

Development and assessment of a concept for a solar thermal assisted biomass district heating system for the municipality of Moosburg / Carinthia considering implemented examples in Austria

A Master's Thesis submitted for the degree of
"Master of Science"

supervised by
Dipl. Päd. Ing. Werner WEISS

Dipl. Ing. Martin DULLNIG
8826110

April 26, 2013, Vienna

Affidavit

I, **Martin Dullnig**, hereby declare

1. that I am the sole author of the present Master Thesis, "Development and assessment of a concept for a solar thermal assisted biomass district heating system for the municipality of Moosburg / Carinthia considering implemented examples in Austria",
238 pages, bound, and that I have not used any source or tool other than those referenced or any other illicit aid or tool, and
2. that I have not prior to this date submitted this Master Thesis as an examination paper in any form in Austria or abroad.

Vienna, _____

Date

Signature

Abstract

During the last 20 years the number of biomass district heating systems in Austria has been continuously growing. The combination of solar thermal technologies with combustion technologies for thermo-chemical conversion of woody biomass is one of the realized concepts to provide useful heat for space heating, domestic hot water preparation and process heat based on renewable energy resources. Several example projects of solar thermal supported biomass district heating systems in Austria have shown that a careful implementation of this concept to use the local solar energy potential and the regionally available solid biomass resources could be a successful approach.

The present work will analyze in detail, if solar thermal technologies can be used in combination with an existing, biomass-fired district heating system to utilize the existent potential in the municipality of Moosburg with respect to technological, ecological and economic feasibility. The outcome of this analysis shall provide a basis for further decision regarding the application of solar thermal systems for useful heat generation.

The selected methods of approach are an evaluation of the district heating system's current status, an analysis of the local solar potential and of the available regional woody biomass resources and the development of an appropriate system concept for later comparison. By modeling the expected heat demand of the investigated biomass district heating system a frame work for energetic analysis is established. A simulation program is applied to determine the energetic effects of a solar thermal system supporting a biomass district heating system with feed-in of solar heat. With the annuity method according to guideline VDI 2067 the economic assessment is carried out. Finally, the proposed solar-assisted biomass district heating application is compared to a reference system realized in Austria.

This thesis shows that an assisting solar thermal plant will substitute a considerable share of district heat produced by boilers, if it is designed properly. The resulting fuel savings, cost savings, and emission savings are the positive effects, which influences the system's economic performance and its ecological sustainability. As worked out by this master thesis the boilers' mode of operation outside the heating season essentially impacts on the district heating plant's emission balance.

With regard to negative consequences this work comes to the conclusion that due to high investment costs the economic feasibility of a solar-assisted biomass district

heating system currently is hard to achieve. The decision pro or contra a solar thermal system supporting a district heating system finally depends on the plant owner's willingness to take a risk and on the support by public funding.

Table of Contents

Abstract.....	ii
Table of Contents	iv
List of Tables	viii
List of Figures.....	xii
List of abbreviations and symbols	xvii
1 Introduction.....	1
1.1 Motivation	1
1.2 Core question and core objective	1
1.3 Structure of work.....	3
2 Basic Principles	5
2.1 Description of concepts and basic principles for solar-assisted biomass district heating systems	5
2.1.1 Terms and classification.....	5
2.1.2 Overview of main components of solar-assisted biomass district heating systems	10
2.1.3 Central heating station	11
2.1.4 Key figures for central heating stations.....	15
2.1.5 Heat distribution network.....	17
2.1.6 Consumer heat sub-stations	24
2.1.7 Key figures for district heating networks	28
2.1.8 Solar thermal collectors.....	32
2.1.9 Solar collector loop, solar pipes and heat exchangers.....	45
2.1.10 Thermal energy storages	47
2.1.11 Key figures of solar thermal systems.....	55
2.2 Hydraulic concepts for solar-assisted biomass district heating systems with central thermal energy storages	61
2.2.1 Hydraulic concepts based on water-operated two-pipe DH network...62	
2.2.2 Hydraulic concepts based on water-operated three-pipe DH network 63	
2.2.3 Hydraulic concepts based on water-operated four-pipe DH network ..65	
2.2.4 Hydraulic concepts based on water-operated six-pipe DH network67	
2.3 Solar-assisted, biomass fired district heating systems in Austria	68
2.3.1 Heating stations in Austria equipped with solid biomass fueled firing applications with a nominal capacity above 100 kW.....	69
2.3.2 Solar-assisted biomass district heating systems in Austria.....	72
2.3.3 Support scheme for solar-assisted biomass district heating systems in Austria	76
3 Methodologies	77
3.1 Method of approach	77
3.1.1 Determination of connected heat load, annual heat demand curve and heat load profile of a biomass district heating system in Moosburg	77
3.1.2 Computing of solar fraction and the share of solar thermal energy fed into a solar-assisted biomass district heating system via simulation program SHWwin.....	81
3.1.3 Ecological appraisal and determination of greenhouse gas savings and air pollutants savings	84
3.2 VDI Guidelines.....	89
3.2.1 Economic appraisal and evaluation of techno-economic feasibility according to guideline VDI 2067: Economic efficiency of building installations	89

4 Analyses of Current Status and Solar Energy Potentials in Moosburg	93
4.1 Current status of the biomass fueled district heating system	93
4.1.1 Technical description of the biomass heating plant	93
4.1.2 Technical description of district heating grid	98
4.1.3 Business use case and thermal energy demand for space heating and hot water preparation in Moosburg.....	101
4.2 Ambient conditions for space heating and hot water preparation	104
4.2.1 Climate data for Moosburg	105
4.2.2 Weather conditions for Moosburg located in central Carinthia	106
4.3 Solar Energy Potential	107
4.3.1 Regional distribution of solar radiation.....	107
4.3.2 Potential for solar thermal energy generation in Moosburg.....	109
4.4 Potential for woody biomass as a renewable energy source for district heating supply.....	112
4.4.1 Regional potential for woody biomass fuels.....	112
4.4.2 Local potential for woody biomass fuels	113
5 Technical Concepts and Proposed Scenarios for a Solar-supported Biomass District Heating System in Moosburg	115
5.1 Definition of system boundaries and boundary conditions	115
5.1.1 Boundary conditions defined by the plant owner and/ or district heating grid operator	115
5.1.2 Technical boundaries for solar technical support.....	117
5.1.3 Boundary conditions with respect to the geographical location of the central heating station.....	118
5.2 Technical concepts, dimensioning and design of a solar-assisted biomass district heating system in Moosburg.....	119
5.2.1 Modeling of an extended district heating grid in year 2013.....	119
5.2.2 Dimensioning of the solar plant based on boundary conditions	121
5.2.3 Design of a solar district heating plant in Moosburg	122
5.3 Reference system for a solar-assisted biomass district heating system in Austria: “Nahwärme Eibiswald”	125
5.3.1 Technical description of “Nahwärme Eibiswald” in year 1997	125
5.3.2 Modeling of a solar-supported district heating network in Eibiswald 1997.....	128
6 Assessments and Comparison.....	130
6.1 Evaluation of scenario specific energy demand and heat production resources for a biomass district heating system with 104 heat consumers in Moosburg 2013.....	130
6.1.1 Evaluation of heat demand and heat production resources for a biomass district heating system with and without solar thermal support in Moosburg 2013.....	130
6.1.2 Evaluation of fuel demand, boiler operation mode and the respective primary energy content in case of a biomass district heating system with and without solar thermal support in Moosburg 2013.....	135
6.1.3 Evaluation of demand for consumables and operation indicators in case of a biomass district heating system with and without solar thermal support in Moosburg 2013	137
6.2 Energetic appraisal of two solar-assisted district heating plants: Solar-assisted biomass district heating system “MS Fernwärme Moosburg” (2013) compared with solar-assisted biomass district heating system “Nahwärme Eibiswald” (1997).....	138

6.2.1 Assessment of two biomass district heating systems located in Moosburg / Carinthia (2013) and Eibiswald / Styria (1997) by simulation program SHWwin.....	138
6.2.2 Evaluation of heat demand and energy balances for two solar-assisted biomass district heating systems: Moosburg 2013 and Eibiswald 1997.....	143
6.2.3 Evaluation of fuel demand, boiler operation mode and the respective primary energy content in case of two solar-assisted biomass district heating systems located in Moosburg (2013) and Eibiswald (1997).....	146
6.2.4 Evaluation of demand for consumables and further operation indicators in case of two solar-assisted biomass district heating systems: Moosburg 2013 and Eibiswald 1997	148
6.3 Evaluation of emissions in case of biomass district heating systems without and with solar support	150
6.4 Evaluation of greenhouse gas and air pollutant savings compared to conventional district heating.....	151
6.4.1 Greenhouse gas and air pollutant savings compared to conventional district heating in case of a solar-assisted biomass district heating system in Moosburg 2013.....	152
6.4.2 Greenhouse gas and air pollutant savings compared to conventional district heating in case of a solar-assisted biomass district heating system in Eibiswald 1997.....	153
6.5 Economic assessment of an extended biomass district heating system with 104 heat consumers in Moosburg 2013.....	153
6.5.1 Economic assessment based on annuity method in case of grid extension for a biomass district heating system without solar support in Moosburg 2013.....	154
6.5.2 Economic assessment based on annuity method in case of a solar-assisted biomass district heating system in Moosburg 2013	160
6.6 Economic assessment based on annuity method in case of reference system “Nahwärme Eibiswald”	167
7 Discussion of Results	174
7.1 Technical and energetic comparison of the proposed applications for district heat supply by biomass district heating systems.....	174
7.1.1 Heating station related key indicators of a biomass district heating system without solar support and a solar-assisted biomass district heating system in Moosburg 2013 compared to heating station related indicators of a solar-assisted biomass district heating system in Eibiswald 1997	174
7.1.2 Distribution grid related key indicators of a biomass district heating system without solar support and a solar-assisted biomass district heating system in Moosburg 2013 compared to distribution grid related indicators of a solar-assisted biomass district heating system in Eibiswald 1997	177
7.1.3 Solar plant related key indicators of a solar-assisted biomass district heating system in Moosburg 2013 compared to heating station related indicators of a solar-assisted biomass district heating system in Eibiswald 1997.....	180
7.2 Ecological comparison of the proposed applications for district heat supply by biomass district heating systems.....	183
7.2.1 Ecological comparison of the proposed applications for biomass district heat supply without and with solar support in Moosburg 2013 with the solar-assisted biomass district heating system in Eibiswald.....	184
7.2.2 Ecological comparison of the proposed applications for district heat supply by solar-assisted biomass district heating systems in Moosburg 2013 and Eibiswald 1997 with respect to relative emission savings	186

7.3 Economic comparison of the proposed applications for district heat supply by biomass district heating systems.....	187
8 Conclusions	191
8.1 Conclusions from a technological point of view.....	191
8.2 Conclusions from an economic point of view.....	192
8.3 Conclusions from an ecological point of view	193
8.4 Conclusions from a plant operator's / plant owner's point of view	194
9 Further Outlooks.....	196
9.1 Perspective for the current owner of the biomass district heating system and district heating grid operator of "MS Fernwärme Moosburg"	196
9.2 Outlook and further measures for the municipality of Moosburg.....	196
10 Acknowledgements	198
11 References	199
11.1 Reports, papers, scripts, and books	199
11.2 Internet resources:	204
12 Annex	206

List of Tables

Table 2-1: Most important types of biomass-fired combustors with automated fuel-feeding system, as well as respective fuel types with related ash and water content (data source: Kaltschmitt, Hartmann & Hofbauer (2009), page 494)	13
Table 2-2: Efficiency expression constants for a global irradiation level of 1000 W/m ² (with reference to the aperture area), collector working temperature and main application of one evacuated tubular collector and two flat plat collectors (data source: SDH (2012), Kaltschmitt, Streicher & Wiese (2010), Weiss (2011))	40
Table 2-3: Storage concepts with respect to heat capacity and geological requirements for large scale or seasonal thermal energy storages (data source: SDH (2012))	52
Table 2-4: Comparison of solar-assisted heating systems with thermal energy storages (i.e. hot water storages) for residential buildings (data source: Weiss & Mahler (2003))	61
Table 2-5: Heating stations in Austria based on firing systems fueled with (forest) wood chips erected in the year 2011 (data source: LWK NÖ (2012))	69
Table 2-6: Biomass district heating systems existing in Austria in the year 2008 with a heat capacity above 150 kW _{th} (data source: LEV (2009))	70
Table 2-7: Key indicators of new biomass district heating systems erected in Austria since 2007 (data source: Promitzer (2011))	71
Table 2-8: Solar-assisted biomass district heating systems in Austria - Status end of 2012 (data source: own research via internet; for more detailed information please refer to the appendix)	72
Table 2-9: Solar-assisted biomass micro grids in Austria - Status end of 2012 (data source: own research via internet; for more detailed information please refer to the appendix)	75
Table 3-1: Emission factors for continuous and start-stop operation of boilers equipped with biomass fired furnaces and oil fueled burners in relation to primary input energy (data source: Heimrath et al. (2002), page 47)	85
Table 4-1: Key indicators of biomass heating plant "MS Fernwärme Moosburg" for year 2011 (data source: Urbas (2009), QM-report (2012) and own calculations)	96
Table 4-2: Key indicators of district heating grid "MS Fernwärme Moosburg" for year 2011 (data source: QM-report (2012) and own calculations)	100
Table 4-3: Income and cost indicators for the business use case of heat generation by a biomass district heating system in Moosburg 2011 (data source: QM-report (2012) and own calculations)	103
Table 4-4: Monthly irradiation, monthly mean temperature, heating days and heating degree days for Moosburg / Carinthia (data source: Meteonorm (2012), BMfWFJ (2013) and own calculations based on ZAMG (2000 - 2011))	105
Table 4-5: Solar irradiation data for selected locations in the region of central Carinthia calculated with PVGIS (data source: Climate-SAF PVGIS (2013))	108
Table 4-6: Estimated technical potentials for useful heat generation by solar thermal collectors feeding into a district heating system without seasonal storage (data source: PVGIS (2013), CPC 14 XL (2012), VK 14 (2008), GK 3100 (2012), HT 4.2 m ² (2009) and own calculations)	111
Table 5-1: Key indicators for an extended district heating grid in Moosburg 2013 (data source: own calculations).	120
Table 5-2: Calculated energy yield of a solar thermal collector field* in Moosburg 2013 (data source: own calculations).	122
Table 5-3: Design details and technical data for a solar-assisted biomass district heating system in Moosburg 2013* (data source: HT 4.2 m ² (2009) and own calculations).	124

Table 5-4: Design details and technical data for a solar-assisted biomass district heating system in Eibiswald 1997* (data source: Streicher & Oberleitner (1998) and own calculations).	127
Table 5-5: Key indicators and technical data for Eibiswald 1997* (data source: Streicher&Oberleitener (1998) and own calculations).	129
Table 6-1: Key indicators for a biomass district heating system without solar thermal support and for a solar-assisted biomass district heating system in Moosburg 2013** (data source: simulation results of SHWwin and own calculations).	131
Table 6-2: Indicators for primary energy content of fuel used in a biomass district heating system without solar thermal support and of fuel used in a solar-assisted biomass district heating system in Moosburg 2013**** (data source: simulation results of SHWwin and own calculations).	136
Table 6-3: Consumables and operation indicators for biomass district heating system without solar thermal support and for a solar-assisted biomass district heating system in Moosburg 2013** (data source: simulation results of SHWwin and own calculations).	137
Table 6-4: Simulation results for a solar thermal system supporting two biomass district heating networks: Moosburg 2013** and Eibiswald 1997*** (data source: simulation results of SHWwin and own calculations).	139
Table 6-5: Simulation results for two biomass district heating systems assisted by a solar thermal system: Moosburg 2013** and Eibiswald 1997*** (data source: simulation results of SHWwin and own calculations).	142
Table 6-6: Comparison of key indicators of 2 solar-assisted biomass district heating systems. Moosburg 2013** and Eibiswald 1997*** (data source: simulation results of SHWwin and own calculations).	143
Table 6-7: Comparison of indicators for primary energy content of fuel used in 2 solar-assisted biomass district heating systems. Moosburg 2013+ and Eibiswald 1997** (data source: simulation results of SHWwin and own calculations).	146
Table 6-8: Comparison of consumables and operation indicators for solar-assisted biomass district heating systems. Moosburg 2013** and Eibiswald 1997*** (data source: simulation results of SHWwin and own calculations).	149
Table 6-9: Total, annual emissions based on primary energy content of fuel of a biomass district heating system without and with solar support in Moosburg 2013* (data source: simulation results of SHWwin and own calculations).	150
Table 6-10: Specific emissions per unit heat fed into district heating system of a biomass district heating system without and with solar support in Moosburg 2013* (data source: simulation results of SHWwin and own calculations).	151
Table 6-11: Annual GHG emission savings and air pollutants savings by a solar-assisted biomass district heating system in Moosburg 2013* compared to conventional district heat supply by a district heating mix (data source: GEMIS (2010), Kaltschmitt & Streicher (2009), own calculations).	152
Table 6-12: Annual GHG emission savings and air pollutants savings by a solar-assisted biomass district heating system in Eibiswald 1997* compared to conventional district heat supply by a district heating mix (data source: GEMIS (2010), Kaltschmitt & Streicher (2009), own calculations).	153
Table 6-13: Initial investment costs and specific investment costs for plant components of a biomass district heating system in Moosburg 2013** (data source: Biermayr, et al. (2012), SDH (2012), Kaltschmitt&Streicher (2009), QM-report (2012)).	154
Table 6-14: Cost items split according to VDI2067, Blatt1 (2012) and income items for a biomass district heating installation in Moosburg 2013* (data source: own calculations). Annuity items calculated according to VDI2067, Blatt1 (2012) (data source: own calculations)	156

Table 6-15: Initial investment costs and specific investment costs for solar plant components of a solar-assisted biomass district heating system in Moosburg 2013** (data source: Biermayr et al. (2012), SDH (2012), Kaltschmitt & Streicher (2009), QM-report (2012)).	161
Table 6-16: Initial investment costs and specific investment costs for plant components (heating station, heat distribution grid) of a solar-assisted biomass district heating system in Moosburg 2013** (data source: Biermayr et al. (2012), SDH (2012), Kaltschmitt & Streicher (2009), QM-report (2012)).	162
Table 6-17: Cost items split according to VDI2067, Blatt1 (2012) and income items for a solar-assisted biomass district heating installation in Moosburg 2013* (data source: own calculations). Annuity items calculated according to VDI2067, Blatt1 (2012) (data source: own calculations)	164
Table 6-18: Initial investment costs for solar plant components of a solar-assisted biomass district heating system in Eibiswald 1997** (data source: Heimrath, et al. (2002), Faninger&Weiss (2002)).	168
Table 6-19: Initial investment costs for plant components (heating station, heat distribution grid) of a solar-assisted biomass district heating system in Eibiswald 1997** (data source: Streicher & Oberleitner (1998), Heimrath, et al. (2002), Faninger&Weiss (2002)).	169
Table 6-20: Cost items split according to VDI2067, Blatt1 (2012) and income items for a solar-assisted biomass district heating installation in Eibiswald 1997* (data source: own calculations). Annuity items calculated according to VDI2067, Blatt1 (2012) (data source: own calculations)	170
Table 7-1: Comparison of heating station related configuration and operating data of biomass district heating systems with and without solar support in Moosburg 2013* and a solar-assisted biomass district heating system in Eibiswald 1997** (data source: simulation results of SHWwin and own calculations).	175
Table 7-2: Comparison of heating station related key indicators of biomass district heating systems with and without solar support in Moosburg 2013* and a solar-assisted biomass district heating system in Eibiswald 1997** (data source: simulation results of SHWwin and own calculations).	176
Table 7-3: Comparison of distribution grid related configuration and operating data of biomass district heating systems with and without solar support in Moosburg 2013 and a solar-assisted biomass district heating system in Eibiswald 1997 (data source: simulation results of SHWwin and own calculations).	178
Table 7-4: Comparison of distribution grid related key indicators of biomass district heating systems with and without solar support in Moosburg 2013 and in Eibiswald 1997 (data source: simulation results of SHWwin and own calculations).	179
Table 7-5: Comparison of solar plant related configuration and operating data of a solar-assisted biomass district heating system in Moosburg 2013 and a solar-assisted biomass district heating system in Eibiswald 1997 (data source: simulation results of SHWwin and own calculations).	181
Table 7-6: Comparison of solar plant related key indicators of a solar-assisted biomass district heating system in Moosburg 2013 and a solar-assisted biomass district heating system in Eibiswald 1997 (data source: simulation results of SHWwin and own calculations).	183
Table 7-7: Total, annual emissions based on primary energy content of fuel utilized by district heating systems without and with solar support in Moosburg 2013 and by a solar-assisted biomass district heating system in Eibiswald 1997 (data source: simulation results of SHWwin and own calculations).	184
Table 7-8: Specific emissions per unit heat fed into district heating system without and with solar support in Moosburg 2013 and per unit heat fed into solar-	

assisted biomass district heating system in Eibiswald 1997 (data source: simulation results of SHWwin and own calculations).	185
Table 7-9: Ecological parameters of a solar-assisted biomass district heating system in Moosburg 2013 compared with a solar-assisted biomass district heating system in Eibiswald 1997 (data source: simulation results of SHWwin and own calculations).	186
Table 7-10: Cost and income related economic parameters of 2 district heating systems without and with solar support in Moosburg 2013 compared with the economic parameters of a solar-assisted biomass district heating system in Eibiswald 1997 (data source: simulation results of SHWwin and own calculations).	188
Table 7-11: Economic key indicators of 2 district heating systems without and with solar support in Moosburg 2013 compared with the economic parameters of a solar-assisted biomass district heating system in Eibiswald 1997 (data source: simulation results of SHWwin and own calculations).	189
Table 12-1: Solar-assisted biomass district heating systems in Austria 2012 (Part 1)	206
Table 12-2: Solar-assisted biomass district heating systems in Austria 2012 (Part 2)	207
Table 12-3: Solar-assisted biomass micro grid systems in Austria – Status 2012	208
Table 12-4: Simulation report of for a solar-assisted biomass district heating system in Moosburg / Carinthia 2013	209
Table 12-5: Simulation report of for a solar-assisted biomass district heating system in Eibiswald / Styria 1997	213
Table 12-6: Total, annual emissions based on primary energy content of fuel and specific emissions per unit heat fed into a biomass district heating system without solar support in Moosburg 2013*** (data source: simulation results of SHWwin and own calculations).	217
Table 12-7: Total, annual emissions based on primary energy content of fuel and specific emissions per unit heat fed into a solar- assisted biomass district heating system in Moosburg 2013*** (data source: simulation results of SHWwin and own calculations).	217
Table 12-8: Total, annual emissions based on primary energy content of fuel and specific emissions per unit heat fed into a solar-assisted biomass district heating system in Eibiswald 1997*** (data source: simulation results of SHWwin and own calculations).	218

List of Figures

Figure 2-1: Categories of solar district heating systems: central district heating system with central solar feed-in and central energy storage as well as distributed district heating system with distributed solar feed-in (data source: SDH (2012))	9
Figure 2-2: Typical scheme of a central biomass heating plant (data source: Ortner (2010))	12
Figure 2-3: Example hydraulic scheme of a district heating plant comprising a biomass boiler, a peak-load oil boiler, a flue gas condenser with economizer and a buffer tank (data source: Stockinger & Obernberger (2005), page 191). There is one hot-water circulation pump for winter operation, one for summer operation and one for reserve.	15
Figure 2-4: Main types of heat distribution networks for district heating systems: radial network, ringed network, and meshed network (data source: Kaltschmitt, Streicher & Wiese (2010), page 451, Zweiler (2011)).	18
Figure 2-5: Example of an annual heat duration line of a district heating system with a correct dimensioned biomass boiler and a peak load boiler (data source: Zweiler (2011)). 85 % of the annual heat demand is covered by the biomass boiler within 4293 nominal power hours (NPH).	22
Figure 2-6: Circuit diagram example and image of an instantaneous water heater (data source: Danfoss TermixNovi (2012)). The substation for instantaneous water heating is designed for the use in one-family houses, apartments and small apartment buildings.	26
Figure 2-7: Circuit diagram example of a district heating substation for indirect heating with tank for DHW preparation (data source: Danfoss Termix BVX RO (2010)). The electronically controlled substation for indirect space heating with tank for domestic hot water preparation is designed for single-family houses or apartments.	27
Figure 2-8: Circuit diagram example and image of an advanced district heating substation from 16 to 90 kW (data source: Danfoss DSA 1 MINI (2012)). The substation is designed for indirect connection to district heating systems in micro and macro networks.	28
Figure 2-9: Principle of energy flows in a solar collector comprising a cover made of glass, an absorber and a collector casing with thermal insulation (data source: Viessmann (2009)). The incident solar radiation consist of the beam or direct radiation onto the solar collector and the diffuse radiation, which is scatter by air molecules in the atmosphere or reflected on clouds or particles in the atmosphere.	33
Figure 2-10: Example of a solar collector's efficiency expression (red line) displayed as a function of temperature difference between mean collector temperature and ambient temperature for a given irradiation level of 1000 W/m^2 (data source: SDH (2012)). For a defined temperature difference the colors indicate the ratio between optical losses (blue), heat losses (orange) and useful energy (green).	35
Figure 2-11: Principle design of a flat plat collector for applications with an operating temperature up to 80°C (data source: Sözen et al. (2008)).	37
Figure 2-12: Principle designs of liquid heaters applied in evacuated tubular collectors (data source: Duffie & Beckman (2006), page 279).	38
Figure 2-13: Heat pipe principle (left) and direct flow principle (right) applied in evacuated tubular collectors (data source: Viessmann (2009)).	39

- Figure 2-14: Manifold designs for evacuated tubular collectors based on direct flow principle (left) and heat pipe principle (right) and (data source: Viessmann (2009)). 39
- Figure 2-15: Examples of collector efficiency curves of three designs of non-concentrating liquid-type collectors (data source: SDH (2012)). The efficiency expression based on the aperture area is plotted as a function of temperature difference between collector fluid and ambient air at a solar irradiation level of 1000 W/m^2 on the collector plane. 41
- Figure 2-16: Definition of gross collector area, aperture area and absorber area for flat plate collectors and evacuated tube collectors (data source: Viessmann (2009)). 42
- Figure 2-17: Annual solar output as a function of collector mean temperature (T_m) for the ETC and the two FPC characterized in Table 2-2 (data source: SDH (2012)). Energy output (Q) is given in kWh per m^2 collector aperture area and year 44
- Figure 2-18: Annual solar output as a function of collector mean temperature (T_m) for the ETC and the two FPC characterized in Table 2 2 (data source: SDH (2012)). Energy output (Q) is given in kWh per m^2 collector gross area and year. 44
- Figure 2-19: Four examples of water-filled tanks with cylinder design used for the storage of potable water, used as buffer tank or for the storage of heating water (data source: Viessmann (2009)). 50
- Figure 2-20: Four main construction concepts for large-scale or seasonal thermal energy storages (data source: SDH (2012)). 51
- Figure 2-21: Example scheme of an above-ground hot water tank used as a seasonal thermal energy storage (data source: SDH (2012). Due to its high investment costs above-ground tank thermal energy storages are in general used as buffer tanks with a maximal volume of 200 m^3 . 54
- Figure 2-22: Hydraulic scheme of a solar-assisted biomass district heating system with two-pipe heat distribution network including two options for consumer heat sub-station * (data source: Fink et al. (2007), page 25). 62
- Figure 2-23: Hydraulic scheme of a solar-assisted biomass district heating system with two-pipe heat distribution network and decentralized apartment heat transfer units * (data source: Fink et al. (2007)). 63
- Figure 2-24: Hydraulic scheme of a solar-assisted biomass district heating system with three-pipe heat distribution network including a separate line for domestic hot water preparation * (data source: Fink et al. (2007)). 64
- Figure 2-25: Hydraulic scheme of a solar-assisted biomass district heating system with three-pipe heat distribution network integrating a separate line for centralized solar thermal feed-in by decentralized mounted collector fields * (data source: Fink et al. (2007)). 65
- Figure 2-26: Hydraulic scheme of a solar-assisted biomass district heating system with four-pipe heat distribution network including a domestic hot water storage tank for central preparation of domestic hot water * (data source: Fink et al. (2007)). 66
- Figure 2-27: Hydraulic scheme of a solar-assisted biomass district heating system with four-pipe heat distribution network including de-centrally installed domestic hot water storage tanks for local preparation of domestic hot water in the connected buildings * (data source: Fink et al. (2007)). 67
- Figure 2-28: Hydraulic scheme of a solar-assisted biomass district heating system with six-pipe heat distribution network including a centrally installed domestic hot water storage tank for central preparation of domestic hot water * (data source: Fink et al. (2007)). 68

Figure 3-1: Linear heat load curve of a district heating system depending on the ambient air temperature (data source: Winter & Obernberger (2002)).	78
Figure 3-2: Heat demand curve of a district heating system depending on time (data source: own calculations).	80
Figure 3-3: Example configuration of a solar-assisted district heating system simulated by simulation program SHWwin (data source: SHWwin (1999)).	82
Figure 3-4: Screen shot of input window for frame conditions of district heating including the control cam for forward and return flow temperature (data source: SHWwin (1999)).	83
Figure 3-5: SO ₂ -equivalents, SO ₂ emissions, NO _x emissions in [g / kWh _{th}] for district heat supply. Air pollutants' balance calculated for the whole life cycle of conventional district heating mix* (data source: GEMIS 4.6 (2010)) compared to the air pollutants' balance of a solar-assisted district heating system** (data source: Kaltschmitt & Streicher (2009), page 144)	87
Figure 3-6: CO ₂ -equivalents in [g / kWh _{th}] for district heat supply. Greenhouse gas emissions' balance calculated for the whole life cycle of conventional district heating mix* (data source: GEMIS 4.6 (2010)) compared to the GHG emissions' balance of a solar-assisted district heating system** (data source: Kaltschmitt & Streicher (2009), page 144)	88
Figure 4-1: Schematic diagram of Urbas' firing technology for district heat generation by woody biomass combustion* (data source: Urbas (2009))	95
Figure 4-2: Schematic diagram of the biomass heating plants hydraulic scheme with parameters measured during summer load operation* (data source: Urbas (2009))	96
Figure 4-3: Behavior of the flow pipe temperature and the return flow pipe temperature in the water-operated two-pipe district heating network of Moosburg *. Temperature difference between flow and return flow varies between a maximum of 40 – 45 °C and a minimum of 15 °C** (data source: Urbas (2009), ESTIF (2007) and own calculations).	99
Figure 4-4: Monthly balances of produced heat, heat fed into the district heating grid and useful heat supplied and sold to the 50 heat consumers in Moosburg 2011* (data source: QM-report (2012))	102
Figure 4-5: Heat demand curve for district heating system "MS Fernwärme Moosburg" based on a maximal effective heat load of 1684.4* kW _{th} and on the climatic conditions for Moosburg in 2011 (data source: Meteonorm (2012) and own calculations).	104
Figure 4-6: Graphical representation of monthly radiation and monthly temperature in Moosburg / Carinthia (data source: Meteonorm (2012))	106
Figure 4-7: Graphical representation of monthly sunshine duration and monthly precipitation in Moosburg / Carinthia (data source: Meteonorm (2012))	107
Figure 4-8: Yearly total of global irradiation on a horizontal surface [kWh/m ²] in Central Carinthia (data source: PVGIS (2013)).	108
Figure 4-9: Annual sum of irradiation on surface [kWh/m ²] within the area of the town of Moosburg / Carinthia (data source: KAGIS (2013)).	110
Figure 4-10: Allocation of areas with different percentage of afforestation in the municipal territory of Moosburg / Carinthia (data source: KAGIS (2013)).	114
Figure 5-1: Heat demand curve for district heating system "MS Fernwärme Moosburg" based on a total effective heat load of 2130 kW _{th} and on the climatic conditions for Moosburg in year 2013 (data source: Meteonorm (2012) and own calculations).	120
Figure 5-2: Visualization of a solar-assisted biomass district heating system from the bird's-eye perspective in Moosburg (data source: Google (2013)).	123
Figure 5-3: Solar-assisted biomass district heating system in Eibiswald /Styria in year 1997 (data source: Eibiswald (2013)).	126

Figure 5-4: Heat demand curve for district heating system “Nahwärme Eibiswald” based on a maximal connected load of 2114* kW _{th} and on the climatic conditions for Eibiswald in 1997 (data source: ZMAG (1971 - 2000) and own calculations).	128
Figure 6-1: Annual energy balances of biomass district heating systems with and without solar support in Moosburg 2013 (data source: simulation results of SHWwin and own calculations).	132
Figure 6-2: Heat demand and assigned heat production resources for a biomass district heating system in Moosburg 2013 (data source: simulation results of SHWwin and own calculations).	133
Figure 6-3: Heat demand and assigned heat production resources for a solar-assisted biomass district heating system in Moosburg 2013 (data source: simulation results of SHWwin and own calculations).	134
Figure 6-4: Monthly balances of global irradiation, useful thermal energy by collectors and solar thermal energy fed into thermal energy storage for solar-assisted biomass district heating system “MS Fernwärme Moosburg” in year 2013 (data source: simulation results of SHWwin).	141
Figure 6-5: Monthly balances of global irradiation, useful thermal energy by collectors and solar thermal energy fed into thermal energy storage for solar-assisted biomass district heating system “Nahwärme Eibiswald” in 1997 (data source: simulation results of SHWwin).	141
Figure 6-6: Annual energy balances of solar thermal supported biomass district heating systems in Moosburg 2013 and in Eibiswald 1997 (data source: simulation results of SHWwin and own calculations).	145
Figure 6-7: Monthly balances of heat produced by boilers, heat fed into the district heating grid, solar thermal energy fed into thermal energy storage and solar heat as a percentage rate of district heat determined for a solar-assisted biomass district heating system “MS Fernwärme Moosburg” in year 2013 (data source: simulation results of SHWwin and own calculations).	147
Figure 6-8: Monthly balances of heat produced by boilers, heat fed into the district heating grid, solar thermal energy fed into thermal energy storage and solar heat as a percentage rate of district heat determined for a solar-assisted biomass district heating system “Nahwärme Eibiswald” in year 1997 (data source: simulation results of SHWwin and own calculation).	148
Figure 6-9: Sensitivity analysis of annuities for a biomass district heating system in Moosburg 2013. Total annuity of a district heating plant investment as a function of electricity costs, consumption costs, maintenance costs, other costs as well as net heat price valid for the year 2014 (Year 5 of operation). Variation done in the range of ± 25 % (data source: own calculations).	159
Figure 6-10: Sensitivity analysis of annuities for a solar-assisted biomass district heating system in Moosburg 2013. Total annuity of a district heating plant investment as a function of electricity costs, consumption costs, maintenance costs, other costs as well as net heat price valid for the year 2014 (Year 5 of operation). Variation done in the range of ± 25 % (data source: own calculations).	167
Figure 6-11: Sensitivity analysis of annuities for a solar-assisted biomass district heating system in Eibiswald 1997. Total annuity of a district heating plant investment as a function of electricity costs, consumption costs, maintenance costs, other costs as well as net heat price valid for the year 1998 (Year 5 of operation). Variation done in the range of ± 25 % (data source: own calculations).	173
Figure 12-1: Annual balances of 2 solar thermal systems feeding into district heating networks of Moosburg 2013 and Eibiswald 1997 (data source: simulation results of SHWwin).	212

- Figure 12-2: Annual energy balances of 2 district heating systems supported by solar thermal systems in Moosburg 2013 and Eibiswald 1997 (data source: simulation results of SHWwin). 216
- Figure 12-3: Total, annual emissions of CO₂, CO, C_xH_x, NO_x and fine particles based on primary energy content of fuel used in biomass district heating systems with and without solar support (data source: own calculations). 219

List of abbreviations and symbols

Abbreviation	Long Text
CHP	Combined Heat & Power
ca.	circa
DHW	Domestic Hot Water
FLH	Full Load Hours
NPH	Nominal Power Hours
ORC	Organic Rankine Cycle
O&M	Operation & Maintenance
HDD	Heating degree days
SNCR	Selective Non Catalytic Reduction
SRM	Schüttraummeter = loose cubic meter
T	Temperature
Hu	Lower heating value
ECO	Economizer
kW	Kilowatt
MW	Megawatt
kW _{el}	Kilowatt electric
MW _{el}	Megawatt electric
kW _{th}	Kilowatt thermal
MW _{th}	Megawatt thermal
kW _{NCV}	Kilowatt net calorific value
MW _{NCV}	Megawatt net calorific value
kg	kilogram
m	meter
Pa	Pascal
J	Joule
PJ	Petajoule
s	second
mbar	millibar
°C	Degree Celsius
K	Kelvin
h	hour
d	day
a	anno (year)
t	ton(s)

Abbreviation	Long Text
wt. %	weight percent
vol.-%	volume per cent
% dm	Per cent dry basis
% w.b.	Per cent wet basis
temp.	temperature
T	temperature [°C], [K]
p	pressure
v	velocity [m/s]
A	Area [m ²]
ρ	density [kg/m ³]
k_f	Hydraulic conductivity [m/s]; A property of vascular plants, soil or rock that describes the ease with which water can move through pore spaces or fractures.
P_{el}	Electric power [W]
W_{el}	Electric work [Wh]
Q'_{th}	Thermal power; thermal capacity [W]
Q_{th}	Thermal energy; heat [Wh], [J]
Q'_{NCV}	Thermal input power of fuel; furnace thermal capacity [W]
GHG	Greenhouse gas
CO ₂	Carbon-di-oxide
SO ₂	Sulfur-di-oxide
y	year
aka.	also known as
n.a.	not available
rel.	relative
ATES	Aquifer thermal energy storage
BTES	Borehole thermal energy storage
TTES	Tank thermal energy storage
DH	District heating
DHW	Domestic hot water
ETC	Evacuated tubular collector
FPC	Flat plate collector
HX	Heat exchanger
ST	Solar thermal
F	Flow (of hot water to load)
RF	Return flow (of cold water from load)
LTRF	Low-temperature return flow (of cold water from load)

1 Introduction

1.1 Motivation

As I have been invited by the community of Moosburg / Carinthia to work in a project group within the “e⁵- program” for energy efficient municipalities in Austria, I would like to develop this master thesis based on site-specific data. It is the aim of this master thesis to provide a basis for further decision regarding the utilization of the regional solar energy potential and to show, which solar energy technologies and alternative concepts could be applied in combination with the already existing, biomass fueled district heating system. A feasible prospect should be outlined in detail and should be analyzed from a techno-economic point of view. Finally, the proposed concept for implementation should be compared with an already existing example for similar projects realized within a municipality in Austria.

1.2 Core question and core objective

In order to define the scope of work for this master thesis the core question and the core objective are defined as followed.

The core question of this master thesis is:

- How can solar thermal technologies be used in combination with a biomass fired district heating system to utilize the solar energy potential available in the municipality of Moosburg with respect to technological, ecological and economic feasibility?

This leads to further questions like as:

- Are there any projects in Austria, where the concept of a biomass district heating system combined with solar-thermal technology have been successfully implemented?
- How can these realized solar energy concepts for a municipality be compared with Moosburg?
- Which of these concepts is the most feasible one from a technological, ecological and economic point of view?
- As there is already a district heating system available, how does the technical potential for solar energy technology within the boundary of the observed area look like?

- Which possibilities do the plant owner and/or the heating grid operator have when utilizing the local solar potential?
- Is there a possibility to combine a solar-thermal system with the biomass district heating plant in order to fully supply the heating grid in summer for hot water preparation?
- Which type of heat storage concept fits best in combination with the solar-supported biomass district heating system?
- Which type of operation mode is the most economic one?
- Which savings and how much savings can be expected, when the solar thermal supported biomass system is put into operation (e.g. operational costs, fuel costs, greenhouse gas savings, fuel savings, etc.)?

The core objective of this master thesis is to provide a basis for further decision regarding the utilization of the regional solar potential by solar thermal technology. As the biomass district heating system is still not used to the full and the provision of heat for hot water preparation during summertime could be improved, alternative scenarios based on renewable energy resources are under further investigation by the plant owner and grid operator.

By focusing on the core objective in the scope of this master thesis the following results are expected:

- As a first result of this master thesis it should turn out to be feasible to support the existing biomass-fired district heating system with a solar-thermal system. During summer time the heat demand for hot water preparation should be mostly be covered by solar heat. Depending on the already implemented mode of operation the need for heat storage should be adapted accordingly.
- As a second result an optimized concept for solar-thermal support of an extended biomass district heating system should be the outcome of this master thesis. Even in case of a larger district heating grid, more heat consumers and a different load profile a continuous operation of the district heating grid with solar support would be more economical and ecological.
- Finally, this master thesis should give an indication to which extend it is possible to utilize the local solar potential in combination with the regional resources of woody biomass. For the municipality of Moosburg this master

thesis should show up further measures and possibilities for using renewable energy sources in the frame of the “e⁵-program”. By a detailed description of the proposed application and it’s energetic, ecologic and economic consequences realistic measures to reach the municipality’s 2020 goals should be outlined.

1.3 Structure of work

The present work is divided into main 12 chapters. Each of the main chapters deals with a specific topic and follows a given formal structure:

- The first chapter introduces to the subject of matter of this master thesis. It describes core question and core objective of this work.
- In the second chapter the basic principles are outlined. It gives a comprehensive overview on the theoretical background of central heating stations, heat distribution networks, consumer heat sub-stations, solar thermal collectors, heat exchangers and thermal energy storages.
- The third chapter deals with the methodologies applied in the frame of this master thesis. Methods for technological, energetic, ecological and economic assessments are presented.
- Chapter four describes the current status of the biomass district heating system in Moosburg / Carinthia. There the ambient conditions, the local solar potential and the available woody biomass resources in the region are analyzed.
- In chapter five technical concepts and proposed scenarios for a solar thermal supported district heating system in Moosburg are described. It defines boundary conditions for realization and gives an overview on the selected reference system in Eibiswald / Styria.
- Chapter six describes the results of energetic, ecological and economic assessments. The outcome of the conducted appraisals is compared to each other with respect to the expected energetic, ecological and economic effects.
- In chapter seven the proposed applications for district heat supply by biomass district heating systems are compared from an energetic, ecologic

and economic point of view. The results of the assessments carried out in chapter six are discussed in detail.

- Chapter eight provides a summary of conclusions and findings with respect to the performed technological, energetic, ecological and economical appraisals.
- In chapter nine further outlooks on future perspectives of the current plant owner and/or grid operator as well as on future perspective of the municipality of Moosburg are given.

The work's formal structure is finalized by with acknowledgements in chapter ten, with references in chapter 11 and with an annex marked as chapter 12.

2 Basic Principles

In the following subchapters an overview on basic principles and concepts applied in the subject area of solar-assisted biomass district heating systems are outlined.

First, this type of heat supply system is classified by classing it with the group of heating systems currently applied in Austria. Second, a detailed description of main components of a solar-assisted biomass district heating systems, of the different types of heating grids and definitions of key figures with respect to the technical, characteristics of a solar-assisted biomass district heating system are provided.

Third, hydraulic concepts of a solar-assisted biomass district heating systems based on a central thermal storage are given and finally the current status of solar-assisted biomass district heating systems in Austria is described.

2.1 Description of concepts and basic principles for solar-assisted biomass district heating systems

2.1.1 Terms and classification

According to Stockinger & Obernberger (2005) heat supply systems for space heating are differentiated by the location, where the heat is generated (see page 3). If the space heating system is installed in the room, where the produced heat is consumed as an energy service, it will be defined as batch fired system for domestic heating. Examples for biomass fired representatives are open fire places or single wood stoves. In case of a so-called central heating system the useful energy is provided by a central energy conversion unit. Examples of such systems for residential heating are wood log boilers, gas or oil-fired boilers, heat pumps or pellet stoves.

To fulfill the heating requirements in multi-story residential buildings by a biomass fired, automatically operated central heat station typically wood chips-fired or pellet-fired boilers with a thermal capacity from 15 kW_{th} to more than 100 kW_{th} are applied (Hofbauer (2010)). The distribution of heat to the rooms within the building or to the flats of a multiple-story block is accomplished by a heat carrier like water or air. In the rooms radiators fed with hot water are the responsible units for heat exchange or the pre-heated air is directly blown into the room. In flats or apartments dedicated apartment heat transfer units take over this task.

A district heating system is a heat supply system which provides heat to several single-family houses, to housing complexes comprising several residential houses

or apartment buildings, to industrial zones including office buildings and industrial buildings or to complete settlements like towns or cities. The conversion of primary energy carriers to useful heat takes place in one or several central heating stations or heating plants. The produced thermal energy is fed into the district heating grid in form of hot water or steam, which carries the heat to heat exchange systems of the connected houses or buildings. There the useful heat is taken over by the buildings heating system.

The centralized provision of heat is done either by dedicated district heating plants or by combined heat and power (CHP) stations. Thermal energy generated by heating plants is the result of thermal conversion of gaseous, liquid or solid fuels in appropriate combustion units or it is waste heat from industrial processes. CHP plants operated in cogeneration mode produce thermal energy in form of hot water or steam and electric energy at the same time. As this study will focus on biomass district heating systems in Austria, which are usually realized as pure heating plants, further on CHP plants and their technology are not discussed any more.

If the annual efficiency of heat provision in heating plants shall be characterized, the total annual energy efficiency for a heating plant ($\zeta_{tot, HP}$) is defined as (see Konstantin (2009)):

$$\zeta_{tot, HP} = \frac{Q_{th, HP, use}}{Q_{NCV}} \quad [1] \quad \text{Equation 1}$$

$Q_{th, HP, use}$... useful heat generated by the heating plant per anno [kWh_{th}/a]
 Q_{NCV} ... input energy per anno related to the net calorific value of the fuel [kWh_{NCV}/a].

As stated by Stockinger & Obernberger (2005) a biomass district heating system in Austria is characterized by the centralized combustion of organic matter providing thermal energy to boilers with a maximal nominal capacity of 10 MW_{th} (see page 3). Usually it is the purpose of a district heating system to supply useful heat for space heating, domestic hot water preparation or process heat via a water-filled district heating network to the heat users. In order to differentiate the heat supply from biomass-fired heating stations via district heating grids from the heat supply via micro-grids Stockinger & Obernberger (2005) propose the following classification (see page 4):

- A heat supply system based on the combustion of biomass fuels will be called micro-grid, if the nominal thermal capacity of the used boiler is lower

than $250 \text{ kW}_{\text{th}}$, if the heat is mainly provided to third parties, and if at least three separate buildings are connected to the micro-grid.

- A heat supply system will be called a biomass district heating system, if the nominal thermal capacity of the biomass-fired boilers in the central heating station exceeds $250 \text{ kW}_{\text{th}}$, if the produced heat is mainly provided to third parties or the connected thermal load of the heat users is greater than $250 \text{ kW}_{\text{th}}$, and if at least three separate buildings are connected to the district heating grid.

In case of a solar district heating system several heat users join to use heat from a single solar plant based on the centralized utilization of solar radiant energy by large-scaled solar collector arrays. These systems are characterized by the provision of low temperature heat ($T < 150 \text{ °C}$) on a diurnal or on a seasonal timeline (see Weiss (2011), page 80). Solar-supported district heating systems are further differentiated with respect to the applied heat storage system (see Kaltschmitt & Streicher (2010), page 157). Basically three concepts for the centralized storage of thermal energy gained by solar collectors are in use (see Weiss & Mahler (2003)):

- The so-called short-term heat storages usually support the preparation of domestic hot water. Solar heat can be stored for a maximal duration of two days.
- The so-called mid-term heat storage can keep the required amount of solar heat up to one week. In order to assist to the preparation of domestic hot water and to space heating the needed storage volume is several times the volume per collector area of a short-term storage system.
- A so-called long-term storage provides the necessary storage capacity to support domestic hot water preparation and space heating via a district heating system with a high rate of solar fraction. For systems with a solar fraction greater than 50% seasonal solar heat storages are required (see Raab (2006), page 2). Due to the requirement to level out the difference of high amount of solar irradiation in summer and the heat demand during the winter time the storage volume of a seasonal solar heat storage system is relatively high.

A solar-assisted biomass district heating system combines two technologies for heat supply out of renewable energy resources in a district heating system. During the

heating period the heat demand of the connected heat clients is mainly covered by the combustion of biomass fuels in the central heating station. Solar gains from the solar thermal collectors are utilized to pre-heat water serving as heat carrier in the heat distribution network.

Outside the heating season the thermal energy provided by the district heating system is primarily intended for domestic hot water preparation. As the required thermal power is low compared to the capacities needed for space heating, in the main solar heat from the solar thermal system shall satisfy the heat demand of the connected heat users outside the heating period and shall cover the unavoidable heat losses in the district heating grid. If more thermal energy is required due to additional heat load in the district heating system or in order to load the thermal energy storage, the biomass-fired boiler or the fossil-fired peak load boiler serve as a reserve.

According to SDH (2012) two categories of solar district heating systems are differentiated related to the feed-in point of the solar system and to the size of the district heating system (see Figure 2-1). In a central solar district heating system the solar thermal system feeds in at the central heating station. The solar collector field is either ground mounted near to the heating plant or the collectors are roof-top mounted on buildings transferring the solar heat to the heating station via a dedicated collection grid. For high solar fractions in the district heating system the central heating plant is connected to single, centralized, long-term energy storage. Central solar DH systems are realized for large-scaled or mid-sized district heating networks and in case of micro- grids in form of central solar block heating system.

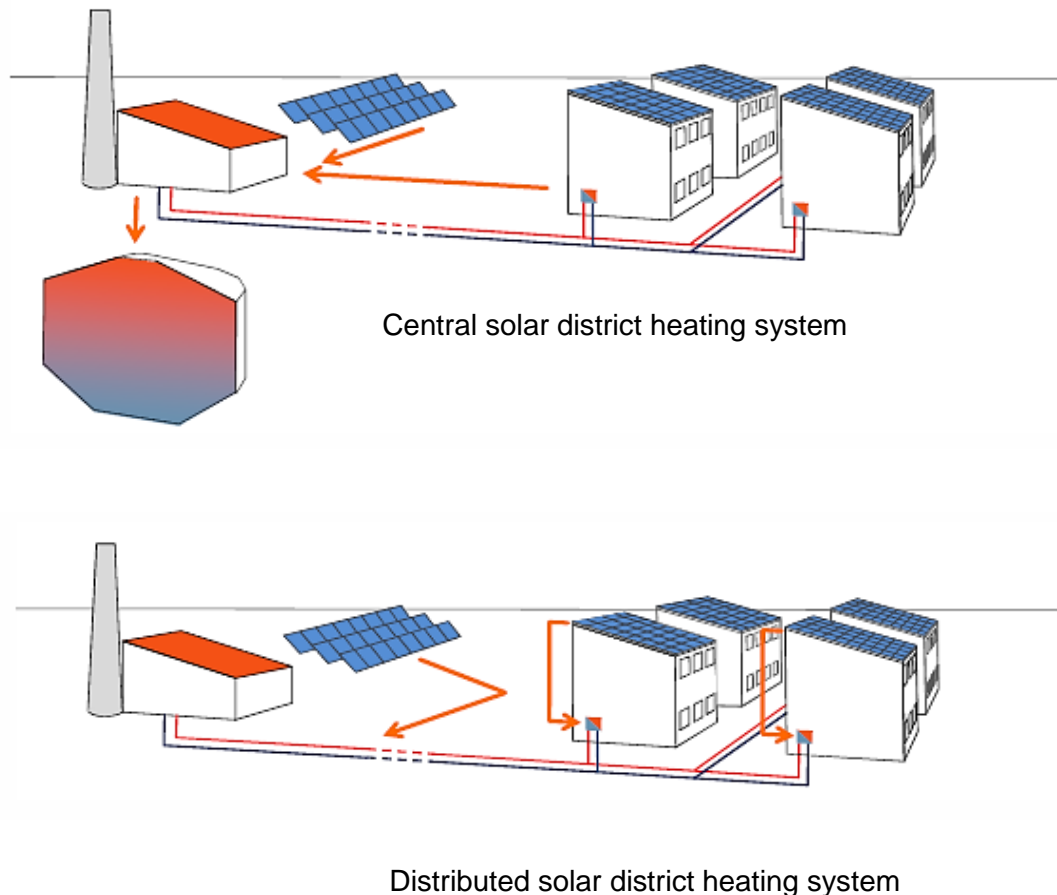


Figure 2-1: Categories of solar district heating systems: central district heating system with central solar feed-in and central energy storage as well as distributed district heating system with distributed solar feed-in (data source: SDH (2012))

Distributed solar district heating systems are characterized by ground mounted or roof-top mounted solar collector fields installed at suitable locations at any place in the district heating network. The solar collector arrays are connected on-site to the primary circuit of the district heating system to directly feed in the solar heat. Based on the amount of solar heat compared to the total load the district heating grid is utilized as a storage in some cases or decentralized solar energy storages are applied. Large distributed solar district heating plants operate with large solar collector fields feeding the solar heat directly into the heating grid without buffering. In case of solar block heating plants net-metering of solar heat coming from the collector fields on top of the connected building is applied.

In general the configuration of the solar thermal collector area, the layout of the district heating grid (i.e. the number of lines), and the design of the central heat

storage system depend on the technical frame conditions of the district heating system (i.e. the thermal capacity of the boilers, the connected heat load, the length of the heat distribution network, the operating mode of the district heating grid, supply and return temperature level), the economic constraints (i.e. the budget for investments, the fuel costs, planned operation and maintenance costs), and the required rate of solar fraction for the total year or the solar fraction during summer months (see Streicher et al. (1999) and Heimrath et al. (2002)).

In the following subsection an overview of the main components of solar-assisted biomass district heating systems is given.

2.1.2 Overview of main components of solar-assisted biomass district heating systems

In general a solar-assisted biomass district heating system comprises the following main components:

- A central heating station or a heating plant for heat generation by combustion of a secondary energy carrier, which is the result of thermo-chemical, physical-chemical or bio-chemical conversion of organic matter. For detailed energy conversion processes and technologies based on biomass please refer to Kaltschmitt, Hartmann & Hofbauer (2009).
- A heat distribution network to connect the heat production units (heating station, solar thermal system) with the heat consumers. Usually the heating grid is built by water-filled pipes, where the circulating water serves as a heat transfer media.
- A set of consumer heat sub-stations, which are the interfaces between the heat distribution network and the internal hydraulic installation of the connected dwelling units, of the connected residential buildings, official buildings, office buildings or even of industrial buildings supplied by district heat. The consumer heat stations work as a heat exchange unit to transfer the required thermal energy supplied by the district heating network to the secondary heating installation of the respective heat consumer.
- A solar thermal system comprising a specific area of solar collectors and usually a thermal energy storage system. By solar collectors solar radiant energy is transformed into heat, which is fed into the thermal energy storage via a heat exchange unit. The type of solar thermal system is determined by

the concept for solar heat storage and the energy service the solar radiant energy is utilized for. Depending on the load management concept of the district heating system central thermal energy storages could also be used as a buffer for load compensation in order to increase the security of heat supply in the district heating system (see Fink et al. (2007)).

For detailed explanation of the main components of a solar-assisted biomass district heating system please refer to the following sub-chapters.

2.1.3 Central heating station

In the frame of a biomass district heating system the central heating station is realized as a pure heating plant or as a cogeneration plant utilizing the energy content of a biomass based secondary energy carrier by combustion. In contrast to cogeneration plants heating plants convert the energy content of a biomass-based fuel into thermal energy for the purpose of heat generation only. The thermal energy, which is released by the combustion of solid, liquid or gaseous fuels, is transferred to a heat carrier like steam or water within a boiler unit.

As the furnace technology for the boiler depends on characteristics of the used fuel, the central heating stations of Austria's biomass district heating systems are for the predominant part based on woody biomass-fuelled hot water boilers. Due to the fact, that the share of alternative solid biomass fuels like straw or other residues from agriculture to be fired in an Austrian heating plant is about 5% (see Stockinger & Obernberger (2005), page 170), hereafter heating stations directly combusting woody biomass fuels are described in more detail.

A central heating station includes the technical equipment for fuel supply and energy conversion in a biomass district heating system (see Figure 2-2). Depending on the kind of solid biomass, the fuel supply system comprises a fuel storage and a device (i.e. a loader or a crane) to manipulate the woody biomass fuel. Typical combustibles are bark or waste wood, forest wood chips made out of forest residues or chopped wood logs, wood chips produced by chopping industrial wood, waste wood from woodworking industry or residues from saw mills, saw dust or wood pellets. The specification of biomass fuels is regulated by international standards and national regulations, which foresee a classification according to the fuel's water content, its density and its ash content. For wood chips and wood pellets also the particle size is of importance in this context.

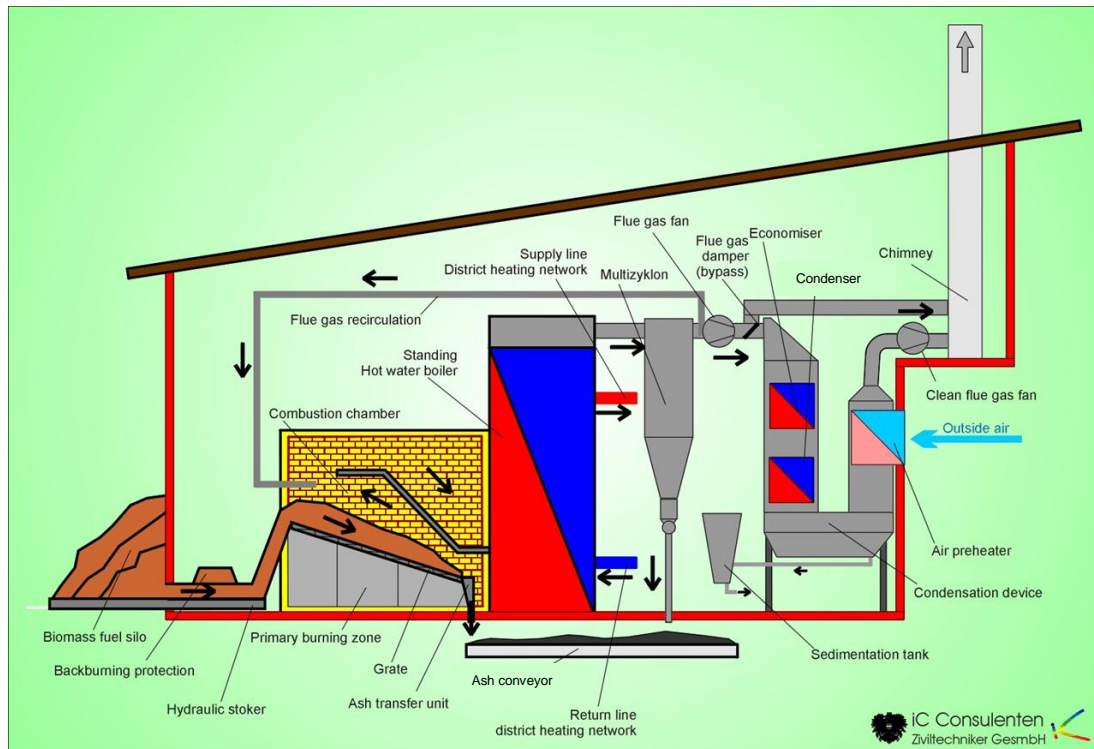


Figure 2-2: Typical scheme of a central biomass heating plant (data source: Ortner (2010))

For energy conversion a typical central heating plant comprises the following technical components (see Stockinger & Obernberger (2005), page 175 as well as Ortner (2010)):

- A dedicated firing technology based on the applied biomass fuel. It comprises a fuel transport system, an automated fuel-fed firing system comprising furnace and boiler, an ash removal facility, a dust separator for flue gas cleaning, and a heat recovery unit usually implemented in the exhaust gas condenser.
- A second combustion unit with boiler usually fueled with fuel oil or natural gas. This second boiler serves as a back-up, as further heat source to cover peak load and as an alternative boiler for heat load outside the heating period.
- A hydraulic system for the energetic and hydraulic interconnection of heat producing units (i.e. biomass boiler, peak load boiler, heat recovery system), heat storage (i.e. buffer storage tank) and heat distribution units. Furthermore it is the task of the hydraulic system to supply the respective

units (i.e. back burning protection, water treatment, condenser cleaning, etc.) inside the heating station with water.

- An electric system for electricity supply of water pumps, fire ventilation systems, flue gas fan, control and monitoring systems as well as for the lighting system.
- A heating house including boiler room, control room, pump room, ash removal unit and fuel transport unit and infrastructure facility like access roads and storage space.

Table 2-1 gives an overview of the most important types of automatically fired biomass combustion systems, which are applied in heating plants for district heating or for industrial heat production. The furnaces are generally equipped with an automated mechanic or pneumatic fuel-feeding system.

Table 2-1: Most important types of biomass-fired combustors with automated fuel-feeding system, as well as respective fuel types with related ash and water content (data source: Kaltschmitt, Hartmann & Hofbauer (2009), page 494)

Type of combustor	Range of fuel power input (Q'_{NCV}) [MW_{NCV}]	Type of biomass fuel	Ash content [% dm]	Water content [% w.b.]
Fixed bed or grate combustors:				
Underfeed stocker	0.01 - 2.5	wood chips, wood pellets	≤ 1%	5% - 50%
Furnace with lateral fuel-feeding	0.05 – 60.0	any kind of woody biomass fuel	≤ 50%	5% - 60%
Spreader stocker	0.006 – 0.06	wood pellets		≤ 20%
Fluidized bed combustors:				
Bubbling (stationary) fluidized bed combustor	5 - 50	any kind of fuel with softening temp. of ashes > 1000 °C; particle size < 100 mm		5% - 60%
Circulating fluidized bed combustor	30 – 100	any kind of fuel with softening temp. of ashes > 1000 °C; particle size < 60 mm		5% - 60%
Pulverized biomass combustors:				
Furnaces with pneumatic fuel injection	0.5 - 10	particle size: 1 – 4 mm		< 20%

Type of combustor	Range of fuel power input (Q'_{NCV}) [MW_{NCV}]	Type of biomass fuel	Ash content [% dm]	Water content [% w.b.]
Dust combustors for co-firing with fossil fuels	tot: 100 – 1000; max. share of biomass: 10 %	wood: particle size < 2 – 4 mm; straw: particle size < 6 mm; miscanthus: particle size < 4 mm		< 20%
<i>Explanations: MW_{NCV} ... Fuel input power in Megawatt referred to net calorific value of fuel; % w.b. ... percentage rate referred to wet basis; % dm ... percentage rate referred to dry matter</i>				

To transfer the thermal energy released during the combustion process to the circulating heat carrier medium, a heat exchange unit, the so-called boiler is placed in the off-gas stream after the firebox. The more thermal energy can be transferred to the heat carrier such as water, steam or thermo oil, the better is the boiler efficiency.

Firing systems in heating plants for district heating systems are usually combined with hot water boilers, which are available as so-called water-tube boilers or as fire-tube boilers. In a water-tube boiler the water circulates in tubes heated externally by hot flue gas coming from the firebox, while in a fire-tube boiler hot flue gases from the firebox pass through one or more tubes running through the heat carrier fluid. However, the most commonly used type of boiler for biomass fired furnaces is the fire-tube boiler, which is applied in small- or mid-sized applications as three tube line boiler (see Kaltschmitt, Hartmann & Hofbauer (2009), page 523).

An example scheme of the hydraulic layout for district heating plant is shown in Figure 2-3. It uses a buffer tank for heat load compensation and a flue gas condenser with economizer for heat recovery. This hydraulic scheme has the advantage of high controllability in case of unstable load behavior of the system and the disadvantage of high investment costs and high costs for auxiliary electricity. In addition to the two-pipe heating network a third pipe for low temperature return flow is used in combination with the condenser.

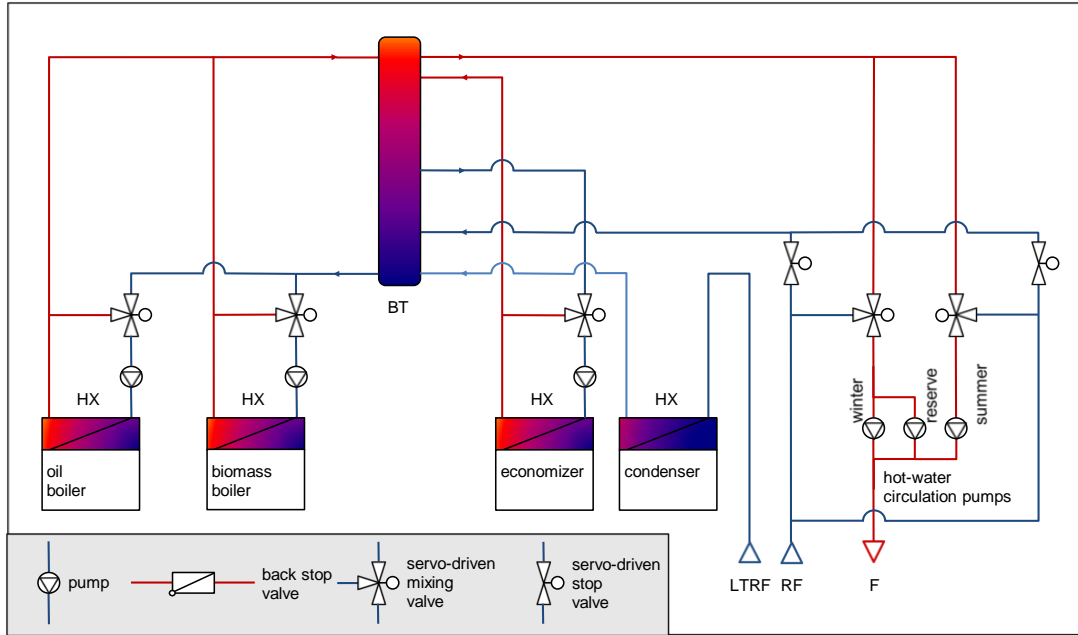


Figure 2-3: Example hydraulic scheme of a district heating plant comprising a biomass boiler, a peak-load oil boiler, a flue gas condenser with economizer and a buffer tank (data source: Stockinger & Obernberger (2005), page 191). There is one hot-water circulation pump for winter operation, one for summer operation and one for reserve.

*Explanations: BT ... buffer tank for heat load management;
HX ... heat exchanger;
LTRF ... low-temperature return flow of cold water;
RF ... return flow of cold water from load;
F ... flow of hot water to load;*

The design of the hot-water circulation pumps with respect to mass flow and operating pressure depend on the pressure rating in the heating network, the heat demand of the connected heat clients and the difference in water temperature between outward flow and return flow (see Stockinger & Obernberger (2005), page 189). In mid-sized heating plants a dedicated circulating pump for operation during the heating period in winter and a second pump for summer operation are the custom. Due to operational safety of heat supply a redundant circulation pump is installed as a reserve.

2.1.4 Key figures for central heating stations

As a main component in a district heating system the central heating station becomes important when assessing the efficiency of energy conversion and the related cost effectiveness of this unit. According to Stockinger & Obernberger (2005) centralized heating stations and the applied boilers can be characterized by the annual boiler utilization ratio ($\zeta_{boiler,an.}$),

$$\zeta_{boiler,an.} = \frac{Q_{th,boiler,an.}}{Q_{NCV,an.}} \quad [1] \quad \text{Equation 2}$$

$Q_{th,boiler,an.}$... annual amount of heat provided by the boiler [kWh_{th}/a]
 $Q_{NCV,an.}$... input of fuel energy with respect to the net calorific value [kWh_{NCV}/a]

the nominal power hours of the boiler (NPH_{boiler}),

$$NPH_{boiler} = \frac{Q_{th,boiler,an.}}{Q'_{th,boiler,nom.}} \quad [h] \quad \text{Equation 3}$$

$Q_{th,boiler,an.}$... annual amount of heat produced by the boiler [kWh_{th}/a]
 $Q'_{th,boiler,nom.}$... nominal thermal power of a boiler measured at specific conditions [kW_{th}]

and the connected heat load per boiler output ($q'_{load,boiler}$):

$$q'_{load,boiler} = \frac{\sum_i Q'_{load,user,nom.,i}}{Q'_{th,boiler,nom.}} \quad [1] \quad \text{Equation 4}$$

$Q'_{load,user,nom.,i}$... nominal connected heat load of user i [kW_{th}]
 $Q'_{th,boiler,nom.}$... nominal thermal power of a boiler measured at specific conditions [kW_{th}].

The specific electricity demand of a district heating plant ($w_{el,HP,aux.}$) producing heat is described as the ratio of annual electricity demand of the heating station per annual heat production:

$$w_{el,HP,aux.} = \frac{W_{el,HP,aux.,an.}}{Q_{th,HP,an.}} \quad [kWh_{el} / MWh_{th}] \quad \text{Equation 5}$$

$W_{el,HP,aux.,an.}$... annual electricity demand of the heating station [kWh_{el}/a]
 $Q_{th,HP,an.}$... annual heat production of the heating station [MWh_{th}/a].

As stated by VDI2067, Blatt 40 (2012) the nominal efficiency of a boiler ($\eta_{boiler,nom.}$) can be described as the ratio of the nominal thermal power of the boiler ($Q'_{th,boiler,nom.}$) to the nominal fuel input power ($Q'_{NCV,nom.}$):

$$\eta_{boiler,nom.} = \frac{Q'_{th,boiler,nom.}}{Q'_{NCV,nom.}} \quad [1] \quad \text{Equation 6}$$

$Q'_{th,boiler,nom.}$... nominal thermal power of a boiler measured at specific conditions [kW_{th}]
 $Q'_{NCV,nom.}$... nominal fuel input power [kW_{NCV}].

The boiler efficiency of a boiler fired with solid biomass results from several types of losses: heat losses via the exhaust gas, heat losses due to radiation, convection

and heat transfer to the ambient air, incomplete combustion and heat losses via the ash. If the average annual efficiency of a boiler ($\eta_{boiler,av.}$) has to be determined for an average load situation including a maintenance period, guideline VDI 2067 recommends the following approach (see Ortner (2010) page 22):

$$\eta_{boiler,av.} = \eta_{boiler,nom.} \cdot \frac{f_p}{\left(\frac{h_{op}}{h_{fl}} - 1\right) \cdot q_b + 1} \quad [1] \quad \text{Equation 7}$$

q_b ... relative heat output (losses) during stand-by [1];
for a boiler fired with solid biomass with fan: $q_b = 14 \cdot (Q'_{th,boiler,nom.} / 1 \text{ kW})^{0.28}$
 f_p ... pollution factor for pipes of heat exchanger [1];
for heat exchangers of a biomass boiler: $f_p = 0.97$
 $\eta_{boiler,av.}$... nominal efficiency of a boiler (average boiler temperature is 70°C) [1]
 h_{op} ... stand-by and operation time within maintenance period [h]
 h_{fl} ... full load hours within maintenance period [h].

Further key figures considering the centralized heating station in connection with the heat distribution network and the heat consumers will be defined later on. The next section deals with another main part of a district heating system responsible for the distribution of heat.

2.1.5 Heat distribution network

In a district heating system or a block heating system several components are responsible for the distribution of the generated heat from the heat sources to the heat consumers. There is the district heating grid or micro-grid based on a specific type of pipes, which are laid in form of a radial, meshed or a ring network. A second type of pipe, sometimes referred to as solar pipe (see SDH (2012)), is used to connect the solar collectors with other components like the heat exchanger within the solar collector loop. The two types of pipes distinguished in a solar-assisted district heating system have to meet specific requirements according to their purpose in the district heating system or block heating system.

At heat client side the consumers' heating sub-stations or heat transfer units are classified as components for heat distribution. Further details will be explained in a separate sub-chapter. Inside the heating plant or heating station further facilities for heat distribution are installed. There are the circulating pumps, the water treatment and water refill unit and the pressure holding device, which are counted as relevant components (see Kaltschmitt & Streicher (2009), page 386).

The technical structure of a heat distribution network mainly depends on the arrangements of the connected buildings, the possibilities for transmission routes and house connections, the grid size and the number of heat sources (heating stations, collector fields) feeding heat into the grid (Kaltschmitt, Streicher & Wiese (2010), page 451). Besides building positions the route planning of a district heating network is based on the expected heat density and the routes of public roads.

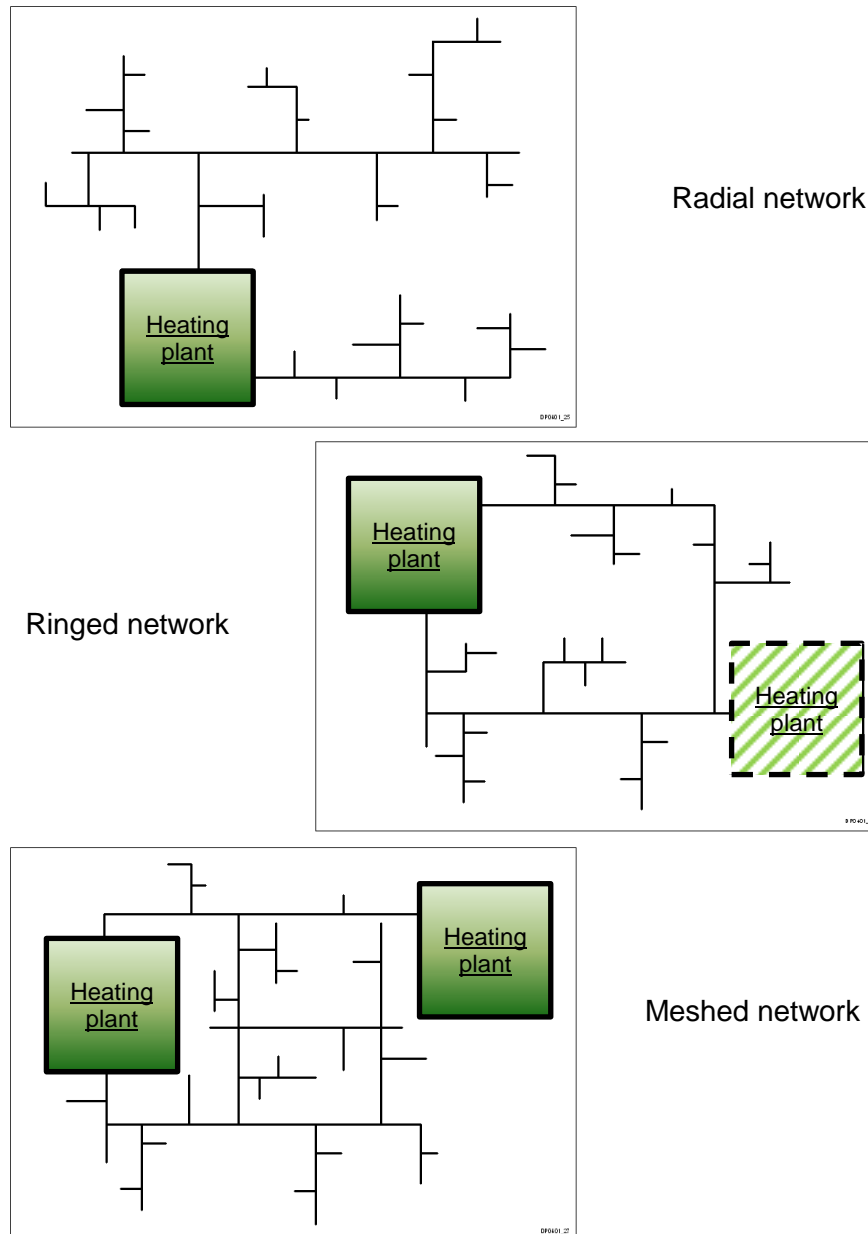


Figure 2-4: Main types of heat distribution networks for district heating systems: radial network, ringed network, and meshed network (data source: Kaltschmitt, Streicher & Wiese (2010), page 451, Zweiler (2011)).

As shown in Figure 2-4 three typical types of district heating systems are differentiated: radial networks, ringed networks and meshed networks. Radial grid systems are mainly applied in case of smaller district heating grids or micro grids. Due to its simple structure and short ways of pipes the building costs and the heat losses are low. Disadvantages of a radial system are the limited options for grid extensions because of hydraulics and a lower heat supply guarantee. In case of a grid failure the radial structured piping system must be turned off (see Zweiler (2011)).

Ringed network systems allow the incorporation of several heating stations and are typically applied in larger heat supply areas. Due to its pipeline route lengths and the nominal diameter of the used pipes the ring grid system needs higher investment costs and shows higher heat losses compared to radial grid systems. However, ring grid systems offer a higher heat supply guarantee and can be easily extended (see Zweiler (2011)).

Meshed network systems are a combination of radial and ringed grid systems. They offer an optimal heat supply guarantee and several possibilities to be extended if necessary. However, due to its increased pipeline lengths and its complicated structure it is only applicable in case of large heat supply networks or large-sized district heating systems including several heating stations. So the investment costs for such type of heating grid are relatively high and the expected operational costs may be above the average.

As stated by Zweiler (2011) the operating costs (costs for auxiliary energy, costs for grid losses, etc.) of a heat distribution network essentially influences the economic efficiency of a district heating system. Consequently the appropriate design of the piping system and an optimized layout of the lines will reduce heat losses in the grid system and will decrease initial investment costs for construction. Solar pipes as well as district heating pipes have to meet technical requirements serving the intended purpose and requirements for and economical operation of the piping system.

From a technical point of view requirements on thermal expansion, thermal insulation, on pressure and temperature conditions, on resistance to effects of the transported heat carrier fluid and on corrosion resistance have to be taken into account. From economic point of view the most important issues are the type of selected installation system, the network parameters (flow temperature, return flow

temperature, temperature difference, pressure rating), sizing, and the mode of operation for the heat distribution network.

According to Kaltschmitt, Streicher & Wiese (2010) the mainly applied installation type for district heating systems are above ground installed pipelines as well as pipelines passed within ducts or directly within the ground (see page 451). Common installation systems are rigidly pipe systems (e.g. pre-insulated (bonded) pipes) or flexible pipe systems (metallic service pipes, polymer service pipes), which can be combined with each other by taking into account the individual installation system parameters (see SDH (2012)). For direct, earth laid pipelines pre-insulated bonded pipes are typically used for the main and distribution lines in radial network systems principally installed in form of horizontal and parallel routes. Usually in modern piping systems the lines are equipped with a leakage detection system during installation.

In radial grid systems, which are mainly applied in small-scale or mid-sized district heating systems or in block heating systems, flow and return pipe temperature are dimensioned symmetrically. One or more routes run from the heat supplier to the consumers' heating sub-stations, while the pipes' diameter decreases in accordance to the decrease of heat demand.

In general the essential nominal diameter of the piping system's segment can be assessed by knowing the temperature deviation and the heat demand of the respective operating part. As a guideline the loss of pressure is nominated with 2 mbar/m of pipe (4 mbar/m of route) for pipes made of steel (see SDH (2012)). For the final house service pipe both the heat demand for space heating during heating period and the corresponding temperature difference as well as the heat demand for summertime and its resulting temperature deviation have to be considered separately.

The most important network parameter influencing the design of the piping system is the flow pipe temperature. In small sized heat distribution networks the flow pipe temperature is typically set to 90 °C, while in heating grid systems with larger extension 110 °C are used (SDH (2012)). The minimum flow temperature (e.g. during summertime) has to exceed 70 °C in order to avoid Legionella for domestic hot water processes.

The temperature of the return flow pipe in district heating systems is set to a maximum of 40 – 45 °C in case of space heating or to 50 – 55 °C in case of

domestic hot water preparation. As a general rule it is mentioned by Zweiler (2011), that the lower the return temperature is, the more efficient the district heating system or block heating system works. Zweiler (2011) recommends a high temperature difference between flow and return temperature level and a small water flow rate at the same thermal power. If the mass flow rate is kept low, circulating pump operation and the related consumption of electricity can be reduced.

In small-scale heat distribution networks like solar-assisted biomass micro-grids or solar-supported block heating systems nominal flow temperature and minimum flow temperature are set on a lower level. In Heimrath et al. (2002) the recommended flow temperature for solar-assisted reference biomass heating systems with a connected heat load below 600 kW_{th} is 85 °C during heating period and 65 °C in summertime. Depending on the connected type of consumer heating sub-station or apartment heat transfer unit (i.e. directly or indirectly connected sub-station) the flow pipe temperature level for solar-assisted two-pipe micro-grids or small-scale district heating systems investigated by Fink et al. (2007) is set to 55 ° – 65 °C.

The lower the flow and return flow temperature in solar-supported biomass district heating systems during summertime, the higher the annual share of solar thermal energy covering the annual heat demand (see Streicher et al. (1999), page 18). Consequently the annual efficiency of the supporting solar thermal collectors and the solar fraction will be higher, if the temperature level in the grid is kept as low as possible.

Besides the temperature level of flow and return flow pipe the selected operating mode determines the economic operation of the district heating system. Heating plants and the corresponding boilers are dimensioned according the so-called heat duration curve. It represents the annual heat load caused by the connected heat customers and grid losses in the course of one year.

As shown by Figure 2-5 representing the annual heat duration line of a district heating system, a correct dimensioned biomass boiler in a two boiler heating station covers 85% of the annual heat production. According to Ortner (2010) the used biomass boilers should provide a nominal thermal power equal to 45% of the maximal total heat load in the district heating system. It should be operated for a minimum of 3000 – 3500 full load hours, while the recommended load level for heat generation plants stated by Zweiler (2011) are 4000 nominal power hours.

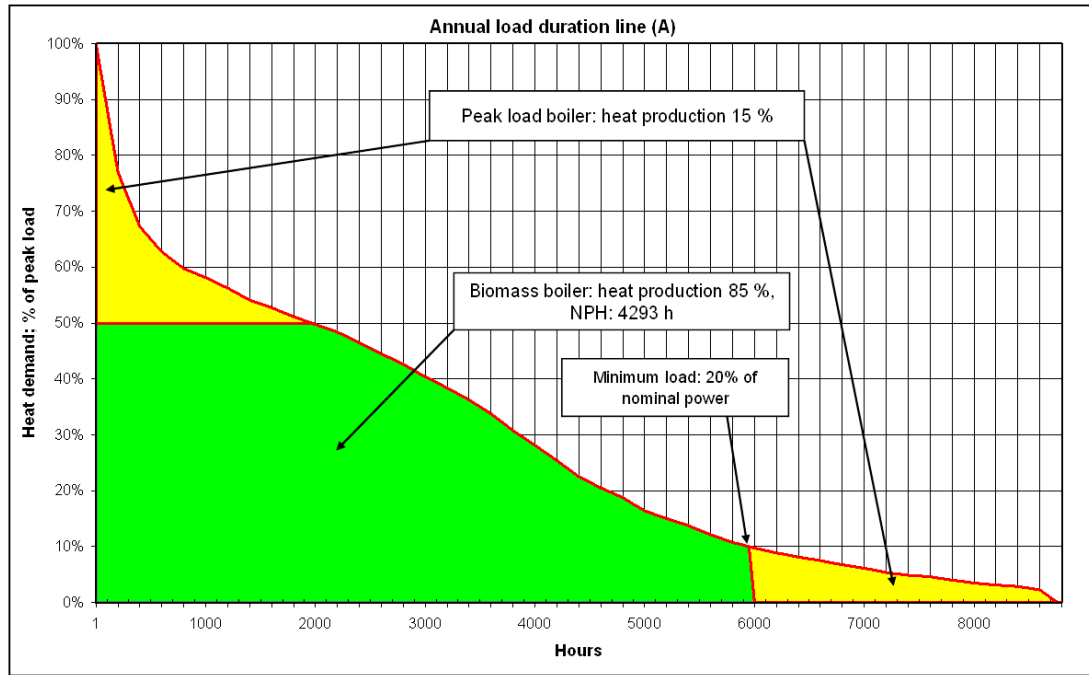


Figure 2-5: Example of an annual heat duration line of a district heating system with a correct dimensioned biomass boiler and a peak load boiler (data source: Zweiler (2011)). 85 % of the annual heat demand is covered by the biomass boiler within 4293 nominal power hours (NPH).

If heat for space heating and domestic hot water preparation is provided by the district heating system, the heat demand during summer time will decrease to about one fifth of the heat demand in wintertime (please refer to SDH (2012)). As stated by Streicher et al. (1999) about 5% of the total heat load can be assigned to domestic hot water preparation, while the other 15% has to be provided for covering of grid losses.

Such type of district heating grid will be operated in continuous mode during summer, if hot water must be provided 24 hours a day. In this case the operation mode of the flow pipe temperature is adapted by defining the required temperature level according to the outside temperature and the related heat demand in the district heating grid or micro-grid. Short-term fluctuations of heat load are controlled by an adjustment of mass flow in the piping system, i.e. by varying the delivery rate of the circulating pumps (see SDH 2012). This type of operation mode is typical for large-scale district heating systems and heating systems with a high level of connected heat load (see Heimrath et al. (2002), page 11).

Another mode of operation applied in heat distribution networks outside the heating period is the so-called intermittent operation. The heating system provides heat during defined time windows once or several times a day. The provided heat is used

to charge de-centrally installed short-term storage tanks for domestic hot water preparation or to heat up domestic hot water storage units located de-centrally in micro-grids of block heating systems. In small-scale systems it is also possible to deliver heat on demand, if one of the de-centrally connected storages needs to be charged.

In contradiction to the continuous mode the intermitted feed-in of heat into the heating grid reduced grid losses and electricity costs. Due to less transported water volume and the lower corresponding heat capacity of the total water mass in the grid this type of heating grid operation mode is put into practice in small-scale heating distribution grids with a low level of connected heat load (see Heimrath et al. (2002), page 12).

A further heating grid operation mode during summer time is the complete shut-down of heating system in case that no domestic hot water preparation has to be done. The heat clients are provided with heat for space heating during heating period only, while in summertime the heat consumers must prepare their domestic hot water by themselves. According Heimrath et al. (2002) biomass district heating systems operated that way are restricted to heating systems up to a connected heat load of 500 kW_{th} typically equipped with one single biomass boiler (see page 12).

Besides the adequate choosing of flow pipe temperature level and the optimal grid operation mode further measures could be taken in order to avoid heat losses in the heat distribution network, as especially with plants operated in summer month for domestic hot water preparation high grid losses can be expected. As mentioned by Zweiler (2011), there is a basic tendency, that a small amount of heat supply per length of piping system will cause higher heat losses compared to heating grid systems with a high amount of supplied heat per length of heating grid.

Consequently a high level of heat connection dense, a sufficient thermal insulation of pipes, plastic jackets to prevent the insulation from moistening and a leakage detection system installed in parallel to the pipelines will be further measures to reduce heat losses in the district heating grid.

As heat distribution networks are in a large part operated based on water-filled pipes, the level of operating pressure in the network influences the necessary effort for pressure stabilization, safety requirements and the construction of circulating pumps. The minimum pressure rating in the grid is determined by the network size and depends on the altitude difference between the highest and lowest point in the grid. The maximum operating pressure is influenced by the heat user with the

highest situated heating sub-station as well as by the consumer heat station at the end of the network. During standstill of the heat supply system this pressure rating is transferred to static pressure in the piping system.

The static pressure and the delivery head of the circulation pumps define the network's nominal pressure. According to SDH (2012) the maximal operating pressure has to be on a lower level than the nominal pressure rating. For the static pressure during standstill of the circulating pumps SDH (2012) recommends a pressure rating level higher than the saturated steam pressure at the highest geodetic point of the network at maximal flow pipe temperature. By keeping this rule evaporating fumes within the piping system will be avoided.

In addition to the effects on requirements and design of the heat distribution network the pressure rating in the district heating grid or micro grid influences the layout of consumer heating sub-stations directly served with hot water from the grid. As described in more detail in the following sub-chapter, the connection of heating sub-stations on heat client's side or heat transfer units in residential living units could be done directly or indirectly.

2.1.6 Consumer heat sub-stations

In a solar-assisted biomass district heating system consumer sub-stations are essential components to link the district heating system to the existing heating system operating within the building or house. In block heating systems applied to terrace houses and compact residential unit blocks (i.e. multistory residential buildings) de-centralized apartment heat transfer units are ideally suited to provide heat from small-scale district heating networks or micro-grids to the heat consumers living in row house units, a single apartment or a single dwelling. Consumer heat substations as well as apartment heat transfer units are available in standardized designs, various sizes and different connected load. They can be distinguished into directly connected sub-stations and substations with an indirect connection to the heat distribution network.

In a directly connected consumer heat substation or in a directly connected apartment heat transfer unit the heat transfer medium (i.e. water) from the district heating system can flow through the components of the heat distribution system installed within the respective house or building. There is no physical separation of the heat distribution network and the heating installations inside the supplied

objects. In most cases the temperature is simply controlled by adding cold water before usage.

The advantage of directly connected consumer substations or direct heat transfer units are lower forward flow and lower return flow temperature due to missing heat exchanger in the circuit. This fact supports the integration of solar thermal systems as a heat resource and reduces the costs compared to substations indirectly connected via a heat exchanger. Substations with a direct connection are mainly connected in new-erected block heating systems and micro grids (see Fink, et al. (2007)). Disadvantages of directly linked substations are the limitations due to pressure drop in the direct system configuration and the high risk of total system break down due to leakages on heat consumer side.

Consumer sub-stations with an indirect connection to the heat distribution network are characterized by a heat exchanger installed between the district heating grid on primary side and the heat distribution system on secondary side (i.e. within the respective building or house or within the supplied dwelling unit). Due to the physically separation of the heat transfer medium in the district heating grid and the heating fluid circulating in the heating circuit of the connected building or in the heating installation of the linked apartment or dwelling, the house heat distribution system or the apartment heating system is independent from the pressure conditions and the water properties in the district heating system (see Kaltschmitt, Streicher & Wiese (2010), page 452).

If an indirectly connected consumer substation fails or an apartment heat transfer unit is out of operation, the district heating system or block heating system will still be operated. Usually indirect connected heat substations and indirectly linked heat transfer units are installed in district heating networks or micro-grid with specific requirements on pressure drop. According to Fink, et al. (2007) indirect systems are mainly applied for the refurbishment of existing house heating systems or for district heating systems with large supply areas and long pipelines in the heat distribution network. New-build micro-grids or block heating systems are less important applications for indirectly connected consumer heat substations or indirect apartment heat transfer units.

Contrary to the advantage of a higher level of heat supply security in heat distribution networks with indirectly connected consumer heat substations, the integration of heat exchangers and more complicated temperature control devices make indirect systems less cost effective compared to direct systems (see

Kaltschmitt, Streicher & Wiese (2010), page 452). However, the efficient integration of solar thermal systems into indirect systems is more challenging, as higher flow and return temperatures in the heat distribution network have to be expected.

According to guideline VDI 2036 (2009) three types of domestic water heating systems are available for the integration with a district heating system:

- The continuous-flow system (CFS),
- the storage system (SS) with direct or indirect connection, and
- the storage charging system (SCS) with direct or indirect connection.

A continuous-flow system (CFS) for domestic hot water preparation heats the drinking water via a directly connected heat exchange unit in the moment the water is tapped. The cold water is heated in the heat exchanger via district heating water. As a result, instantaneous water heaters deliver a constant supply of hot water. The maximum hot water flow rate depends on the connected head load of the heat exchanger and the desired temperature level of the delivered hot water. Figure 2-6 shows an example of an instantaneous water heater with heat exchanger and flow compensated temperature controller.

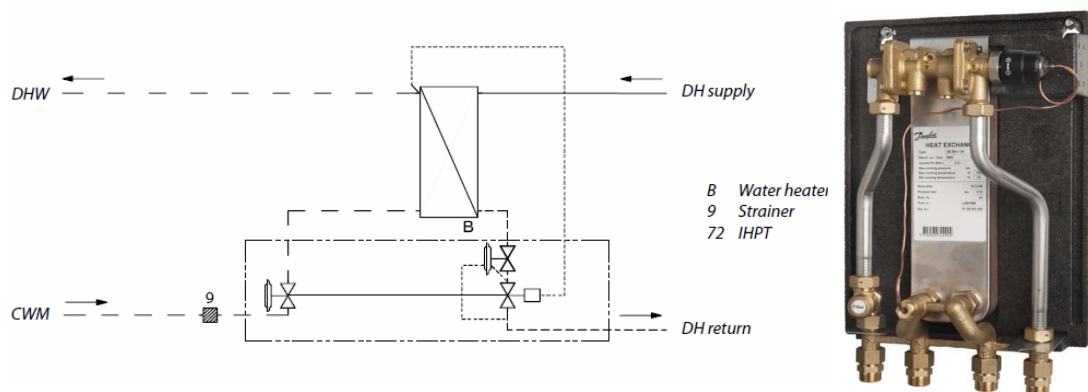


Figure 2-6: Circuit diagram example and image of an instantaneous water heater (data source: Danfoss TermixNovi (2012)). The substation for instantaneous water heating is designed for the use in one-family houses, apartments and small apartment buildings.

Explanations: DHW ... domestic hot water;
DH ... district heating;
CWM ... cold water mains;
IHPT ... flow-compensated temperature controller with built-in Δp controller

A storage system with direct connection to the district heating grid heats up the drinking water in a storage tank via an internal heat exchanger such as a pipe coil, which is flown through by the district heating water. Usually these storage heaters

are installed with a separate circulation connection for the drinking water supply on secondary side. Figure 2-7 gives an example of a substation for indirect heating and a primary connected storage system (cylinder with pipe coil). In case of a storage charging system with indirect connection combined with indirect space heating, the storage charging system is integrated into the secondary circuit of the substation's heat exchanger.

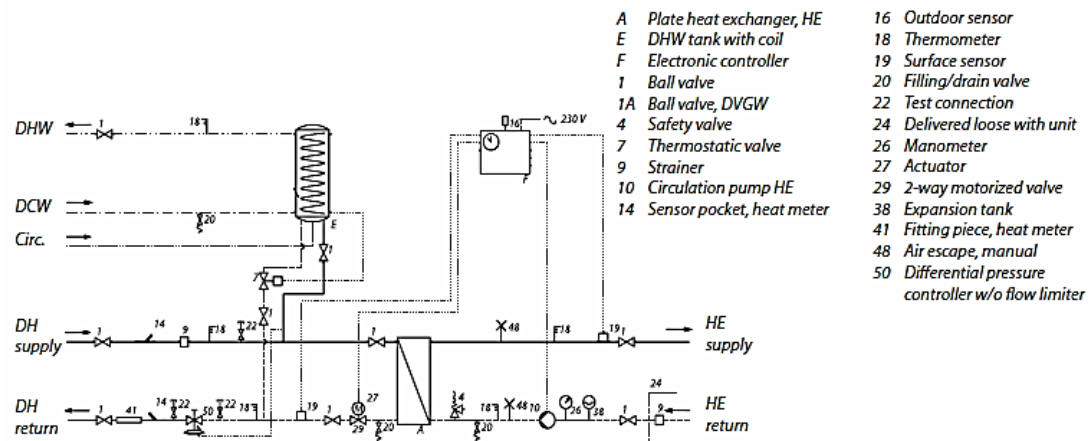


Figure 2-7: Circuit diagram example of a district heating substation for indirect heating with tank for DHW preparation (data source: Danfoss Termix BVX RO (2010)). The electronically controlled substation for indirect space heating with tank for domestic hot water preparation is designed for single-family houses or apartments.

Explanations: DHW ... domestic hot water;
DH ... district heating;
CWM ... cold water mains;
HE ... heating

Depending on the connected load standardized indirect consumer heat substation in compact design (16 – 90 kW_{th}) for the usage in micro or macro networks (see Figure 2-8) are available. However, these substations are designed for use in district heating networks in low temperature and also in high temperature range without incorporating the idea of a supporting solar thermal system.

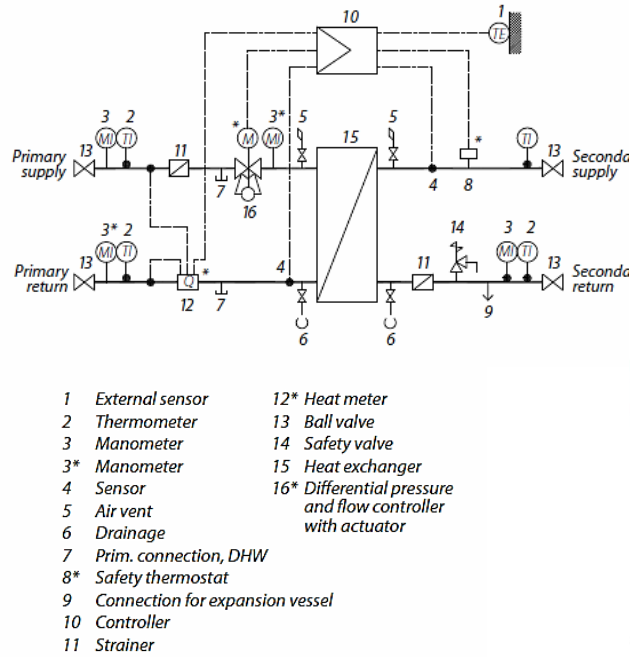


Figure 2-8: Circuit diagram example and image of an advanced district heating substation from 16 to 90 kW (data source: Danfoss DSA 1 MINI (2012)). The substation is designed for indirect connection to district heating systems in micro and macro networks.

Explanations: DHW ... domestic hot water

The heat distribution network and the consumer heating stations can be summarized to the district heating network connecting the heat producing resources with the heat consumers. In the following sub-chapter several key figures for district heating networks are explained in detail.

2.1.7 Key figures for district heating networks

From a technical point of view a heat distribution network is characterized by several key figures, which will be calculated out of a given set of known parameters defined for the grid. As stated by Ortner (2010) the total connected heat load in the district heating grid ($Q'_{load,grid,tot.}$) is the sum of the effective maximal heat load ($Q'_{load,max.,eff.}$) and the thermal power losses in the network (Φ'_{grid}):

$$Q'_{load,grid,tot.} = \underbrace{\sum_i (Q'_{th,user,nom.,i} \cdot f_u)}_{Q'_{load,max,eff.}} + \Phi'_{grid} \quad [kW_{th}]$$

Equation 8

$Q'_{th,user,nom.,i}$... nominal connected heat load of user i [kW_{th}]

f_u ... utilization factor [1]

$Q'_{load,max.,eff.}$... maximal effective heat load in the district heating grid [kW_{th}]

Φ'_{grid} ... thermal power losses in the district heating grid [kW_{th}].

Consequently, the utilization factor f_u , which is typically in the range of 0.5 up to 1.0, is the ratio of the effective maximal heat load in the heating network to the sum of nominal connected heat load of users. For the utilization factor $f_u(n)$ in small- or mid-sized district heating networks ($1 < n < 200$) Winter, Haslauer & Obernberger (2001) propose the following approximation (see page 12):

$$f_u(n) = a + \frac{b}{1 + \left(\frac{n}{c}\right)^d} \quad [1] \quad \text{Equation 9}$$

$f_u(n)$... utilization factor as a function of number of heat consumers [1]

$a = 0.449677646267461$

$b = 0.551234688$

$c = 53.84382392$

$d = 1.762743268$

n ... number of heat consumers

scope of application: $1 < n < 200$; $f_u(1) = 1$

For the thermal power losses per trench meter ($\varphi'_{hl,grid}$) of buried, parallel pipelines with a specific inner diameter, a specific type and thickness of insulation and known operation temperatures for forward and return flow of the heat transfer media (i.e. water) Obernberger (1997) uses the following approach (see page 7):

$$\varphi'_{hl,grid}(t_a) = S \cdot \lambda_E \cdot ((t_{FF}(t_a) - t_{ES}(t_a)) + (t_{RF}(t_a) - t_{ES}(t_a))) \quad [W_{th}/m] \quad \text{Equation 10}$$

$\varphi'_{hl,grid}(t_a)$... thermal power losses per unit length as a function of t_a [W_{th}/m]

S ... form coefficient for parallel running pipelines with a circular cross section [1]

λ_s ... heat transfer coefficient of the surrounding soil [$W_{th}/(m \text{ K})$]

t_a ... ambient air temperature [K].

$t_{FF}(t_a)$... forward flow temperature dependent on the ambient temperature [K].

$t_{ES}(t_a)$... temperature on earth's surface dependent on the ambient temperature [K].

$t_{RF}(t_a)$... return flow temperature dependent on the ambient temperature [K].

$$S = \left(\frac{1}{2} + \frac{1}{\pi} \cdot a \cdot \tan \frac{a \cdot \lambda_s}{h \cdot \lambda_{in}} \right) \cdot \frac{2\pi}{\frac{\lambda_s}{\lambda_{in}} \cdot \ln \frac{d_o}{d_i} + \operatorname{arccosh} \frac{2 \cdot h}{d_o}} \quad [1] \quad \text{Equation 11}$$

S ... form coefficient for parallel running pipelines with a circular cross section [1]

a ... distance of pipe's cross section centers [m]

h ... utilization factor [m]

λ_s ... heat transfer coefficient of the surrounding soil [$W_{th}/(m \text{ K})$]

λ_{in} ... heat transfer coefficient of the used insulation material [$W_{th}/(m \text{ K})$]

d_i ... inner diameter of pipe [m].

d_o ... outer diameter of pipe [m].

In order to assess the effectiveness of a heat distribution grid, two key parameters are in use indicating the load level. For the energy load level (ELL_{grid}) it is recommended to reach a value of 1200 kWh_{th}/m per anno at minimum (see Zweiler (2011)):

$$ELL_{grid} = \frac{Q_{th,useful,an.}}{l_{grid}} \quad [kWh_{th} / m] \quad \text{Equation 12}$$

$Q_{th,useful,an.}$... useful heat supplied and sold to the users per anno [kWh_{th}/a]
 l_{grid} ... length of grid in trench meter (including the connection lines) [m].

For an economical system operation the heat connection dense (HCD_{grid}) of a heat distribution grid should be at least at a level of 1 to 2 kW_{th}/m (see Zweiler (2011)):

$$HCD_{grid} = \frac{Q'_{load,grid,tot.}}{l_{grid}} \quad [kW_{th} / m] \quad \text{Equation 13}$$

$Q'_{load,grid,tot.}$... total heat load in the district heating network [kW_{th}]
 l_{grid} ... length of grid in trench meter (including the connection lines) [m].

According to Stockinger & Obernberger (2005) further indicators are the network allocation related to connected heat load of users (NWA_{HL}) and the network allocation with respect to the nominal thermal power of the boiler (NWA_{TP}) (see page 5):

$$NWA_{HL} = \frac{\sum_i Q'_{th,user,nom.,i}}{l_{grid}} \quad [kW_{th} / m] \quad \text{Equation 14}$$

$Q'_{th,user,nom.,i}$... nominal connected heat load of user i [kW_{th}]
 l_{grid} ... length of grid in trench meters (including the connection lines) [m]

$$NWA_{TP} = \frac{Q'_{th,boiler,nom.}}{l_{grid}} \quad [kW_{th} / m] \quad \text{Equation 15}$$

$Q'_{th,boiler,nom.}$... nominal thermal power of a boiler measured at specific conditions [kW_{th}]
 l_{grid} ... length of grid in trench meter [m].

The specific heat losses in the heat distribution network ($\phi_{grid,an.}$) are defined as the ratio of heat losses per year to length of the grid (see Stockinger & Obernberger (2005), page 5):

$$\varphi_{grid,an.} = \frac{\Phi_{grid,an.}}{l_{grid}} [(kWh_{th} / a) / m] \quad \text{Equation 16}$$

$Q_{th,feed-in,an.} - Q_{th,useful,an.} = \Phi_{grid,an.}$... amount of heat lost in the grid per year $[(kWh_{th}/a)]$
 l_{grid} ... length of grid in trench meter $[m]$.

The specific electricity demand of a district heating network ($w_{el,grid,aux.}$) distributing heat to heat consumers is described as annual electricity demand in the heat distribution grid in relation to useful heat supplied and sold to the users per anno:

$$w_{el,grid,aux.} = \frac{W_{el,grid,aux,an.}}{Q_{th,useful,an.}} [kWh_{el} / MWh_{th}] \quad \text{Equation 17}$$

$W_{el,grid,aux,an.}$... annual electricity demand for heat distribution in the heating grid $[kWh_{el}/a]$
 $Q_{th,useful,an.}$... useful heat supplied and sold to the users per anno $[MWh_{th}/a]$.

The annual grid utilization factor ($\varsigma_{grid,an.}$) is determined by dividing the amount of useful heat sold to the users ($Q_{th,useful,an.}$) by the produced heat in the heating station.

$$\varsigma_{grid,an.} = \frac{Q_{th,useful,an.}}{Q_{th,HP,an.}} [1] \quad \text{Equation 18}$$

$Q_{th,useful,an.}$... annual amount of useful heat supplied and sold to heat consumers $[MWh_{th}/a]$
 $Q_{th,HP,an.}$... annual heat production of the heating station $[MWh_{th}/a]$

Including the connected heat consumers two key figures can be defined (see Stockinger & Obernberger (2005), page 4), which represent a mean value per single heat consumer. The nominal power hours per heat consumer (NPH_i) and the average connected heat load per user ($Q'_{th,user,av.}$):

$$NPH_i = \frac{Q_{th,useful,i,an.}}{Q'_{th,user,nom.,i}} [h / a] \quad \text{Equation 19}$$

$Q_{th,useful,i,an.}$... annual amount of useful heat supplied and sold to heat consumer i $[kWh_{th}/a]$
 $Q'_{th,user,nom.,i}$... nominal connected heat load of user i $[kW_{th}]$

$$Q'_{th,user,av.} = \frac{\sum_i Q'_{th,user,nom.,i}}{i} [kW_{th}] \quad \text{Equation 20}$$

$Q'_{th,user,nom.,i}$... nominal connected heat load of user i $[kW_{th}]$
 i ... number of connected heat consumers $[m]$.

Besides the central heating station and the heat distribution network a further source for useful heat in the solar-assisted district heating systems are solar thermal

collectors. The following sub-sections deal with solar thermal collectors, solar pipes and thermal energy storages in more detail.

2.1.8 Solar thermal collectors

In a solar-assisted biomass district heating system besides the thermo-chemical conversion of biomass, solar radiant energy is utilized as a second renewable energy resource for generation of usable heat. Parts of the solar radiation energy can be converted into heat by a solar collector, which is a special kind of heat exchanger. In a solar collector the energy transfer is from a distant source of radiant energy to a fluid via an energy-absorbing surface, the so-called absorber. The absorber as part of the solar collector as well as other collector components and further necessary components like

- the heat transfer medium (i.e. the used solar fluid),
- the used pipes connecting the single parts of the system,
- the heat exchangers transferring heat from solar fluid to a second heat carrier like water,
- and the integrated pumps forcing a controlled circulation of solar fluid within this solar circuit

build up a solar thermal system. A control and monitoring system, as well as a heat storage unit make the solar thermal system complete, as solar thermal energy can be only harvested by day.

The basic principle of the energy conversion process taking place in solar collectors can be described as photo-thermal conversion (see Kaltschmitt, Streicher & Wiese (2010), page 123). If solar radiation either direct or diffuse solar radiation, incidence on material, a certain part will be absorbed. A part of the incident radiation is reflected on several boundary layers (e.g. air-to-cover junction or air-to-absorber junction) within the construction of a solar collector or it is absorbed in the collector's transparent cover. These losses are summarized as optical losses compared with thermal losses, to which the results of radiation emission effect, thermal conduction effect and thermal convection inside the solar collector are counted. In Figure 2-9 the different energy flows in a solar collector are shown, which influences the collector's efficiency when converting radiant energy to useful heat.

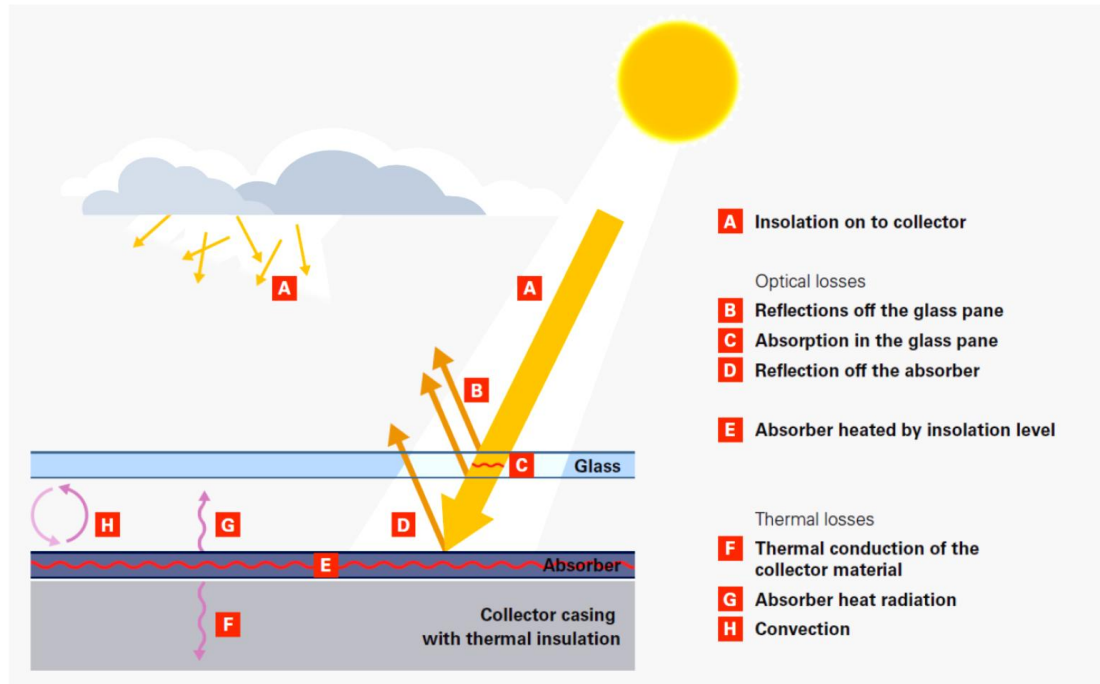


Figure 2-9: Principle of energy flows in a solar collector comprising a cover made of glass, an absorber and a collector casing with thermal insulation (data source: Viessmann (2009)). The incident solar radiation consist of the beam or direct radiation onto the solar collector and the diffuse radiation, which is scatter by air molecules in the atmosphere or reflected on clouds or particles in the atmosphere.

In steady state the solar collector's performance is described by an energy balance equitation. This equitation indicates the distribution of incident solar energy into useful energy gain and into thermal as well as optical losses (see Duffie & Beckmann (2006), page 239). The useful energy output of a solar collector with a defined area is determined by the difference between absorbed solar radiation and the losses. A collector removes the utilizable heat by a heat transfer medium (i.e. the solar fluid) flowing through the collector in fluid conduits. Consequently, the efficiency η_c of conversion of solar radiating energy into usable heat results from the ratio of useful thermal flow (Q'_{useful}) transported by the fluid to global radiation incident onto the collector (see Kaltschmitt, Streicher & Wiese (2010), page 128).

The total collector efficiency can be calculated with 3 parameters usually given by the collector's data sheet. With the so-called optical efficiency η_0 , and the 1st and 2nd order heat loss coefficient (a_1 , a_2) the efficiency expression is defined as a function of temperature difference ($T_m - T_a$) (see SDH (2012)):

$$\eta_c = \eta_0 - a_1 \frac{(T_m - T_a)}{G} - a_2 \frac{(T_m - T_a)^2}{G} \quad [1] \quad \text{Equation 21}$$

η_0 ... optical efficiency; maximum efficiency of the collector, if no heat losses occur [1]
 a_1 ... 1st order heat loss coefficient [$W / (K m^2)$]
 a_2 ... 2nd order heat loss coefficient [$W / (K^2 m^2)$]
 G ... total (global) irradiance on the collector surface (i.e. based on aperture area) [W / m^2]
 T_m ... mean collector fluid temperature [$^{\circ}C$]
 T_a ... temperature of ambient air [$^{\circ}C$].

The collector's thermal power output ($Q'_{th,col}$) can then be calculated as the product of collector efficiency (η_c), collector aperture area (A_{col}) and global irradiation G in plane of the collector's aperture area:

$$Q'_{th,col} = A_{col} \cdot \eta_c \cdot G \quad [W] \quad \text{Equation 22}$$

η_c ... total collector efficiency [1]
 A_{col} ... aperture area of collector [m^2]
 G ... total (global) irradiance on the collector surface (i.e. based on aperture area) [W / m^2].

For a more detailed calculation of the collector performance the share of direct and diffuse radiation, as well as the amount of irradiation reflected at the glass and absorber surface has to be considered. As direct and diffuse solar irradiation show a different reflecting behavior, a separate incidence angel modifier (IAM = K_{θ}) is applied. The IAM as a function of incident angle θ can be given as one of the following expressions (see SDH (2012)):

$$K_{\theta} = 1 - b_0 \cdot \left(\frac{1}{\cos \theta} - 1 \right) \quad [1] \quad \text{Equation 23}$$

b_0 ... constant provided by the manufacturer and/or test institute [1]
 θ ... incident angle on collector plane [$^{\circ}$]

$$K_{\theta} = 1 - \tan^p \left(\frac{\theta}{2} \right) \quad [1] \quad \text{Equation 24}$$

p ... constant provided by the manufacturer and/or test institute [1]
 θ ... incident angle on collector plane [$^{\circ}$].

Taking into account beam (direct) irradiation (G_b) and diffuse irradiation (G_d) and separate IAMs, the collector's thermal power output ($Q'_{th,col}$) can then be calculated as (see SDH (2012)):

$$Q'_{th,col} = A_{col} \cdot (\eta_0 \cdot (G_b \cdot K_{\theta} + G_d \cdot K_{60^{\circ}}) - a_1(T_m - T_a) - a_2(T_m - T_a)^2) [W] \quad \text{Equation 25}$$

η_0 ... optical efficiency [1]
 A_{col} ... aperture area of collector [m^2]
 G_b ... beam (direct) irradiation on collector plane (i.e. based on aperture area) [W / m^2]
 G_d ... diffuse irradiation (i.e. based on aperture area) [W / m^2]
 K_{θ} ... IAM for the incident angle at the given time step [1]

K_{60° ... IAM for diffuse radiation; average value of IAM at $\theta = 60^\circ$ is used for G_d [1].

While the optical losses of a collector are constant regardless of the temperature, losses due to convection to ambient air, long-wave radiation losses as well as thermal conductivity losses of the absorber can approximately be expressed in the collector's efficiency expression by a dependency on temperature difference between mean collector temperature and ambient temperature.

In Figure 2-10 an example of an efficiency expression is plotted as a function of temperature difference ($T_m - T_a$). The different colors illustrate optical losses, heat losses and the useful energy gain for a given irradiation level. With given material parameters the highest conversion efficiency is achieved, when the temperature difference between the absorber, the environment and the maximum radiation reaches its possible minimum (see Kaltschmitt, Streicher & Wiese (2010), page 128).

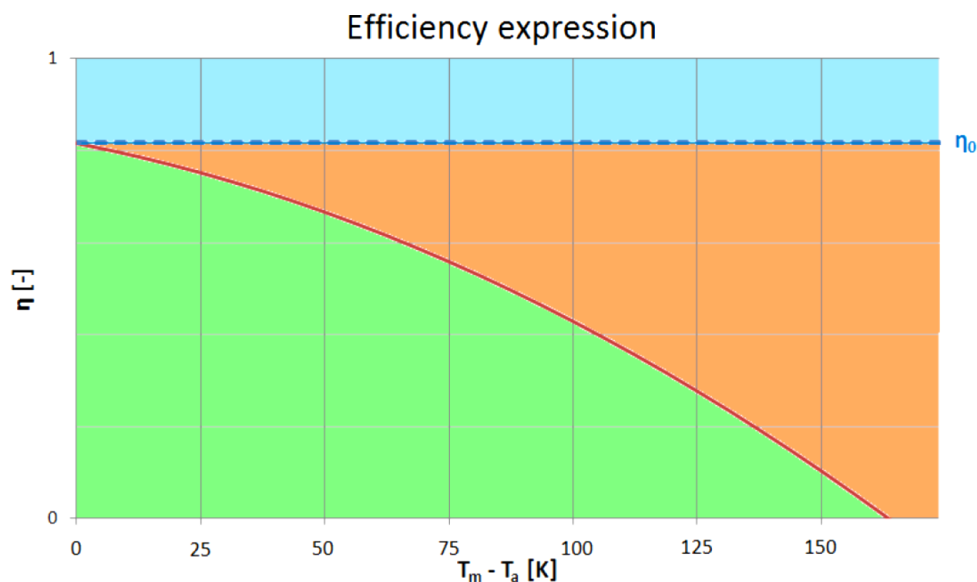


Figure 2-10: Example of a solar collector's efficiency expression (red line) displayed as a function of temperature difference between mean collector temperature and ambient temperature for a given irradiation level of 1000 W/m^2 (data source: SDH (2012)). For a defined temperature difference the colors indicate the ratio between optical losses (blue), heat losses (orange) and useful energy (green).

Explanations: η ... efficiency of a solar collector for an irradiation of 1000 W/m^2 [-];
 η_0 ... maximum efficiency in case only optical losses occur [-];
 T_m ... mean collector temperature [K];
 T_a ... ambient air temperature [K].

Besides the optical characteristics and the heat loss coefficients of the used materials the effectiveness of a solar collector is influenced by the flow rate of the

liquid or gaseous heat transfer medium removing the absorbed radiant energy from the absorber plate. On the one hand the efficiency of the collector will be high, if the flow is maximized and thus the collector's operating temperature is minimized. Consequently, collector heat losses will be lower as well. According to Duffie & Beckman (2006) the maximal useful energy gain can be achieved in a solar collector, if the whole collector is at the inlet fluid temperature (see page 265), as heat losses to the surrounding are at a minimum in this case.

On the other hand high flow rates require more pump power and larger pipe diameters, which would have a negative effect on the overall system efficiency of the solar thermal system. Moreover, there is a system specific upper limit with respect to mass flow rate in a collector in order to avoid erosion corrosion. In some collector types there is also a minimum level of mass flow required, as a uniform flow distribution in the absorber should be ensured. Usually the efficiency factors given in data sheets of solar collectors are based on standard test procedures executed beside other predefined conditions with a certain mass flow level (e.g. 0.02 kg/s per m² of collector area). However, the flow rate distribution in a solar collector depends on several construction details, fluid temperature as well as fluid viscosity and differs for each collector model.

The most common types of solar collectors used in solar-assisted biomass district heating systems are evacuated tubular collectors (ETC) and flat plate collectors (FPC). Both collector types are classed as non-concentrating liquid-type collectors (see Kaltschmitt, Streicher & Wiese (2010), page 134). Compound parabolic concentrators (CPC) combine the principles of flat plate collectors and parabolic through collectors, but the market share of this collector type is rather limited (see Weiss (2011), page 28). Other types, like concentrating collectors or uncovered collectors (i.e. simple absorbers) are either not applicable under Northern and Central European atmospheric conditions, since a large share of irradiation is diffuse. Furthermore these collectors are not sufficient since simple absorbers cannot provide the required operating temperature for domestic hot water preparation, space heating and process heat supply.

Flat plate collectors can utilize both beam and diffuse solar radiation and do not need tracking of the sun. Their mechanically simple design makes this type of solar collector reliable in operation and cost-saving in installation and maintenance. Typically an FPC consists of a collector box, the absorber, heat insulation and a transparent cover.

The absorber plate is made of copper, aluminum or stainless steel, which is simply painted black or is coated with a more sophisticated selective coating layer. In order to reduce the optical losses the transparent cover (made of glass or plastics) can have an anti-reflective coating. To minimize heat losses due to convection a so-called convective barrier between absorber plate and glass cover can be introduced. It reduces the circulation of air between the hot absorber and the colder glass cover.

Furthermore, flat plate collectors combining double anti-reflective glazing with gas filling of the collector box are in use. Figure 2-11 shows the typical components and construction details of a basic flat plate collector used for applications up to working temperatures of 80°C.

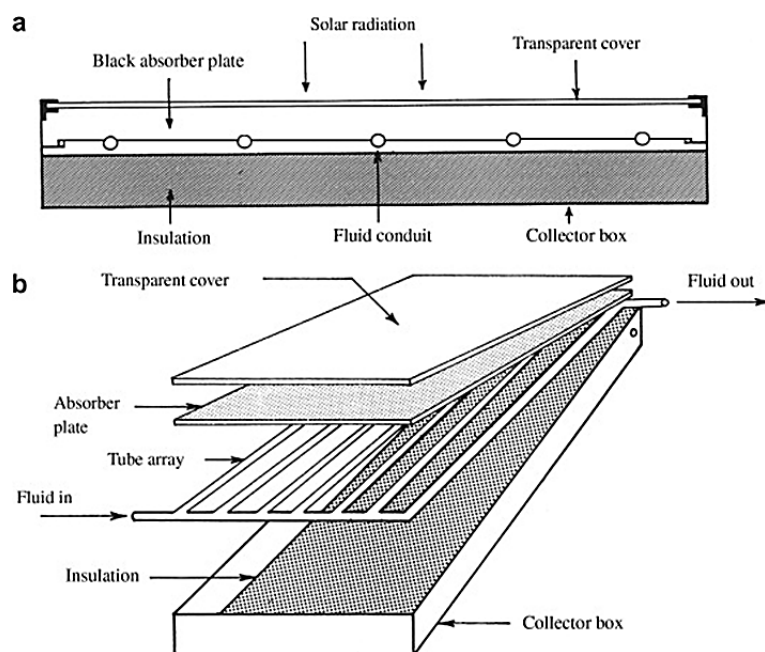


Figure 2-11: Principle design of a flat plate collector for applications with an operating temperature up to 80°C (data source: Sözen et al. (2008)).

Explanations: (a) ... cross-sectional view of a basic flat plate collector;
(b) ... isometric view of the basic design of a simple flat plate collector.

The tubes transporting the heat transfer fluid are fixed in close contact onto the absorber plate (e.g. by high frequency or ultrasonic welding). The piping can be either designed as a set of parallel tubes connected by a distributor and a collector pipe (i.e. manifold) in the absorber or as a single, bent tube in meander shape covering the whole absorber area. A parallel tube layout (harp absorber) is characterized by a high total mass flow, but a low temperature lift (high flow principle). In the latter case (meander tube) the mass flow is low, but the

temperature lift is high (low flow principle) (see Kaltschmitt, Streicher & Wiese (2010), page 133).

Evacuated tubular collectors (ETC) summarize a group of collector types, where long, narrow flat absorbers are mounted inside evacuated glass tubes (see Duffie & Beckman (2006), page 279). Conductive and convective heat losses are reduced to a minimum or are even eliminated by evacuating the space between the absorber and the tubular glass envelope. The three main concepts of vacuum tube collectors are shown in Figure 2-12.

Collector type (d) and (e) are based on the direct flow principle, where the heat transfer fluid flows directly through the absorber via a tube. Instead of co-axial direct flow (see type (d)) like in a single riser tube of a flat plate collector the liquid in the U-pipe type of evacuated tubular collectors runs through a single U-tube joining the two flow conduits (see type (e)).

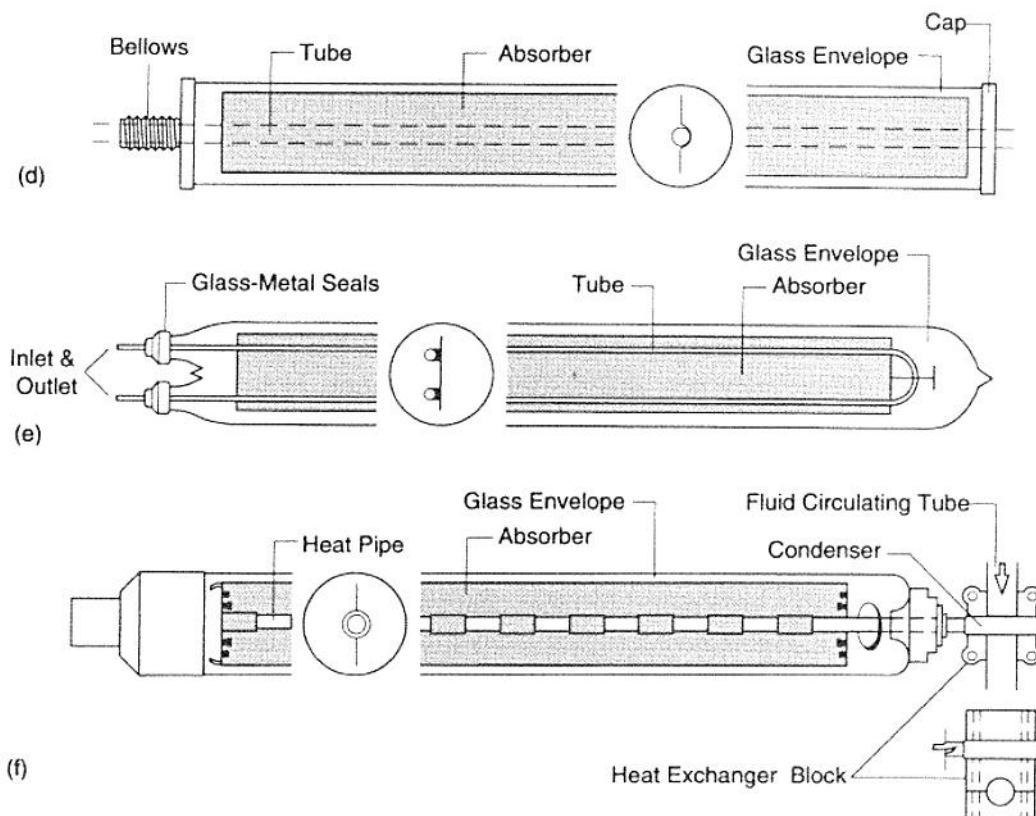


Figure 2-12: Principle designs of liquid heaters applied in evacuated tubular collectors (data source: Duffie & Beckman (2006), page 279).

Explanations: (d) ... evacuated glass tube with single metal fin and tube and glass-to-metal seals at both ends (direct flow principle);
 (e) ... evacuated glass tube with single metal fin and U-tube joining the two conduits. 2 glass-to-metal seals at the same end of the glass envelope (direct flow principle);

(f) ... heat pipe in contact with a metal fin in an evacuated glass tube. Only one seal at the end of the tube, so heat pipe and fin are free to expand inside the evacuated space.

In ETC type (f) shown in Figure 2-12 the heat is collected by means of the heat pipe principle. Inside each evacuated tube a small amount of fluid is sealed, which will be evaporated by the solar radiation energy converted in the absorber. After rising to the condenser, the vapor condenses and the latent heat of phase change is transferred to the circulating fluid in the header pipe via the heat exchanger block. Finally the condensed fluid runs back to the bottom of the heat pipe, where it is evaporated again. The different working principle of ETCs based on the heat pipe principle and ETCs based on the direct flow principle can be seen in Figure 2-13.

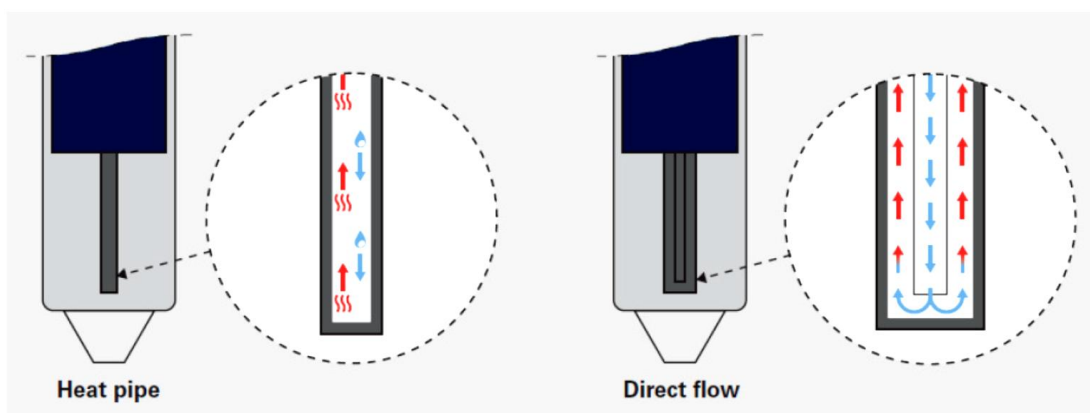


Figure 2-13: Heat pipe principle (left) and direct flow principle (right) applied in evacuated tubular collectors (data source: Viessmann (2009)).

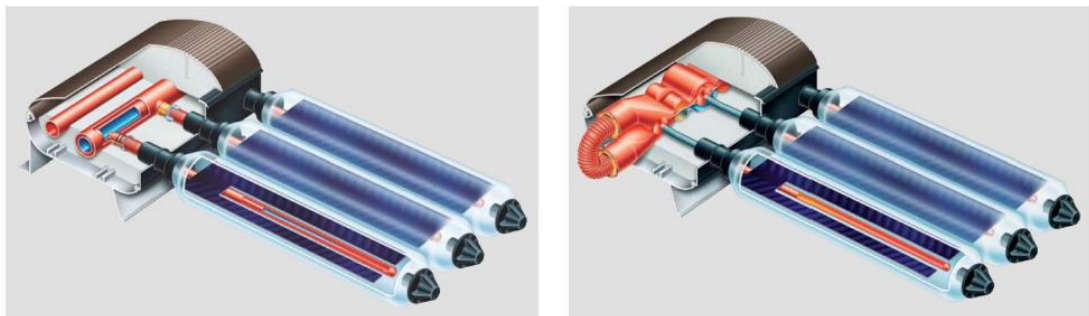


Figure 2-14: Manifold designs for evacuated tubular collectors based on direct flow principle (left) and heat pipe principle (right) and (data source: Viessmann (2009)).

The design of an evacuated tubular collector unit is characterized by a row of parallel glass tubes which are evacuated ($p < 10^{-2}$ Pa) in order to reduce conduction losses and to eliminate convection losses. The upper end of the glass tubes is connected to header pipes, which are available in various manifold designs (see Figure 2-14). In order to utilize a maximum of the incident radiation onto the ETC

unit concave mirrors, so-called CPC reflectors are placed behind the glass tubes. In this case in addition to the front side of the absorber plate also the back side requires a selective coated surface. In Table 2-2 representative parameters of two types of non-concentrating liquid-type collector designs are listed. The given efficiency expression constants for a global radiation of 1000 W/m^2 are indicative, as collector efficiencies may vary even within the same category of collectors.

Table 2-2: Efficiency expression constants for a global irradiation level of 1000 W/m^2 (with reference to the aperture area), collector working temperature and main application of one evacuated tubular collector and two flat plate collectors (data source: SDH (2012), Kaltschmitt, Streicher & Wiese (2010), Weiss (2011))

Name	Type of collector design	Optical efficiency (η_0) [-]	1 st order heat loss coefficient (a_1) [W / m ² K]	2 nd order heat loss coefficient (a_2) [W / m ² K ²]	Collector's working temp. range [°C]	Main application
ETC A	High performing ETC with selective surface	0.75	1.0	0.005	90° - 130°	DHW; SH; PH
FPC B	High performing FPC with anti-reflective coated cover and convection barrier	0.80	3.0	0.008	40° – 90°	DHW; SH
FPC C	Medium performing FPC with simple glass cover	0.75	4.0	0.010	30° - 80°	DHW

Explanations: ETC ... evacuated tubular collector; FPC ... flat plate collector; DHW ... domestic hot water preparation; SH ... space heating; PH ... process heat supply.

Due to its high collector working temperature the ETC type can be applied for space heating, cooling and process heat supply, while the typical application for an FPC is domestic hot water preparation and space heating. As displayed in Figure 2-15 the collector efficiencies based on the aperture area show a different curve behavior per collector type when plotted as a function of temperature difference between mean collector fluid and ambient air.

The efficiency of ETCs is significantly higher compared to FPCs at high collector temperatures. If the collector temperature is near to the temperature level of ambient air, the flat plate collector type's efficiency exceeds the collector efficiency of ETCs. However, due to the higher price-to-performance ratio of evacuated tubular collectors, the flat plate collector type shows better results with respect to the economic efficiency of solar district heating plants (see SDH (2012)).

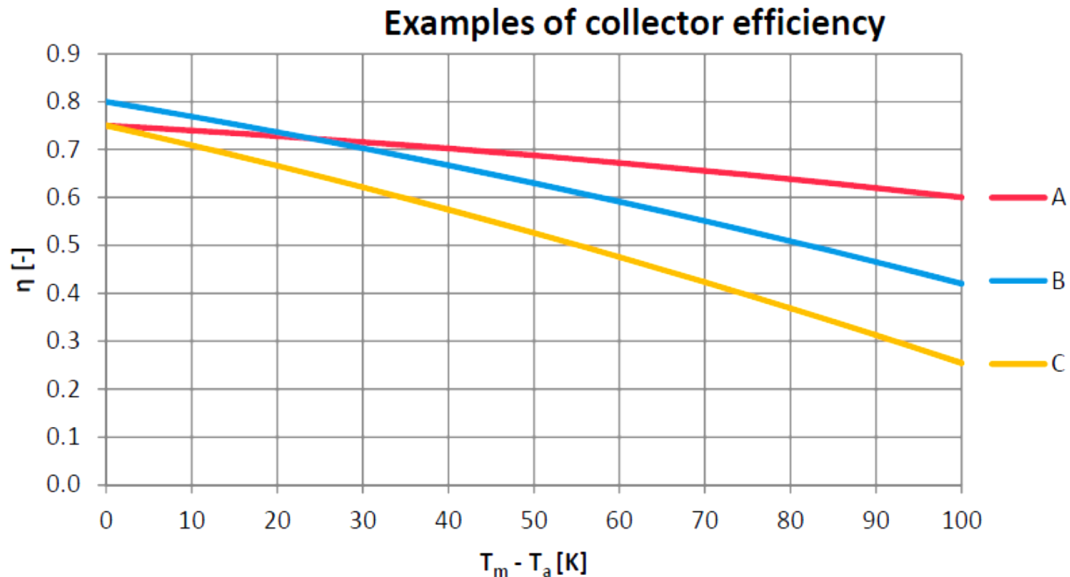


Figure 2-15: Examples of collector efficiency curves of three designs of non-concentrating liquid-type collectors (data source: SDH (2012)). The efficiency expression based on the aperture area is plotted as a function of temperature difference between collector fluid and ambient air at a solar irradiation level of 1000 W/m^2 on the collector plane.

Explanations: A ... High performing evacuated tubular collector with selective surface;
B ... High performing flat plate collector with anti-reflective coated cover and convection barrier ;
C ... Medium performing flat plate collector with simple glass cover.

For solar collectors three different area designations are in use as a reference unit in order to refer power output, energy yield or other performance details to a reference value. As shown in Figure 2-16 the definition of gross collector area, absorber area and aperture area depends on the type of collector. The gross collector area describes the external dimension of a collector unit as a result of lengths times the width. It is used for calculating the required roof area or the needed space for installation. The absorber area exclusively refers to the dimension of the absorbers active area. For circular absorbers the total area is counted, even though not the complete absorber is exposed to direct insolation.

The aperture area is the area of a collector, which takes part in the energy conversion as this is the maximum projected surface through which un-concentrated solar radiation can enter the collector. It is the usual standard variable for the definition of collector efficiency parameters. In case of flat plate collectors, the aperture area is equal to the visible part of the glass pane. In evacuated tubular collectors without reflectors the aperture area is defined as the total of the longitudinal cross-sections of all glass envelopes. For vacuum tube collectors with back-mounted reflectors the aperture area is defined by the projection of these mirror areas (see Weiss (2011)).

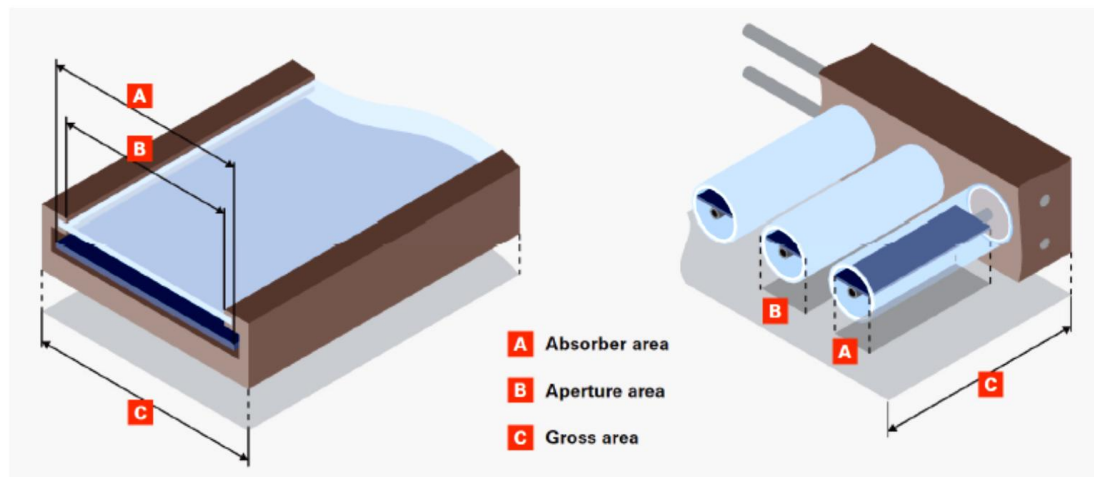


Figure 2-16: Definition of gross collector area, aperture area and absorber area for flat plate collectors and evacuated tube collectors (data source: Viessmann (2009)).

If the performance of two different solar collector designs is compared, it is necessary to use characteristic parameters (e.g. optical efficiency, 1st order heat loss coefficient, 2nd order heat loss coefficient) measured with respect to the same area designation. In the United States usually the instantaneous efficiency of a collector is determined as a function of the difference of inlet temperature (T_i) and ambient temperature (T_a) as well as a function of fluid flow rate referred to the gross collector area. In Europe the practice is to base the instantaneous collector efficiency on the difference between $T_{f,av}$, which is the arithmetic average of fluid inlet and outlet temperature (see Duffie & Beckman (2006), page 292), and T_a , which is the ambient temperature outside the collector. Together with the optical efficiency the determined parameters refer to the aperture area of the collector.

According to ESTIF (2007) the values of G , T_a and T_m have to be known at all time to calculate the annual energy output of the collector. While G and T_a are weather data defined by the location the collector is installed, T_m depends on several influencing

facts, like weather, connected heat load, design and components of the solar thermal system and the actual operating conditions at a given point in time.

Consequently a typical operation temperature in the collector must be assumed at a constant level in order to keep the calculation simple.

An annual energy output can be derived by integrating Equation 22 or Equation 25 over the period of one year. Assuming, that the collector loop will not be operated when the contribution is negative and the average fluid temperature in the collector is constant, the resulting annual energy output based on the thermal power output described in Equation 22 is:

$$Q_{th,an.} = \int_{year} [A_{col} \cdot (\eta_0 G - a_1(T_{m,const} - T_a) - a_2(T_{m,const} - T_a)^2)]^+ dt \quad [Ws] \quad \text{Equation 26}$$

A_{col} ... aperture area of the collector [m^2]
 η_0 ... optical efficiency; maximum efficiency of the collector, if no heat losses occur [1]
 a_1 ... 1st order heat loss coefficient [$W / (K m^2)$]
 a_2 ... 2nd order heat loss coefficient [$W / (K^2 m^2)$]
 G ... total (global) irradiance on the collector surface (i.e. based on aperture area) [W / m^2]
 $T_{m,const}$... mean collector fluid temperature at a given point in time [$^{\circ}C$]
 T_a ... temperature of ambient air [$^{\circ}C$].

As recommended by ESTIF (2007) this simple approach to calculate the real collector output at a given location can be used to estimate the system output and the system savings, if a mean operating temperature in typical applications is defined. For a conversion of collector output to the system output and system savings conversion factors $F_{col-sys}$ and $F_{col-sav}$ have to be applied. Both, factor $F_{col-sys}$ and factor $F_{col-sav}$ take into account the losses in the solar system and the losses in the back-up system.

With the help of Figure 2-17 and Figure 2-18 a comparison of the annual energy output as a function of mean collector temperature (T_m) based on the collectors' gross area and based on the collectors' aperture area can be done. The displayed curves represent the annual energy yield achieved for a high performing ETC, a high performing FPC and a medium performing FPC investigated in the sections before. As the collector's aperture area can be much less than the gross area (i.e. the area corresponding to the collector's outer dimensions), the ETC shows a significant different curve behavior and an obviously lower energy yield at low mean collector temperatures when referring to gross collector area.

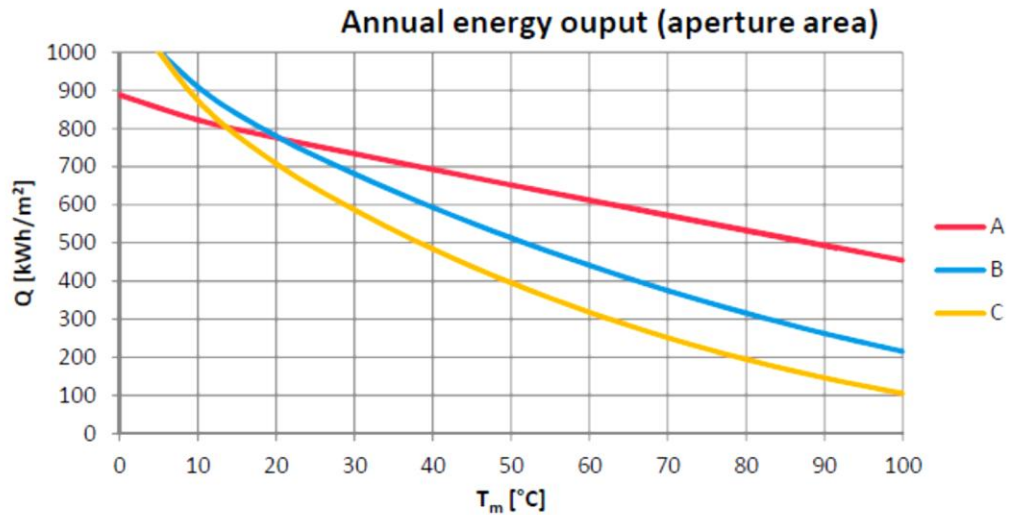


Figure 2-17: Annual solar output as a function of collector mean temperature (T_m) for the ETC and the two FPC characterized in Table 2-2 (data source: SDH (2012)). Energy output (Q) is given in kWh per m^2 collector aperture area and year

Explanations: A ... High performing evacuated tubular collector with selective surface;
B ... High performing flat plat collector with anti-reflective coated cover and convection barrier ;
C ... Medium performing flat plat collector with simple glass cover.

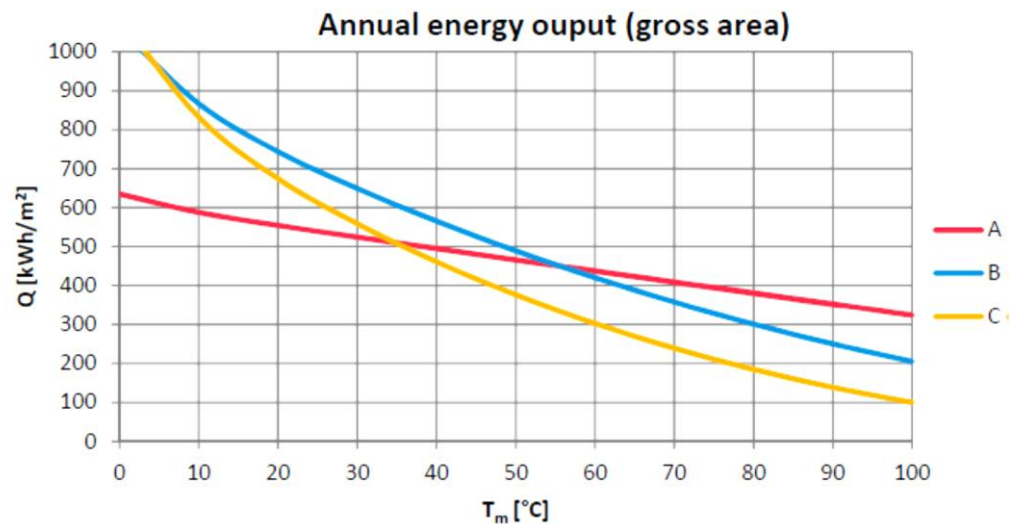


Figure 2-18: Annual solar output as a function of collector mean temperature (T_m) for the ETC and the two FPC characterized in Table 2 2 (data source: SDH (2012)). Energy output (Q) is given in kWh per m^2 collector gross area and year.

Explanations: A ... High performing evacuated tubular collector with selective surface;
B ... High performing flat plat collector with anti-reflective coated cover and convection barrier ;
C ... Medium performing flat plat collector with simple glass cover.

In the following section solar pipes and heat exchangers completing the solar collector loop are described.

2.1.9 Solar collector loop, solar pipes and heat exchangers

Most of the solar thermal applications in Northern or Central Europe are installed in combination with a heat exchanger (HX) between collector on the one side and district heating network or solar heat storage on the other side. Typically a circulation pump is pumping the solar fluid through the solar pipes. The solar pipes connect the components of the solar collector loop, forming the primary side of the heat exchanger. In forced circulation systems the collector circuit is actively controlled by a control device measuring the difference of temperature in the collector and the heat storage or the district heating system respectively.

Due to presence of the heat exchanger the collector is forced to operate on a higher temperature level than it otherwise would. Consequently, the collector's efficiency will decrease, when the mean collector temperature increases. So the selection of a well performing heat exchanger linking the solar heat to the heat storage or the district heating network is crucial for the overall plant efficiency (see SDH (2012).

Heat exchangers serve as a device to transfer heat from one media to another, while the two heat transfer media are physically separated (see Kaltschmitt, Streicher & Wiese (2010), page 146). They are distinguished into groups according their characteristics. There are parallel-flow and counter-flow as well as internal in contradiction to external heat exchangers. Based on their design they are also classed into shell and tube heat exchangers differentiated from plate heat exchangers.

In large solar systems normally counter-flow plate heat exchanger are used, but external heat exchangers are also available as shell and tube (for large systems) or coaxial heat exchangers (see Kaltschmitt, Streicher & Wiese (2010), page 147). Due to their limited size and their relatively low heat output internal heat exchangers in straight-tube, double-mantle or ribbed-tube design are more suitable to be applied in smaller units like domestic hot water tanks or buffer tanks for a one-family house.

The heat, which can be transferred from the primary side (i.e. solar collector loop) to the secondary side (i.e. heat storage, district heating network) depends on (see Kaltschmitt, Streicher & Wiese (2010), page 146):

- The temperature difference between the two media,
- the area of heat exchanger, and

- the type of heat transfer medium and its flow speed on both sides of the heat exchanger (i.e. the heat exchanger's heat transfer coefficient (UA)).

It is equal to the heat exchanger's heat transfer coefficient (UA) times the temperature difference (ΔT) between solar loop and secondary side.

The heat transfer medium used in the solar collector loop, also called collector fluid, has to meet several requirements due to the specific ambient conditions in Central and Northern Europe. The heat transfer medium should have (see Kaltschmitt, Streicher & Wiese (2010), page 145):

- A high specific heat capacity,
- a low viscosity,
- no freezing or boiling at operating temperature,
- non-corrosion in the conduit system,
- non-flammable,
- non-toxic and biologically degradable.

A mixture of water and antifreeze like glycol is the most commonly used collector fluid, even though the specific heat capacity is lower compared to pure water. In addition the mixture shows a higher viscosity and a reduced area tension. So it is one strategy to reduce the percentage of glycol in the mixture, while in case of minimum ambient temperature the collectors are operated in reverse operation mode by taking heat from the district heating network and heating the collectors. The pumps are activated when the temperature in the solar collector loop falls below a certain level of ambient temperature. So the annual efficiency of the plant due to lower viscosity and higher heat capacity is increased, while the collectors and solar pipes are prevented from freezing and damaging (see SDH (2012)).

Like the heat transfer medium used in the solar collector loop also the solar system piping have to meet requirements on functionality and resistance to the ambient conditions. On the one hand, the dimension of the pipes has to match the size of the used pumps in order to achieve the right flow corresponding with a temperature difference (ΔT) over the collector in the range of 25° to 45° Kelvin. On the other hand an increase of the pipe's diameter means an increase of piping costs, while the pressure loss and the corresponding pump power will decrease.

Furthermore, the setup of the collector area will influence the pressure drop in the collector field, which could be either collectors coupled in series or which are collectors connected in a parallel setup. Depending on the size of the solar thermal application either steel pipes or copper pipes are used. Since the pipes in the solar collector loop have to handle more thermal expansion and since they are exposed to much more fluctuating temperatures than the ordinary district heating pipes special measures have to be taken in to account (e.g. built-in lyre) to withstand stress in the pipe system (see SDH (2012)).

However, thermal losses will occur in the pipes of the collector circuit. Even though the collector circuit is insulated with materials like mineral wool, polyurethane-shells or foam rubber, 10% to 15% of the energy released by the collector field might be lost via the solar piping system (see Kaltschmitt, Streicher & Wiese (2010), page 146). Thermal insulation is also relevant for thermal energy storages described in the next section.

2.1.10 Thermal energy storages

In solar thermal systems the thermal energy storage is an essential component. As solar energy is a time-dependent energy resource, the system performance of a solar thermal system strongly depends on the availability to store the captured solar gains for utilization at a different point in time. The main reason is that the storage of thermal energy in dedicated storage systems enables to cope with the deviation of solar heat production during the course of one day, several days or even of a year (SDH 2012). According to Duffie & Beckman (2006) the optimum capacity of an energy storage system depends on several parameters when investigating solar energy processes (see page 376):

- The expected time dependence of solar radiation availability,
- the nature of loads to be expected on the process,
- the degree of reliability needed for the process,
- the way, auxiliary energy is supplied, and
- the economic conditions determining the share of the annual load carried by the solar energy resource.

Consequently, the choice for the right type of storage media according to the nature of process applied and the solar process's dimensioning essentially influences the solar fraction to be achieved by the solar thermal system.

As stated by Duffie & Beckman (2006) the energy storage capacity of a storage unit at uniform temperature (Q_s), which is filled with fully mixed or unstratified water or other liquid, operating over a finite temperature difference is given by (see page 379):

$$Q_s = (m \cdot c_p)_s \Delta T_s \quad [J] \quad \text{Equation 27}$$

Q_s ... total heat capacity for a cycle operating through the temperature range ΔT_s [J]
 m ... mass of water (or liquid) in the storage unit [kg]
 c_p ... specific heat of water (4.1855 J/(g·K)) or liquid serving as storage medium [J/(kg K)]
 ΔT_s ... temperature range over which such storage unit can operate [K].

The maximal energy storage capacity $Q_{stor.,max.}$ of a water-filled storage tank within a defined period of time (e.g. one year) can be calculated according to Equation 28. When the volume of the storage tank, the specific heat capacity of the storage medium, the density of the storage medium, as well as the maximal and the minimal temperature in the storage tank during the operating period are known, the maximal energy storage capacity can be calculated to (see Raab (2006), page 7):

$$Q_{stor.,max.} = V_{stor.} \cdot \rho_{H_2O} \cdot c_{H_2O} \cdot (\theta_{stor.,max.} - \theta_{stor.,min.}) \quad [kJ] \quad \text{Equation 28}$$

$V_{stor.}$... storage volume of the hot water tank [m^3]
 ρ_{H_2O} ... density of the storage medium (i.e. water) [kg/m^3]
 c_{H_2O} ... specific heat capacity of the storage medium [$kJ/(kg K)$]; $c_{H_2O} = 4.1855 \text{ J/(g·K)}$
 $\theta_{stor.,max.}$... max. temperature in the storage tank during the course of one operation year [$^{\circ}C$]
 $\theta_{stor.,min.}$... min. temperature in the storage tank during the course of one operation year [$^{\circ}C$].

In biomass district heating systems usually water-filled tanks serve as thermal energy storage, which have to fulfill two tasks. First, the water storage has to hydraulically de-couple the distribution system from the heat production by the biomass boiler. Second, the so-called buffer tank is implemented within the district heating system in order to balance heat demand and heat generation, as biomass boilers are limited by their minimal load level and their capability to level out heat load changes.

In district heating systems the use of thermal energy storages (i.e. water storages) enables the operator to cover load peaks of heat. Furthermore, it allows leveling out load changes in the heating system, if the heat storage capacity of the water-filled piping system is not sufficient (see Kaltschmitt & Streicher (2009), page 383).

As stated by Duffie & Beckmann (2006) the major characteristics of a thermal energy storage system are (see page 378):

- Its capacity per unit volume,
- the temperature range, over which the energy storage operates (i.e. the temperature level, heat is added and heat is removed),
- the means of addition or removal of heat and the associated temperature differences,
- the stratification of heat in the storage unit,
- the power requirements for addition and removal of heat,
- the structural elements like containers or tanks, etc. associated with the storage system, and
- the costs related to construction and operation of a storage system.

As described there the energy storage in a solar process system may be in form of sensible heat of a liquid or solid medium, as heat of fusion in chemical systems, or as chemical energy of products in a reversible chemical reaction (see Duffie & Beckman (2006), page 378). Besides the utilized form of stored energy thermal energy storage systems can be categorized by the intended period of time they are designed for. Due to SDH (2012) three types of applications can be differentiated:

- Buffer storages for short time energy storage, sub-divided into the category of short-term storage systems storing heat for one or two days and the category for storage of thermal energy for the course of one week.
- Large-scale thermal energy storages for long-term or even seasonal thermal energy storage
- Large-scale thermal energy storages for multiple users like the combined storage of solar heat and waste heat from industrial processes or from electric power generation.

Due to its ideal characteristics as a storage medium and transport fluid for solar thermal heat, water is the favorable material to store thermal energy in solar systems. Typically water-filled storage tanks designed for pressurized or non-pressurized storage of hot water are used in the field of short-term thermal energy storages in solar-assisted district heating systems. Charging of the water storage

tanks can be done either by internal heat exchangers or by external ones like plate heat exchangers or ribbed pipe heat exchangers.

De-centrally installed storage tanks are mainly applied for the preparation of and the supply of domestic hot water for residential buildings or even single dwelling units in apartment buildings. Due to their intended purpose this type of short-term storages has to comply with high standards of hygiene. So it is typically manufactured out of stainless, galvanized or enamel-coated steel or it is made of plastics. If the water storage is used as buffer tank with integrated domestic hot water tank (e.g. in solar thermal combi systems) the water utilized as storage media is separated from the potable water kept in a dedicated device (see Weiss (2011)).

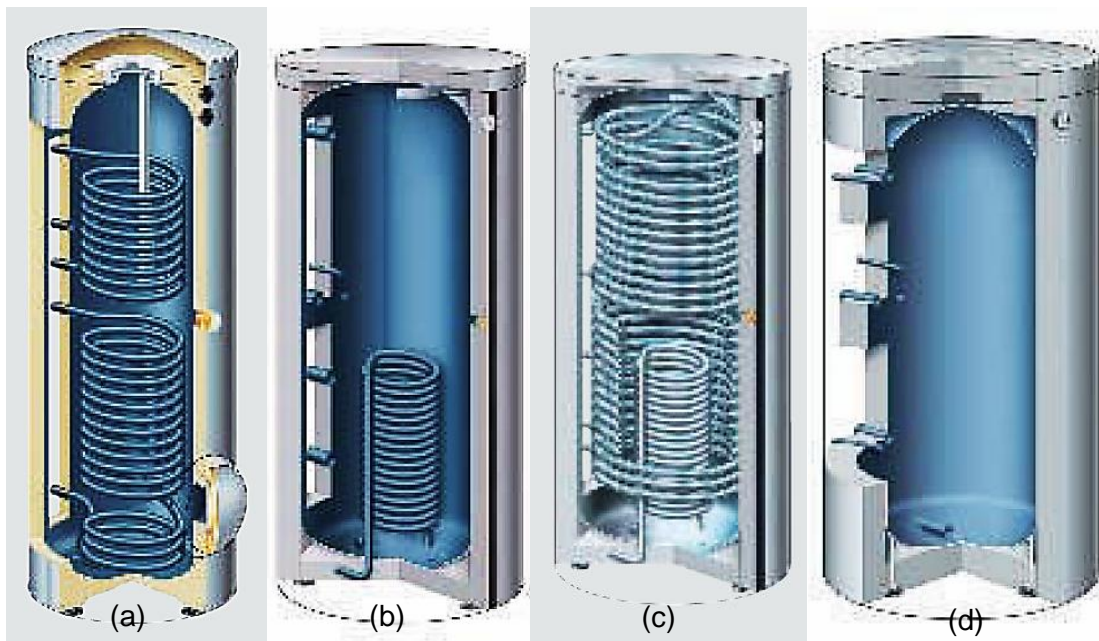


Figure 2-19: Four examples of water-filled tanks with cylinder design used for the storage of potable water, used as buffer tank or for the storage of heating water (data source: Viessmann (2009)).

Explanations: (a) ... dual-mode domestic hot water cylinder with 1 indirect coil connected to the collector circuit and 1 indirect coil to provide reheating by a boiler;
(b) ... heating water buffer tank with an internal indirect solar coil to be integrated with a solar thermal system;
(c) ... multi-mode heating water buffer tank with integral domestic hot water heating via an indirect coil made of corrugated stainless steel pipes;
(d) ... domestic hot water tank for storing potable water with an external heating by a plate-type heat exchanger.

Buffer tanks designed for the purpose of storing the fed-in heat at different levels within the water column in the tank are equipped with stratification devices.

According to Duffie & Beckman (2006) two categories of stratified tank models have been developed (see page 382). First, water tanks with the multi-node approach,

and second, water tanks with the plug flow approach. The degree of stratification in a real water tank will depend on size, location and design of inlets and outlets, as well as on flow rates of entering and leaving water stream. However, the calculation of the energy balance equation for a tank with some degree of stratification can not be done by hand, but have to be simulated by using the appropriate stratified tank model.

Within a district heating network with large-scale solar thermal collector fields the sub-function of large-scale thermal energy storages is of special interest. According to SDH (2012) four main types of large-scale or seasonal thermal energy storages are differentiated. Figure 2-20 shows the construction concepts of the four main types of seasonal storages.

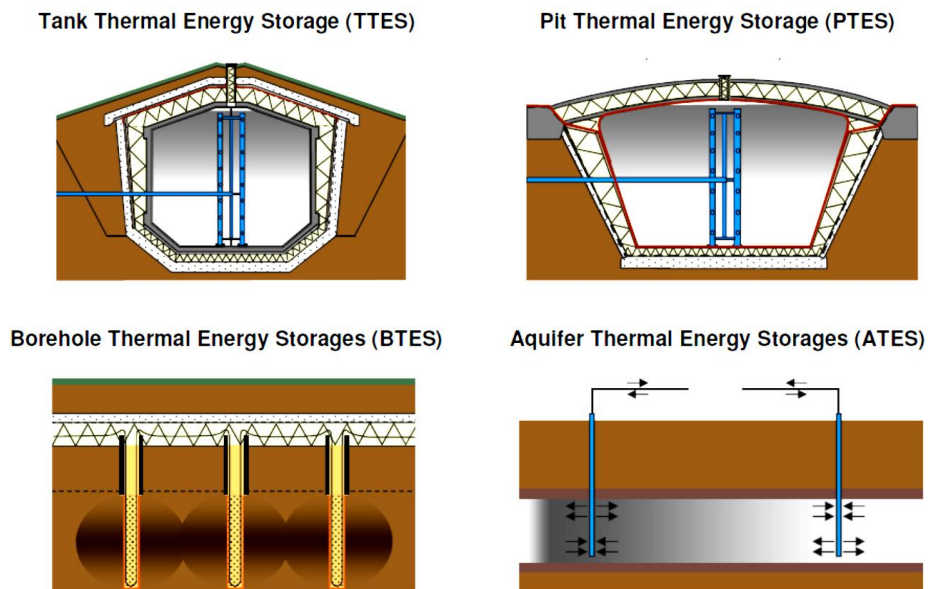


Figure 2-20: Four main construction concepts for large-scale or seasonal thermal energy storages (data source: SDH (2012)).

There are tank thermal energy storages (TTES) and pit thermal energy storages (PTES) in use, where the storage medium is water or gravel-water. The transfer of heat into the storages takes place via water-filled piping system feeding a stratification device. For charging a defined quantity of water is extracted from the bottom and the same quantity of heated water is injected on a higher level of the water column. For discharging the procedure is done in reversed mode in order not to mix the temperature layering.

In borehole thermal energy storages (BTES) the underground, i.e. the soil or rock below the surface of earth is utilized as a storage medium. The technical fluid (e.g. water) is pumped through heat exchangers (e.g. vertical borehole heat exchangers) in a closed loop, so heat is charged and discharged without direct connection to the storage medium. Consequently, BTES are classed with closed storage systems.

Table 2-3: Storage concepts with respect to heat capacity and geological requirements for large scale or seasonal thermal energy storages (data source: SDH (2012))

Type	Storage medium	Heat capacity [kWh/m ³]	Storage volume for 1 m ³ water equivalent [m ³ /m ³ _{w.equ.}]	Geological requirements
Tank Thermal Energy Storage (TTES):	water	60 - 80	1	- stable ground conditions - preferably no ground water - 5 – 15 m deep
Pit Thermal Energy Storage (PTES):	water* gravel-water*	60 - 80 30 - 50	1 1.3 - 2	- stable ground conditions - preferably no ground water - 5 – 15 m deep
Borehole Thermal Energy Storage (BTES):	soil / rock	15 - 30	3 – 5	- drillable ground - ground water favorable - high heat capacity - high thermal conductivity - low hydraulic conductivity ($k_f < 10^{-10}$ m/s) - natural ground water flow < 1 m/a - 30 – 100 m deep
Aquifer Thermal Energy Storage (ATES):	sand - water	30 - 40	2 - 3	- natural aquifer layer with high hydraulic conductivity ($k_f > 10^{-5}$ m/s) - confining layers on top and below - no or low natural ground water flow - suitable water chemistry at high temperatures - aquifer thickness of 20 – 50 m

*Explanations: * ... Water is the more favorable storage media from thermodynamic point of view. Gravel-water is often used, if the storage's surface is designed for further usage*

Aquifer thermal energy storages (ATES) are storage systems, where ground water is pumped out of the ground and injected again. Prerequisite is the availability of an aquifer, a water-filled layer of sand, gravel, or a permeable layer of sandstone or limestone with high hydraulic conductivity. If the layer is enclosed by impervious layers on top and at the bottom and if there is no or minimal natural flow of ground

water, the aquifer could be used as thermal energy storage. ATEs are open storage systems with a high level of heat transfer capacity due to the use of wells, which are drilled into the layer for extraction and injection (see Figure 2-20). The four concepts described above are summarized in Table 2-3 taken from SDH (2012).

As advanced storage techniques like phase change materials (PCM), thermo chemical storages or sorption storages do not have reached the necessary stage of development to be applied in seasonal thermal energy storage applications, mainly hot water storage concepts are in use due to their relatively low specific costs (see Raab (2006), page 15). Hot water storage systems are either realized in form of above-ground tank thermal energy storages or as ground buried storages with a structure made of concrete, steel or glass fiber reinforced plastic.

Above-ground water tanks (see Figure 2-21) are in general only used as buffer tanks with volumes up to 200 m³. Ground-buried TTES and PTES constructions have been realized for solar-assisted district heating systems in a storage volume range of 100 m³ up to 75000 m³ (see SDH (2012)). Due to the thermodynamic characteristics of water, hot water storage tanks can be either operated as non-pressurized storage systems up to a temperature of 95°C or as pressurized thermal storages with a pressure level of several bars and a maximum temperature of about 115°C (see Raab (2006), page 16).

Pit thermal energy storages are constructed as ground-buried facilities filled with pure water, gravel-water, sand-water or soil-water. Typical operation temperatures are 80° to 90°C depending on the temperature stability of the liner mounted in the pit. Due to their layout PTES can provide the necessary storage capacity combined with low static requirements and relatively low specific costs for construction.

As stated by Duffie & Beckman (2006) the volume of a storage unit roughly increase as the cube of its characteristic dimension, while the area for heat losses via the storage's outer casing increases as the square (see page 397). Consequently the increase of storage size reduces the loss-to-capacity ratio for a storage system. As a rule of thumb in solar thermal systems Duffie & Beckman (2006) recommend a 2 to 3 orders of magnitude larger storage capacity per unit collector area for a seasonal storage than for an overnight storage (see page 397).

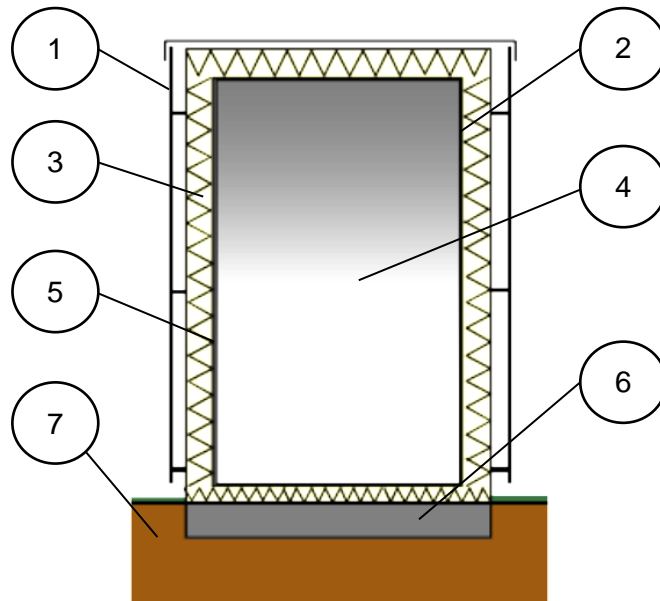


Figure 2-21: Example scheme of an above-ground hot water tank used as a seasonal thermal energy storage (data source: SDH (2012)). Due to its high investment costs above-ground tank thermal energy storages are in general used as buffer tanks with a maximal volume of 200 m³.

Explanations:

- 1 ... outer shell for weather protection;
- 2 ... structure made of steel;
- 3 ... insulation e.g. made of mineral wool ;
- 4 ... water column with thermal stratification ;
- 5 ... stainless steel liner for water- and steam diffusion tightness;
- 6 ... foundation made of concrete;
- 7 ... stable ground.

On the one hand the economic efficiency of a storage concept for a solar-assisted district heating system depends on the costs for construction, operation and maintenance of the selected system. From investment costs' point of view tank thermal energy storages are the most expensive one followed by PTES. Lowest costs can be reached with borehole or aquifer thermal energy storages, even though additional equipment for operation of these storage types like buffer tanks or water treatment units are necessary. There will be also a decrease of costs with increasing storage volume, if specific storage costs per storage volume (in water equivalents) are compared (see SDH (2012)).

On the other hand the economy of a storage system is also influenced by the thermal performance of the selected storage type and of the connected system. The efficiency of a solar-assisted district heating system is mainly influenced by the choice of a suitable storage concept, which has to consider the local geological situation, the system integration, the required size of storage, the power rates, the

number of storage cycles per year, legal restrictions and the temperature levels in the district heating system.

Especially the return temperatures from the heat distribution system are a crucial point with respect to the used storage application. As the return flow temperature determines the lowest temperature level in the system, the lowest usable temperature for discharging the heat storage is defined as well (see SDH (2012)). However, it has been found out, that in many installations the designed values for return temperature deviates significantly from the higher measured temperature levels. An increase of return flow temperature directly reduces the storage's heat capacity and decreases the solar fraction of the system (see Raab (2006), page 21).

2.1.11 Key figures of solar thermal systems

For the assessment and comparison of solar thermal systems it is useful to determine a set of key figures, which have been introduced and applied in different variants (see Heimrath et al. (2002), page 137, Raab (2006), page 6). To focus on the most common key figures characterizing solar thermal systems the following indicators are described in more detail:

- The solar savings fraction or solar fraction (f_{sol}),
- the share of solar energy for domestic hot water preparation ($f_{sol,DHW}$),
- the solar energy utilization ratio of a solar thermal system (ζ_{sol}),
- the specific energy yield of a solar collector (y_{col}),
- the system efficiency of a solar- assisted heating system ($\zeta_{sys.,sol}$), and
- the degree of utilization of a solar thermal collector field (DU_{col}).

For the the characterization of thermal energy storages Raab (2006) proposes the following key figures (see page 7):

- The utilization ratio of the thermal energy storage ($\zeta_{stor.}$), and
- the number of cycles per year of operation (CN).

The most used key figure to assess a solar thermal system is the solar savings fraction or solar fraction (f_{sol}). Several definitions are in use to describe the share of solar energy covering parts of the total useful energy demand in the (district) heating system. In most cases the period of time used to determine the amount of energy required and the amount of useful energy provided by the solar thermal system is

one calendar year. According to Heimrath et al. (2002) one definition for the solar savings fraction or solar fraction (f_{sol}') is (see page 136):

$$f_{sol}' = 1 - \frac{Q_{add.}}{Q_{demand,DH}} \quad [1] \quad \text{Equation 29}$$

$Q_{add.}$... conventional energy carrier savings (e.g. by an additional heating system) [kWh/a]
 $Q_{demand,DH}$... total annual energy demand covered by (district) heating system [kWh/a].

This definition is applicable for solar thermal systems used for domestic hot water preparation and for space heating, while the losses of the thermal energy storage are completely assigned to the solar thermal system. Another definition for the solar fraction (f_{sol}'') is the ratio of the useful solar energy (supplied by the collector circuit) to the amount of the total energy demand covered by the heating system (see Raab (2006), page 6):

$$f_{sol}'' = \frac{Q_{sol.}}{Q_{demand,DH}} \quad [1] \quad \text{Equation 30}$$

$Q_{sol.}$... useful solar energy provided by the collector circuit to the heating system [kWh/a]
 $Q_{demand,DH}$... total annual energy demand covered by (district) heating system [kWh/a].

The annual losses of the thermal energy storage sub-system are allocated to the solar thermal collector sub-system. In case a buffer tank is used key figure f_{sol}'' is defined as (see Streicher et al. (2002), page 137):

$$f_{sol}'' = \frac{Q_{sol.,in,stor.}}{Q_{demand,DH}} \quad [1] \quad \text{Equation 31}$$

$Q_{sol.,in,stor.}$... solar thermal energy fed into storage by the collector circuit per year [kWh_{th}/a]
 $Q_{demand,DH}$... total annual energy demand covered by (district) heating system [kWh_{th}/a].

Losses by the storage system are taken into account by the conventional heating system. Further more a definition for the solar fraction (f_{sol}^*) is typically applied in case of a tank storage system used as buffer tank for thermal energy provided by a solar thermal system and a conventional boiler (or biomass boiler). This definition represents the ratio of useful solar energy fed into the buffer tank to the total amount of energy provided by the solar thermal collectors and the boiler (see Heimrath et al. (2002), page 137).

$$f_{sol}^* = \frac{Q_{sol.,in.,stor.}}{Q_{sol.,in.,stor.} + Q_{aux.,in.,stor.}} \quad [1] \quad \text{Equation 32}$$

$Q_{sol.,in.,stor.}$... annual amount of useful solar heat fed into the storage tank [kWh_{th}/a]
 $Q_{aux.,in.,stor.}$... annual amount of useful heat fed into storage by the biomass boiler [kWh_{th}/a].

Heat losses of the thermal energy storage are equally assigned to the two heat sources. The annual demand of auxiliary electricity for pump operation and system controlling is neither considered in *Equation 31* nor in *Equation 32*. The share of solar energy for domestic hot water preparation ($f_{sol,DHW}$) is expressed by the following equation:

$$f_{sol,DHW} = \frac{Q_{sol.,in.,stor.}}{Q_{demand,DHW}} \quad [1] \quad \text{Equation 33}$$

$Q_{sol.,in.,stor.}$... solar thermal energy fed into storage by the collector circuit per year [kWh_{th}/a]
 $Q_{demand,DHW}$... annual energy demand for domestic hot water preparation [kWh_{th}/a]

The solar energy utilization ratio of a solar thermal system (ζ_{sol}) describes the efficiency of energy utilization by a solar thermal system influenced by the dimensioning of the system and the system quality (efficiency of collectors, heat losses in solar pipes, etc.).

$$\zeta_{sol} = \frac{Q_{sol.,in.,stor.}}{E_{irr.,col.}} \quad [1] \quad \text{Equation 34}$$

$Q_{sol.,in.,stor.}$... solar thermal energy fed into storage by the collector circuit per year [kWh_{th}/a]
 $E_{irr.,col.}$... energy amount of solar irradiation onto the collector area per year [kWh_{th}/a].

Heat losses by the solar pipes are considered in this case (see Raab (2006), page 7).

The specific energy yield of a solar collector (y_{col}) indicates the annual amount of solar energy per unit of collector area fed into the thermal energy storage. It has to be differentiated between absorber area (net collector area) and gross collector area when the unit of collector area is defined (see Heimrath et al. (2002), page 138):

$$y_{sol} = \frac{Q_{sol.,in.,stor.}}{A_{col.}} \quad [kWh/(a \cdot m^2)] \quad \text{Equation 35}$$

$Q_{sol.,in.,stor.}$... solar thermal energy fed into storage by the collector circuit per year [kWh_{th}/a]
 $A_{col.}$... collector area (gross collector area or absorber area) [m²].

The degree of utilization of a solar thermal collector field (DU_{col}) characterizes the operation of a solar thermal collector field. It is defined as the relation between the total annual energy demand covered by the (district) heating system compared to the applied collector area:

$$DU_{col} = \frac{Q_{demand,DH}}{A_{col}} \quad [kWh/(a \cdot m^2)] \quad \text{Equation 36}$$

$Q_{demand,DH}$... total annual energy demand covered by (district) heating system [kWh_{th}/a]
 A_{col} ... collector area (gross collector area or absorber area) [m^2].

The system efficiency of a solar- assisted heating system ($\zeta_{sys.,sol}$) compares the heat demand with the provisioned useful heat in the heating system. On one side there is annual useful heat demand for space heating and domestic hot water preparation (useful energy without losses due to storage and distribution), on the other side there is energy spent by the energy resources like the solar thermal system and the biomass boiler (see Heimrath et al. (2002), page 139):

$$\zeta_{sys.,sol} = \frac{Q_{demand,SH} + Q_{demand,DHW}}{Q_{sol.,in,stor.} + Q_{aux.,in,stor.}} \quad [1] \quad \text{Equation 37}$$

$Q_{demand,SH}$... annual energy demand for space heating (SH) [kWh_{th}/a]
 $Q_{demand,DHW}$... annual energy demand for domestic hot water (DHW) preparation [kWh_{th}/a]
 $Q_{sol.,in,stor.}$... annual amount of solar heat feed into the storage tank [kWh_{th}/a]
 $Q_{aux.,in,stor.}$... amount of heat provided to storage by the biomass boiler per year [kWh_{th}/a].

As the thermal energy storage usually is an essential part of a solar thermal system, key figures for thermal energy storages are in use (see Raab (2006), page 7). The utilization ratio of the thermal energy storage ($\zeta_{stor.}$) is the relation between the amount of thermal energy (heat) taken from the storage system ($Q_{stor.,out}$) to the amount of thermal energy (heat) fed into the storage ($[Q_{stor.,in} - Q_{stor.,diff}]$) within a defined time interval. $Q_{stor.,diff}$ is the difference of heat content determined between start and end of the investigated time interval.

$$\zeta_{stor.} = \frac{Q_{stor.,out}}{Q_{stor.,in} - Q_{stor.,diff.}} \quad [1] \quad \text{Equation 38}$$

$Q_{stor.,out}$... heat taken from the storage within a defined time interval (i.e. year) [kWh_{th}/a]
 $Q_{stor.,in}$... heat fed into the storage [kWh_{th}/a]
 $Q_{stor.,diff}$... difference of heat content determined between start and end of interval [kWh_{th}/a].

The number of charging cycles per year of operation (CN) for a thermal energy storage can be calculated based on the heat taken from the storage during a year

($Q_{stor.,out}$) and the maximal storage capacity ($Q_{stor.,max.}$) determined according to Equation 28.

$$CN = \frac{Q_{stor.,out}}{Q_{stor.,max.}} [a^{-1}] \quad \text{Equation 39}$$

$Q_{stor.,out}$... heat taken from the storage within a defined time interval (i.e. year) [kWh_{th}/a]
 $Q_{stor.,max.}$... max. heat storage capacity of a storage tank within a defined period of time [kWh_{th}]

If a seasonally operated adiabatic heat storage is charged and discharged once a year $CN = 1 a^{-1}$. For a daily charged and discharged adiabatic buffer tank the number of charging cycles per year of operation equals $CN = 365 a^{-1}$.

As described by Heinz & Streicher (1999) the total connected heat load in the district heating grid ($Q'_{load,grid,tot.}$, see Equation 8), the specific collector area ($a_{col.}$) with respect to the total heat load and the specific storage volume ($v_{stor.}$) in relation to the total connected heat load in the district heating grid are the main input parameters for the Nomogram-Algorithmus suggested for an initial configuration of the solar-assisted district heating system. The ratio $a_{col.}$ is calculated assuming that the gross collector area of the installed collector field is known:

$$a_{col.} = \frac{A_{col.}}{Q'_{load,grid,tot.}} [m^2 / kW_{th}] \quad \text{Equation 40}$$

$A_{col.}$... gross collector area of the installed collector field [m^2]
 $Q'_{load,grid,tot.}$... total connected heat load in the district heating grid [kW_{th}].

For the specific storage volume ($v_{stor.}$) the storage volume of the thermal energy storage is taken, which is normally the volume of a cylindrical hot water storage tank:

$$v_{stor.} = \frac{V_{stor.}}{Q'_{load,grid,tot.}} [m^3 / kW_{th}] \quad \text{Equation 41}$$

$V_{stor.}$... volume of the installed hot water storage tank [m^3]
 $Q'_{load,grid,tot.}$... total connected heat load in the district heating grid [kW_{th}].

For a rough assessment of the required storage volume needed to keep the thermal energy provided by a collector field for a defined period of time Meißner & Abrecht (2012) propose the following estimate:

$$V_{stor.} = \frac{q_d t_{stor.} A_{col.}}{c_{H2O} \rho_{H2O} (\theta_{stor.,max.} - \theta_{sol.,ret.,av.})} \quad [m^3] \quad \text{Equation 42}$$

$V_{stor.}$... storage volume of the hot water tank [m^3]
 q_d ... specific energy yield per unit gross collector area and day [$kWh/(m^2 d)$];
 $t_{stor.}$... required period of time to store the heat at a certain temperature level [h]
 $A_{col.}$... gross collector area of the collector field [m^2]
 ρ_{H2O} ... density of the storage medium (i.e. water) [kg/m^3]; $\rho_{H2O} = 980 \text{ } [kg/m^3]$ at $70^\circ C$
 c_{H2O} ... specific heat capacity of the storage medium [$kWh/(kg K)$]; $c_{H2O} = 1.1639 \text{ } [kWh/(kg \cdot K)]$
 $\theta_{stor.,max.}$... max. temperature in the storage tank [$^\circ C$]
 $\theta_{sol.,ret.,av.}$... average temperature of return flow in the solar circuit [$^\circ C$].

By taking into account a cylindrical hot water tank with a height-to-cross-section ratio of 1.5 the surface area of the storage tank (A_{st}) and the area relevant for heat losses (A_{hl}) through the insulated exterior surface can be determined. Based on this area, the average temperature difference between hot water and ambient air, the thickness of insulation and the specific heat transfer coefficient of the applied insulation material an average heat loss per unit of time ($Q'_{hl,v}$) can be calculated for the storage volume according to (see Meißner & Abrecht (2012), page 95):

$$Q'_{hl,v} = \frac{\lambda_l \cdot A_{hl} \cdot \Delta T_v}{d_l} \quad [W] \quad \text{Equation 43}$$

λ_l ... specific heat transfer coefficient of the applied insulation material [$W/(m K)$]
 A_{hl} ... surface area of the insulated cylindrical storage tank relevant for heat losses [m^2]
 ΔT_v ... average temperature difference between stored hot water and ambient air [K]
 d_l ... thickness of the insulation layer [m]

Knowing the average heat loss per unit of time ($Q'_{hl,v}$) a magnitude of order for the annual thermal energy lost by heat transfer through the exterior surface of the storage tank is calculated by simply multiplication with 8760 hours.

Pilot plants with seasonal thermal energy storages realized in Germany and Sweden typically show a volume-to-area ratio in the range of $0.865 \text{ } m^3/m^2$ up to $23.148 \text{ } m^3/m^2$. These of solar-assisted district heating systems have been designed in order to reach an annual solar fraction of more than 30% up to 100% (see Raab (2006), saisonalspeicher.de (2009)).

In more concrete figures a categorization of different thermal storages system types and the related storage volume of water per unit collector area is given by Weiss & Mahler (2003) in Table 2-4 for domestic hot water preparation and space heating in residential buildings.

Table 2-4: Comparison of solar-assisted heating systems with thermal energy storages (i.e. hot water storages) for residential buildings (data source: Weiss & Mahler (2003))

System type	Utilization of solar energy for	Solar fraction of the total heat demand [%/a]	Collector area per residential unit [m²]	Storage volume per unit collector area [m³/m²]
Solar-assisted heating system with short-term thermal energy storage	preparation of DHW	10% - 20%	2 - 4	0.05 – 0.07
Solar-assisted heating system with weekly thermal energy storage	preparation of DHW and space heating	30% - 40%	4 - 10	0.2 – 0.4
Solar-assisted heating system with seasonal (long-term) thermal energy storage	preparation of DHW and space heating	40% - 70%	10 - 40	2 - 4

Explanations: DHW ... Domestic Hot Water.

In the following section the layout and the characteristics of the main hydraulic schemes applied in solar-assisted district heating systems are discussed. In each of the described examples the central thermal energy storage is an important issue of the overall concept.

2.2 Hydraulic concepts for solar-assisted biomass district heating systems with central thermal energy storages

In the following sub-chapters several hydraulic concepts for solar-assisted biomass district heating systems with central thermal energy storages are outlined. Besides concepts with centralized energy storages also layouts with decentralized short-term or mid-term storages per heat supplied dwelling unit or even per building are applied. According to Fink et al. (2007) hydraulic concepts for solar-assisted space heating and domestic hot water supply with decentralized collector areas and decentralized energy storages have been developed in the field of energy and building technology for developing areas in cities and municipalities. As described by Fink et al. (2007) these concepts are especially suitable for a modular design and a step-by-step approach in several construction phases. However, the following examples of hydraulic schemes for solar-assisted biomass district heating systems deal only with central energy storages.

2.2.1 Hydraulic concepts based on water-operated two-pipe DH network

The hydraulic concept shown in Figure 2-22 is applied in case of solar-assisted biomass district heating systems with two-pipe district heating grids or solar-supported block heating systems based on two-pipe micro-grids. Each heat producing component feeds the heat into the central thermal energy storage. For local hot water preparation the connected buildings are equipped with decentralized domestic hot water storage tanks using the charge-store principle. The DHW tanks are heated either by an external heat exchange unit (see option 1) or by an internal heat exchanger (see option 2). The consumers' heating sub-stations are either connected directly or are supplied indirectly via an internal heat exchanger.

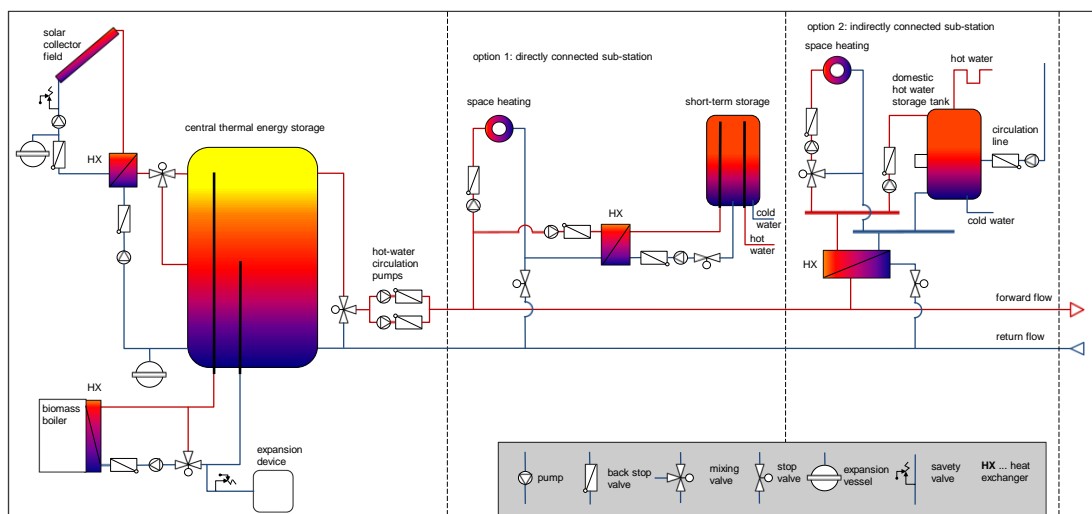


*Figure 2-22: Hydraulic scheme of a solar-assisted biomass district heating system with two-pipe heat distribution network including two options for consumer heat sub-station * (data source: Fink et al. (2007), page 25).*

*Explanations: * ... The 2 options are a directly connected and an indirectly connected sub-station. In addition to the central energy storage decentralized short-term storages or domestic hot water storage tanks for the daily domestic hot water demand are implemented.*

The type of two-pipe heating grid shown in Figure 2-22 can be operated in two different ways. During the heating period the grid will either keep a fixed temperature level or the circulating water's temperature is controlled according to the ambient temperature. Depending on operation mode for space heating the preparation of hot water takes place continuously or during planned time slots for charging the decentered storages (see Fink, et al. (2007), page 25).

Figure 2-23 displays a hydraulic concept for solar-assisted, biomass fired two-pipe district heating grids or micro-grids in supplying areas with high building density (i.e. areas with multiple-story residential buildings or areas with row houses). There is on

central energy storage near to the heat producing units but no decentralized storages in the heat supplied buildings or apartments. Domestic hot water is prepared in a decentralized manner by apartment heat transfer units in the respective residential unit via continuous flow water heaters (refer to Fink & Riva (2004), page 66). The consumers' space heating sub-stations are either connected directly (see Figure 2-23) or are supplied indirectly via an internal heat exchanger.

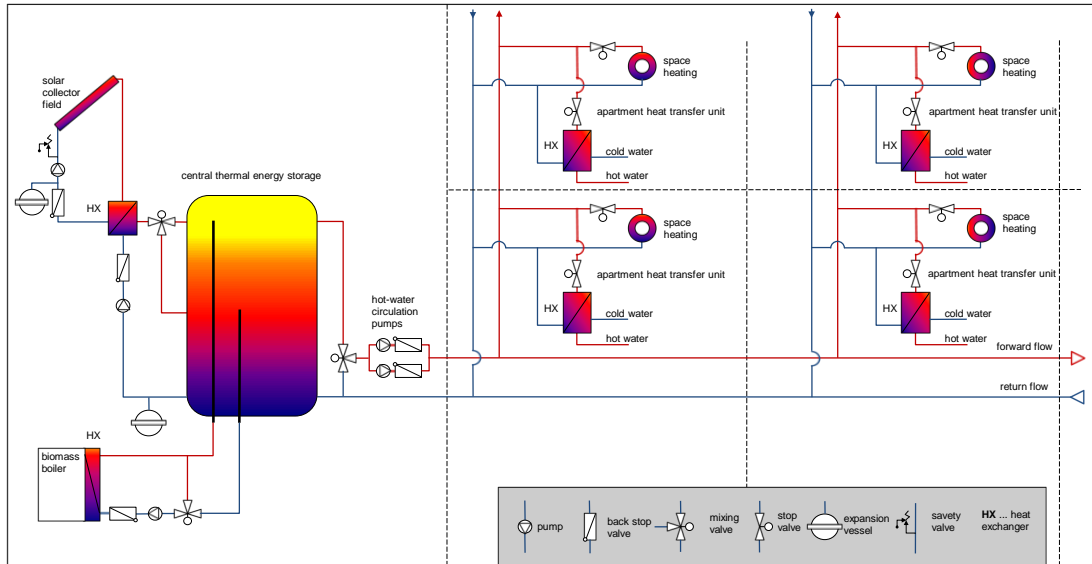


*Figure 2-23: Hydraulic scheme of a solar-assisted biomass district heating system with two-pipe heat distribution network and decentralized apartment heat transfer units * (data source: Fink et al. (2007)).*

*Explanations: * ... The domestic water is heated by means of constant flow water heater equipped with a plate heat exchanger. Consumer sub-station for space heating can be directly connected (see above) or can be indirectly connected via a heat exchanger.*

Due to the operation of continuous flow water heaters the two-pipe network shown in Figure 2-23 has to be supplied with circulating heated water on a constant temperature level during the whole year. As there are no decentralized storages the heating grid has to be designed in order to deal with peaks in demand.

2.2.2 Hydraulic concepts based on water-operated three-pipe DH network

In Figure 2-24 the hydraulic scheme of a solar-assisted biomass district heating system with three-pipe heat distribution network is shown. This concept is typically applied in micro-grids with a high density of heat consumers. In addition to the central energy storage the connected buildings are equipped with de-central domestic hot water storages, where a decentralized preparation of domestic hot water takes place. Due to a separate line for domestic water preparation and a

separate pipe for space heating the flow temperatures in these pipelines can be controlled independently. Sub-stations for space heating are connected directly or available as indirectly connected heating units.

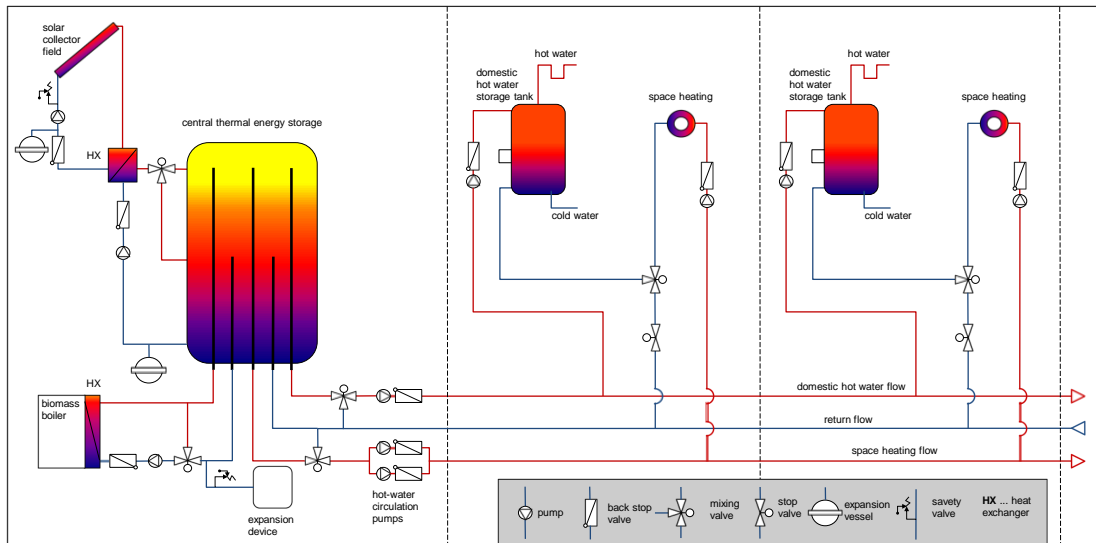
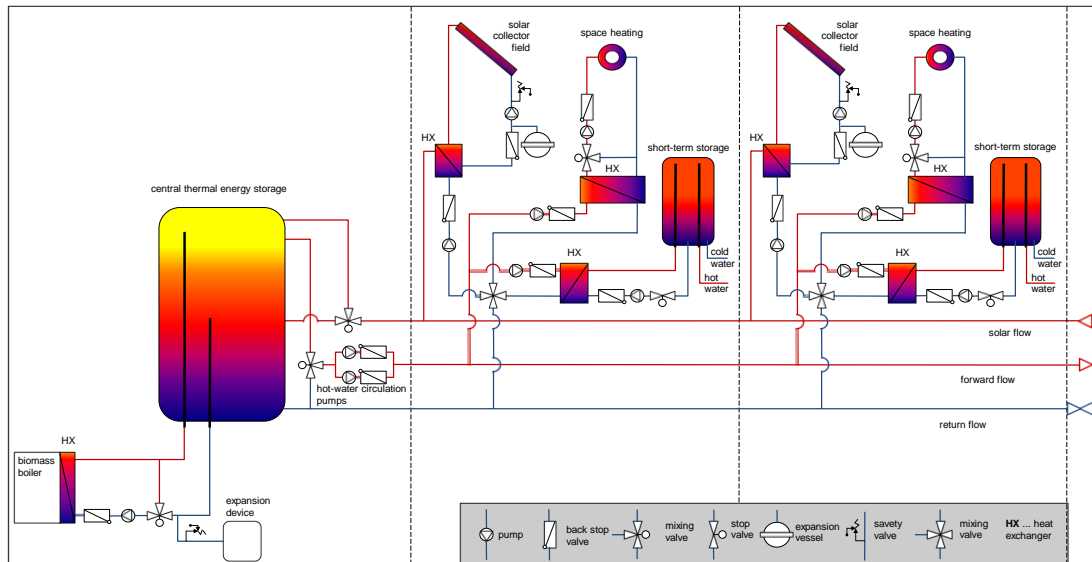


Figure 2-24: Hydraulic scheme of a solar-assisted biomass district heating system with three-pipe heat distribution network including a separate line for domestic hot water preparation * (data source: Fink et al. (2007)).

Explanations: * ... In addition to the central energy storage decentralized domestic hot water storage tanks for the daily domestic hot water demand are implemented.

The supply of heat for space heating during the heating period is characterized by a flow temperature adapted to the ambient temperature. For domestic hot water preparation the concept in Figure 2-24 foresees either fixed planned time windows for heat charge of decentralized storage units or a charging on demand, if one of the connected DHW storage requires a re-charging with heat.

The hydraulic scheme for a solar-assisted biomass district heating system shown in Figure 2-25 represents a concept for integrating decentralized mounted solar thermal collectors into a water-operated two-pipe district heating grid. Via a separate solar flow the de-centrally gained solar heat of the solar thermal system is fed into central energy storage. This three-pipe concept is applicable for mid-sized heating systems with a moderate density of heat consumers supplying areas of settlement developed with row houses or multiple-storey residential buildings. The preparation of domestic hot water is done by the support of decentralized short-term storages.



*Figure 2-25: Hydraulic scheme of a solar-assisted biomass district heating system with three-pipe heat distribution network integrating a separate line for centralized solar thermal feed-in by decentralized mounted collector fields * (data source: Fink et al. (2007)).*

*Explanations: * ... In addition to the central energy storage decentralized short-term storage tanks for the daily domestic hot water demand are implemented. The consumer heating sub-stations are indirectly connected to the district heating grid.*

Depending on the mode of operation used for the heat supply of the connected heat consumers, the pipe assigned for the return flow of the heating system will transport the return water in two different directions. Either it is the return flow of the conventional heat distribution grid or it water supply for the solar system.

2.2.3 Hydraulic concepts based on water-operated four-pipe DH network

As shown in Figure 2-26 the hydraulic concept of the solar-assisted biomass district heating system is based on a central thermal energy storage feeding a two-pipe heating grid for space heating and a central domestic hot water storage tank, which provides domestic water to a second pair of pipes for the dwelling units. The consumer sub-stations for space heating can be directly connected or can be indirectly connected via a heat exchanger.

Besides the functionality of energy storage the central thermal energy storage operates as a buffer tank or hydraulic switch, respectively. It has to level out the heat flows coming from the solar collector field, the biomass boiler and the four-pipe heat distribution network. Due to its high level of heat distribution losses this concept is applied in biomass fired block heating systems characterized by a micro-grid with a high consumer density.

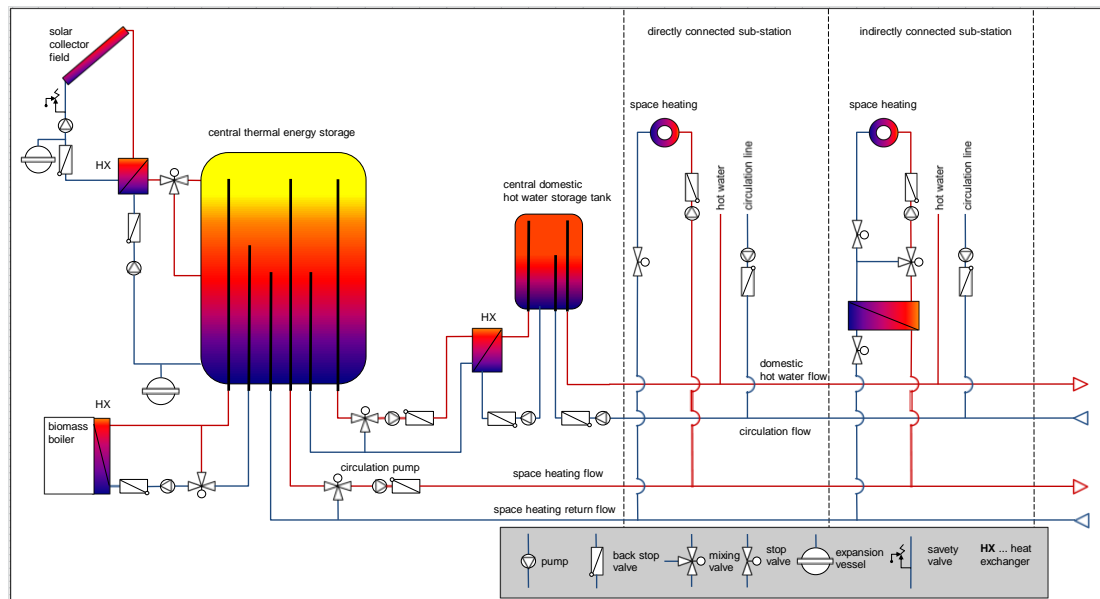


*Figure 2-26: Hydraulic scheme of a solar-assisted biomass district heating system with four-pipe heat distribution network including a domestic hot water storage tank for central preparation of domestic hot water * (data source: Fink et al. (2007)).*

*Explanations: * ... Heat supply for the consumers' directly or indirectly connected heating sub-stations is provided by a dedicated two-pipe heating grid. The second pair of pipes provides domestic water for the connected dwelling units.*

The pipes for space heating flow and space heating return flow (see Figure 2-26) will only be used during the heating period by applying flow temperatures according to the ambient conditions. For a permanent availability of domestic hot water in the connected residential units the circulating domestic water flow is constantly kept on a relatively high temperature level of about 65 °C (see Fink, et al. (2007)).

The hydraulic concept of a four-pipe heat distribution network for a solar-assisted biomass district heating system shown in Figure 2-27 is applied in micro-grid applications with a high density of heat consumers. In addition to a central thermal energy storage fed by the solar thermal collectors and the biomass boiler, a set of de-centrally installed short-term storage tanks provides the capacity to cover the daily demand of domestic hot water in the supplied buildings. There is a pair of pipes providing circulating hot water to the directly or indirectly connected consumers' heating sub-stations (see space heating flow and space heating return flow in Figure 2-27) and a second pair of pipes supplying heat to the heat exchangers for local domestic hot water preparation (see DHW flow and DHW return flow in Figure 2-27).

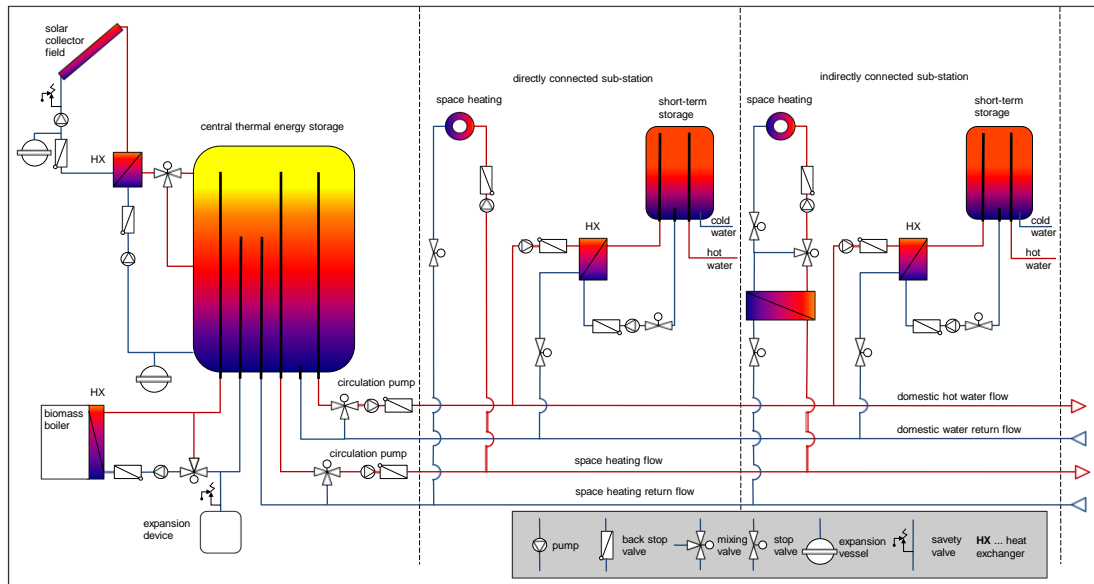


*Figure 2-27: Hydraulic scheme of a solar-assisted biomass district heating system with four-pipe heat distribution network including de-centrally installed domestic hot water storage tanks for local preparation of domestic hot water in the connected buildings * (data source: Fink et al. (2007)).*

*Explanations: * ... Heat supply for the consumers' directly or indirectly connected heating sub-stations is provided by a dedicated two-pipe heating grid. The second pair of pipes provides the heated water for domestic hot water preparation.*

As in the four-pipe network described before the separate two-pipe grid for space heating is only operated during the heating period by applying a temperature level according to the ambient conditions. The preparation of domestic hot water in the de-centrally installed short-term storages can be done in form of scheduled heat re-charging one or two times a day or by heat charges on demand, if one of the connected short-term storages requires a re-charging.

2.2.4 Hydraulic concepts based on water-operated six-pipe DH network

The hydraulic scheme for a solar-assisted biomass district heating system shown in Figure 2-28 represents a concept for integrating decentralized mounted solar thermal collectors into a water-operated six-pipe district heating grid. Based on a four-pipe network described in Figure 2-26 this concept includes an additional pair of pipes for a separate solar flow and solar return flow, feeding solar heat coming from centralized or decentralized mounted solar collector fields into a central thermal energy storage. This hydraulic concept is recommended by Fink, et al. (2007) in case of micro-grids characterized by a small number of heat consumers with an individually high level of connected heat load.

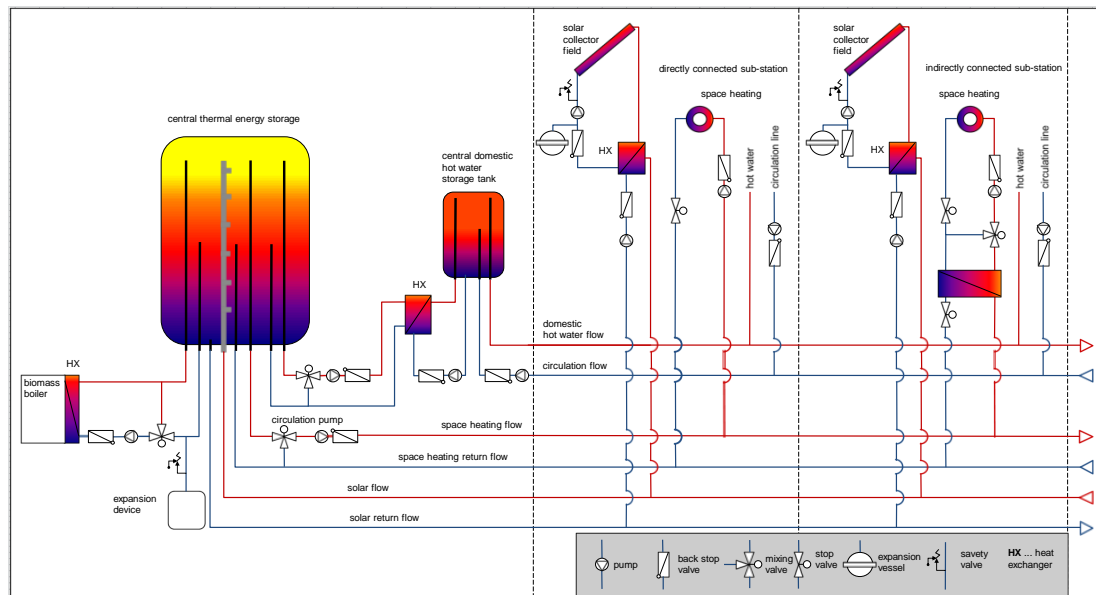


Figure 2-28: Hydraulic scheme of a solar-assisted biomass district heating system with six-pipe heat distribution network including a centrally installed domestic hot water storage tank for central preparation of domestic hot water * (data source: Fink et al. (2007)).

Explanations: * ... Heat supply for the consumers' directly or indirectly connected heating sub-stations is provided by a dedicated two-pipe heating grid. The second pair of pipes provides the centrally heated water for domestic hot water preparation. The third pair of pipes integrates the de-centrally mounted solar thermal collectors to the heating system. Solar heat from several solar thermal systems is fed into the central thermal energy storage.

Like in the four-pipe concept the domestic water circuit requires a permanent circulation of heated water on a relatively high temperature level during the whole year. This means a high level of heat losses with respect to domestic hot water preparation. Directly or indirectly connected heating sub-stations in the residential units are only supplied with heat from the central energy storage during the heating period.

Besides the applied hydraulic concept also the current status of solar-assisted biomass district heating systems in Austria shall to be investigated for further assessment. In the following chapter an overview on biomass (district) heating systems, solar-assisted district heating systems and the applicable support scheme for this combination of renewable energy based heating application in Austria is given.

2.3 Solar-assisted, biomass fired district heating systems in Austria

Since the year 1980 the provincial Chamber of Agriculture of Lower Austria have been collecting data of solid biomass fueled firing systems in Austria. Starting with

boilers fueled with (forest) wood chips or bark, also pellet boilers have been evaluated since 1997 based on data given by 57 manufacturers and suppliers. In 2001 the types of relevant firing systems to be counted has been extended to log wood boilers (see LK NÖ (2012)). Looking back the last 22 years the number of installed firing systems converting solid biomass as a fuel to heat in a thermo-chemical process has been continuously growing. Nevertheless after a booming period in 2006 and 2007 due to applications for green electricity the total capacity of newly installed firing systems decreased in order to continue the positive trend in the following years.

2.3.1 Heating stations in Austria equipped with solid biomass fueled firing applications with a nominal capacity above 100 kW

As wood chips fueled firing applications typically provides the heat for district heating grids, micro-grids, industrial or agricultural buildings and public facilities, this type of firing technology is of special interest when investigating biomass district heating systems. A closer look on the development of heating stations fired with (forest) wood chips above a nominal capacity of 100 kW shows that the number of installed biomass fired boilers with a capacity in the range of 101 up to 1000 kW increased from 46 in 1980 to a total number of 8867 until the year 2011. Installments of wood chips fueled firing systems with a boiler capacity above 1000 kW increased from 10 in 1980 up to a maximum of 88 in 2007, so that in total 1066 biomass fired heating stations have been erected till the year 2011. Table 2-5 gives the numbers and the capacities of this type of firing application for the year 2011, split into 3 capacity ranges and determined according their location in one of Austria's federal countries (see LWK NÖ (2012), page 9).

Table 2-5: Heating stations in Austria based on firing systems fueled with (forest) wood chips erected in the year 2011 (data source: LWK NÖ (2012))

Country	Number			Installed capacity in 2011 [kW]		
Range	101-500 kW	501-1000 kW	> 1000 kW	101-500 kW	501-1000 kW	> 1000 kW
Lower Austria	109	24	13	23089	17375	28050
Styria	60	10	9	12670	7530	19000
The Tyrol	40	16	5	8490	11300	8300
Upper Austria	122	33	13	23669	23330	23050
Carinthia	42	8	6	8170	5990	21700
Salzburg	39	12	3	8129	8490	4400

Country Range	101-500 kW	Number 501-1000 kW	> 1000 kW	Installed 101-500 kW	capacity 501-1000 kW	in 2011 [kW] > 1000 kW
Burgenland	10	6	2	2040	4400	2400
Vorarlberg	14	6	3	2910	4150	5000
Vienna	7	2	2	1731	1400	2400
Austria (2011)	443	117	56	90898	83965	114300

Based on evaluation done by provincial Chamber of Agriculture of Lower Austria the LandesEnergieVerein Steiermark as well as the Biomasseverband Oberösterreich have published statistical data in form of maps representing the existing biomass district heating systems or biomass micro-grids (see LEV (2008) and biomass fired heating plants and biomass fueled combined heat and power plants in Austria (see OeBV (2011)), respectively. In 2008 in total 1224 biomass district heating systems with a heat capacity above 150 kW and a total installed capacity of 1667407 kW existed in Austria (see Table 2-6).

Table 2-6: Biomass district heating systems existing in Austria in the year 2008 with a heat capacity above 150 kW_{th} (data source: LEV (2009))

Country	Accumulated number of systems > 150 kW	Accumulated installed capacity [kW] > 150 kW
Lower Austria	221	362962
Styria	415	327399
The Tyrol	59	162630
Upper Austria	259	332650
Carinthia	89	166840
Salzburg	66	191589
Burgenland	50	64957
Vorarlberg	65	58380
Vienna	-	-
Austria (acc.)	1224	1667407

According to information given by LandesEnergieVerein Steiermark (see LEV (2013)) there are about 20 up to 30 new biomass district heating systems and 50 up to 70 new biomass micro-grids erected and put into operation in Austria per year. These biomass heating plants and biomass block heating systems are realized by the support of public funding. In order to guarantee an optimal planning, construction and an efficient operation a quality management program for biomass heating plants

and biomass district heating system called “*qm-heizwerke*” (see *qm-heizwerke* (2013)) has been initiated by the Austrian Ministry of Life. Besides technical support for biomass heating plant operators a standardized and cost effective monitoring system and a project data base managed by the LandesEnergieVerein Steiermark (see LEV (2013)) give the possibility for further improvement.

Based on technical and business data collected by the *qm-heizwerke* project database since 2007 new biomass district heating systems in Austria are characterized by the following key indicators (see Table 2-7).

Table 2-7: Key indicators of new biomass district heating systems erected in Austria since 2007 (data source: Promitzer (2011))

Indicator	Symbol	Unit	Minimum	Average	Maximum
Specific electricity demand of for grid operation	$w_{el,grid,aux.}$	[kWh _{el} /MWh _{th}]	3.5	6.9	14.1
Specific electricity demand of for heat generation	$w_{el,hg,aux.}$	[kWh _{el} /MWh _{th}]	7.1	n.a.	20.3
Annual grid losses	$\Phi_{grid,an.} / Q_{th,feed-in,an.}$	[%]	n.a.	12.4	28.1
Energy load level	ELL_{grid}	[(kWh _{th} /a)/ m]	n.a.	1700	n.a.
Specific investment costs of heat generation	$inv_{hg,an.}$	[€ / (MWh _{th} /a)]	99	309	559
Specific investment costs of heat distribution	$inv_{grid,an.}$	[€ / (MWh _{th} /a)]	43	191	554

Explanations: $w_{el,grid,aux.}$... Amount of electricity needed per unit of sold heat [kWh_{el}/MWh_{th}];
 $w_{el,hg,aux.}$... Amount of electricity needed per unit of generated heat [kWh_{el}/MWh_{th}];
 $\Phi_{grid,an.}/Q_{th,feed-in,an.}$... Ratio of lost heat to fed-in heat per year [%];
 $Q_{th,feed-in,an.}-Q_{th,useful,an.} = \Phi_{grid,an.}$... Amount of heat lost in the district heating network per year [(MWh_{th}/a)];
 $Q_{th,feed-in,an.}$... Amount of heat fed into the district heating grid per year [MWh_{th}/a)];
 $Q_{th,useful,an.}$... Useful heat supplied and sold to the users per anno [MWh_{th}/a];
 ELL_{grid} ... Annual useful heat supplied and sold to the users per unit length of grid [(kWh_{th}/a)/m)];
 $inv_{hg,an.}$... Investment costs per unit of generated heat per year [€/(MWh_{th}/a)];
 $inv_{grid,an.}$... Investment costs per unit of useful heat distributed per year [€/(MWh_{th} / a)].

Out of the number of biomass district heating systems described above a distinct share of applications is assisted by solar-thermal systems in terms of domestic hot water preparation, space heating or process heat supply. These solar-assisted

biomass district heating systems in Austria are described in more detail in the following sub-section.

2.3.2 Solar-assisted biomass district heating systems in Austria

Starting in the year 1994 the first solar-assisted biomass district heating systems have been put into operation in Austria. It was the goal to replace the heat inefficiently produced by the biomass boilers outside the heating season by solar thermal energy directly gained via solar thermal collectors. At the end of 1998 a number of 444 biomass district heating systems were operated all over the federal territory. A share of 12 applications already supported their summer mode of operation by a solar thermal system feeding solar heat into the district heating network or the micro grid of the block heating system (Heimrath, et al. (2002), page II). During this early phase of development the combination of solar plants and biomass boilers has been promoted in order to utilize the irradiation during the summer month for covering more than 90% of the networks heat demand in July and August.

Four years later about 20 solar-assisted biomass district heating systems were in operation. Especially in case of a system equipped with a single biomass boiler, which have to be replaced by a fossil fueled boiler outside the heating season, the combination with a solar thermal system could allow a perennial operation based on renewable primary energy resources only (see Streicher, et al. (1999), page 5). Up to now (status end of 2012) 36 biomass district heating systems with solar support (see Table 2-8) and 15 biomass solar-assisted micro-grids (see Table 2-9) could be identified as the result of an internet research.

Table 2-8: Solar-assisted biomass district heating systems in Austria - Status end of 2012 (data source: own research via internet; for more detailed information please refer to the appendix)

Plant site	Start of Op. [year]	Biomass boiler(s) [kW]	Length of district heating grid [m]	Volume of central thermal storage [m ³]	Collector area [m ²]	Storage volume per unit collector area [m ³ /m ²]
Deutsch Tschantschendorf / Burgenland	1994	600	2910	34	350	0.097
Bildein / Burgenland	1995	1000	4500	38	450	0.084
Obermarkersdorf /	1995	840 + 340	3400	80	567	0.141

Plant site	Start of Op. [year]	Biomass boiler(s) [kW]	Length of district heating grid [m]	Volume of central thermal storage [m ³]	Collector area [m ²]	Storage volume per unit collector area [m ³ /m ²]
Lower Austria						
Unterrabnitz / Burgenland	1996	640 + 500	4500	58	477	0.122
Lindgraben / Burgenland	1997	450	2000	37	350	0.106
Gnas / Styria	1996	1000 + 640	2800	60	441	0.136
Urbersdorf / Burgenland	1996	650	2500	30 + 30	340	0.176
Bad Mitterndorf / Styria	1997	4000	13000	130	1120	0.116
Eibiswald / Styria	1997/ 2012	2000 + 500	9500	175	2450	0.071
Poysbrunn / Lower Austria	1997	1000	3870	80	870	0.092
Nikitsch / Burgenland	1997	1650 + 600	10258	70	780	0.090
Kroatisch Minihof / Burgenland	1997	700 + 150	6000	60	626	0.096
Soboth / Styria	1998	300	n.a.	10	200	0.050
Schwanberg / Styria *	1998/ 2009	1500	4200	45	non ^a	non ^a
Stadl a. d. Mur / Styria	1998	1200	4420	60	454	0.132
Winklern / Carinthia	1999	1200	6000	120	1295	0.093
Obsteig / Tyrol	2003/ 2004	440	1250	34	115	0.296
Lienz / Tyrol	2001/ 2005	7000 + 6000 ^b + 8700 ^b	53000	400	630	0.635
Ebenau / Salzburg	2005	500	1050	32	128	0.250
Gleinstätten / Styria	2006	2500 + 400	5700	90	1315	0.068
Aich-Assach i. Ennstal / Styria	2006	500	1150	n.a.	327	n.a.
Oberzeiring / Styria	1998/ 2007	800 + 1000	4700	non ^c	408	non ^c
Scharnstein / Upper Austria	1992/ 1996/ 2009	1000 + 1600 + 1200	19817	48 + 60	685	0.158

Plant site	Start of Op. [year]	Biomass boiler(s) [kW]	Length of district heating grid [m]	Volume of central thermal storage [m ³]	Collector area [m ²]	Storage volume per unit collector area [m ³ /m ²]
Saxen / Upper Austria	2007/ 2009	500 (+300) ^h	n.a. (+500) ^h	24	300	0.080
Mattsee / Salzburg	2009	1300 + 200	2600	40	260	0.154
Oberlech / Vorarlberg	2009	2500	3500	67	621	0.108
Pölling / Upper Austria	2009	800 + 100	2250	n.a.	198	n.a.
Obertrum / Salzburg	2010	6000 ^d (+500) ^h	7000 + 3000	n.a. ^e	405	n.a. ^e
Eugendorf / Salzburg	2010	3500 (+700) ^h	11000	94	772	0.122
Weichstetten / Upper Austria	2010	750	3000	20	250	0.080
Sirnitz / Carinthia	1990/ 1998/ 2011	500 + 350 + 1500	>1300	40	218	0.183
Hirschegg / Styria	2011	n.a. ^f	> 250	20	102	0.196
Tillmitsch / Styria	2011	n.a. ^g	4200	n.a.	287	n.a.
Bregenz / Vorarlberg	2007/ 2012	540 + 300	500	8	171	0.047
Seekirchen / Salzburg	2012	1900 (+400) ^h	3500	n.a.	250	n.a.
Freistadt / Upper Austria	2012	850 (+850) ^h	2500	n.a.	250	n.a.

Explanations: a ... originally installed solar collectors replaced by PV panels in 2009;
b ... thermo oil boilers for an Organic Rankine Cycle application;
c ... no central storage tank but return flow booster, water content of district heating pipeline (incl. boilers) = 30,000 liters;
d ... boiler for combined heat & power application;
e ... no central storage tank but solar collectors works with decentralized energy storage with 3000 l per supplied building;
f ... 1 biomass boiler with unknown capacity;
g ... 2 biomass boilers with unknown capacity;
h ... planned but not yet installed.

In comparison to solar-assisted biomass district heating systems listed in Table 2-8 the following summary comprises block heating systems or micro-grids, where the nominal thermal capacity of the used boiler is lower than 250 kW_{th} or less than three separate buildings are connected to the micro-grid (see Table 2-9).

Table 2-9: Solar-assisted biomass micro grids in Austria - Status end of 2012 (data source: own research via internet; for more detailed information please refer to the appendix)

Plant site	Start of Op. [year]	Biomass boiler(s) [kW]	Length of district heating grid [m]	Volume of central thermal storage [m ³]	Collector area [m ²]	Storage volume per unit collector area [m ³ /m ²]
Weibern / Upper Austria	1996	100	n.a.	1 + 0.5 ^a	44	0.034
Gleisdorf / Styria	1998	40	n.a.	14	233	0.060
Judendorf-Strassengel / Styria	1999	125	135	5	106	0.047
St. Florian / Upper Austria	2000	700	100	n.a.	n.a.	n.a.
Wettmannstätten / Styria	2001	125	95	5	106	0.047
Salzburg / Salzburg	2002	150	n.a.	n.a.	400	n.a.
Salzburg / Salzburg	2003	150	n.a.	n.a.	160	n.a.
Weyregg / Upper Austria	2004	110	n.a.	7	46	0.152
Villach / Carinthia	2003	32 + 32 + 32 ^b	120	3.05	78	0.039
Asbach / Upper Austria	2004 / 2006	500	n.a.	2 + 2 + 1 ^c	30	0.167
Zemendorf / Burgenland	2007	110	100	1.5	n.a.	n.a.
Unterschützen / Burgenland	2007	110	80	1.4	n.a.	n.a.
Steinhaus / Upper Austria	2009 / 2010	960	700	30	100	0.300
Gleisdorf / Styria	2010	220	n.a.	6	92	0.065
St. Pantaleon- Erla / Upper Austria	2010	165	n.a.	6	60	0.100

Explanations: a ... 1 buffer tank 1000 l + 1 domestic hot water tank 500 l;
b ... original bio-diesel BHKW has been replaced by a 3. pellets boiler, each of the 6 residential buildings is equipped with a 300 l tank for DHW preparation;
c ... 3 separated hot water tanks used for space heating and domestic hot water preparation.

Besides the systems listed in Table 2-8 and Table 2-9 there are further solar-assisted district heating system in operation in Austria, which do not fulfill the criteria to be counted as solar-assisted biomass district heating system. Either the solar

thermal collector field directly feeds into a conventional district heating system with or without of the use of a buffer tank or the auxiliary heating system is exclusively fueled by natural gas or fuel oil.

2.3.3 Support scheme for solar-assisted biomass district heating systems in Austria

In 2007 Austrian's Federal Government set up the Climate and Energy Fund (Klima- und Energiefonds) in order to fund climate protection and energy projects. Since its foundation the fund has supported around 43000 projects within the last 5 years in the field of research & development, electric mobility, transportation, renewable energies, energy efficiency, model regions, as well as projects in sustainable building construction and renovation (see klimafonds (2013)).

Within the subject area of "renewable energy projects" the topic "solarthermics – large-scale solar thermal plants" has been promoted with a total budget of 3.694 million Euros dedicated to the third call for proposals and 6.008 million Euros dedicated to the second run. Until September 2012 three tender procedures have been executed collecting grant applications with respect to the following sub-topics:

- Solar process heat for production plants,
- Feed-in of solar heat into district heating systems or micro-grids,
- High solar fractions (above 20%) of total heat demand for business and service enterprises,
- Solar-assisted air conditioning and its combination with domestic hot water preparation and space heating outside the heating season.

As a prerequisite to apply for a maximal investment incentive of 450000 Euro per single project, the applicant has to prove that the installed solar collector fields will be in the range of 100 m² to 2000 m². If the project is selected to be part of an accompanying research program, the project owner will have to install appropriate measuring equipment and will have to agree to a publication of results (see Leitfaden (2012)).

According to the project data base of already funded projects during the first, second and third call for proposals 117 grant applications have been accepted in the field of "solarthermics – large-scale solar thermal plants". Out of this 49 projects dealing with the feed-in of solar heat into district heating systems or micro grids have been granted a non-refundable investment incentive (see klimafonds (2013)).

3 Methodologies

In the following chapters the methodologies applied in the frame of this master thesis are outlined. For the energetic assessment of the observed scenarios first the determination of the connected heat load, the annual heat demand curve and heat load profile of a biomass district heating system in Moosburg/Carinthia is shown. Second, the computing of solar fraction and the share of solar thermal energy fed into a solar-assisted biomass district heating system via the simulation program SHWin is described. Third, the methods to assess the ecological effects by gaseous and dust particle emissions are outlined. Finally an overview of the economic assessment of the investigated biomass district heating systems with or without solar thermal support is given. Following the usual approach for heating plants the dynamic annuity method proposed by guideline VDI 2067, Blatt 1 (2012) shall be applied.

3.1 Method of approach

3.1.1 Determination of connected heat load, annual heat demand curve and heat load profile of a biomass district heating system in Moosburg

The shape of the curve describing the annual heat demand of a district heating network depends on the ambient temperature conditions. Due to the behavior of the ambient air temperature it is split into two sections, which represents the heat load during the heating season and the heat load during summer time. If the air temperature is below the heating limit temperature, the useful heat fed into the district heating grid is used for space heating in addition to domestic hot water preparation, process heat supply and the coverage of heat losses in the grid.

As shown by several detailed studies, the connected heat load of a single heat consumer's space heating system is linearly dependent on the ambient air temperature (see Winter & Obernberger (2002), page 4). Based on this behavior the connected heat load (Q'_{CL}) of a district heating system comprising the load for space heating of several connected heat consumers could be calculated by the following approximation:

$$Q'_{CL}(\theta_a) = \left[\frac{\theta_{in} - \theta_a}{\theta_{in} - \theta_{a,nom.}} \right]^+ \cdot Q'_{max.,eff.} \quad [kW_{th}] \quad \text{Equation 44}$$

θ_a ... temperature of ambient air measured at a specific point in time [°C]

θ_{in} ... inner temperature of the heated room or building [°C], e.g. +20°C for required comfort

$\theta_{a,nom.}$... min. temperature measured at the location the heating system is configured for [°C]
 $Q'_{max,eff.}$... effective maximal heat load of space heating system [kW_{th}]; see Equation 8
⁺ ... only positive values for $\theta_a \leq +12^\circ\text{C}$ (= heating limit temperature)

The effective heat demand for space heating ($Q_{eff.,H,op.}$) within the heating system's operation period ($\Delta t_{H,op.}$) is approximately calculated by summing up the connected heat load ($Q'_{CL,i}$; assumed to be constant during time interval i) times the time interval Δt_i over the period of time the heating system is evaluated, multiplied by a service factor (see Kranzl (2010)):

$$Q_{eff.,H,op.} = f_s \cdot \sum_i Q'_{CL,i} \cdot \Delta t_i \quad [\text{kWh}_{th}] \quad \text{Equation 45}$$

f_s ... service factor for central heating of multiple dwellings [-]; $f_s = 0.9$ for district heating
 $Q'_{CL,i}$... connected heat load assumed to be constant during time interval Δt_i [kW_{th}]
 Δt_i ... time interval i within the operating period of the heating system

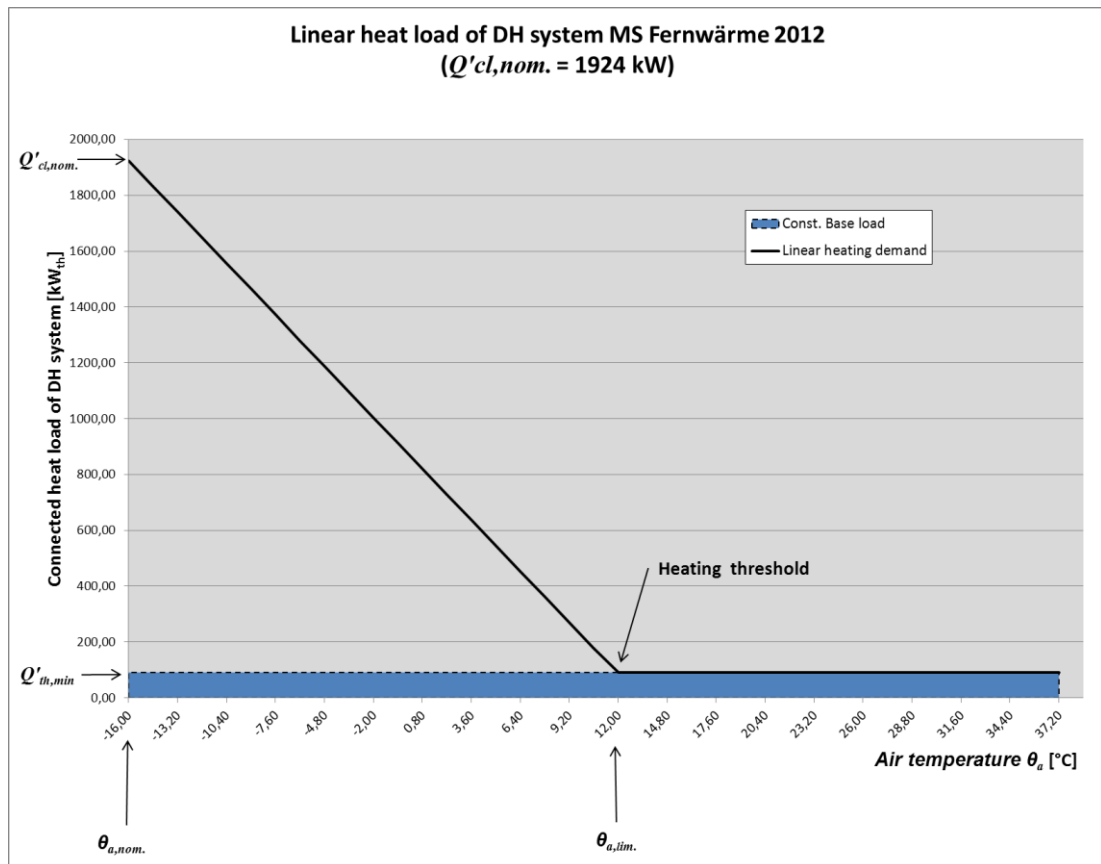


Figure 3-1: Linear heat load curve of a district heating system depending on the ambient air temperature (data source: Winter & Obernberger (2002)).

Explanations: $Q'_{th,nom.}$... Nominal heat load [kW_{th}];
 $Q'_{th,min.}$... Minimal load for heating [kW_{th}];
 $\theta_{a,lim.}$... Heating limit temperature [°C], e.g. 12 °C;
 $\theta_{a,nom.}$... Nominal air temperature [°C], e.g. - 16 °C;
 θ_a ... Ambient air temperature [°C].

If the air temperature is above the temperature threshold ($\theta_a > 12 \text{ }^\circ\text{C}$), no space heating will be required and the heat demand becomes approximately constant (see Figure 3-1). In order to estimate the head demand for grid losses a monthly percentage rate of the fed-in heat is applied, as the evaluation of empirical data provides an indication of the expected losses depending on the mode of operation and the season of year.

For determination of the annual head demand curve of the district heating system the approach of Sochinsky is chosen. A real annual heat demand curve can be approximated by the following time-dependent function $Q'_{th}(t)$ (see Schallenberg (1998)):

$$Q'_{th}(t) = Q'_{th,max} \cdot \alpha(\tau) = Q'_{th,max} \cdot (1 - (1 - \alpha_{min}) \cdot \tau^b) \quad [kW_{th}] \quad \text{Equation 46}$$

$Q'_{th,max}$... Maximal heat load demanded by the district heating network $[kW_{th}]$

$\tau = t / t_{H,Op}$... Ratio of variable time to overall operating time for heat supply [-]

$\alpha(\tau)$... Exponential function according to Sochinsky [-]

$\alpha_{min} = Q'_{th,min} / Q'_{th,max}$ [-]

$Q'_{th,min}$... Minimal heat load demanded by the district heating network $[kW_{th}]$

$\alpha_m = Q'_{th,m} / Q'_{th,max} = t_{H,V} / t_{H,Op}$ [-]

$Q'_{th,m}$... Mean heat load demanded by the district heating network $[kW_{th}]$

$t_{H,V}$... Number of full load hours per anno $[h/a]$

$t_{H,Op}$ [-] ... Number of operating hours per anno $[h/a]$

$b = (\alpha_m - \alpha_{min}) / (1 - \alpha_{min})$

Sochinsky's function is an approximate model to predict the annual behavior of the effective, connected heat load of a district heating network. The total amount of heat (Q_{th}) demanded by the heat users in the district heating system is calculated by integrating the area below the exponential heat duration curve (see Schallenberg (1998)):

$$Q_{th} = \int_0^{t_{H,Op}} 1 - (1 - \alpha_{min}) \cdot \left(\frac{t}{t_{H,Op}} \right)^{\frac{\alpha_m - \alpha_{min}}{1 - \alpha_{min}}} \cdot Q'_{th,max} dt \quad [kWh_{th}] \quad \text{Equation 47}$$

As a model applicable for the biomass district heating system investigated in this study it is assumed, that the heat demand for space heating during the heating season and the heat losses in the grid behave like Sochinsky's exponential function ($\alpha(\tau)$). Outside the heating period the base load (i.e. the heat demand for domestic hot water preparation plus the heat load lost due to circulation in the grid) shall be constant.

Consequently the area below the curves describing the heat demand for space heating and for grid losses can be calculated by integration of the related Sochinsky function over the observed period of time (i.e. $\Delta t_{H,Op}$). The heat demand to be covered for domestic hot water preparation and for coverage of base load outside the heating season is represented by areas in the shape of rectangles (see Figure 3-2).

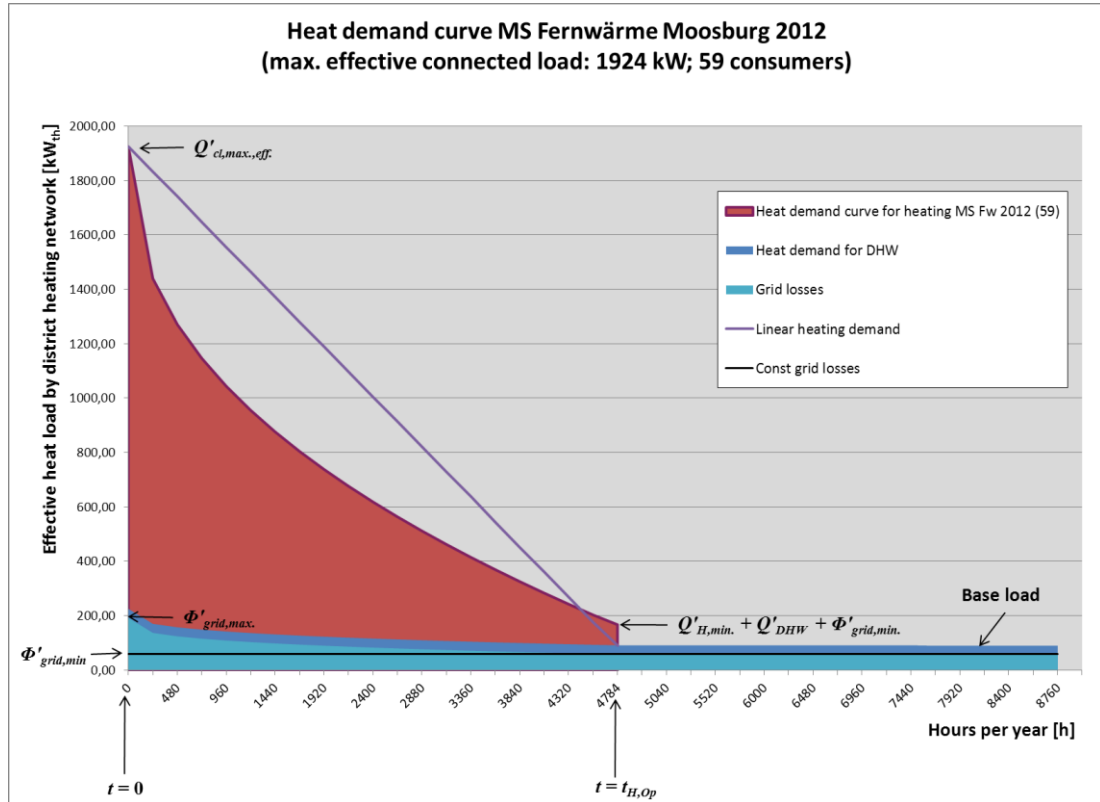


Figure 3-2: Heat demand curve of a district heating system depending on time (data source: own calculations).

Explanations: $Q'_{cl,max,eff.}$... Maximal effective connected heat load [kW_{th}];
 $\Phi'_{grid,max.}$... Maximal heat load for grid losses [kW_{th}];
 $\Phi'_{grid,min.}$... Minimal heat load for grid losses [kW_{th}];
 $Q'_{H,min.}$... Minimal heat load for space heating [kW_{th}];
 Q'_{DHW} ... Heat load for domestic hot water preparation [kW_{th}];
 $t_{H,Op}$... Operating time for heating [h].

Knowing the heat demand curve for a given district heating system, it is possible to dimension the nominal capacity of the installed biomass boiler as well as the necessary capacity of the required peak-load boiler in the central heating station. Furthermore, due to the evaluated heat demand based on the area below the heat demand curve, the heat input ($Q_{th,NCV}$) and the respective furnace thermal capacity ($Q'_{th,NCV}$) can be determined. With the help of these indicators the annual fuel input for the respective thermo-chemical conversion unit (i.e. firing box for solid biomass

and heating oil burner) can be estimated. As a prerequisite the related energy conversion efficiency during the applied mode of operation must be known.

The total amount of thermal energy produced in the central heating station of the district heating system will be fed into the district heating network in order to cover the connected heat users' heat demand. Losses due to distribution and storage of heat inside the heating station are not considered by this approach. However, the next section will show how to allocate the share of produced heat to several renewable energy resources. Via the simulation program SHWwin the solar fraction and the share of solar thermal energy fed into a solar-assisted biomass district heating system are computed.

3.1.2 Computing of solar fraction and the share of solar thermal energy fed into a solar-assisted biomass district heating system via simulation program SHWwin

Based on the evaluation of the expected heat load and the heat consumers' user profile done with the methods described above, the effects of a solar thermal system feeding into a biomass district heating system are studied. In order to get reasonable values for solar fraction and the share of solar thermal energy substituting a considerable amount of heat generated by the heating station's boilers, a Microsoft Windows based simulation program is used. In the frame of this study the program is applied on two different configuration scenarios of the district heating system in Austria. The scenario in Moosburg/Carinthia represents a different stage of expansion of the current district heating grid, a different biomass boiler capacity and the layout of a newly built solar thermal system supporting the current district heating grid. In addition, the performance of the reference system erected in the year 1997 in Eibiswald/Styria is simulated based on historical irradiation and temperature data.

The program, called SHWwin, has been developed by members of the Technical University of Graz since 1993 and was released in the year 1999 by the Institute of Thermal Engineering (see SHWwin (1999)). SHWwin has been verified in the frame of several research projects and has shown realistic results when compared with measurements taken at solar-assisted heating systems.

It is possible to simulate solar thermal systems for the purpose of domestic hot water preparation as well as solar thermal combi-systems, which are applied to meet the requirements for hot water preparation and space heating at the same time. For each system variant the integration with a domestic hot water tank, a

buffer tank or heating water storage can be considered for computing. Finally SHWwin enables the user to simulated solar-assisted district heating systems including a centralized hot water storage tank. Figure 3-3 gives an overview on an example system configuration.

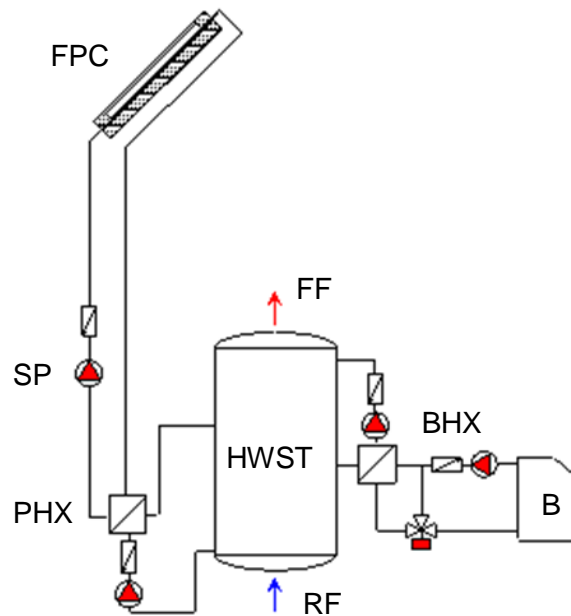


Figure 3-3: Example configuration of a solar-assisted district heating system simulated by simulation program SHWwin (data source: SHWwin (1999)).

Explanations: FPC ... Flat plate collectors;
SP ... Circulation pump of solar circuit;
PHX ... Plate heat exchanger;
FF ... Forward flow;
HWST ... Hot water storage tank;
RF ... Return flow;
BHX ... Heat exchange unit of boiler;
B ... Boiler.

As the simulation program is equipped with a graphical user interface, the input of project specific data, frame conditions and characteristic parameters of the applied system components could be easily done via desktop PC or Laptop. The following components can be either selected from a pre-filled and extendable date base or can be configured in dedicated input windows:

- The solar thermal collector,
- the storage tank (hot water tank or buffer storage),
- the control system (for collector field, storage tank, hot water circulation and boiler),

- the daily demand for domestic hot water in the network,
- building parameters & space heating characteristics or frame conditions for district heating, and
- boiler parameters.

For meteorological data of the selected plant site, the simulation program must be linked to a simple file containing hourly irradiation data of global and diffuse radiation on-site as well as ambient air temperature values on hourly basis.

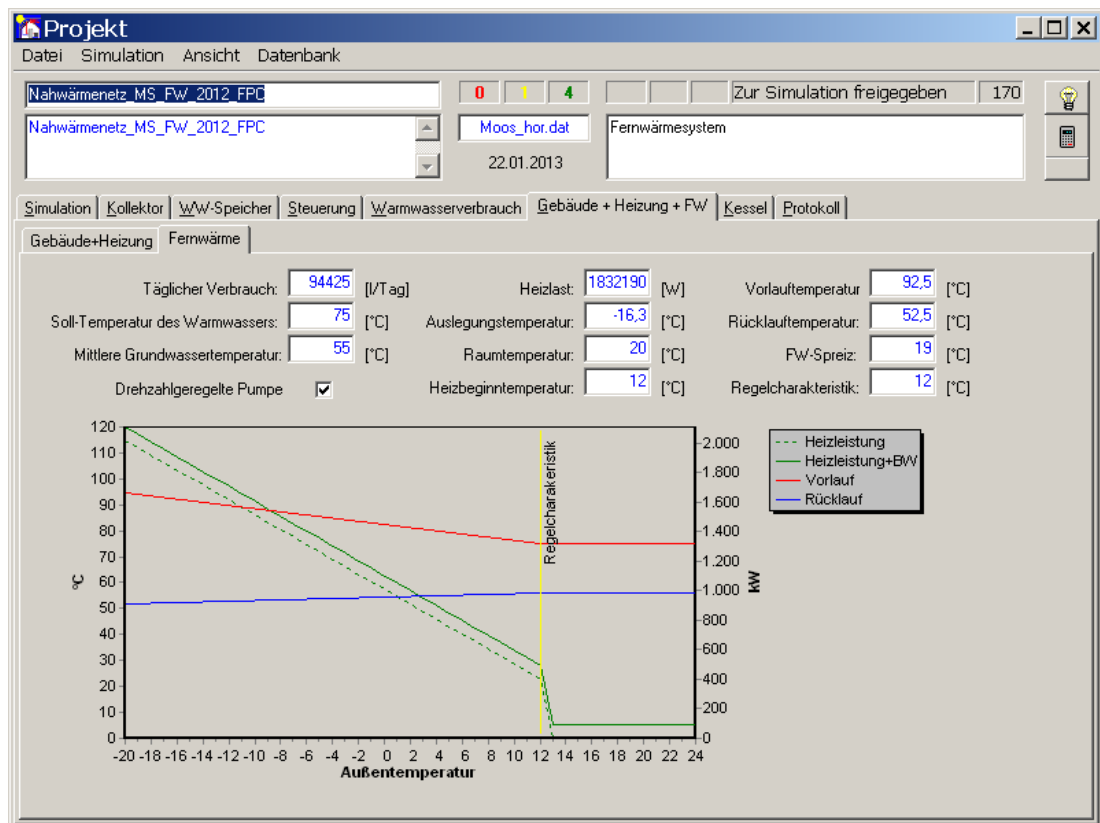


Figure 3-4: Screen shot of input window for frame conditions of district heating including the control cam for forward and return flow temperature (data source: SHWwin (1999)).

Explanations:

- ... Connected heat load for space heating;
- ... Connected heat load for space heating + load for DHW preparation;
- ... Forward flow temperature;
- ... Return flow temperature;
- ... Heating limit temperature.

In case of a solar-assisted district heating system, the forward flow temperature, the return flow temperature as well as the mass flow in the district heating network have

to be predefined. According to the discussion of methods for heat load prediction done before, the temperature dependent heat load measured at the feed-in point to the district heating grid follows the course of the curve shown in Figure 3-1.

Consequently SHWwin determines the necessary flow temperature, return flow temperature and the required difference in flow temperatures according to the control cam displayed in Figure 3-4.

The user of simulation program SHWwin can choose one out of the following options to define the appropriate heat demand in the district heating network, which determines the control cam for flow temperature control. In any case the total heat load is a sum of loads for space heating, domestic hot water preparation and grid losses as part of base load in the grid (see SHWwin (1999)):

- In option one the forward flow is controlled with a constant mass flow according to the control cam. If the space heating demand decreases to zero, the mass flow will be reduced according to the heat load required for DHW preparation at the consumers' sub-stations. The temperature difference of supply and return flow is set up as a fix value during summer operation.
- In option two the heat load in the grid as well as the forward flow temperature and the return flow temperature is predefined according to the expected behavior of the outside temperature. The simulation program computes the resulting mass flow in this case, which is a more realistic operation scenario for district heating systems, as in most systems speed-controlled hot water circulation pumps are applied.

However, the operation time of the hot water circulation pumps and the respective electricity do have a small impact on the ecological effects of a solar-assisted district heating plant. Nevertheless, the ecological effects with respect to gaseous and particle emissions should be considered as well. The next sub-chapter will deal with a method to assess this type of emissions and to compare the ecological effects of solar-assisted district heating systems with conventional district heating systems.

3.1.3 Ecological appraisal and determination of greenhouse gas savings and air pollutants savings

To assess the ecological effects of solar thermal supported district heating applications a two-step approach has been chosen. At first gaseous emissions as well as other recognizable emissions of biomass-fueled furnaces and heating oil

fueled burners are calculated in case of continuous operation and clocked operation. As an input parameter the annual demand of primary energy ($Q_{NCV,an.}$) in form of wood chips or heating oil is used as basis to compute the emissions of carbon dioxide (CO_2), carbon monoxide (CO), hydro carbons (C_xH_y) and nitric oxide (NO_x), as well as the emission of dust particles.

Heimrath et al. (2002) propose a list of emission factors applicable for continuous operation and start-stop operation of a biomass fueled firing system and an oil burner (please refer to Table 3-1). It is assumed, that the continuous operation is related to a load situation, which is greater than 30% of the boiler's nominal thermal power. The start-stop operation, which includes the clocked operation mode, will refer to a load situation, which requires less than 30% of the boiler's nominal thermal power.

As the head demand curve of the investigated district heating system has been predicted before, the share of heat produced by the biomass boiler and the heat from the oil boiler can be calculated by using the approach of Sochinsky-Jung. With the help of average boiler efficiencies the annual fuel demand in continuous operation and start-stop operation mode can be calculated. Consequently, the primary energy content of the converted amount of solid biomass and fossil fuel can be determined via the net calorific value. For wood chips, which are a mixture of spruce, pine and beech with a water content of 30%, a net calorific value per unit volume ($NCV_{wc30\%,vol.}$) equal to 795.1 kWh/SRM has been taken as a basis. For heating oil a net calorific value per unit mass ($NCV_{oil,mas.}$) equal 11.8 kWh/kg is used.

Table 3-1: Emission factors for continuous and start-stop operation of boilers equipped with biomass fired furnaces and oil fueled burners in relation to primary input energy (data source: Heimrath et al. (2002), page 47)

Type of fuel	Mode of operation	CO_2 [g/kWh _{NCV}]	CO [g/kWh _{NCV}]	C_xH_y [g/kWh _{NCV}]	NO_x [g/kWh _{NCV}]	Particles [g/kWh _{NCV}]
Biomass	Continuous operation	0.000	0.117	0.005	0.374	0.120
Biomass	Start-stop-operation	0.000	4.069	0.281	0.374	1.955
Heating oil	Continuous operation	270.000	0.060	0.010	0.234	0.000*
Heating oil	Start-stop-operation	270.000	0.391	0.046	0.234	0.000*

*Explanations: * ... For heating oil no particle emissions are considered.*

In case of a solar-assisted district heating system a considerable share of the annual heat production of the plant, the so-called solar fraction savings are covered by the thermal energy output of the solar thermal system. Depending on the way the biomass boiler and oil boiler are operated in parallel to the solar thermal system the result will be a specific amount of annual primary energy savings. The positive savings gained within one year of operation can be measured in form of wood chips left in the storage or heating oil still available in the oil tank.

For both configurations, either the solar-assisted or the simple biomass district heating system, the emissions of carbon dioxide (CO_2), carbon monoxide (CO), hydrocarbons (C_xH_y) and nitric oxide (NO_x), as well as the emission of dust particles (i.e. fine particles) are determined based on the emission factors defined in Table 3-1. Then the results are compared with each other in order to determine a positive or negative ecological effect with respect to emissions.

The comparison could have two contrasting results representing the change in boiler operation when the assisting solar thermal system is integrated in the district heating plant. On the one hand there could be an effective emission saving due to the share of solar heat produced especially outside the heating period. On the other hand there could be an increase of emissions, as more heating oil is burned as before. This would be the case, if the oil boiler is applied as a peak-load boiler outside the heating season, while the biomass boiler is not operated during summertime at all.

In a second step the greenhouse gas (GHG) emissions as well as air pollutants savings compared to conventional district heating systems should be evaluated. According to Kalt & Kranzl (2009) the GHG emissions of the reference systems are mainly the result of CO_2 release by combustion of fossil energy carriers. In case of solid biomass-fueled district heating applications the main part of GHG emissions can be assigned to energy and fuel consumption within the supply chain of wood chips done beforehand. The minor part of GHG emissions can be assigned to the fossil fuels burned in order to cover peak loads or a biomass boiler outage.

The generation of heat with solar thermal systems is characterized by normal operation without any emission of greenhouse gases, air pollutants or other toxic substances (Kaltschmitt & Streicher (2009), page 150). If the whole life cycle of a solar thermal system is analyzed, one will find the biggest share of emissions when balancing the fossil energy used during production process of solar collectors or thermal storages. Further emissions can be assigned to transport of components to the plant site and to the construction work on site.

In order to quantify the emitted greenhouse gases and air pollutants during the whole life cycle the following formula should be used (see Kalt & Kranzl (2009)):

$$\Delta EMI = EMI_{ref,heat} - EMI_{SADHP,heat} \quad [kg / MWh] \quad \text{Equation 48}$$

$EMI_{ref,heat}$... emissions based on used final energy at the consumer sub-station
[kg/MWh]

$EMI_{SADHP,heat}$... greenhouse gas or air pollutants emissions for the solar-assisted district heating system based on used final energy at the consumer sub-station
[kg/MWh]

ΔEMI ... emission savings by considering the cumulative, non-regenerative emissions of the production process & supply chain (net savings) [kg/MWh]

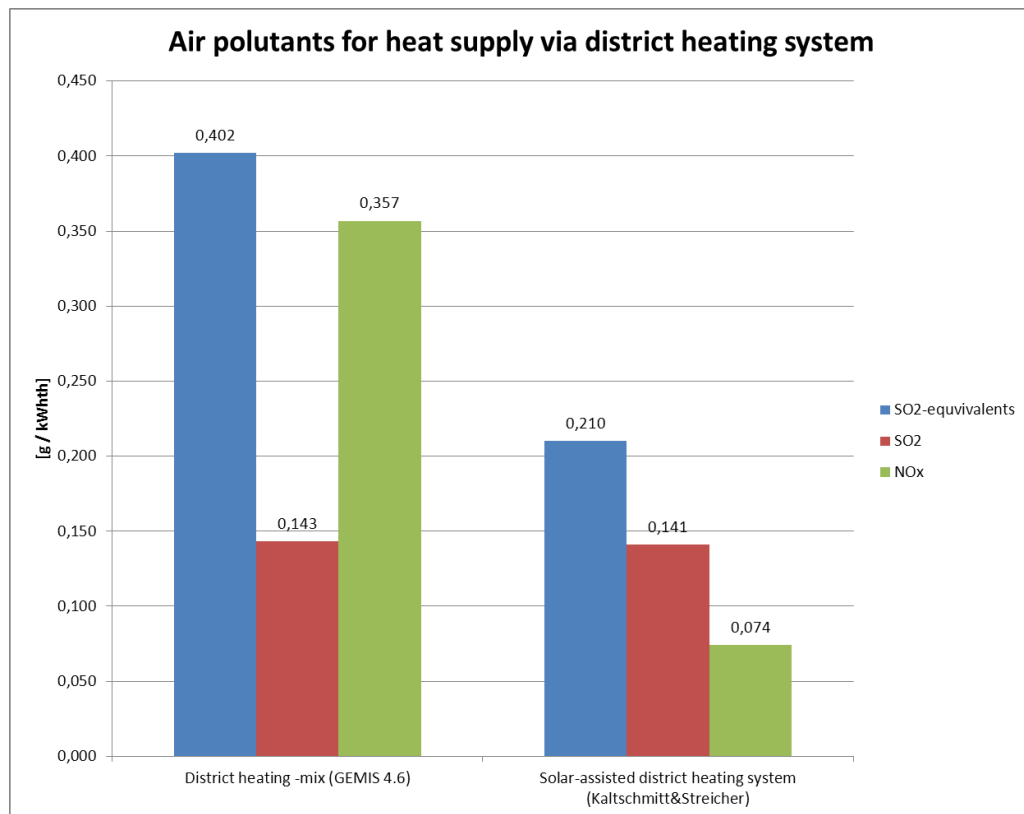


Figure 3-5: SO₂-equivalents, SO₂ emissions, NO_x emissions in [g / kWh_{th}] for district heat supply. Air pollutants' balance calculated for the whole life cycle of conventional district heating mix* (data source: GEMIS 4.6 (2010)) compared to the air pollutants' balance of a solar-assisted district heating system** (data source: Kaltschmitt & Streicher (2009), page 144)

Explanations: * ... Final energy utilization of district heat at the consumers' heating sub-stations with a heat utilization factor of 1;

** ... DH system with 15% grid losses and an average heat utilization factor of 0.95 for consumers heating sub-stations: network length: 2000 m, heat supply: 2750 MWh/a, collector area: 650 m², steel tank: 55 m³.

If Equation 48 is used as a basis, the air pollutants savings (in SO₂-equivalents) and the greenhouse gas emission savings (in CO₂- equivalents) compared to a

reference system will be evaluated. As a reference the greenhouse gas emissions balance and the air pollutant emissions balance evaluated for a district heat supply mix by GEMIS 4.6 (2010) is introduced. In addition the life cycle data for a solar-supported district heating system given by Kaltschmitt & Streicher (2009) are taken as input data (see Figure 3-5 and Figure 3-6).

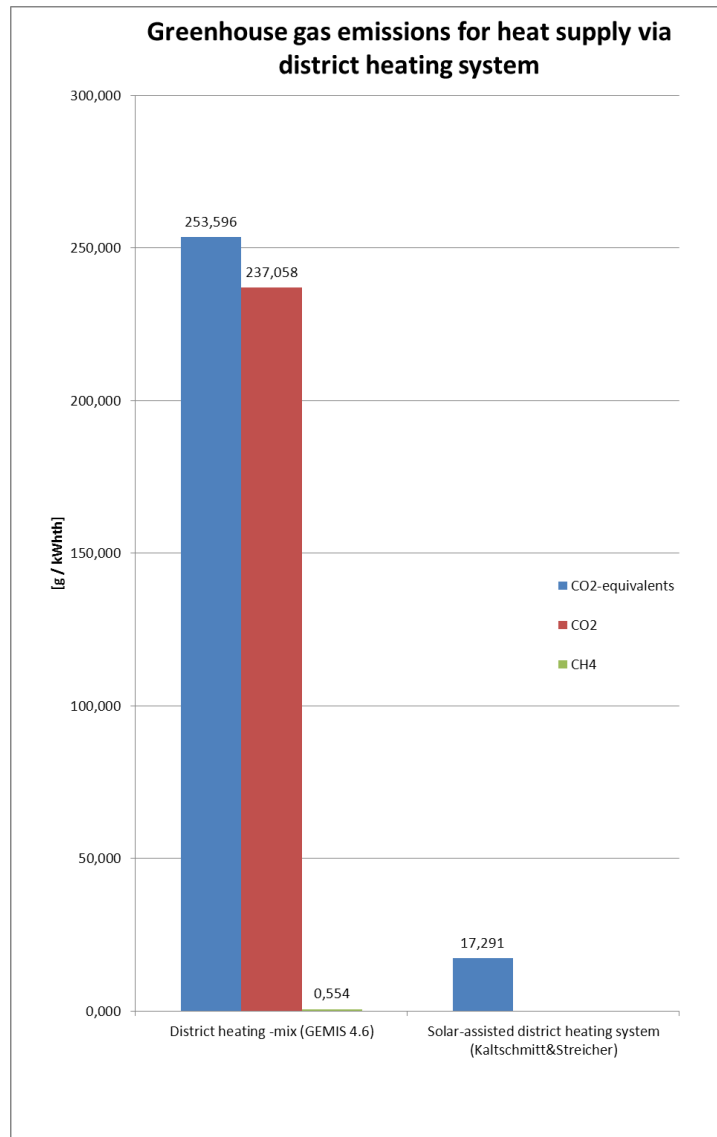


Figure 3-6: CO₂-equivalents in $[g / kWh_{th}]$ for district heat supply. Greenhouse gas emissions' balance calculated for the whole life cycle of conventional district heating mix* (data source: GEMIS 4.6 (2010)) compared to the GHG emissions' balance of a solar-assisted district heating system** (data source: Kaltschmitt & Streicher (2009), page 144)

Explanations: * ... Final energy utilization of district heat at the consumers' heating sub-stations with a heat utilization factor of 1;
** ... DH system with 15% grid losses and an average heat utilization factor of 0.95 for consumers' heating sub-stations: network length: 2000 m, heat supply: 2750 MWh/a, collector area: 650 m², steel tank: 55 m³.

Besides the ecological effect the fuel demand of a heating plant influences the system's economic performance due to its costs. In the following chapter the method used to evaluate the techno-economic feasibility of the applications is outlined in more detail.

3.2 VDI Guidelines

As a district heating system operator is mainly interested in the economic feasibility of his heating plant, the economic performance of a heating plant should be assessed in advance. Guideline VDI 2067, Blatt1 (2012) provides an established method for a dynamic approach.

3.2.1 Economic appraisal and evaluation of techno-economic feasibility according to guideline VDI 2067: Economic efficiency of building installations

As the technology described in this study is considered to be state-of-the-art and well proven, one could assume that it is easy to get proper information about investment and operation costs of such applications. Unfortunately the overall investment depends on the individual project, the local conditions and other specific factors. That is because no standard prices and costs can be found. In order to get an overview of some reasonable figures a set of sources have been used to calculate the initial investment costs for solar thermal systems (see Kaltschmitt & Streicher (2009), SDH (2012), Biermayr, et al. (2012)).

For an economical appraisal of the selected solar-assisted biomass district heating projects the approach suggested by VDI 2067, Blatt1 (2012) has been chosen. As described in this guideline costs for maintenance can be calculated based on the investment for the specific plant configuration as a percentage rate. For insurance costs and administration costs a similar approach can be used. Due to the fact that for some components like a loader the life time is lower than the investment horizon of 20 years, a re-investment has to be considered in the evaluated projects. VDI 2067, Blatt1 (2012) gives also suggestions for the life time of the other installed components. It proposes the mathematical way to compute the terminal value of these parts with a life time exceeding the investment horizon.

However, in this study an overall project life time of 20 years is taken as a basis. While during the first years the plant is operated as a pure biomass district heating plant, the investments for a solar thermal extension are foreseen 3 to 4 years after the start of operation. Consequently, the observation period for the combination of

solar thermal plant and biomass heating plant is either 17 or 16 years, which is a quite short period of time to show positive economic feasibility.

Following the approach of VDI 2067, Blatt1 (2012) the costs of project are evaluated by splitting them into 4 groups: capital costs, consumption costs, operations and maintenance costs, and other costs. Typically each cost item is determined for the period of one year. One-time costs like project development costs, construction costs and engineering costs are summed up as initial investment. They are assigned to year zero. Re-investments are done in the year the life time of the component is over. Current costs for capital, consumption, operation and maintenance are adapted with a fixed rate of price increase and incomes are reduced by an annual inflation rate. For the income from supplied and sold heat a dedicated rate of heat price increase is applied.

VDI 2067, Blatt1 (2012) suggests the annuity method in order to calculate the economic feasibility of an investment. As described there the total annuity (A_N) of all costs of an installation equals the difference between the annuity of proceeds ($A_{N,E}$) and the sum of the annuities of the capital-related, demand-related, operation-related and other costs:

$$A_N = A_{N,E} - (A_{N,K} + A_{N,V} + A_{N,B} + A_{N,S}) \quad [\text{€}] \quad \text{Equation 49}$$

$A_{N,E}$... annuity of proceeds
 $A_{N,K}$... annuity of capital-related costs
 $A_{N,V}$... annuity of demand-related costs
 $A_{N,B}$... annuity of operation-related costs
 $A_{N,S}$... annuity of other costs

For a given period under observation (T), usually a period of several years ending at the investment horizon, one-time investments, current costs and incomes can be summarized with the use of the annuity factor a into yearly constant cash flows.

$$a = \frac{i \cdot (1+i)^T}{(1+i)^T - 1} = \frac{q^T \cdot (q-1)}{q^T - 1} \quad [1] \quad \text{Equation 50}$$

a ... annuity factor [1] aka. Capital Recovery Factor (CRF)
 i ... interest rate [1]
 T ... observation period aka. period of several years ending at the investment horizon [a]
 q ... interest factor [1]; $q = (1+i)$

Like the method of calculating the Net Present Value (NPV) of an investment the annuity calculation is a dynamic approach to evaluate the economic feasibility of an investment. If the total annuity (A_N) is positive, the investment project could be

accepted. If it is negative, the project should be rejected. In case two similar projects are compared, the project with the greater positive total annuity is the more economic one (see VDI 2067, Blatt 1 (2012), page 11). The determination of the Net Present Value (*NPV*) of the investment project should result in the same total annuity according to

$$A_N = NPV \cdot CRF = NPV \cdot a \quad [\text{€}] \quad \text{Equation 51}$$

A_N ... total annuity determined for an installation's investment project [€]

NPV ... Net Present Value of an investment project evaluated over observation period [€]

a ... annuity factor [1]

CRF ... Capital Recovery Factor [1]

In this case the *NPV* will be calculated based on the nominal cash flow per year without considering depreciation and taxes.

As a part of the economic appraisal the total annuity of a project will be analyzed in the frame of a sensitivity analysis. The influence on the project's total annuity by the variation of fuel costs for wood chips and costs for heating oil, the variation of electricity costs, consumption costs, maintenance costs, operational costs, and other costs as well as the variation of net heat price determined at a specific point in time shall be displayed as graphs. The point of intersection with the zero line represents the necessary percentage rate for variation, which is necessary to change the total annuity from positive to negative or vice versa.

Finally, the Long Run Generation Costs ($LRGC_H$) for useful heat generation by a solar-assisted biomass district heating system shall be calculated. To do this Kalt & Kranzl (2009) propose the following formula (see page 18):

$$LRGC_H = \frac{a \cdot c_{inv}}{T_{H,fl}} + SRMC_H = \underbrace{\left(\frac{a \cdot c_{inv}}{T_{H,fl}} \right)}_{c_{fix}} + \underbrace{\left(\frac{c_{fuel}}{\zeta_{H,an.}} + \frac{c_{O\&M}}{T_{H,fl}} \right)}_{c_{var}} \quad [\text{€} / \text{kWh}_{th}] \quad \text{Equation 52}$$

a ... annuity factor [1]

c_{inv} ... specific investment costs [€/kW_{th}]

$T_{H,fl}$... annual full load hours of the district heating system producing useful heat [h/a]

$SRMC_H$... Short Run Marginal Costs of heat generation [€/kWh_{th}]

c_{fix} ... unitized fixed costs [€/kWh_{th}]

c_{var} ... variable costs [€/kWh_{th}]

c_{fuel} ... specific fuel costs [€/kWh_{NCV}]

$c_{O\&M}$... specific operation and maintenance (O&M) costs [€/(kW_{th} a)]

$\zeta_{H,an.}$... annual heat utilization factor for heat generation [kWh_{th}/kWh_{NCV}]

The quantity $T_{H,\text{fl}}$ represents the equivalent full load hours calculated in using the installed heat capacity of the district heating system and the useful thermal energy fed into the district heating grid ($Q_{th,useful,an.}$) within a year. The amount of useful heat shall be predicted based on the heat demand curve according to Sochinsky by excluding the grid losses.

Unfortunately the calculation of Long Run Generation Costs ($LRGC_H$) for useful heat generation based on *Equation 52* requires several input parameters, which are hard to define. By way of comparison the same result can be obtained for $LRGC_H$ when the Annuity of Costs ($A_{N,C}$) is considered according to

$$LRGC_H = A_{N,C} \frac{1}{Q_{th,useful,an.}} \quad [\text{€} / kWh_{th}] \quad \text{Equation 53}$$

$A_{N,C}$... annuity of costs

$Q_{th,useful,an.}$... useful thermal energy fed into the district heating grid [kWh_{th}]

The Annuity of Costs ($A_{N,C}$) is the sum of annuity of capital-related costs, annuity of demand-related costs, annuity of operation-related costs, and annuity of other costs:

$$A_{N,C} = A_{N,K} + A_{N,V} + A_{N,B} + A_{N,S} \quad [\text{€}] \quad \text{Equation 54}$$

$A_{N,K}$... annuity of capital-related costs

$A_{N,V}$... annuity of demand-related costs

$A_{N,B}$... annuity of operation-related costs

$A_{N,S}$... annuity of other costs

While the Short Run Marginal Costs ($SRMC_H$) characterizes the heat generation costs for the existing heating plant, Long Run Generation Costs ($LRGC_H$) are taken into account for the installation of additional capacity (see Weissensteiner (2010)). If the determined $LRGC_H$ for heat production are below the feed-in tariff for heat, it can be assumed, that the heat generation facility will operate economically.

4 Analyses of Current Status and Solar Energy Potentials in Moosburg

In the next chapter an overview of the current status of the investigated biomass district heating system, the ambient conditions and the available solar potential as well as the potential of woody biomass fuels for this region of Austria will be given.

4.1 Current status of the biomass fueled district heating system

After a three years period of pre-planning and pre-studies, in December 2007 the limited company “MS Fernwärme Moosburg” was founded. Scope of business was in a first step the erecting of a biomass heating plant and a district heating network in the town of Moosburg. In a second step the operation of the district heating system by supplying and selling environmental-friendly generated heat to a number of about 65 heat consumer was planned.

Nearly two years later the first couple of heat consumers had been connected to the district heating network, while after a 2-years construction phase the central heating station started to operate ready before heating season. Up to the year 2012 the number of connected objects and the number of heating sub-stations were continuously growing, as the grid was extended to further service areas like a residential building area in the south of the municipality and the SOS Children's Village in Moosburg. During heating season 2011 / 2012 the current stage of expansion has been reached, so the next sub-chapters will describe the technical status of the biomass-fueled district heating system. Further on the local operating conditions are discussed in more detail.

4.1.1 Technical description of the biomass heating plant

The central heating station of the district heating application is located in the industrial zone north of the town of Moosburg. The plant-site can be easily accessed by trucks or heavy tractors with freight trailers (full-trailers), as it is situated near to a heavily frequented federal highway. So the solid biomass fuel in form of wood chips is mainly transported via truck to the site. In addition regional farmers can directly supply their forest residues in form of wood chips to the plant (just- in-time delivery). Before the fuel is stored at a dedicated storage area the volume of the solid biomass fuel is determined and the water content is measured. Finally the wood chips are unloaded to fuel storage (bunker).

In case of the heating station in Moosburg the separate fuel storage unit is integrated into the heating house, which is covered by a slightly tilted flat roof with a total area of 1020 m². Assuming a biomass fuel demand of 511.6 kg/h ($q_{NCV} = 3.42$ kWh_{NCV}/kg ; 30 wt.% (w.b.)) at nominal load conditions, that are 12.28 tons /day or 52.82 loose cubic meters per day (SRM/day), a fuel bunker capacity of 3600 cubic meters inside the storage facility provides a reserve of about 68 days. According to the biomass fuel demand in 2011 (7340 SRM/a), the storage capacity is sufficient for half a year of operation.

Forest wood chips (including bark) from the regional forestry with an average water content of 30 wt.% are utilized as biomass fuel. Due to the specifications given by ÖNORM M7133 this solid biomass fuel can be classified as wood chips G50/ W30/ S200/ A2 (see FNR (2010)). As mainly a mixture of spruce (70%) and pine (20%) with a small share of hard wood (e.g. beech: 10%) will be provided as a raw material for wood chips production, solid biomass fuel with an average lower heating value of 3.42 kWh_{NCV}/kg based on an average moisture content of about 30 wt.% (w.b.) is taken as a basis for further calculations of the woody biomass fuel's primary energy content.

From the storage the fuel is filled into the hydraulically-driven moving-floor conveyance system by a telescope loader. With a hydraulic stoker the wood chips are feed into an inclined, water-cooled moving grate furnace, where the thermal conversion of the solid biomass via combustion ($T > 800$ °C) takes place. The firing system is combined with a hot water boiler, which is constructed as a fire-tube boiler. The primary air is controlled in three zones underneath the grate, where as the secondary air is added with high impulse at the entrance to the combustion chamber. The hot flue gases from the firebox pass through a two-tube-line heat exchange unit (see Figure 4-1), transferring heat from medium gas to the heat carrier fluid (i.e. hot water). The system is not equipped with a hot water economizer, usually recovering energy from the flue gases from the outlet of the hot water boiler.

Urbas' hot water boiler unit is characterized by nominal thermal power of 1500 kW. This thermal capacity is transferred via a heating surface of 117 m², when the hot water in water cycle passes with a flow rate of 97 m³/h. Consequently, the furnace thermal capacity is set to $\dot{Q}_{NCV} = 1750$ kW assuming a boiler efficiency of 85.7% at nominal conditions.

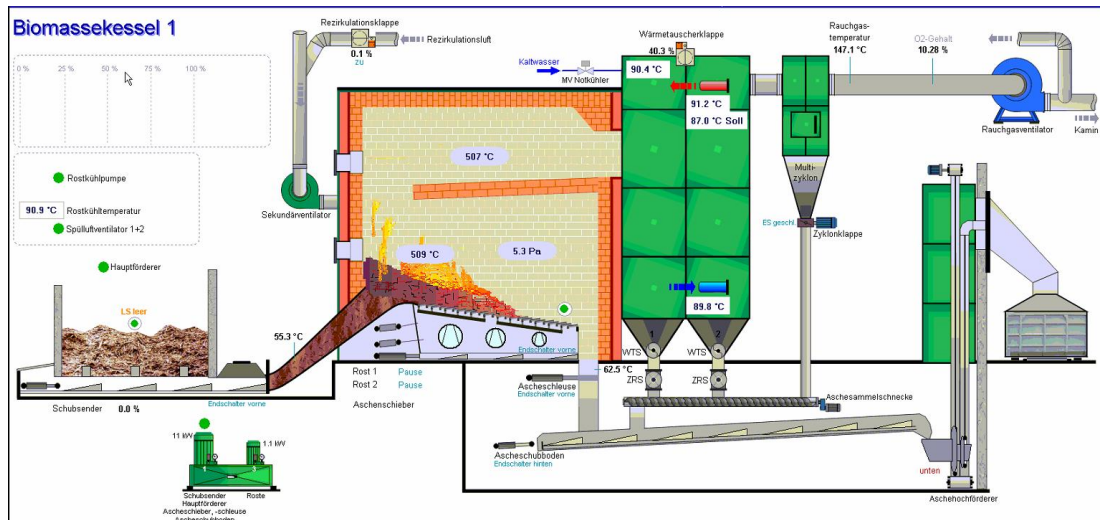


Figure 4-1: Schematic diagram of Urbas' firing technology for district heat generation by woody biomass combustion* (data source: Urbas (2009))

Explanations: * ... The displayed operating state shows parameters measured during start/stop-operation mode. The fed-in biomass fuel is glowing at a temperature of 509 °C, while the boiler's thermal capacity is sufficient to cover the connected heat load during summer period.

Subsequently, the flue gas is cleaned by one stage, where the precipitation of larger dust particles takes place in multi-cyclones. After the flue gas cleaning unit the flue gas driven by a flue gas fan enters the chimney. Bottom ash from the biomass fired grate furnace and ash from the multi-cyclones are collected by an ash removal unit. Finally these fractions are transported to the ash containers by a dedicated ash conveyor. Boiler ash, which is removed from the fire-tubes inside the heat exchanger, is also disposed via the ash containers. Due to the type of biomass fuel the ash content in relation to dry matter combusted in the fire box is slightly more than 1%.

The heating plant is operated in heat-controlled operation mode. As a basic requirement for heating plants based on biomass combustion, the heating station covers the base thermal load of the connected district heating grid. Peak thermal load in the district heating system is provided by an oil-fired peak load boiler, which also serves as a reserve. For immediate switch-over the oil boiler with a nominal capacity of 1500 kW is always in stand-by mode. Consequently, the circulation pump in the oil boiler's circuit has to run permanently in order to keep the necessary supply flow temperature (see Figure 4-2).

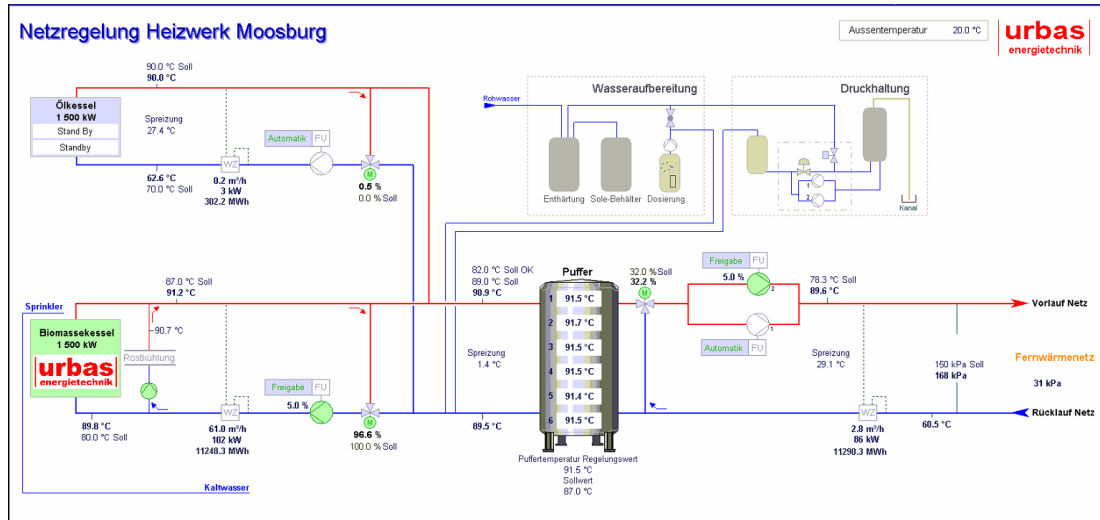


Figure 4-2: Schematic diagram of the biomass heating plants hydraulic scheme with parameters measured during summer load operation* (data source: Urbas (2009))

Explanations: * ... The displayed state of the hydraulic system shows parameters measured during summer operation mode. While the biomass boiler feeds hot water into the buffer tank at minimal load conditions, the oil boiler is in stand-by mode. Due to a low heat demand in the district heating grid supply flow and return flow temperature are relatively high.

The heating plant's hydraulic system has integrated a buffer storage tank for hydraulic interconnection of heat producing units and heat distribution units. The insulated steel tank with a volume of 35 m³ is installed inside the heating house. It is designed as hot water tank for heat load compensation (see Figure 4-2) and can store hot water in several stratified layers. As shown in Figure 4-2 the hydraulic system also includes a water treatment unit and a pressurizer. The central heating station's the connection to the two-pipe heating network is established by two hot water circulation pumps, which automatically alternate with one another during operation.

To get an overview of type and technical data of the central heating station of "MS Fernwärme Moosburg", the main key indicators are summarized in Table 4-1.

Table 4-1: Key indicators of biomass heating plant "MS Fernwärme Moosburg" for year 2011 (data source: Urbas (2009), QM-report (2012) and own calculations)

Parameter	Symbol	Value	Unit
Total heat produced by heat resources per year	$Q_{th,produced,an.}$	4232000	[kWh _{th} /a]
Heat fed into the district heating grid per year	$Q_{th,demand,DH}$	4203000	[kWh _{th} /a]
Useful head supplied and sold to the users	$Q_{th,useful,an.}$	3369000	[kWh _{th} /a]

Parameter	Symbol	Value	Unit
per year			
Heat produced by biomass boiler per year	$Q_{bio,prod.,an.}$	4189000	[kWh _{th} /a]
Heat produced by oil boiler per year	$Q_{oil,prod.,an.}$	43000	[kWh _{th} /a]
Heat lost in the heating plant (e.g. buffer tank losses) per year	$\Phi_{HP,av.}$	29000	[kWh _{th} /a]
Annual efficiency of heat provision of heating plant	$\zeta_{tot.,HP}$	0.79608	[kWh _{th} /kWh _{NCV}]
Annual biomass boiler utilization ratio	$\zeta_{bio,an.}$	0.71778	[kWh _{th} /kWh _{NCV}]
Annual oil boiler utilization ratio	$\zeta_{oil,an.}$	0.89844	[kWh _{th} /kWh _{NCV}]
Nominal power hours of biomass boiler	NPH_{bio}	2792.7	[h/a]
Nominal power hours of oil boiler	NPH_{oil}	28.7	[h/a]
Connected heat load per boiler output	$q'_{load,boiler}$	0.73133	[1]
Total annual electricity demand of heating plant	$W_{el,HP,aux.}$	70480	[kWh _{el} /a]
Annual electricity demand for biomass boiler	$W_{el,bio,aux.}$	49180	[kWh _{el} /a]
Annual electricity demand for oil boiler	$W_{el,oil,aux.}$	2100	[kWh _{el} /a]
Annual electricity demand for hot water circulation pumps	$W_{el,Circ.,aux.}$	16800	[kWh _{el} /a]
Annual electricity demand for further devices (lighting, IT, etc.)	$W_{el,etc.,aux.}$	2400	[kWh _{el} /a]
Specific electricity demand of heating station	$w_{el,HP,aux.}$	11.62	[kWh _{el} /MWh _{th}]
Nominal efficiency of biomass boiler	$\eta_{bio,nom.}$	0.85714	[kW _{th} /kW _{NCV}]
Nominal efficiency of oil boiler	$\eta_{oil,nom.}$	0.89000	[kW _{th} /kW _{NCV}]
Biomass fuel demand per year	$FD_{bio,vol.}$	7340.0	[SRM/a]
Primary energy content of biomass fuel input per year	$Q_{NCV,bio.,an.}$	5836034	[kWh _{NCV} /a]
Heating (fuel) oil demand per year	$FD_{oil,vol.}$	4800	[l/a]
Primary energy content of heating oil input per year	$Q_{NCV,oil,an.}$	47861	[kWh _{NCV} /a]

Explanations: IT ... Information Technology.

For a more detailed view on the district heating grid, please refer to the next sub-chapter.

4.1.2 Technical description of district heating grid

With a total grid length of 3838 trench meters including 234 meters of connection lines the heat distribution network in Moosburg can be classified as a mid-sized district heating grid. The radial grid system is based on direct, earth laid pipelines with pre-insulated bonded pipes, which are typically used for the main and distribution lines in radial network systems. The piping system is installed in form of horizontal and parallel routes and the lines are equipped with a leakage detection system.

In case of Moosburg's district heating system the operation mode of the flow pipe temperature is adapted by defining the required temperature level according to the outside temperature and the related heat demand in the district heating grid. So the flow pipe temperature (i.e. the supply flow temperature) is typically set to a maximum of 92°C for a nominal temperature of -15°C during wintertime, while the minimum flow temperature (e.g. during summertime) has to exceed a minimum of 75 °C for domestic hot water processes (see Figure 4-3).

The return flow temperature in district heating grid varies in the range of 52°C up to 60°C, depending on the seasonal heat demand. Consequently, the temperature difference between flow and return temperature level is set to a maximum of 40 – 45 °C in case of heat supply in wintertime or to less than 15 ° C in case of pure summer load conditions (see Figure 4-3). This type of water-operated two-pipe district heating network is operated in continuous mode during summer, as hot water must be provided 24 hours a day.

In the year 2011 a number of 50 heat consumers created a connected heat load of 2194 kW with an estimated annual heat demand of 3363 kWh/a. The majority of the objects supplied with district heat are one-family houses or commercial houses. But also the local schools, the kindergarten and official buildings of the municipality have been converted to district heat supply. Especially the integration of several residential complexes and the Children's Village of Moosburg into the district heating system could noticeably improve the air quality in the town of Moosburg, as coal-

and oil-fired central heating systems had been exchanged by environmental-friendly district heating.

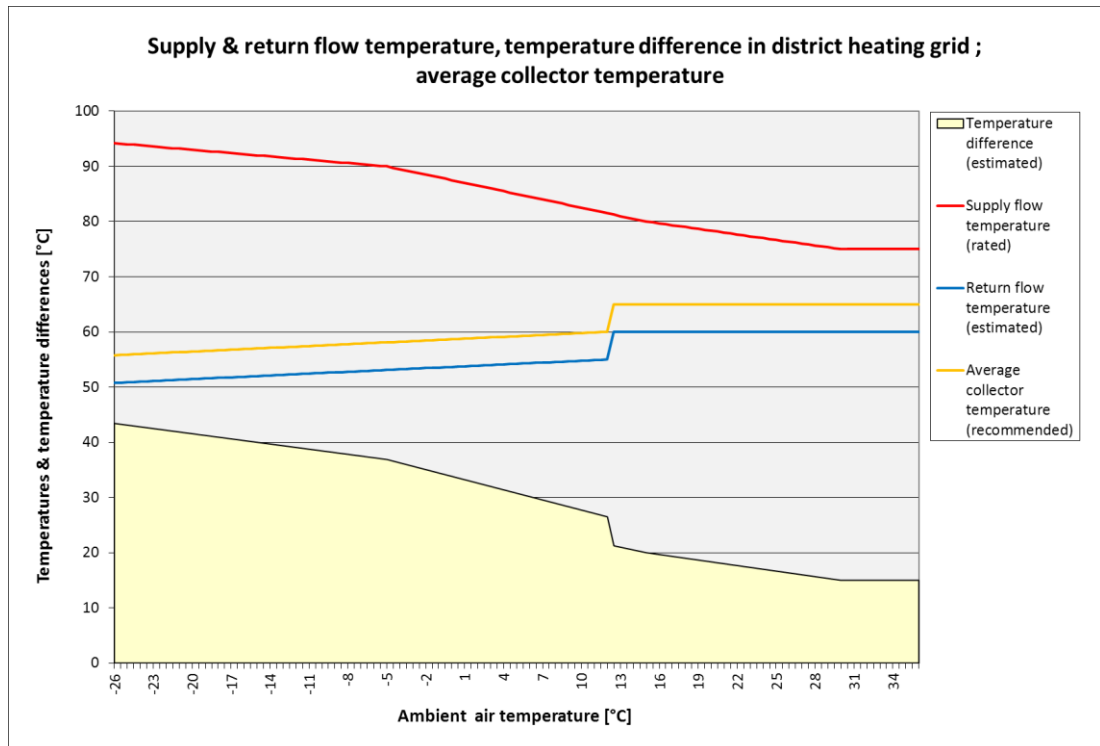


Figure 4-3: Behavior of the flow pipe temperature and the return flow pipe temperature in the water-operated two-pipe district heating network of Moosburg *. Temperature difference between flow and return flow varies between a maximum of 40 – 45 °C and a minimum of 15 °C** (data source: Urbas (2009), ESTIF (2007) and own calculations).

Explanations: * ... As recommended by ESTIF (2007) the average collector temperature of an optional assisting solar thermal system feeding into a district heating system without seasonal storage is set to return flow temperature plus 5 °C; ** ... The temperature difference in summer season mainly depends on the grid losses and the heat demand due to domestic hot water preparation.

All consumer sub-stations are installed with an indirect connection to the heat distribution network. The indirect substations are either for space heating purposes only or are equipped with an indirect connected hot water tank. This tank is applied for domestic hot water preparation and DHW storage. Based on an average heat demand of 726 kWh per day during summertime, in 2011 about 560 persons consumed about 21240 liters of domestic hot water per day. This is represented by an average base load of about 84.2 kW_{th} in the district heating grid. The base load is the sum of 30.5 kW_{th} for DHW preparation plus 53.7 kW_{th} of average grid losses (see Figure 4-5). However, about 834 MWh/a of heat has been lost by the circulating water in the pipelines, which is equal to a percentage rate of 19.84%

compared to the annually fed-in amount of heat. During summer operation of year 2011 more than 66% of grid losses had been measured at the maximum.

To get an overview of type and technical data of the district heating grid of “MS Fernwärme Moosburg”, the network’s main key indicators are summarized in Table 4-2.

Table 4-2: Key indicators of district heating grid “MS Fernwärme Moosburg” for year 2011 (data source: QM-report (2012) and own calculations)

Parameter	Symbol	Value	Unit
Sum of nominal connected heat load of users	$\sum Q'_{th,user,nom.,i}$	2194	[kW _{th}]
Total connected heat load in the district heating grid	$Q'_{load,grid,tot.}$	1684	[kW _{th}]
Maximal effective heat load in DHG	$Q'_{load,max.,eff.}$	1631	[kW _{th}]
Average thermal power losses in DHG	$\Phi'_{grid,av.}$	54	[kW _{th}]
Average heat load for domestic hot water preparation	$Q'_{load,DHW,av.}$	31	[kW _{th}]
Average base load in DHG	$Q'_{load,base,av.}$	84	[kW _{th}]
Length of grid in trench meters (including connection lines)	l_{grid}	3838	[m]
Utilization factor in the district heating grid (calculated)	f_u	0.74326	[1]
Energy load level in the district heating grid	ELL_{grid}	877.8	[kWh _{th} /m]
Heat connection dense	HCD_{grid}	0.43889	[kW _{th} /m]
Network allocation related to connected heat load of users	NWA_{HL}	0.57165	[kW _{th} /m]
Network allocation with respect to nom. thermal power of boiler	NWA_{TP}	0.78166	[kW _{th} /m]
Annual thermal energy losses in DHG	$\Phi_{grid,an.}$	834000	[kWh _{th} /a]
Annual thermal energy losses in DHG (calculated)	$\Phi_{grid,an.}$	812807	[kWh _{th} /a]
Average power losses per trench meter in the DHG	$\varphi'_{grid,av.}$	0.02481	[kW _{th} /m]
Average heat losses per trench meter and year in the DHG (calculated)	$\varphi_{grid,av.}$	211.8	[(kWh _{th} /a)/m]

Parameter	Symbol	Value	Unit
Average heat losses per trench meter and year in the DHG	$\varphi_{grid,av.}$	245.3	[(kWh _{th} /a)/m]
Specific electricity demand of district heating grid	$w_{el,grid,aux.}$	0.00499	[kWh _{el} /kWh _{th}]
Annual grid utilization factor	$\zeta_{grid,an.}$	0.79608	[1]
Number of connected heat users (consumer heating sub-stations)	$n_{user,i}$	50	[1]
Average connected nom. heat load per heat consumer	$Q'_{th,user,av.}$	43.88	[kW _{th} /user]
Average nominal power hours per heat consumer	$NPH_{user,av.}$	1506.6	[(h/a)/user]

Explanations: DHG ... District Heating Grid.

In the next sub-chapter an overview on the heating system's business use case is given. In addition the thermal energy demand of the connected heat consumers depending on the ambient conditions in the year 2011 will be discussed in more detail.

4.1.3 Business use case and thermal energy demand for space heating and hot water preparation in Moosburg

According to the annually report about the business year 2011 the net income for sold heat resulted in an average heat price per unit useful energy of $p_{heat,av.} = 74.72$ €/MWh. It is calculated based on the sum of basic charges, the sum of meter charges and the Megawatt-hour rate invoiced per unit of sold thermal energy. About 98.98% of the generated heat was provided by the woody biomass fueled conversion unit. Consequently, the biomass boiler was not stopped outside the heating period, but had to cover the district heating system's summer load by start/stop operation on a minimal load level.

The oil boiler was applied for peak load coverage and in order to function as a reserve. The amount of 43 MWh_{th}/a was generated within 33 nominal power hours, which is equal to 1.02% of the total amount produced by the plant's heat resources. Figure 4-4 displays the monthly balances of produced heat, heat fed into the district heating grid and useful heat supplied and sold to the 50 heat consumers within the business year 2011. Obviously, the minimum of heat supplied and sold to the heat

consumers is reached in August, while the maximal percentage of grid losses in relation to the fed in heat is determined in the same month.

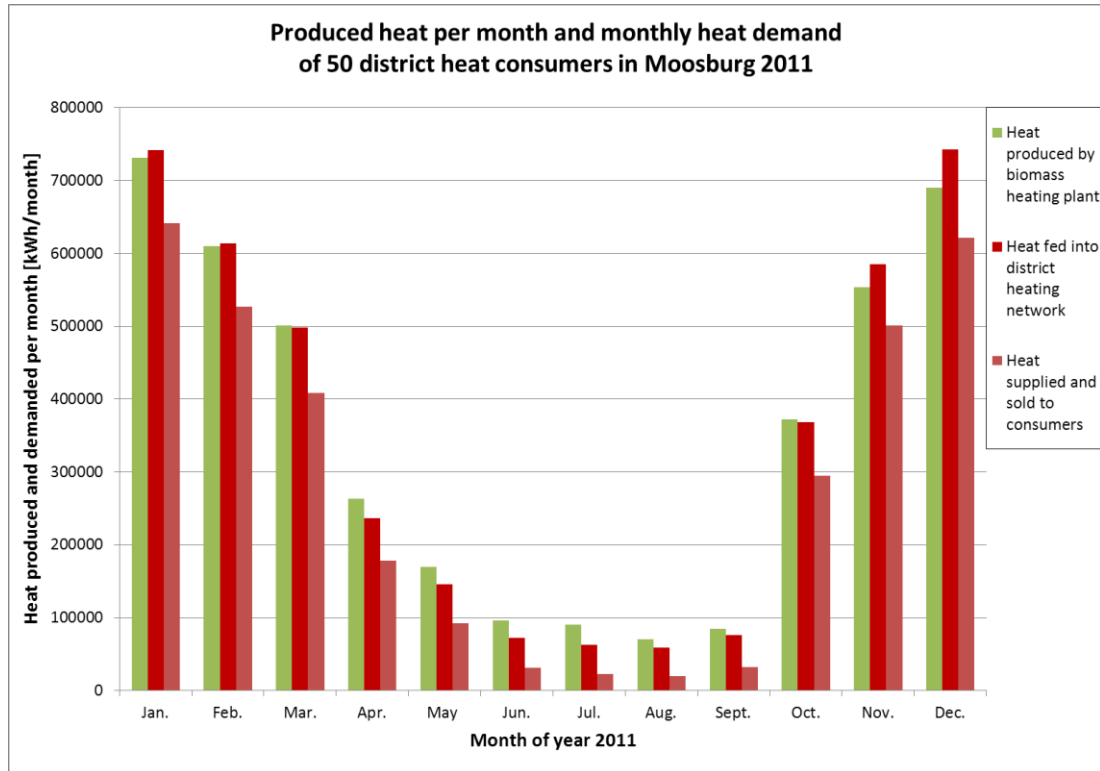


Figure 4-4: Monthly balances of produced heat, heat fed into the district heating grid and useful heat supplied and sold to the 50 heat consumers in Moosburg 2011* (data source: QM-report (2012))

Explanations: * ... District heating system with 20% grid losses: network length: 3838 m, estimated heat demand: 3364 MWh/a.

In Table 4-3 the relevant income and cost indicators for the business use case of heat generation are listed. The price for woody biomass correlates with a fuel wood price of $p_{bio,atro} = 103.51 \text{ €/t}_{atro}$, what is acceptable from an economic point of view. However, the yearly price index for fuel oil (21.4%) and diesel (9.7%) reached a relatively high level in 2011 compared to the year before (see AEA (2011)). In 2012 the yearly price indices for fossil fuel types (heating oil: 8.4%; diesel: 6.1%) were slightly above the average energy price index of 2012 (AEA (2012)).

Based on the ambient conditions in Moosburg the heat demand curve of the district heating network could look like as displayed in Figure 4-5. The maximal thermal power of the biomass heating plant installation (i.e. the nominal biomass boiler capacity: $Q'_{th,HP,max.}$) is 89% of the maximal thermal power required for the coldest day in the year (i.e. the maximal, effective connected heat load: $Q'_{cl,max,eff.} = 1684.4 \text{ kW}_{th}$). About 5% of this maximal heat load shall be assigned for hot water

preparation and grid losses. This part of the thermal load typically represents a constant base load for a number of 50 heat consumers supplied with district heat during the whole year.

Table 4-3: Income and cost indicators for the business use case of heat generation by a biomass district heating system in Moosburg 2011 (data source: QM-report (2012) and own calculations)

Indicator	Symbol	Value	Unit
Total heat produced by heat resources per year	$Q_{th,produced,an.}$	4232.0	[MWh _{th} /a]
Heat fed into the district heating grid per year	$Q_{th,demand,DH}$	4203.0	[MWh _{th} /a]
Useful heat supplied and sold to the users per year	$Q_{th,useful,an.}$	3369.0	[MWh _{th} /a]
Average heat price for sold heat	$p_{heat,av.}$	74.41	[€/MWh]
Heat produced by biomass boiler per year	$Q_{bio,prod.,an.}$	4189000.0	[kWh _{th} /a]
Biomass fuel demand per year	$FD_{bio,vol.}$	7340.0	[SRM/a]
Fuel costs for wood chips (30 wt.%; net price *)	$p_{bio.,30\%wt}$	15.91	[€/SRM]
Heat produced by oil boiler per year	$Q_{oil,prod.,an.}$	43000.0	[kWh _{th} /a]
Heating oil (fuel) demand per year	$FD_{oil,vol.}$	4800.0	[l/a]
Fuel costs for heating oil (net price *)	$p_{oil,light}$	0.63	[€/l]
Total annual electricity demand of heating plant	$W_{el,HP,aux.}$	70480.0	[kWh _{el} /a]
Industrial electricity price (consumption < 1 GWh/a)	$p_{el.,light}$	13.58	[€ct/kWh]
Biomass fuel manipulation rate of telescope loader	MR_{loader}	80.0	[SRM/h]
Operation hours of telescope loader per year	OpH_{loader}	91.8	[OpH/a]
Diesel demand per operation hour	fd_{diesel}	13.29	[l/OpH]
Total diesel demand of telescope loader per year	FD_{diesel}	1219.68	[l/a]
Fuel costs for diesel (net price *)	p_{diesel}	0.63	[€/l]
Average working hours personnel (boiler man)	$WH_{pers,av.}$	270	[h/a]
Hourly rate - personal costs (net rate *)	$hr_{pers.}$	35.00	[€/h]

*Explanations: * ... Prices and rates are net values without considering taxes*

If a total heat production of 4232.0 MWh_{th}/a by the biomass district heating plant is taken as a basis, a number of about 157 households will be powered with thermal energy during heating season and summertime. This rough calculation is based on an annual average heat consumption of 21.406 MWh_{th}/a per household in central Carinthia (average heat demand for space heating: 19.756 MWh_{th}/a; average heat demand for DHW preparation: 1.650 MWh_{th}/a). On the average the heating plant gives an annual useful heat output of 67.380 MWh_{th}/a per heat consumer and year. This means, that about three households per heated object can be assumed.

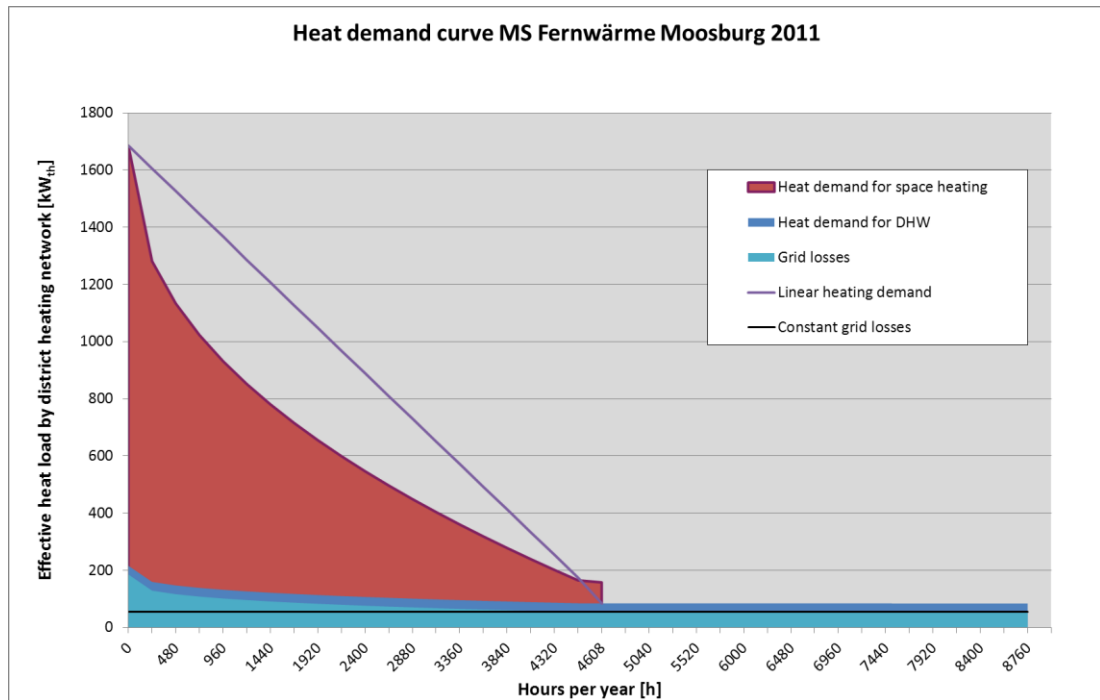


Figure 4-5: Heat demand curve for district heating system “MS Fernwärme Moosburg” based on a maximal effective heat load of 1684.4 kW_{th} and on the climatic conditions for Moosburg in 2011 (data source: Meteonorm (2012) and own calculations).

Explanations: * ... According to the approach by Sochinsky the annual heat demand comprises a base load and a heat load for space heating. For room heating a maximal heat load of 1600.2 kW_{th} has been assumed, while the average base load of 84.2 kW_{th} is a sum of 30.5 kW_{th} load for DHW preparation and 53.7 kW_{th} of average grid losses.

In the next sub-chapter the ambient conditions for heating and hot water preparation in Moosburg are discussed. Due to its geographical location the solar radiation and the weather conditions differ from the Austrian's average.

4.2 Ambient conditions for space heating and hot water preparation

The main purpose of a heating system in central Europe is the provision of useful heat for space heating, domestic hot water preparation and for some dedicated applications the supply with process heat. While domestic hot water and process heat is required throughout the whole year at a more or less constant level the demand for space heating strongly depends on the climatic conditions of the site the heated object is located. In the following sub-sections an overview on climate data for the investigated municipality and the weather conditions for this location in central Carinthia is given.

4.2.1 Climate data for Moosburg

The direct utilization of the available solar potential for generation of useful heat by solar collectors is particularly influenced by the solar radiation energy which can be absorbed by the solar collectors' active area. However, about 75% of the incident solar energy is lost in relation to insulation on collector area. About 25% of solar radiation energy incident on collector area are gained as useful energy. This percentage is typical for solar thermal applications operating under central European meteorological conditions (see Kaltschmitt, Streicher & Wiese (2010), page 149).

Besides the radiation energy onto the solar thermal system's collector area the system efficiency is also influenced by the ambient air temperature and the purpose the useful thermal energy is utilized later on. Table 4-4 summarizes the relevant monthly climate data and the related monthly values for heating days ($HD_{12^{\circ}\text{C}}$) and heating degree days ($HDD_{12^{\circ}\text{C}/20^{\circ}\text{C}}$) indicating the heat demand for space heating.

Table 4-4: Monthly irradiation, monthly mean temperature, heating days and heating degree days for Moosburg / Carinthia (data source: Meteonorm (2012), BMFWFJ (2013) and own calculations based on ZAMG (2000 - 2011))

Month	H_{G_h} [kWh / m ²]	H_{D_h} [kWh / m ²]	$H_{B_{n\text{hor}}}$ [kWh / m ²]	T_a [°C]	$HD_{12^{\circ}\text{C}}$ [d]	$HDD_{12^{\circ}\text{C}/20^{\circ}\text{C}}$ [Kd]
January	41	22	62	-2.7	31.0	693.1
February	66	27	98	0.4	28.3	560.3
March	108	48	120	4.9	30.2	479.0
April	128	62	111	9.9	20.0	278.5
May	168	82	137	15.4	3.7	85.0
June	173	74	148	18.5	1.0	13.1
July	181	77	159	19.8	0.1	1.8
August	158	75	135	19.2	0.1	1.8
September	115	51	121	14.2	6.1	34.6
October	71	41	69	9.9	18.5	260.8
November	37	22	47	4.0	29.7	487.3
December	30	18	43	-1.1	31.0	652.4
Year	*1274	600	*1251	*9.4	199.5	3547.7

Explanations: H_{G_h} ... Irradiation of global radiation on a horizontal plane [kWh/m²]
 H_{D_h} ... Irradiation of diffuse radiation on a horizontal plane [kWh/m²]
 $H_{B_{n\text{hor}}}$... Irradiation of direct radiation (beam) with high horizon [kWh/m²]
 T_a ... Mean air temperature [°C]
 $HD_{12^{\circ}\text{C}}$... Heating days [d]; Sum of days with daily mean temp. < 12°C;
 $HDD_{12^{\circ}\text{C}/20^{\circ}\text{C}}$... Heating degree days [K d]; Monthly sum of differences between average room temperature of 20°C and daily mean temperature below heating limit temperature of 12°C. The summed up temperature differences are multiplied with all heating days of the respective month;
 * ... Uncertainty of yearly values: $\Delta G_h = 3\%$, $\Delta B_h = 6\%$, $\Delta T_a = 0.8\%$.

While the generation of heat in heat oriented operation mode is controlled according to the behavior of the ambient air temperature on-site, the monthly energy yield of a solar thermal system varies with the duration of sunshine as well as its intensity. Both influencing factors depend on the time of year, the geographical location and also on the weather conditions, which are outlined in the next sub-section.

4.2.2 Weather conditions for Moosburg located in central Carinthia

As the global radiation and the proportion of diffuse radiation are mainly dependent on the condition of the atmosphere and the cloud conditions, Figure 4-6 displays the typical behavior of monthly solar radiation in combination with monthly temperature change determined for Moosburg in Carinthia.

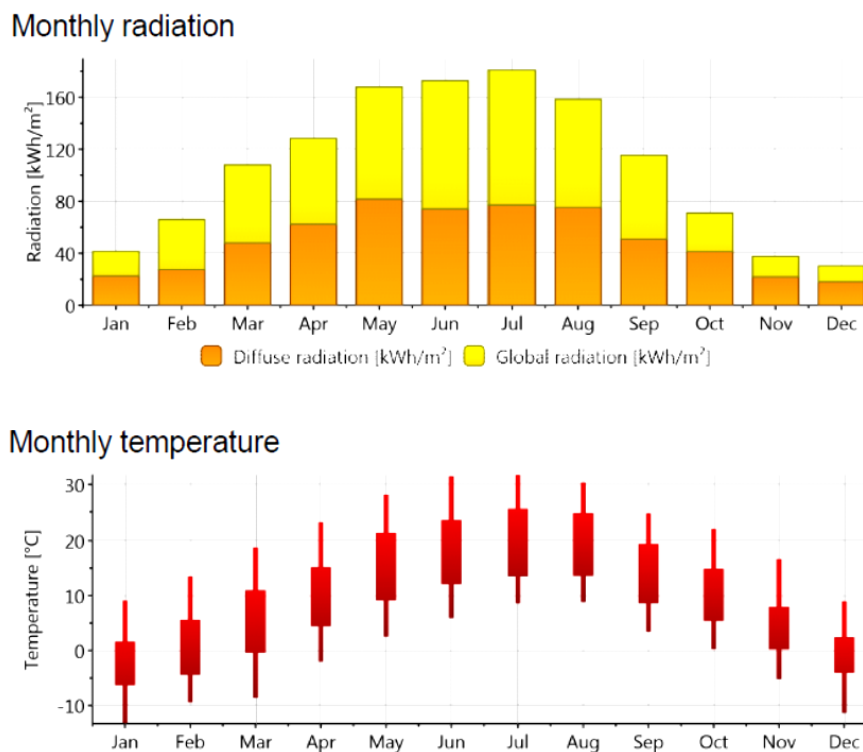
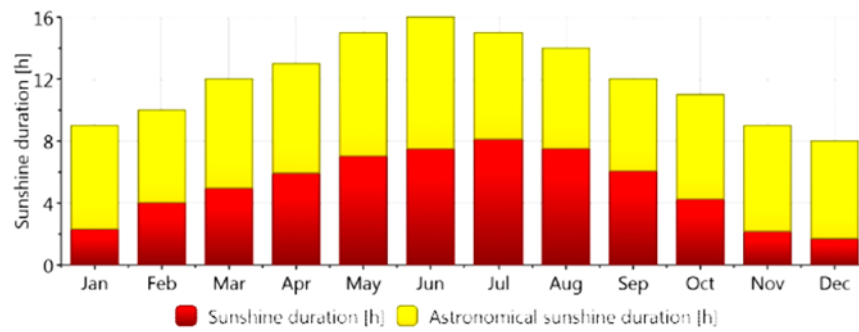


Figure 4-6: Graphical representation of monthly radiation and monthly temperature in Moosburg / Carinthia (data source: Meteonorm (2012))

In Figure 4-7 seasonal duration of sunshine and the precipitation in the course of one year is shown. Depending on the cloud conditions the diffuse fraction of global radiation will change from 10% up to 100% (clear blue sky: 10% - 20%, scattered clouds: 20% - 80%, overcast sky: 80% - 100%). The higher the diffuse fraction, the lower is the energy content of global solar radiation (see Weiss (2011), page 14).

Sunshine duration



Precipitation

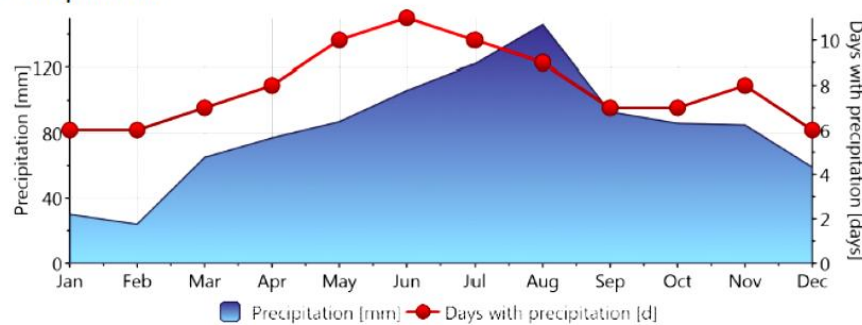


Figure 4-7: Graphical representation of monthly sunshine duration and monthly precipitation in Moosburg / Carinthia (data source: Meteonorm (2012))

In the following sub-sections a closer look to the available solar energy potential is given. Either it is global radiation ready for direct conversion by solar collectors, or it is transformed solar radiation energy in form of biomass.

4.3 Solar Energy Potential

As the generation of useful heat by solar thermal systems und biomass district heating systems directly or indirectly depends on the available solar energy potential, the following chapters deal with the regional and local energy potentials of the renewable energy resources called solar radiation and woody biomass.

4.3.1 Regional distribution of solar radiation

In order to evaluate accurate data regarding global irradiation and solar thermal potential at the selected region of central Carinthia, the solar radiation database from climatologic data homogenized for Europe prepared by the European Joint Research Centre, Institute for Energy, Renewable Energy Unit is used. The so-called Photovoltaic Geographical Information System (PVGIS) provides online access to a tool set for geographical assessment of solar resource and performance

of photovoltaic technology (see PVGIS (2013)). Based on the PVGIS radiation databases (e.g. Climate-SAF PVGIS) it is possible to make estimates of the performance of solar thermal systems. Further on this web page provides an interactive map as well as ready made maps for solar radiation potential in Europe. Figure 4-8 gives an example for the interactive map result for the region of central Carinthia as well as the map for global solar irradiation on the surface of earth in Austria.

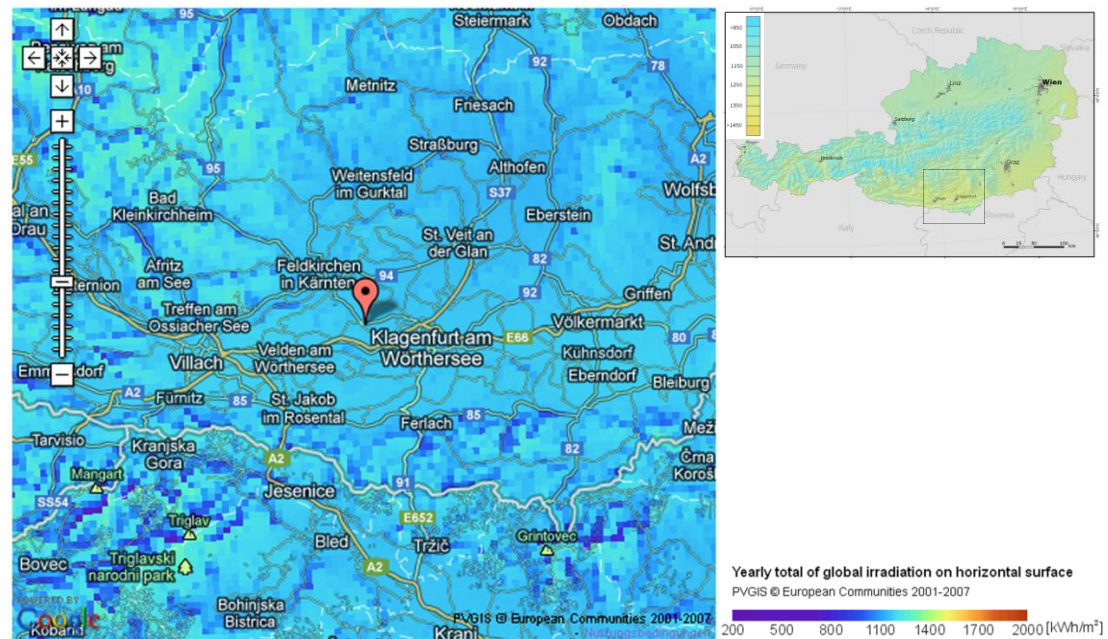


Figure 4-8: Yearly total of global irradiation on a horizontal surface [kWh/m²] in Central Carinthia (data source: PVGIS (2013)).

Explanations: ■ ... The town of Moosburg is located at 46° 39' 32", North and 14° 10' 38", East; Elevation: 497 m a.s.l..

Using this web tool the following irradiation data for selected locations in Carinthia have been calculated (see Table 4-5):

Table 4-5: Solar irradiation data for selected locations in the region of central Carinthia calculated with PVGIS (data source: Climate-SAF PVGIS (2013))

Location	Elevation [m a.s.l.]	$H_{h,a}$ [kWh / m²]	H_h [Wh / (m²*d)]	$H_{(30),a}$ [kWh / m²]	$H_{(30)}$ [Wh / (m²*d)]	DNI [Wh / (m²*d)]	D/G [-]
Moosburg:	497	1300	3580	1510	4150	3410	0.47
Klagenfurt:	448	1310	3590	1520	4160	3470	0.46
Villach:	498	1290	3530	1500	4120	3340	0.48
Ferlach:	460	1210	3330	1380	3780	2860	0.51
St. Veit:	484	1310	3590	1520	4170	3410	0.47

Average:	477	1284	3524	1486	4076	3298	0.48
-----------------	------------	-------------	-------------	-------------	-------------	-------------	-------------

Explanations: $H_{h,a}$... Average annual irradiation on horizontal plane [kWh/m^2];
 H_h ... Average daily irradiation on horizontal plane [$\text{Wh}/(\text{m}^2 \cdot \text{d})$];
 $H_{(30),a}$... Average annual irradiation on plane at angle: 30 deg. [kWh/m^2];
 $H_{(30)}$... Average daily irradiation on plane at angle: 30 deg. [$\text{Wh}/(\text{m}^2 \cdot \text{d})$];
DNI ... Direct normal irradiation [$\text{Wh}/(\text{m}^2 \cdot \text{d})$];
D/G ... Ratio of diffuse to global irradiation [-].

If the region's global irradiation on horizontal plane per year is compared to data evaluated for the rest of Austria, the annual amount of solar radiation received per unit area is above the Austrian average (i.e. $H_{h,a} = 1100 \text{ kWh}/(\text{m}^2 \cdot \text{a})$; see Kaltschmitt & Streicher (2009), page 158). Taking into account an average annual irradiation of $H_{h,a} = 1284 \text{ kWh}/\text{m}^2$ on horizontal plane and an area of 1750 km^2 valid for the geological basin around Klagenfurt, the theoretical potential of global radiation irradiated on this area is calculated to $Pot_{solar,th.} = 8089.2 \text{ PJ/a}$. This value is a percentage rate of 2.44% compared to the theoretical solar potential in Austria (i.e. $Pot_{solar,th.} = 332200 \text{ PJ/a}$; see Kaltschmitt & Streicher (2009), page 160).

Although the conditions for heat generation by solar thermal systems are quite promising in Carinthia, only 7% of Austria's total collector area in 2011 has been installed in Carinthia. Summing up the area evaluated for un-glazed collectors (i.e. simple absorbers) and glazed collectors (i.e. flat plate collectors and evacuated tube collectors) a number of 16100 m^2 has been put into operation within entire year (see Biermayr, et al. (2012), page 116). That is an increase of 7% compared to the year before. As stated there, there is a promotion program in form of directly paid subsidies for solar thermal system by the federal country of Carinthia.

However, the penetration rate of solar thermal systems within the municipal territory of Moosburg is obviously on the average of Carinthia, what is discussed in more detail in the following part.

4.3.2 Potential for solar thermal energy generation in Moosburg

In order to assess the possibilities for heat generation by solar thermal energy conversion technology a closer look to the solar potential of the municipality of Moosburg shall be done. As the municipal territory is situated in the south of Austria, the potential sites for solar thermal plants are located in the range of a geographic latitude from $46^\circ 38'$, north up to $46^\circ 42'$, north and in the range of a geographic longitude from $14^\circ 06'$, east to $14^\circ 13'$, east. Based on an average annual global irradiation of $H_{h,a} = 1300 \text{ kWh}/(\text{m}^2 \cdot \text{a})$ within this geographical zone, the theoretical

solar potential on the surface of earth for these 36.76 square kilometers can be estimated to $Pot_{solar,th.} = 172.0 \text{ PJ/a}$.

If an average area of 564 m^2 of operating solar thermal collectors per 1000 Austrians are taken as a basis (see Biermayr, et al. (2012), page 112), in the year 2011 about 2480 m^2 of solar thermal collectors have been operated in Moosburg, which is equal to a total capacity of 1736 kW_{th} .

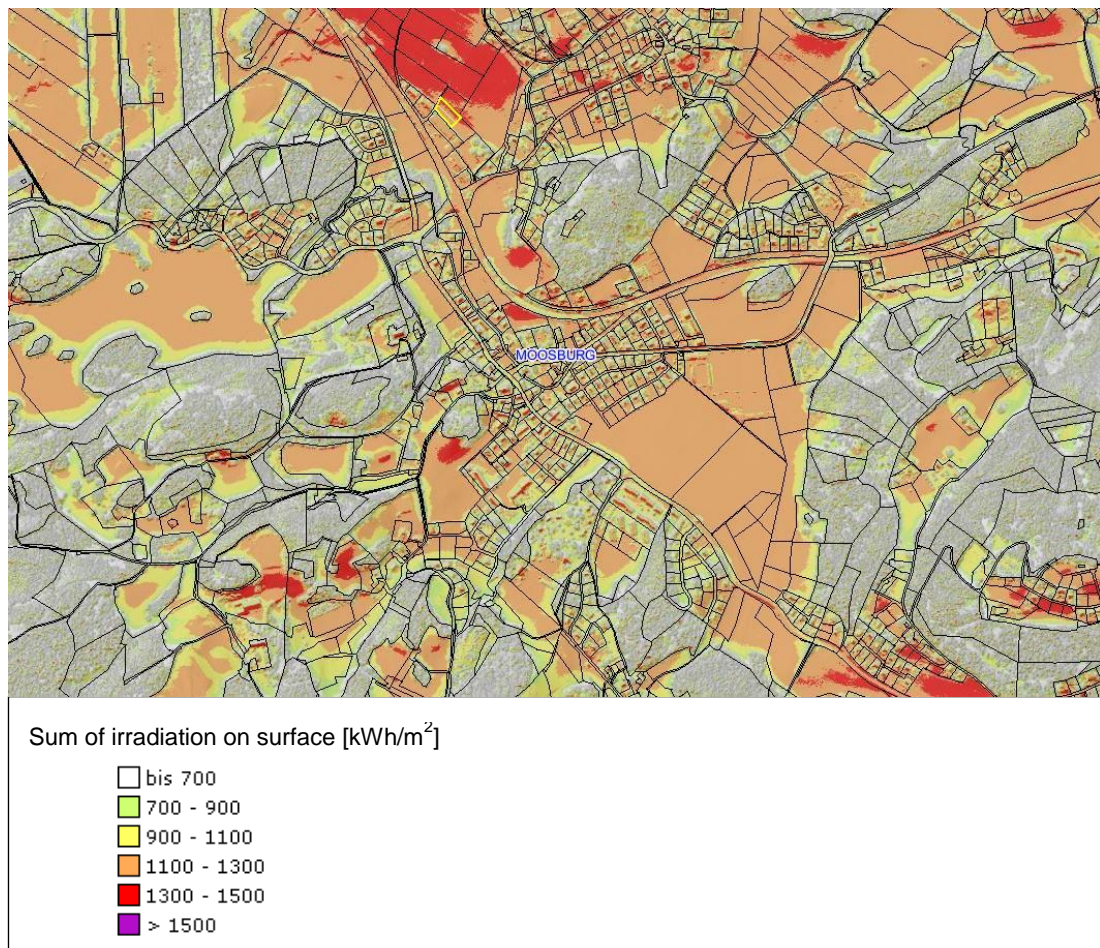


Figure 4-9: Annual sum of irradiation on surface [kWh/m^2] within the area of the town of Moosburg / Carinthia (data source: KAGIS (2013)).

Explanations: □ ... The section of land, where the biomass heating plant is located, is marked with a yellow frame.

As shown by the so - called “Solarpotentialkataster”, an online tool of Carinthia’s geographical information system (see KAGIS (2013)), the potential sites with promising solar irradiation on surface of earth are limited. In Figure 4-9 an extract of the interactive map for the town of Moosburg is shown. Obviously the annual sum of irradiation on surface [kWh/m^2] reaches its maximum at open space situated on a hillside with proper orientation. However, the plant site of the district heating

system's central heating station is located in the northern part of Moosburg, which is near to a potential location for a solar thermal plant (see Figure 4-9).

The technical potential of generating useful heat by solar thermal collectors shall be assessed in roughly calculating the average annual energy yield per unit installed collector area. As input data the amount of monthly irradiation and the monthly mean temperature for Moosburg as given by PVGIS is used. The estimates listed in Table 4-6 are the results of applying Equation 26 on the local climate data and a set of characteristic collector parameters. These values are normally taken from the selected collector type's data sheets. Taking into account the planned integration of the solar thermal installment into a district heating system without seasonal storage, even the system output per unit aperture area can be predicted. As a precondition it is assumed, that the selected solar collectors are inclined to 30 degrees and that are oriented exactly to south.

Table 4-6: Estimated technical potentials for useful heat generation by solar thermal collectors feeding into a district heating system without seasonal storage (data source: PVGIS (2013), CPC 14 XL (2012), VK 14 (2008), GK 3100 (2012), HT 4.2 m² (2009) and own calculations)

Collector type	Tilt / Azimuth	Collector output per unit aperture area & year	Collector output per unit aperture area & summer period *	System output per unit aperture area & year	System output per unit aperture area & summer period *
	[°]	[kWh/(m ² *a)]	[kWh/(m ²)]	[kWh/(m ² *a)]	[kWh/(m ²)]
Ritter Solar CPC 14 XL (ETC)	30° / 0° (South)	769	286	731	272
GREENoneTEC VK 14 (ETC)	30° / 0° (South)	647	249	615	237
GREENoneTEC GK 3100 (FPC)	30° / 0° (South)	513	228	487	217
ÖkoTech HT 4.2 m ² (FPC)	30° / 0° (South)	639	269	607	256

Explanations: * ... June, July & August (01.06. – 31.08.);

ETC ... Evacuated tube collector;

FPC ... Flat plate collector.

Obviously the theoretical energy yield per collector area for ETCs is higher than the theoretical energy yield per collector area of FPCs. However, Equation 26 deals with a recommended value for mean collector fluid temperature. It depends on the average return temperature from district heating network, which does not reflect the exact operating conditions on site. As shown in chapter 2, flat plate collectors and

evacuated tube collectors would require different types of heat storages to optimally utilize the solar gains. Further more, the used irradiation data taken from PVGIS (2013) represents mean monthly values taken per quarter of an hour.

As the successful operation of a solar-assisted biomass district heating system mainly depends on the provision of useful heat by thermo-chemical conversion of solid biomass fuels, the next section will deal with the potential for woody biomass as a renewable energy source for district heating supply.

4.4 Potential for woody biomass as a renewable energy source for district heating supply

Biomass can be defined as solar energy, which is transformed into organic matter by plants via the process of photo-synthesis. About 15% of the solar radiation energy impinging on the plant will be converted into chemical energy, which is stored in form of binding energy in the plant's material. As during the photo-synthesis the greenhouse gas carbon dioxide (CO₂) is taken by the plant to build up high-energetic carbon compounds, plants are a main factor in influencing the atmosphere's CO₂-balance. In case biomass is utilized for the production of useful energy, the conversion process is considered to be neutral in terms of greenhouse gas emissions and the related global climate change.

For the provision of useful heat by biomass district heating systems for the most part woody biomass fuels are used. The process of thermo-chemical conversion takes place in dedicated combustion units, where the primary energy content of these solid biomass fuels is transferred to a heat carrier. Typical combustibles are bark or waste wood, forest wood chips made out of forest residues or chopped wood logs, wood chips produced by chopping industrial wood, waste wood from woodworking industry or residues from saw mills, saw dust or wood pellets. In the following sub-chapters a rough overview on the regional potential for woody biomass fuels in Carinthia is given, followed by a closer look on the local potential, which can be obtained within Moosburg's municipal territory.

4.4.1 Regional potential for woody biomass fuels

Potentials for the renewable energy source called solid biomass can be found in agriculture and forestry. Besides Styria, Carinthia is one of the federal countries with the biggest share of forest area in Austria. About 60% of the entire territory can be classified as forest. The stock of wood available in Carinthia's commercial

timberland is estimated at 178 millions of solid cubic meters. About 72% of the forest consist of conifers, where as 28% can be assigned to deciduous trees and shrubs (see Wald&Holz (2012)). Theoretically this amount of woody biomass is equivalent to a primary energy content of 1101.792 PJ, if the available biomass would be converted to heat by combustion and if the net calorific value of one solid cubic meter of fresh-harvested timber (60% spruce , 10% pine, 10% beech, 10% oak, 10% poplar) would be taken as a basis (see FNR (2010)). In the year 2011 about 2.1 % of woody biomass stocks, which are equal to a theoretical energy content of 22.902 PJ, have been effectively used (see Wald&Holz (2012)).

About 60% of the annual lumbering in Carinthia is utilized as round wood, 25% as feedstock for industrial purposes and 15% as firewood. According to Wald&Holz (2012)) in 2011 more than 1.25 million solid cubic meters of woody biomass have been utilized for heat and power generation (i.e. 1.25 millions of solid cubic meters are equal to 7.737 PJ of primary energy content)). Compared with the total gross demand of solid biomass fuels, i.e. pellets, briquets, wood chips, bark and log wood consumed in Austria in the year 2011 (12953413 tons or 168.9 PJ; see Biermayr, et all. (2012)), the share is relatively low. For the production of useful heat about 310000 solid cubic meters per year were burned by biomass-fueled heating plants in Carinthia.

But also woodworking industries, saw mills and small enterprises, like joineries or carpentries could be considered as a source for woody biomass fuels in form of waste wood, residues from woodworking, wood shavings, and saw dust. As stated by Wald&Holz (2012) in Carinthia 163 firms working in timber industries, 182 carpentries and 749 joineries handle wood or wood products. A decreasing number of saw mills (in 2011: 151) is processing an increasing amount of timber (in 2011 about 3 millions of solid cubic meters). However, the number of industrial plants and enterprises in the field of woodworking are limited, if the municipal area of Moosburg is taken as a basis.

4.4.2 Local potential for woody biomass fuels

The main local resources for woody biomass fuels in the municipality of Moosburg can be determined on the 4000 hectares of arable land or wood land farmed by 170 agricultural or forestry enterprises. As shown in Figure 4-10 the percentage of afforestation within the municipal area is in the range of 20% to 60%. Nevertheless, local farmers can directly supply their forest residues or wood fuel in form of wood

chips to the plant (just- in-time delivery). Due to the small scale of the district heating plant and the location of the heating station near to the residential zone of Moosburg, an on-site chopping is not possible.

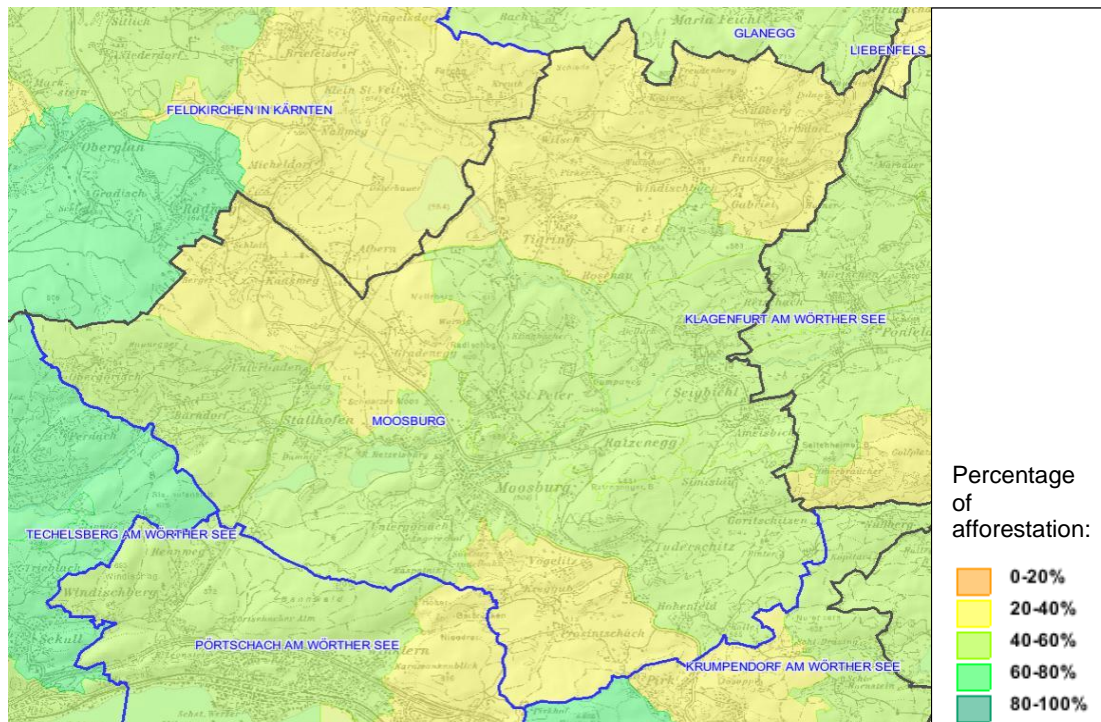


Figure 4-10: Allocation of areas with different percentage of afforestation in the municipal territory of Moosburg / Carinthia (data source: KAGIS (2013)).

From an economic and ecological point of view, the provision of wood fuel is recommended within a distance of 70 to 100 km (see Ortner (2010)). The reason for this limitation is the growing transport costs and the related demand of diesel fuel. However, the geographic position of Moosburg in the basin of Klagenfurt enables an economic supply with forest wood chips delivered from the south of Styria as well as from northern Italy or northern Slovenia. Besides a stable and assessable price of wood fuel the security of supply are the bases for a continuous, economic operation of the biomass heating plant.

5 Technical Concepts and Proposed Scenarios for a Solar-supported Biomass District Heating System in Moosburg

In the frame of chapter 5 first the system boundaries and boundary conditions for a solar-assisted district heating system shall be described. Second, the technical concept for a solar thermal plant feeding into an extended district heating network is introduced. Third, the modeling, dimensioning and design of district heating networks and solar thermal plants are roughly outlined. Finally, the reference system in Eibiswald / Styria shall be described from a technical point of view. Its district heating network operating in season 1997 / 1998 should be modeled according to the approach of Sochinsky.

5.1 Definition of system boundaries and boundary conditions

The system boundaries and boundary conditions for solar thermal support of an extended biomass district heating system in Moosburg can be split into three topics according to the following list:

- Boundary conditions defined by the plant owner and/or district heating grid operator,
- technical boundaries due to the heat load of the supplied district heating network, and
- boundary conditions with respect to the geographical location of the central heating station.

In the following sub-chapters these boundary conditions are discussed in more detail.

5.1.1 Boundary conditions defined by the plant owner and/ or district heating grid operator

In preparation for the feasibility study of a future investment project the current owner of the heating plant “MS Fernwärme Moosburg” was interviewed in order to define his requirements. His main aspects for a future extension of his plant are:

- An increase of the economic performance: At least an economic operation within the plant’s lifetime of 20 years should be possible.
- No additional personnel effort: It should be possible to handle the newly introduced plant components by the currently enabled boiler man.

- **Efficient investments:** There should be utilization of synergies with the available plant infrastructure. The currently installed buffer tank should be reused.
- **State-of-the-art technology:** The applied components should be characterized by an appropriate price-performance ratio.
- **If possible, no additional land use:** The roof area of the heating house should be equipped with solar collectors.
- **Positive ecological effects:** By saving greenhouse gas or air pollutants emissions the public acceptance for environmentally-friendly heat generation should be increased.

From the district heating grid operator's point of view the following conditions should be fulfilled in order to accept an extension of the current biomass district heating system:

- **No change of operation mode:** The heat consumers must be supplied with district heat throughout the whole year 24 hours a day.
- **No change of supply flow and return flow temperature:** The maximum flow pipe temperature in winter should stay on a level of 92 °C. The return flow temperature should be in the range of 50 °C to 55 °C. During summer operation the flow pipe temperature must fulfill a minimum of 75 °C, while the return flow temperature could change from 55 °C to 60 °C.
- **No change of hydraulic concept of the current district heating network:** Solar thermal heat must be fed into the supply network via a buffer storage located at the central heating station.
- **The storage volume of the newly erected thermal energy storage should provide a reserve of several days,** as the current buffer tank volume is sufficient for one day of boiler outage.
- **The solar fraction saving during summer months should be greater than 90%:** In order to shut down the biomass boiler during summer season (July, August) the main resource for district heat supply should be the solar thermal system.
- **Peak loads and longer phases of adverse weather conditions should be covered with the existing oil boiler.** No additional biomass boiler for summer operation should be installed.

- Easy and smooth operation of the additional solar thermal plant components must be possible. No specialists or experts to run the solar thermal parts should be required.
- There should be considerable, effective fuel cost savings, as a yearly solar fraction of more than 10% should be achieved.
- Control and monitoring devices as well as the required control and monitoring software should be easily integrated into the already available control and monitoring infrastructure.

Besides the operator's and owner's requirements also the technical system boundaries have to be considered when planning the extension of an up and running biomass heating system. The next section deals with these technical boundaries in more detail.

5.1.2 Technical boundaries for solar technical support

According to Streicher, et al. (1999) the main technical criteria when deciding pro or contra a solar thermal support of a biomass district heating system are a state-of-the-art concept and the quality of dimensioning. A main indicator is the specific energy yield of the collectors, which depends on the installed collector area, the volume of the solar thermal storage, the connected heat load of the district heating network, and the temperature level of supply and return flow.

Starting point for a possible extension of the district heating system are the operating conditions of Moosburg's heating network in year 2012. After 9 additional consumer's heating sub-stations had been installed and several meters of additional connection lines had been buried, in 2012 in total 59 heat consumers have been supplied with district heat via a heating grid of 3850 trench meters of total length. The connected load of 2653 kW_{th} generated a maximal effective heat load of 1924 kW_{th} at the coldest day (-16.3 °C) during heating season (see Figure 3-2 in chapter 3). The effective heat load could be split into a maximal load of 1832 kW_{th} for space heating, a constant load of 33 kW_{th} for DHW preparation and an average load for grid losses of about 58 kW_{th}. Heat connection dense (HCD_{grid}) was equal to 0.5 kW_{th}/m, while the energy load level (ELL_{grid}) was calculated to 981 kWh_{th}/m. Supply flow and return flow temperatures were set to the same level as in 2011 ($T_{FF,max}$: 92°C, $T_{FF,min}$: 75 °C; $T_{RF,max}$: 60 °C, $T_{RF,min}$: 50 °C). For flow temperature levels please refer to Figure 4-3 in chapter 4.

Heat was produced by a 1500 kW_{th} biomass boiler in continuous mode during heating season. During summer season the biomass boiler changed to start/stop-operation providing the minimal heat output for summer load. The 1500 kW_{th} oil boiler was started only in case of maintenance outage of the main boiler and in case of peak load.

As the specific energy yield of the collector arrays in the first instance is influenced by the available solar potential the next part summarizes the local conditions for a solar thermal system installed near to the central heating station of “MS Fernwärme Moosburg”.

5.1.3 Boundary conditions with respect to the geographical location of the central heating station

As the concept of a central solar district heating system shall be realized, the local conditions at plant site have to be investigated before planning. As already shown in chapter 5, the conditions for solar thermal heat generation are quite promising in the basin of Klagenfurt. The estimations based on data given by PVGIS (2013) result in a solar yield per unit collector area and year of 487 kW_{th}/(m² a) up to 731 kW_{th}/(m² a) depending on the used type of collector (see Table 4-6).

The available free space at plant site shall be utilized as a construction area for collector arrays installed with a specific orientation and inclination. Considering this, either the heating house's flat roof with a roof area of 1020 m² will be available or, if not roof-top mounted an open space area at the hill side could be used for ground mounted collector rows. The roof's plane is slightly tilted with 3 degrees and is oriented to southwest (Azimuth: -45 ° (west)). For an open area installation the sloped area located northwest to the heating station would be a potential installation area with on average tilt of 8.51 degrees and an orientation to south-southwest (Azimuth: -25 ° (west)).

Unfortunately, a roof-top mounted solar plant with inclined collectors is not allowed due to regulatory restrictions. However, due to the defined goal of at least 90 % of solar fraction the available roof area would not be sufficient. Taking into account all aspects leads on to a technical concept which will be described in the next chapter.

5.2 Technical concepts, dimensioning and design of a solar-assisted biomass district heating system in Moosburg

Knowing the requirements and boundary conditions allows going further with planning and design. The next sub-chapters deals with the modeling of an extended heat distribution grid planned to be introduced in 2013, the proposed dimensioning of a central solar district heating system based on a nomogram algorithm and the out coming design adapted to the local conditions at plant site.

5.2.1 Modeling of an extended district heating grid in year 2013

It is planned to extend of the current district heating network to a new service area. The current owner and operator of “MS Fernwärme Moosburg” foresees at least a number of 45 additional consumers’ heating sub-stations to be installed in the eastern part of town. In addition to the existing 59 heating sub-station 45 buildings, mainly one-family houses, an official building and a supermarket shall be connected to the existing grid. In total the 45 heat consumers would bring in 901 kW_{th} of connected load. A lengthening of pipeline by further 1905 trench meters including 575 meters of additional connection lines would result in a total grid length of 5755 trench meters.

Based on the ambient conditions valid for Moosburg (see Meteonorm (2012)) the new frame conditions for the district heating grid are modeled. Thanks to the approach of Sochinsky the heat demand curve is determined for the extended district heating network, which is shown in Figure 5-1.

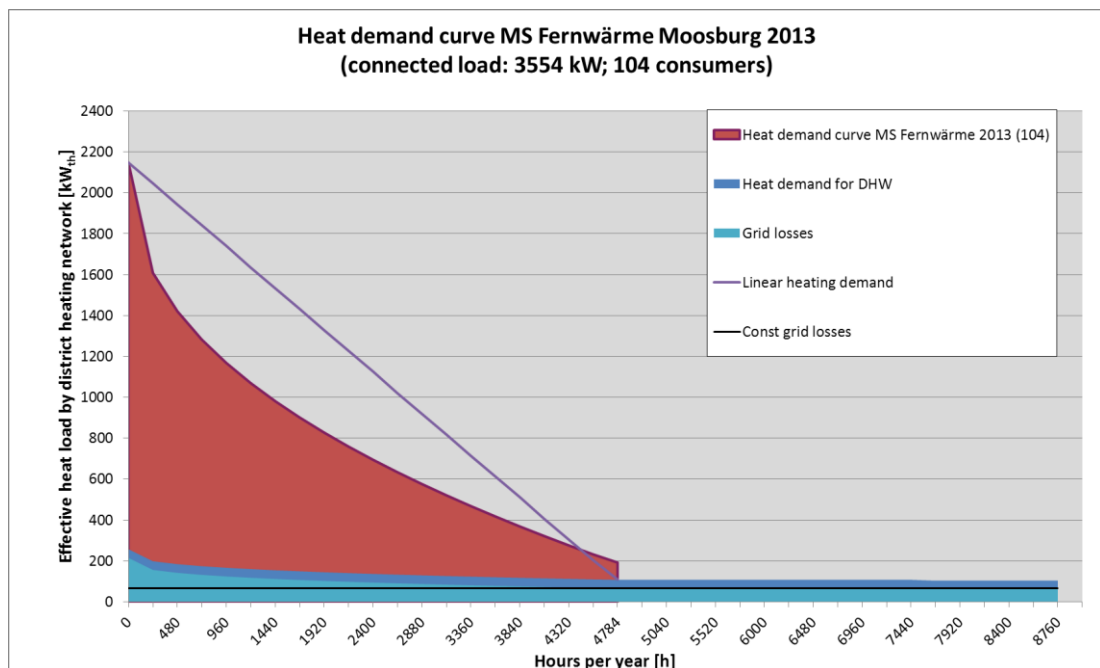


Figure 5-1: Heat demand curve for district heating system “MS Fernwärme Moosburg” based on a total effective heat load of 2130 kW_{th} and on the climatic conditions for Moosburg in year 2013 (data source: Meteonorm (2012) and own calculations).

If the expected grid losses are calculated for a two-line, water-operated heating grid made of insulated steel pipes (DN 100) with a total grid length of 5755 trench meters, the result will be an amount of $\Phi_{grid,an.} = 1218787$ kWh_{th} per year. The calculation takes into account average heat losses per trench meter and year of 211.8 (kWh_{th}/a)/ m. The key indicators determined for the new district heating network supplied by “MS Fernwärme Moosburg” in year 2013 are summarized in Table 5-1.

Table 5-1: Key indicators for an extended district heating grid in Moosburg 2013 (data source: own calculations).

Indicator of district heating network	Symbol	Value	Unit
Sum of nominal connected heat load of users	$\sum Q'_{th,user,nom.,i}$	3554	[kW _{th}]
Total connected heat load in the district heating grid	$Q'_{load,grid,tot.}$	2130	[kW _{th}]
Maximal effective heat load in DHG	$Q'_{load,max.,eff.}$	2066	[kW _{th}]
Average thermal power losses in DHG	$\Phi'_{grid,av.}$	65	[kW _{th}]
Average heat load for domestic hot water preparation	$Q'_{load,DHW,av.}$	42	[kW _{th}]
Average base load in DHG	$Q'_{load,base,av.}$	107	[kW _{th}]
Length of grid in trench meters (including connection lines)	l_{grid}	5755	[m]
Utilization factor in the district heating grid (calculated)	f_u	0.581	[1]
Energy load level in the district heating grid	ELL_{grid}	731	[kWh _{th} /m]
Heat connection dense	HCD_{grid}	0.370	[kW _{th} /m]
Network allocation related to connected heat load of users	NWA_{HL}	0.618	[kW _{th} /m]
Annual thermal energy losses in DHG	$\Phi_{grid,an.}$	1122269	[kWh _{th} /a]
Annual thermal energy losses in DHG (calculated)	$\Phi_{grid,an.}$	1218787	[kWh _{th} /a]
Average power losses per trench meter in the DHG	$\phi'_{grid,av.}$	0.022	[kW _{th} /m]
Average heat losses per trench meter and year in the DHG (calculated)	$\phi_{grid,av.}$	211.8	[(kWh _{th} /a)/m]
Average heat losses per trench meter and year in the DHG	$\phi_{grid,av.}$	195.0	[(kWh _{th} /a)/m]
Annual grid utilization factor	$\zeta_{grid,an.}$	0.789	[1]
Number of connected heat users (consumer heating sub-stations)	$n_{user,i}$	104	[1]
Average connected nom. heat load per heat	$Q'_{th,user,av.}$	34.2	[kW _{th} /user]

Indicator of district heating network	Symbol	Value	Unit
consumer			
Average nominal power hours per heat consumer	$NPH_{user,av.}$	1183.4	[(h/a)/user]
Maximal forward flow temperature (winter)	$T_{FF,max}$	92	[°C]
Minimal forward flow temperature (summer)	$T_{FF,min}$	75	[°C]
Minimal return flow temperature (winter)	$T_{RF,min}$	50	[°C]
Maximal return flow temperature (summer)	$T_{RF,max}$	60	[°C]

Explanations: DHG ... District Heating Grid.

As the capacity of the current installed biomass boiler ($Q_{th,bio,nom.} = 1500 \text{ kW}_{th}$) is not sufficient to cover the increased heat load during heating season, a capacity extension of biomass boiler is planned in this case. With additional 250 kW_{th} the total boiler capacity in the heating plant is set to 3250 kW_{th} , including the unchanged capacity of the oil boiler.

The results of the grid model will be used as input for dimensioning and design of the required solar thermal plant supporting the existing biomass district heating system. The next sub-chapters will show the subsequent dimensioning and design steps.

5.2.2 Dimensioning of the solar plant based on boundary conditions

According to the nomogram algorithm presented in Streicher, et al. (1999) a district heating system with a maximal effective heat load of about 1684 kW_{th} requires a specific storage volume of about $0.1 \text{ m}^3/\text{kW}_{th}$ and a specific collector area of about $1 \text{ m}^2/\text{kW}_{th}$ to achieve an annual solar fraction rate of 14%. With the same input values the nomogram delivers a specific annual energy saving of about $285 \text{ kWh}_{th}/(\text{m}^2 \text{ a})$ and a solar fraction of about 95% during summer month. Prerequisites are a summer load ratio of 5% compared of a maximal heat load, a collector inclination of 30 degrees and a supply flow temperature range of $95^\circ\text{C} / 70^\circ\text{C}$ and return flow temperature range of $60^\circ\text{C} / 50^\circ\text{C}$.

Based on this rough check a collector field comprising 120 units of ground mounted flat plate collectors with a total net area of 1827.6 m^2 is chosen for the planned application in Moosburg. As a storage volume the currently maximal available storage volume for steel tanks is selected, which is in size of 200 m^3 at the moment. For a connected effective load of 2130 kW_{th} the input values for the nomogram algorithm are a specific collector area of $0.858 \text{ m}^2/\text{kW}_{th}$ and a specific storage volume of $0.0939 \text{ m}^3/\text{kW}_{th}$. The resulting annual solar fraction is evaluated to $f_{sol,an.} =$

13.25%, which is more than the required 10%. For the average solar fraction during summer season a percentage rate of $f'_{sol, sum.} = 91.79\%$ is determined, which exceeds the required threshold of 90%.

In order to check the potential annual yield of the solar system comprising 1827.6 m² of active area Equation 26 (see chapter 2.1.8) is applied on the hourly irradiation data given by Meteonorm (2012) and the collector parameters for FPC type “Gluatmugl HT 16.7” (see HT 4.2 m² (2009)). The result is listed in Table 5-2, considering losses of about 5 % when calculating the system output.

Table 5-2: Calculated energy yield of a solar thermal collector field in Moosburg 2013 (data source: own calculations).*

Indicator	Symbol	Value	Unit
Net area of solar thermal collector field	$A_{col., net}$	1827.6	[m ²]
Annual collector output (calculated: Ti:30°, Az: 0°)	$Q_{col., out., an.}$	966965	[kWh/a]
Annual collector output per net area of collector field & year (calc.: Ti:30°, Az: 0°)	$q_{col., out., an.}$	529	[kWh/(a m ²)]
Annual solar thermal system output (calculated: Ti:30°, Az: 0°)	$Q_{col., sys., an.}$	918617	[kWh/a]
Annual solar thermal system output per net area & year (calc.: Ti:30°, Az: 0°)	$q_{col., sys., an.}$	503	[kWh/(a m ²)]
Collector output during summer time (1.6. - 31.8.; calc.: Ti:30°, Az: 0°)	$Q_{col., out., sum.}$	476454	[kWh/a]
Collector output per net area & summer time (1.6. - 31.8.; calc.: Ti:30°, Az: 0°)	$q_{col., out., sum.}$	261	[kWh/(a m ²)]
Solar system output during summer time (1.6. - 31.8.; calc.: Ti:30°, Az: 0°)	$Q_{col., sys., sum.}$	4526331	[kWh/a]
Solar system output per net area & summer time (1.6. - 31.8.; calc.: Ti:30°, Az: 0°)	$q_{col., sys., sum.}$	248	[kWh/(a m ²)]

Explanations: * ... Collector type: Gluatmugl HT 16.7; Tilt: $Ti_{col} = 30^\circ$; Azimuth: $Az_{col.} = 0^\circ$ (South); Net collector area: $A_{col., net} = 1827.6 \text{ m}^2$,
Ti. ... Tilt;
Az. ... Azimuth.

However, the real conditions on-site require an adaptation of the collector arrays orientation and arrangements. In the next sub-chapter the proposed design of a solar thermal plant supporting a biomass district heating system is described in more detail.

5.2.3 Design of a solar district heating plant in Moosburg

Based on the dimensioning done in the chapter before, a possible design of a solar district heating plant should be worked out in the next step. Because of regulatory restrictions, it has been decided to install the collectors as open field application

near to the plant site. In order to make use of the available slope the collector arrays are installed in form of 10 rows a' 12 solar modules each. In total 120 units of flat plate collectors type "Gluatmugl HT 16.7" should be erected as ground mounted collector arrays. The collectors shall be operated in matched flow mode keeping a fixed temperature difference between the collector outlet's temperature and the supply flow temperature in the district heating grid.

The collector rows are interrupted by a 4 m wide pathway, which should provide access for vehicles. As the hillside is inclined with an average tilt of 8.5° against horizontal plane, a shade calculation would recommend a row distance of about 1.63 m. For an optimal utilization of ground conditions at construction side the collector arrays should be arranged in parallel to the slope's surface. As the hillside is oriented to south-southwest, the resulting azimuth for the flat plate collectors is -25° from south.

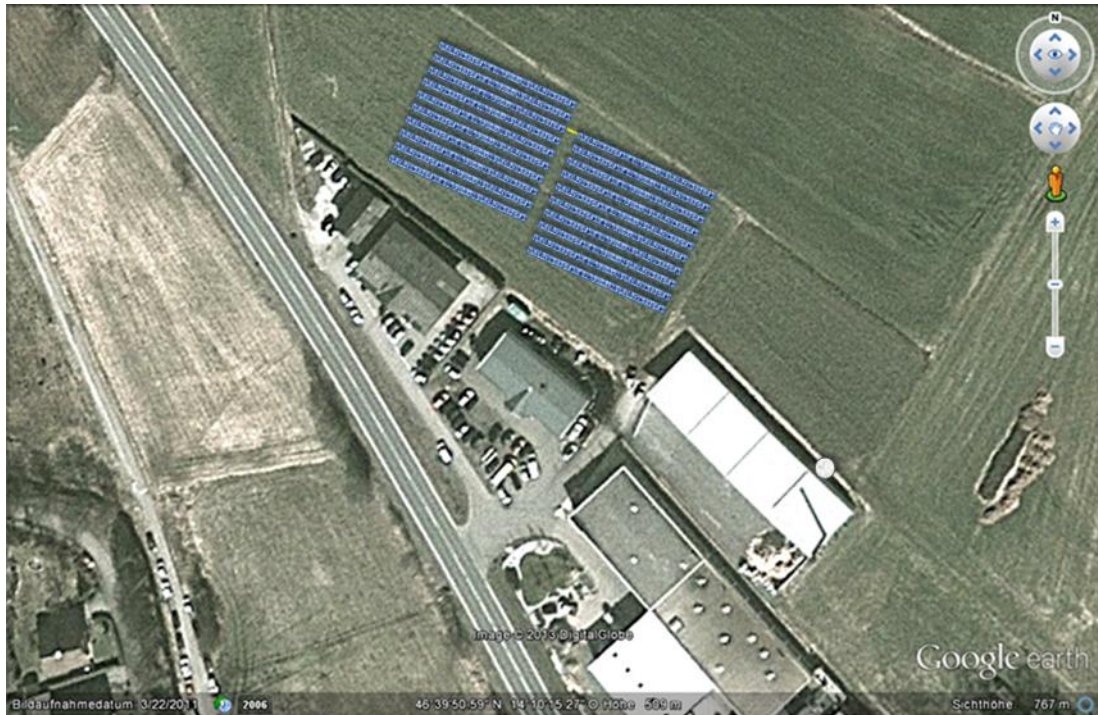




Figure 5-2: Visualization of a solar-assisted biomass district heating system from the bird's-eye perspective in Moosburg (data source: Google (2013)).

Explanations:  ... Solar collector arrays made of 120 units; type: Gluatmugl HT 16.7;
 ... Hot water storage tank made of steel: volume 200 m^3 , $\varnothing 5.8 \text{ m}$.

The total land requirement for collector field is an area of 3153 m^2 not considering the inner and the two outer pathways used for maintenance reasons. In sum a gross collector area of $A_{\text{col.,gross}} = 2034 \text{ m}^2$ are installed, which is equal to 1827.6 m^2 of

aperture area. The total land area used for the ground mounted flat plate collectors comprises 5500 m² including excess roads, pathways for maintenance, fixing system and a fence for security reasons. In Figure 5-2 the possible plant configuration is displayed from the bird's-eye perspective.

Table 5-3: Design details and technical data for a solar-assisted biomass district heating system in Moosburg 2013 (data source: HT 4.2 m² (2009) and own calculations).*

Description	Symbol	Value / Type	Unit
Thermal energy storage installation			
Storage volume of hot water tank	$V_{stor.}$	200	[m ³]
Type of hot water storage		Insulated cylindrical steel tank	
Height	h_V	10	[m]
Outer diameter	\varnothing_{out}	5.8	[m]
Type of installation		Above ground installation; partly buried into ground	
Type of insulation material		Mineral wool	
Thickness of insulation layer		0.4	[m]
Maximal energy storage capacity of hot water tank (calculated)	$Q_{stor.,max.}$	39049041	[kJ]
Number of charging cycles	CN	491	[a ⁻¹]
Solar plant installation			
Aperture area of solar thermal collector field	$A_{col.,net}$	1827.6	[m ²]
Total gross area of solar thermal collector field	$A_{col.,gros}$	2034.0	[m ²]
Type of installation		Ground mounted collector arrays on open field	
Name of collector		Solid Gluatmugl HT16.7	
Type of collector		Flat plate collectors (FPC)	
Number of installed units		120	[pcs]
Tilt of collector plane	$Ti_{col.}$	30	[°]
Azimuth (-90°:W, 0°:S, 90°:E)	$Az_{col.}$	-25	[°]
Optical efficiency	η_0	0.811	[1]
1 st order heat loss coefficient	a_1	2.710	[W/(m ² K)]
2 nd order heat loss coefficient (a_2	0.010	[W/(m ² K ²)]
Operation mode of collectors		Matched flow with a fixed ΔT	
Specific collector area	$a_{col.}$	0.8580	[m ³ /kW _{th}]
Specific storage volume	$v_{stor.}$	0.0939	[m ² /kW _{th}]
Storage volume per unit collector area	$v_{col.}$	0.1094	[m ³ /m ²]
Expected annual solar savings fraction	$f_{sol.,exp.}$	>10%	[1]
Expected solar savings fraction for summer month (July, August)	$f_{sol.,sum.,exp.}$	>90%	[%]

Explanations: * ... Connected load: $Q'_{cl.,DHN} = 3554$ [kW_{th}]; maximal effective connected load: $Q'_{cl,max.,eff.} = 2130$ [kW_{th}].

Besides the collector arrays a thermal energy storage tank made of steel is the most costly component of the proposed installment. Due to its size the cylindrical tank construction will be welded on-site. With a height of 10 m and an inner diameter of 5 m the steel tank must be buried up to half height into earth, because a maximal height of 5 m above ground should not be exceeded. With a layer of 40 cm of mineral wool the outer diameter will reach a dimension of 5.8 m.

As shown by Figure 5-2 the cylindrical hot water tank should be attached to the heating house near to the biomass boiler inside. As mentioned before, the biomass boiler capacity is assumed to reach a nominal value of $1750 \text{ kW}_{\text{th}}$ in order to cover the increased heat load of the extended district heating grid (see Figure 5-1). Basis for dimensioning of boiler capacity is a total effective connected heat load of $2130 \text{ kW}_{\text{th}}$. For supply flow and return flow temperature levels no changes are taken into account (please refer to Table 5-1).

For transmission pipes from collector field to central thermal energy storage a distance of 180 m has to be considered. Like in district heating grids the buried pipes should be made of steel with an appropriate insulation layer. For a better overview of dimension and design please refer to Table 5-3.

The next chapter gives a short description of the biomass district heating system in Eibiswald / Styria, which has been selected as a reference system for further comparison.

5.3 Reference system for a solar-assisted biomass district heating system in Austria: “Nahwärme Eibiswald”

Since the year 1997 the district heating system in Eibiswald / Styria is operated as a solar-assisted biomass district heating plant. However, since 2012 the plant is running with an extended solar collector field of 2450 m^2 in total (plus 1200 m^2 of gross collector area) and an additional storage volume of 70 m^3 (175 m^3 in total; see Eibiswald (2013)), which should not be taken into account for further comparison. Therefore the following technical description of “Nahwärme Eibiswald” and the model of the expected heat demand are based on the technical status in season 1997/1998 given by Streicher & Oberleitner (1998).

5.3.1 Technical description of “Nahwärme Eibiswald” in year 1997

Three years before 1997 the biomass boiler started to operate in Eibiswald providing a maximal capacity of $2000 \text{ kW}_{\text{th}}$ for district heat supply. Due to a summer load level

equal to 5 % of the grid's nominal heat load, the thermal system had been introduced in spring 1997 in order to switch off the ineffective biomass boiler during summer load operation. Thanks to the simulation program SHWin the system was dimensioned to achieve a solar fraction of more than 90 % during the summer month July and August. A 500 kW_{th} oil boiler was ready to cover the remaining 10 % during holiday season in case the required supply flow temperature could not be provided by solar feed-in.

A total net collector area of $A_{col,net} = 1150 \text{ m}^2$ provided the necessary heat output during daytime. The majority of the collector arrays had been installed as roof-integrated flat plate collectors on top of the biomass storage unit (see Figure 5-3), which was characterized by storage volume of 4000 SRM. The rest of the collector area was mounted on the heating house's roof.



Figure 5-3: Solar-assisted biomass district heating system in Eibiswald /Styria in year 1997 (data source: Eibiswald (2013)).

In order to buffer the solar gains a cylindrical steel tank was integrated into the heating house. Due to its height of 12 m the storage tank towered over the roof ridge (see Figure 5-3). With a storage volume 105 m³ the tank was dimensioned as a short-term storage providing a heat reserve for one to two days.

Table 5-4: Design details and technical data for a solar-assisted biomass district heating system in Eibiswald 1997* (data source: Streicher & Oberleitner (1998) and own calculations).

Indicator	Symbol	Value / Type	Unit
Boiler equipment			
Nominal capacity of biomass boiler	$Q'_{th,bio,nom.}$	2000	[kW _{th}]
Nominal capacity of oil boiler	$Q'_{th,oil,nom.}$	500	[kW _{th}]
Thermal energy storage installation			
Storage volume of hot water tank	$V_{stor.}$	105	[m ³]
Type of hot water storage		Insulated cylindrical steel tank	
Height	h_V	12	[m]
Outer diameter	\varnothing_{out}	n.a.	[m]
Type of installation		Heating house-integrated	
Type of insulation material		Mineral wool	
Thickness of insulation layer		0.2	[m]
Maximal energy storage capacity of hot water tank (calculated)	$Q_{stor,max.}$	23300218	[kJ]
Number of charging cycles	CN	696	[a ⁻¹]
Solar plant installation			
Aperture area of solar thermal collector field	$A_{col,net}$	1150.0	[m ²]
Total gross area of solar thermal collector field	$A_{col,gros}$	1250.0	[m ²]
Type of installation		Roof-integrated collector arrays	
Name of collector		Gluatmugl Großfläche (1996)	
Type of collector		Flat plate collectors (FPC)	
Number of installed units		n.a.	[pcs]
Tilt of collector plane	$Ti_{col.}$	30	[°]
Azimuth (-90°:W, 0°:S, 90°:E)	$Az_{col.}$	-20	[°]
Optical efficiency (rel. to aperture area)	η_0	0.754	[1]
1 st order heat loss coefficient (rel. to aperture area)	a_1	3.000	[W/(m ² K)]
2 nd order heat loss coefficient (rel. to aperture area)	a_2	0.002	[W/(m ² K ²)]
Operation mode of collectors		Matched flow with a fixed ΔT	
Specific collector area	$a_{col.}$	0.5441	[m ³ /kW _{th}]
Specific storage volume	$v_{stor.}$	0.0497	[m ² /kW _{th}]
Storage volume per unit collector area	$v_{col.}$	0.0913	[m ³ /m ²]
Measured annual solar savings fraction	$f_{sol,mes.}'$	8%	[1]
Measured solar savings fraction for summer month (July, August)	$f_{sol, 'sum,mes.}$	90%	[%]

The solar-assisted biomass heating system was designed based on a two-pipe, water-operated hydraulic scheme with a central buffer tank. Collectors as well as the biomass boiler feed into the storage tank via separate inlets mounted at different heights. To get an overview on the main technical data of the solar supported reference plant valid for 1997 please refer to Table 5-4.

Following the approach of Sochinsky in a final step the possible heat demand curve for Eibiswald's district heating system shall be modeled. The next section shows how the resulting heat demand during the course of year 1997 could have looked like.

5.3.2 Modeling of a solar-supported district heating network in Eibiswald 1997

Due to the fact, that the exact number of heating sub-stations are not mentioned by Streicher&Oberleitner (1998) 64 heat consumers are taken as a basis for further calculation. Based on a total connected heat load of 3000 kW_{th} and ambient conditions valid for Eibiswald in 1997 (see ZAMAG (1971 – 2000)) the appropriate frame conditions for the district heating grid are modeled. Thanks to the approach of Sochinsky the resulting heat demand curve can be determined (see Figure 5-4).

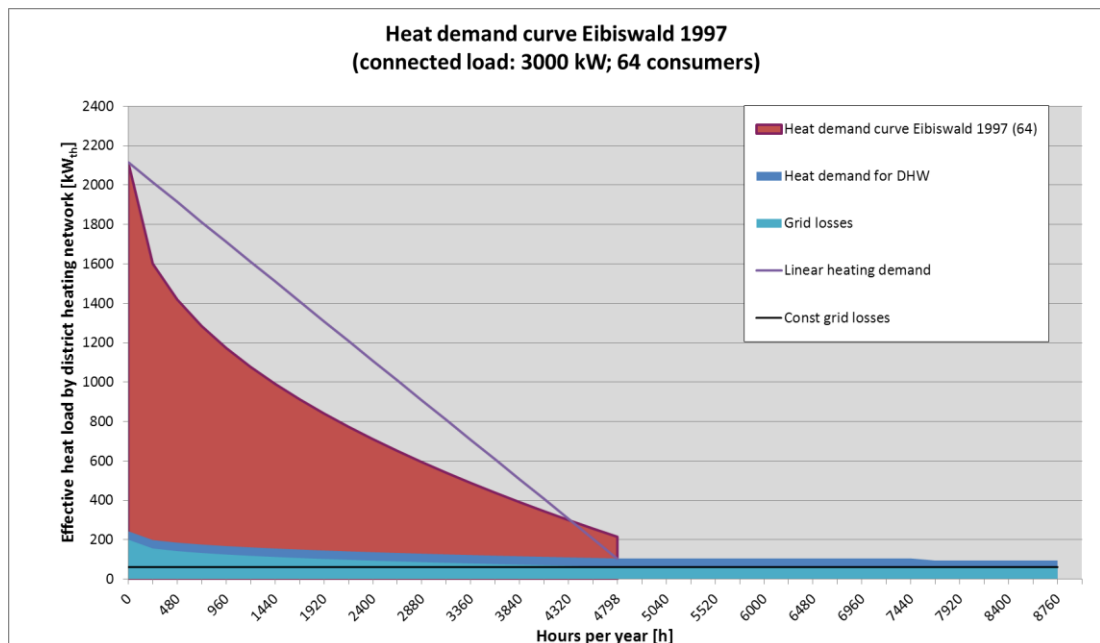


Figure 5-4: Heat demand curve for district heating system “Nahwärme Eibiswald” based on a maximal connected load of 2114* kW_{th} and on the climatic conditions for Eibiswald in 1997 (data source: ZMAG (1971 - 2000) and own calculations).

Explanations: * ... According to the approach by Sochinsky the annual heat demand comprises a base load and a heat load for space heating. For room heating a maximal heat load of 2051 kW_{th} has been assumed, while the average base load of 106 kW_{th} is a sum of 43 kW_{th} load for DHW preparation and 63 kW_{th} of average grid losses.

For further calculation and simulations the above created model will be taken as a basis for further study and simulation. The following Table 5-5 gives an overview on the determined indicators and technical data of the district heating network modeled for Eibiswald in the year 1997.

Table 5-5: Key indicators and technical data for Eibiswald 1997* (data source: Streicher&Oberleitener (1998) and own calculations).

Indicator	Symbol	Value for Eibiswald 1997	Unit
Sum of nominal connected heat load of users	$\sum Q'_{th,user,nom.,i}$	3000	[kW _{th}]
Total connected heat load in the district heating grid	$Q'_{load,grid,tot.}$	2114	[kW _{th}]
Maximal effective heat load in DHG	$Q'_{load,max.,eff.}$	2051	[kW _{th}]
Average thermal power losses in DHG	$\Phi'_{grid,av.}$	63	[kW _{th}]
Average heat load for domestic hot water preparation	$Q'_{load,DHW,av.}$	43	[kW _{th}]
Average base load in DHG	$Q'_{load,base,av.}$	106	[kW _{th}]
Length of grid in trench meters (including connection lines)	l_{grid}	4000	[m]
Utilization factor in the district heating grid (calculated)	f_u	0.6836	[1]
Energy load level in the district heating grid	ELL_{grid}	912.5	[kWh _{th} /m]
Heat connection dense	HCD_{grid}	0.5284	[kW _{th} /m]
Network allocation related to connected heat load of users	NWA_{HL}	0.7500	[kW _{th} /m]
Network allocation with respect to nom. thermal power of boiler	NWA_{TP}	0.6250	[kW _{th} /m]
Annual thermal energy losses in DHG (measured)	$\Phi_{grid,an.}$	850000	[kWh _{th} /a]
Average power losses per trench meter of DHG	$\varphi'_{grid,av.}$	0.0243	[kW _{th} /m]
Average heat losses per trench meter and year in the DHG	$\varphi_{grid,av.}$	212.5	[(kWh _{th} /a)/m]
Annual grid utilization factor	$\zeta_{grid,an.}$	0.8074	[1]
Number of connected heat users (consumer heating sub-stations)	$n_{user,i}$	64	[1]
Average connected nom. heat load per heat consumer	$Q'_{th,user,av.}$	46.9	[kW _{th} /user]
Average nominal power hours per heat consumer	$NPH_{user,av.}$	1216.7	[(h/a)/user]
Maximal forward flow temperature (winter)	$T_{FF,max}$	95	[°C]
Minimal forward flow temperature (summer)	$T_{FF,min}$	70	[°C]
Minimal return flow temperature (winter)	$T_{RF,min}$	50	[°C]
Maximal return flow temperature (summer)	$T_{RF,max}$	60	[°C]

Explanations: DHG ... District Heating Grid;

* ... Connected load: $Q'_{cl,DHN} = 3000$ [kW_{th}]; maximal effective connected load: $Q'_{cl,max.,eff.} = 2114$ [kW_{th}]; base load: $\Phi'_{grid,min.} + Q'_{DHW} = 106$ [kW_{th}]; grid length: $l_{grid} = 4000$ [m]; number of heat consumers: $n_{user,i} = 64$ [1].

6 Assessments and Comparison

The entire chapter provides a comprehensive summary of results, which are the outcome of energetic, ecological and economic assessments. As described in chapter 3, different methods of approach have been applied to analyze the selected biomass district heating applications with or without solar thermal support.

6.1 Evaluation of scenario specific energy demand and heat production resources for a biomass district heating system with 104 heat consumers in Moosburg 2013

The upcoming chapters have the goal to evaluate the differences in operating a biomass district heating plant without solar thermal support compared to a system with an assisting solar plant. Basis for calculation is the extended district heating network planned for year 2013 in Moosburg. As shown before in chapter 5.2.1 a connected load of 3554 kW_{th} results in a total, effective connected load of 2130 kW_{th}, which is expected for the coldest day (-16.3 °C) during heating period.

6.1.1 Evaluation of heat demand and heat production resources for a biomass district heating system with and without solar thermal support in Moosburg 2013

In the following table the annual energy balances, the expected losses and the expected annual electricity demand of the two compared configurations are shown (see Table 6-1). In order to get a quick impression of differences, the delta values are listed in a separate column.

Due to the fact that a different approach for evaluating the annual energy balance has been chosen (Sochinsky or SHWwin), the results for the total amount of feed-in heat slightly differs but still shows a quite good consistency (see Figure 6-1). As SHWwin will not give any results of district heat consumed by the connected heat consumers the method according to Sochinsky provides an acceptable outcome.

Table 6-1: Key indicators for a biomass district heating system without solar thermal support and for a solar-assisted biomass district heating system in Moosburg 2013** (data source: simulation results of SHWin and own calculations).

Indicator	Symbol	Value for DHS w/o solar support	Value for solar- assisted DHS	Delta value (*)	Unit
Total heat produced by heat resources per year	$Q_{th,produced,an.}$	5333547	5330960	-2587	[kWh _{th} /a]
Heat fed into the district heating grid per year	$Q_{th,demand,DH}$	5328213	5326745	-1468	[kWh _{th} /a]
Useful heat supplied and sold to the users per year	$Q_{th,useful,an.}$	4205945	4205945	0	[kWh _{th} /a]
Heat produced by biomass boiler per year	$Q_{bio,prod.,an.}$	5226613	4525581	-701032	[kWh _{th} /a]
Heat produced by oil boiler per year	$Q_{oil,prod.,an.}$	106933	119804	12870	[kWh _{th} /a]
Heat produced by solar thermal system per year	$Q_{sol.,prod.,an.}$	0	685575	685575	[kWh _{th} /a]
Heat lost in the heating plant (e.g. buffer tank losses) per year	$\Phi_{HP,av.}$	5334	4215	-1119	[kWh _{th} /a]
Solar heat fed into the storage tank per year	$Q_{sol.,in,stor.}$	0	676823	676823	[kWh _{th} /a]
Annual amount of heat fed into the storage tank by boiler(s)	$Q_{aux.,in,stor.}$	0	4645389	4645389	[kWh _{th} /a]
Heat lost in the solar circuit per year	$\Phi_{sol.,av.}$	0	8752	8752	[kWh _{th} /a]
Heat lost in the hot water storage tank per year	$\Phi_{stor.,av.}$	0	10664	10664	[kWh _{th} /a]
Total annual electricity demand of heating plant	$W_{el,HP,aux.}$	88312	90839	2527	[kWh _{el} /a]
Annual thermal energy losses in DHG	$\Phi_{grid,an.}$	1122269	1120800	-1468	[kWh _{th} /a]
Annual thermal energy losses in DHG (calculated)	$\Phi_{grid,an.}$	1218787	1218787	0	[kWh _{th} /a]

Explanations: * ... Delta of solar-assisted DHS minus DHS w/o solar support;

** ... Connected load: $Q'_{cl,DHN} = 3554$ [kW_{th}]; maximal effective connected load: $Q'_{cl,max,eff.} = 2130$ [kW_{th}]; base load: $\Phi'_{grid,min.} + Q'_{DHW} = 107$ [kW_{th}]; grid length: $l_{grid} = 5755$ [m]; number of heat consumers: $n_{user,i} = 104$ [1];
DHG ... District Heating Grid;
DHS ... District Heating System.

The model, which has been used to determine the heat demand curve, has been verified with real operating data of year 2011. Based on these data given in QM-report (2012) the calculated values match very well. So for both scenarios the same

amount of useful heat supplied and sold to the 104 heat consumers will be used for further calculations (e.g. for relative greenhouse gas emissions).

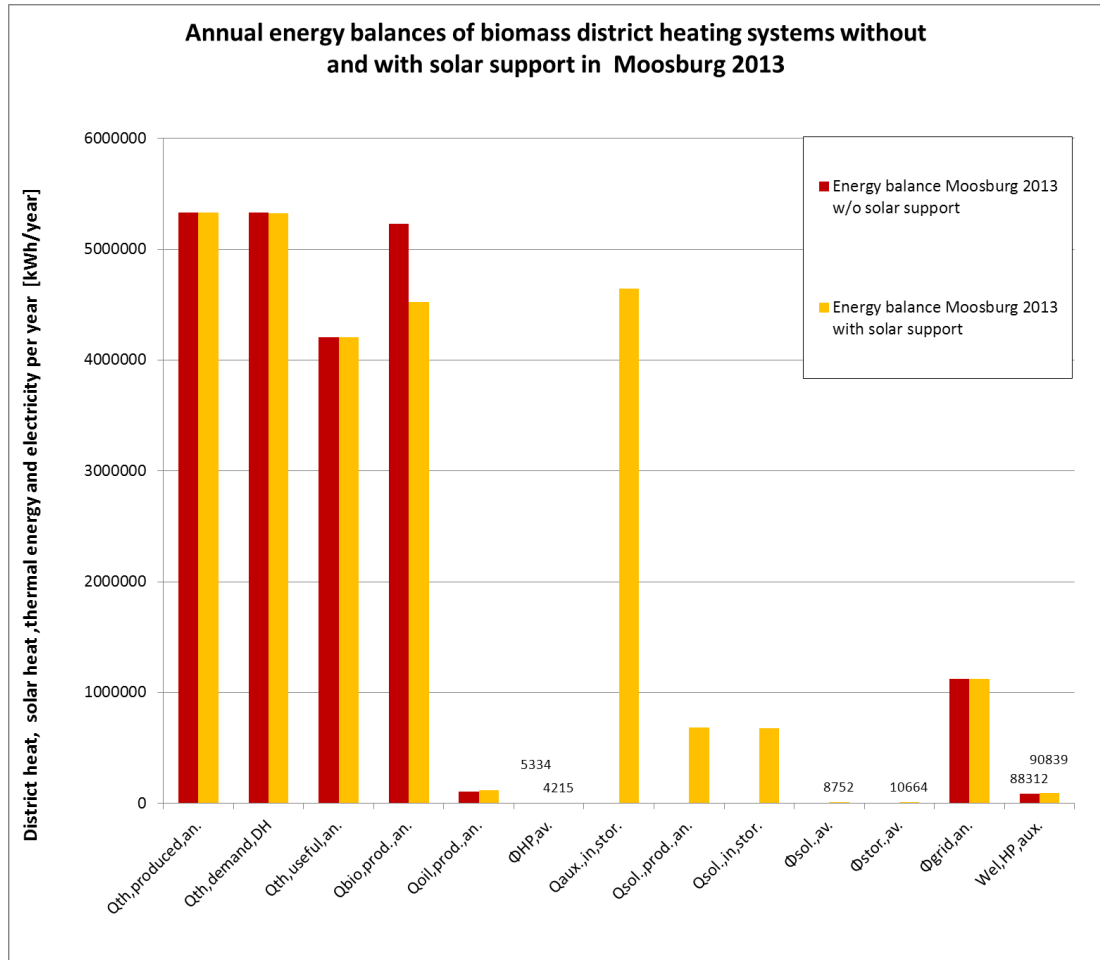


Figure 6-1: Annual energy balances of biomass district heating systems with and without solar support in Moosburg 2013 (data source: simulation results of SHWin and own calculations).

Explanations: $Q_{th,produced,an.}$... Total heat produced by heat resources per year [kWh_{th}];
 $Q_{th,demand,DH}$... Heat fed into the district heating grid per year [kWh_{th}];
 $Q_{th,useful,an.}$... Useful head supplied and sold to the users per year [kWh_{th}];
 $Q_{bio,prod.,an.}$... Heat produced by biomass boiler per year [kWh_{th}];
 $Q_{oil,prod.,an.}$... Heat produced by oil boiler per year [kWh_{th}];
 $\Phi_{HP,av.}$... Heat lost in the heating plant (per year [kWh_{th}];
 $Q_{aux.,in,stor.}$... Annual amount of heat fed into storage tank by boiler(s) [kWh_{th}];
 $Q_{sol.,prod.,an.}$... Heat produced by solar thermal system per year [kWh_{th}];
 $Q_{sol.,in,stor.}$... Solar heat fed into the storage tank per year [kWh_{th}];
 $\Phi_{sol.,av.}$... Heat lost in the solar circuit per year [kWh_{th}];
 $\Phi_{stor.,av.}$... Heat lost in the hot water storage tank per year [kWh_{th}];
 $\Phi_{grid,an.}$... Annual thermal energy losses in DHG [kWh_{th}];
 $W_{el,HP,aux.}$... Total annual electricity demand of heating plant [kWh_{el}].

For the calculation of losses in the heating plant a percentage rate of the produced heat has been taken. It represents more or less the heat losses of the 35 m³ buffer tank, which is available in both configurations, but is not integrated as a solar

thermal storage device (see e.g. $\Phi_{HP,av.}$ in Table 6-1). The heat losses of the 200 m³ solar thermal energy storage are represented by a separate figure (see $\Phi_{stor.,av.}$ in Table 6-1). When applying the simulation program SHWwin the additional buffer storage volume of 35 m³ is not considered for solar thermal feed-in.

As the heating house's equipment stays the same with respect to boiler capacity and the related fuel utilization ratio, the heat producing units differ because of the solar supporting plant. Obviously, the number of NPH_s for the biomass boiler is reduced in case of solar support, as an amount of 676.8 MWh_{th} of solar heat is fed into the thermal energy storage (see $Q_{sol.,in,stor}$ in Table 6-1). The effect of solar thermal feed-in is shown in Figure 6-3.

Figure 6-2 and Figure 6-3 represents the heat demand of the district heating system within the course of one year. Red colored areas are equal to the heat demand covered by the oil boiler, while the green parts of the annual heat demand are assigned to the biomass boiler. The yellow colored, fluctuating area in Figure 6-3 is introduced because of solar heat fed into the district heating grid. Obviously, the share of solar thermal heat is sufficient to provide the required solar power to cover the heating system's base load during summer season.

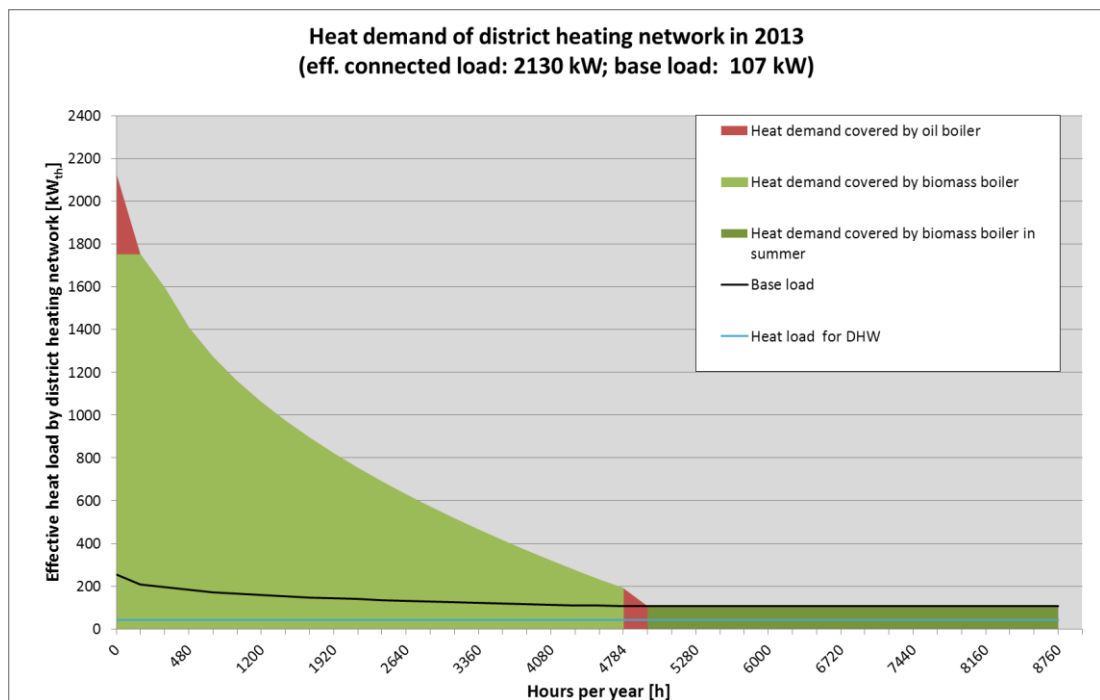


Figure 6-2: Heat demand and assigned heat production resources for a biomass district heating system in Moosburg 2013 (data source: simulation results of SHWwin and own calculations).

While the biomass boiler is operated for about 8610 hours in case of no solar support, it is switched off after running 6550 hours in case of the solar-assisted heating plant. For peak load coverage during summer load operation only the oil boiler is used. For further effects on primary energy demand as a consequence of boiler operation at different load levels, please refer to chapter 6.1.2.

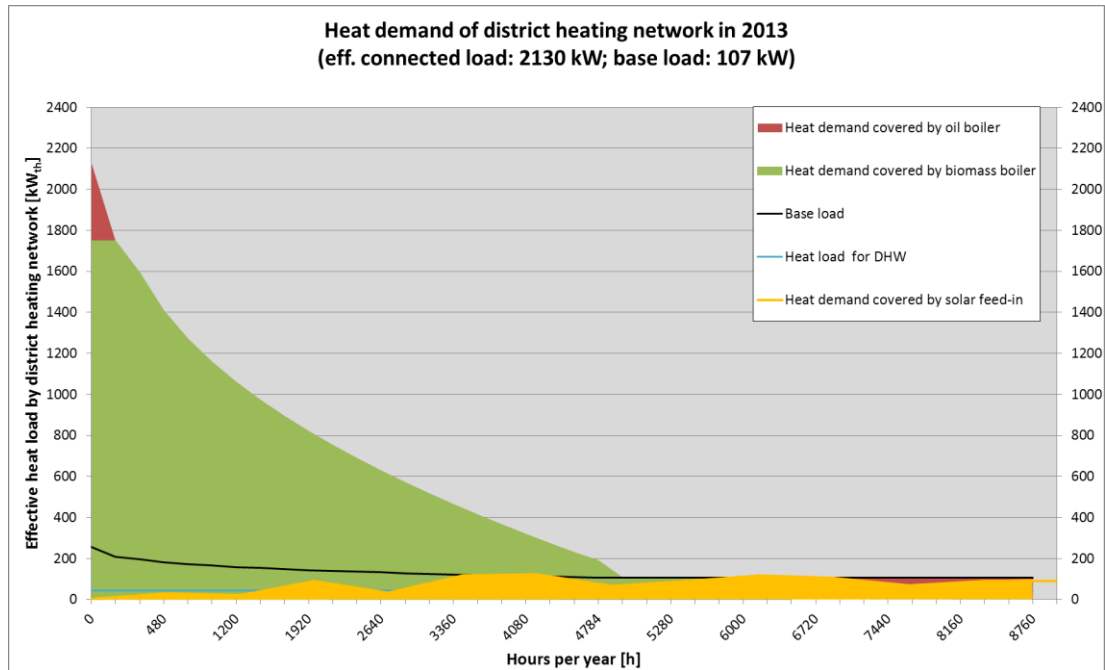


Figure 6-3: Heat demand and assigned heat production resources for a solar-assisted biomass district heating system in Moosburg 2013 (data source: simulation results of SHWin and own calculations).

A quite interesting fact that can be determined in case of a solar-assisted district heating plant is the increased demand of auxiliary electricity (see $W_{el,HP,aux}$ in Table 6-1 and Figure 6-1). For the main part the additional electric energy is needed to run the solar circulation pumps. For details about electricity demand of different electric devices, please refer to the following sub-section 6.1.3.

From the grid's point of view the annual thermal energy losses slightly differ for the compared scenarios. The reason is a different amount of fed in heat but the same amount of district heat consumed on heat consumer side. Consequently, the grid utilization factor, which depends on the amount of produced heat, differs as well.

For evaluated results regarding key indicators and characteristic parameters of the assisting solar plant, please refer to chapter 6.2.2. The interesting results with respect to savings of consumables like wood chips, fuel oil, auxiliary electricity, etc.,

which have a direct impact on the profitability of a solar-assisted biomass heating system, are outlined in chapter 6.1.3.

The next sub-chapter presents the calculated results regarding the primary energy content of fuel consumed by the biomass boiler and the oil boiler in both of the investigated configurations.

6.1.2 Evaluation of fuel demand, boiler operation mode and the respective primary energy content in case of a biomass district heating system with and without solar thermal support in Moosburg 2013

As the annual energy balances are known and the relevant heat resources have been identified in chapter 6.1.1 before, the following table presents the outcome of evaluating the primary energy content of utilized fuel types with respect to two investigated scenarios. The determined figures for the scenario without solar support takes the following considerations into account:

- The biomass boiler operates throughout the whole year. Outside the heating season it runs on a load level less than 30 % of nominal capacity in start / stop operation.
- The oil boiler is started for peak load coverage only and a reserve for maintenance outage of the main boiler.
- For a fast switch-over the oil boiler is permanently in stand-by mode. Consequently, the electricity demand for the oil boiler is relatively high.

In case of operation with solar thermal support the following premises are taken into account:

- The biomass boiler operates until the thermal power of solar feed-in is sufficient to cover the summer load.
- During summer season (June, July, and August) the biomass boiler is switched off. Any additional feed-in of heat during summer load operation must be provided by the oil boiler.
- In case of peak load situation during heating season the oil boiler is still used for peak load coverage.

Results for the predicted boiler operating mode in case of scenario one without solar support and scenario two with solar assistance are listed in Table 6-2.

Table 6-2: Indicators for primary energy content of fuel used in a biomass district heating system without solar thermal support and of fuel used in a solar-assisted biomass district heating system in Moosburg 2013**** (data source: simulation results of SHWin and own calculations).

Indicator for primary energy content	Symbol	Value for DHS w/o solar support	Value for solar-assisted DHS	Delta value (***)	Unit
Annual biomass boiler utilization ratio	$\zeta_{bio,an.}$	0.7178	0.7178	0.0000	[kWh _{th} /kWh _{NCV}]
Annual oil boiler utilization ratio	$\zeta_{oil,an.}$	0.8984	0.8984	0.0000	[kWh _{th} /kWh _{NCV}]
Nominal capacity of biomass boiler	$Q'_{th,bio,nom.}$	1750	1750	0	[kW _{th}]
Nominal capacity of oil boiler	$Q'_{th,oil,nom.}$	1500	1500	0	[kW _{th}]
Nominal power hours of biomass boiler	NPH_{bio}	2987	2586	-401	[h/a]
Nominal power hours of oil boiler	NPH_{oil}	0.7178	0.7178	0.0000	[h/a]
Biomass fuel demand per year	$FD_{bio,vol.}$	9158	7930	-1228	[SRM/a]
Heating oil (fuel) demand per year	$FD_{oil,vol.}$	11937	13373	1437	[l/a]
Primary energy content of biomass fuel input per year*	$Q_{NCV,bio.,an.}$	7281617	6304952	-976665	[kWh _{NCV} /a]
Primary energy content of heating oil input per year**	$Q_{NCV,oil,an.}$	119021	133347	14325	[kWh _{NCV} /a]
Primary energy content of biomass converted above 30% capacity	$Q_{NCV,bio.,>30\%}$	5716477	5119396	-597081	[kWh _{NCV} /a]
Primary energy content of biomass converted below 30% capacity	$Q_{NCV,bio.,<30\%}$	1565140	1185556	-379583	[kWh _{NCV} /a]
Primary energy content of oil converted above 30% boiler capacity	$Q_{NCV,oil,>30\%}$	100865	100865	0	[kWh _{NCV} /a]
Primary energy content of oil converted below 30% boiler capacity	$Q_{NCV,oil,<30\%}$	18157	32482	14325	[kWh _{NCV} /a]
Sum of primary energy content	$Q_{NCV,tot.,an.}$	7400638	6438299	-962339	[kWh_{NCV}/a]

Explanations: * ... Wood chips (30%w.b.): $NCV_{wc30\%,vol.} = 795.1$ [kWh_{NCV}/SRM];
 ** ... Heating oil (0.845 kg/l): $NCV_{oil,mas.} = 11.8$ [kWh_{NCV}/kg];
 *** ... Delta of solar-assisted DHS minus DHS w/o solar support;
 **** ... Connected load: $Q'_{cl,DHN} = 3554$ [kW_{th}]; maximal effective connected load: $Q'_{cl,max,eff.} = 2130$ [kW_{th}]; base load: $\Phi'_{grid,min.} + Q'_{DHW} = 107$ [kW_{th}]; grid length: $l_{grid} = 5755$ [m]; number of heat consumers: $n_{user,i} = 104$ [1].

Obviously, the total amount of primary energy decreases as a considerable share is substituted by solar thermal energy. Nevertheless, the heating oil demand and the related primary energy content increases in case of the solar-assisted scenario. As shown later on, this fact will lead to a higher CO₂ emission for this case.

However, the mode of operation influences the annual fuel demand and the consumption of other resources needed for plant operation. The next sub-section summarizes the annual balance of fuel demand, the demand of consumables and gives an indication for savings because of solar feed-in.

6.1.3 Evaluation of demand for consumables and operation indicators in case of a biomass district heating system with and without solar thermal support in Moosburg 2013

From plant operator's point of view the main reason to extend the existing biomass plant by a solar thermal system would be an increase of economic performance. The most important drivers are savings to be achieved in terms of woody biomass fuel, heating oil and fuel manipulation. In the following table the annual results of the evaluated scenario without solar support and the predictions for solar-assisted operation are shown (see Table 6-3).

*Table 6-3: Consumables and operation indicators for biomass district heating system without solar thermal support and for a solar-assisted biomass district heating system in Moosburg 2013** (data source: simulation results of SHWwin and own calculations).*

Consumable or indicator	Symbol	Value for DHS w/o solar support	Value for solar- assisted DHS	Delta value (*)	Unit
Total annual electricity demand of heating plant	$W_{el,HP,aux.}$	88312	90839	2527	[kWh _{el} /a]
Annual electricity demand for biomass boiler	$W_{el,bio,aux.}$	61618	53132	-8487	[kWh _{el} /a]
Annual electricity demand for oil boiler	$W_{el,oil,aux.}$	2664	5851	3187	[kWh _{el} /a]
Annual electricity demand for solar circulation pumps	$W_{el,sol.,aux.}$	0	7445	7445	[kWh _{el} /a]
Annual electricity demand for hot water circulation pumps	$W_{el,Circ.,aux.}$	21138	21294	156	[kWh _{el} /a]
Biomass fuel demand per year	$FD_{bio,vol.}$	9158	7930	-1228	[SRM/a]
Heating oil (fuel) demand per year	$FD_{oil,vol.}$	11937	13373	1437	[l/a]
Operation hours of telescope loader per year	OpH_{loader}	114	99	-15	[OpH/a]

Consumable or indicator	Symbol	Value for DHS w/o solar support	Value for solar- assisted DHS	Delta value (*)	Unit
Total diesel demand of telescope loader per year	FD_{diesel}	1522	1318	-204	[l/a]
Annual working hours of personnel (e.g. boiler man)	$OpH_{pers.}$	270	255	15	[OpH/a]

Explanations: * ... Delta of solar-assisted DHS minus DHS w/o solar support;
 ** ... Connected load: $Q'_{cl,DHN} = 3554 [kW_{th}]$; maximal effective connected
 load: $Q'_{cl,max,eff.} = 2130 [kW_{th}]$; base load: $\Phi'_{grid,min.} + Q'_{DHW} = 107 [kW_{th}]$; grid
 length: $l_{grid} = 5755 [m]$; number of heat consumers: $n_{user,i} = 104 [1]$;
 DHS ... District Heating System.

As already mentioned before, the electricity demand for the heating plant will increase due to the additional electric driven circulation pumps in the solar circuit. A second driver could be found in the oil boiler running with low capacity, but permanently during summer season.

The following sub-chapter deals with two solar-assisted biomass heating systems designed to achieve a similar annual solar fraction as well as a solar fraction above 90 % during holiday season.

6.2 Energetic appraisal of two solar-assisted district heating plants: Solar-assisted biomass district heating system “MS Fernwärme Moosburg” (2013) compared with solar-assisted biomass district heating system “Nahwärme Eibiswald” (1997)

In the following sub-sections, first the results of an assessment of two biomass district heating systems located in Moosburg and Eibiswald by simulation program SHWwin are presented. Second, an energetic assessment and technological appraisal is described, summarizing the outcome of simulation and its consequences in terms of differences. The third sub-section provides the results of evaluating the primary energy content of the used fuel types in the compared scenarios. Finally, the demand for fuels and consumables predicted in case of solar supported operation in Moosburg 2013 and the evaluated figures for Eibiswald 1997 are listed and compared.

6.2.1 Assessment of two biomass district heating systems located in Moosburg / Carinthia (2013) and Eibiswald / Styria (1997) by simulation program SHWwin

According to the simulation reports the most important simulation output and the calculated differences of simulation results of the two scenarios are summarized in

Table 6-4 and Table 6-5. For details regarding the original simulation reports, please refer to the annex (see Table 12-4 and Table 12-5). First, the scenario of a solar-assisted district heating system in Moosburg is evaluated based on irradiation data provided by Meteonorm (2012). The simulation is based on the frame conditions defined above. A district heating grid with 104 connected heating sub-stations causes a total effective connected load of 2130 kW_{th} and shall be supported by a solar thermal plant. The solar thermal installation comprises a collector field with an area of 1827.6 m² and a thermal energy storage with a volume of 200 m³.

Second, the configuration of a solar-assisted biomass heating plant in Eibiswald operating in the year 1997 to year 1998 is simulated. As input data the predicted effective total load of 2114 kW_{th} for a district heating network connecting 64 heat users is taken.

*Table 6-4: Simulation results for a solar thermal system supporting two biomass district heating networks: Moosburg 2013** and Eibiswald 1997*** (data source: simulation results of SHWwin and own calculations).*

Description	Symbol*	Value for Moosburg	Value for Eibiswald	Unit
Year of operation		2013	1997	[year]
Collector net area	$A_{col,net}$	1827.6	1150.0	[m ²]
Storage volume	$V_{stor.}$	200	105	[m ³]
Storage volume per unit collector area	$v_{col.}$	0.1094	0.0913	[m ³ /m ²]
Total operating time of collectors per year	BeDauKol	1730.6	1876.9	[h]
Global irradiation on total collector area with inclined plane	Global	2588745	1659827	[kWh]
Global irradiation onto collector area, while the collectors are operating	BetrStr	1600540	1173486	[kWh]
Useful energy gained by collectors	NutzKol	685575	467906	[kWh]
Annual amount of heat losses due to circulation in collector loop	ZirkVer	8752	7144	[kWh]
Solar thermal energy fed into storage by collectors	SolSpei	676823	460762	[kWh]
Average energy conversion efficiency of collectors per year	KolWiGr	42.83%	39.87%	[%]
Annual utilization ratio of collectors	KolNuGr	26.48%	28.19%	[%]
Annual solar saving fraction	DeckGr	12.79%	9.97%	[%]

Explanations: * ... Symbols according to simulation reports by SHWwin;
 ** ... Connected load: $Q'_{cl,DHN} = 3554$ [kW_{th}]; maximal effective connected load: $Q'_{cl,max,eff.} = 2130$ [kW_{th}]; base load: $\Phi'_{grid,min.} + Q'_{DHW} = 107$ [kW_{th}]; grid length: $l_{grid} = 5755$ [m]; number of heat consumers: $n_{user,i} = 104$ [1];
 *** ... Connected load: $Q'_{cl,DHN} = 3000$ [kW_{th}]; maximal effective connected load: $Q'_{cl,max,eff.} = 2114$ [kW_{th}]; base load: $\Phi'_{grid,min.} + Q'_{DHW} = 106$ [kW_{th}]; grid length: $l_{grid} = 4000$ [m]; number of heat consumers: $n_{user,i} = 64$ [1].

Table 6-4 summarizes the simulation outcome for the solar thermal part of the investigated plant configurations. In Table 6-5 the simulation results for the part concerning district heat is listed. For a detailed summary of the simulation results and the used input data, please refer to Table 12-4 and Table 12-5, for a graphical representation please see Figure 12-1 and Figure 12-2 in the annex.

Due to different pre-conditions concerning plant configuration heat load of grid, supply flow and return flow temperature and ambient conditions the total operating time of solar pumps in Eibiswald is longer. Consequently, the annual utilization ratio of collectors in Eibiswald shows a higher percentage rate. However, despite the better performance indicators of the plant in Eibiswald the annual solar saving fraction is calculated to 10%, which is a lower value than in Moosburg ($DeckGr = 12.79\%$).

As the simulation tool SHWin calculates the values for global irradiation (G_{global}), for useful energy gained by collectors (N_{utzKol}) and the value for solar thermal energy fed into storage (So/Sp_{el}) on a monthly basis the output for the simulated configuration of “MS Fernwärme Moosburg” is displayed as a bar diagram in Figure 6-4. The determined monthly solar fraction is represented as crosses connected by a line. Obviously, the solar fraction reaches its maximum during summer season, when the global irradiation is high but the heat demand of the district heating system reaches its seasonal minimum.

Figure 6-5 shows the simulation’s outcome with respect to monthly balances of global irradiation (G_{global}), for useful energy gained by collectors (N_{utzKol}) and the value for solar thermal energy fed into storage (So/Sp_{el}) for a solar-assisted biomass district heating system in Eibiswald in year 1997. Again, the maximal monthly solar fraction of more than 90% is reached in August. However, the maximum of global irradiation is measured one month later in September, when the monthly solar fraction is at a level of 84%.

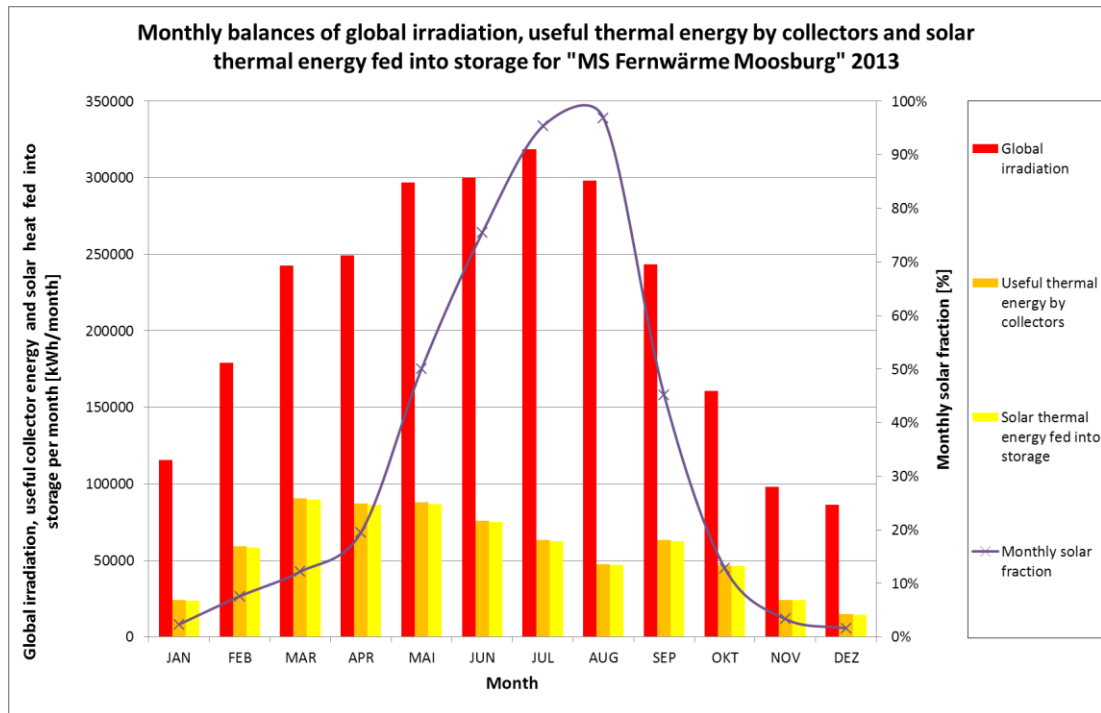


Figure 6-4: Monthly balances of global irradiation, useful thermal energy by collectors and solar thermal energy fed into thermal energy storage for solar-assisted biomass district heating system "MS Fernwärme Moosburg" in year 2013 (data source: simulation results of SHWin).

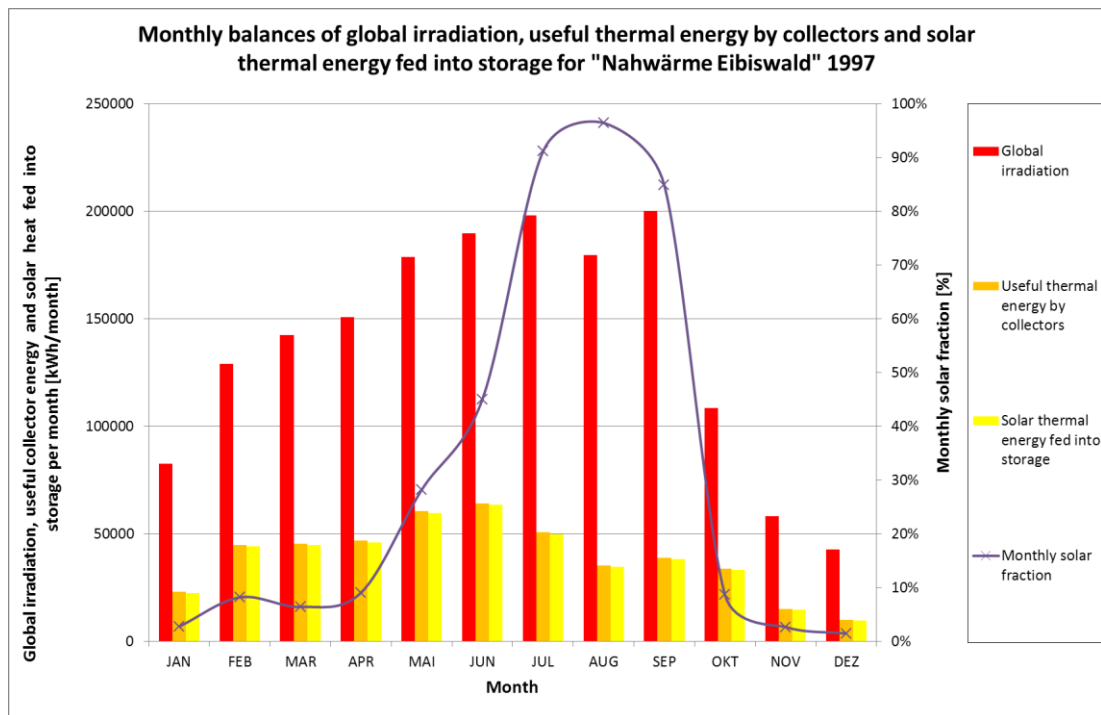


Figure 6-5: Monthly balances of global irradiation, useful thermal energy by collectors and solar thermal energy fed into thermal energy storage for solar-assisted biomass district heating system "Nahwärme Eibiswald" in 1997 (data source: simulation results of SHWin).

When analyzing the collected results for the district heating part of SHWwin's simulation report in Table 6-5, obviously the amount of heat produced by boilers (*Kessel*) and the amount of thermal energy fed into the district heating grid (*FwSpent*) is higher in Moosburg than in Eibiswald. Also the solar thermal gains, which are fed into the storage (*SolSpei*), are lower in Eibiswald.

*Table 6-5: Simulation results for two biomass district heating systems assisted by a solar thermal system: Moosburg 2013** and Eibiswald 1997*** (data source: simulation results of SHWwin and own calculations).*

Description	Symbol*	Value for Moosburg	Value for Eibiswald	Unit
Year of operation		2013	1997	[year]
Total operating time of collectors (i.e. of solar circulation pumps) per year	BeDauKol	1730.6	1876.9	[h]
Maximal temperature of water in thermal storage due to solar thermal feed-in	FwSpTmax	103.5	103.9	[°C]
Minimal temperature of water fed into district heating grid	FwentTmi	55.9	49.8	[°C]
Annual amount of thermal energy fed into district heating grid	FwSpent	5326745	4501483	[kWh]
Annual amount of heat losses by thermal energy storage	FwSpVerl	10664	11891	[kWh]
Produced heat by boilers fed into thermal energy storage	Kessel	4645389	4052605	[kWh]
Solar energy utilized by collectors, which is fed into thermal storage	SolSpei	676823	460762	[kWh]
Electric energy utilized for heat generation	Elektr	0	0	[kWh]
Solar thermal energy as a percentage of useful heat supplied to the consumers' heating sub-stations	DeckFw	12.79%	9.97%	[%]

Explanations: * ... Symbols according to simulation reports by SHWwin;

** ... Connected load: $\dot{Q}'_{cl,DHN} = 3554 [kW_{th}]$; maximal effective connected load: $\dot{Q}'_{cl,max,eff.} = 2130 [kW_{th}]$; base load: $\Phi'_{grid,min.} + \dot{Q}'_{DHW} = 107 [kW_{th}]$; grid length: $l_{grid} = 5755 [m]$; number of heat consumers: $n_{user,i} = 104 [1]$;

*** ... Connected load: $\dot{Q}'_{cl,DHN} = 3000 [kW_{th}]$; maximal effective connected load: $\dot{Q}'_{cl,max,eff.} = 2114 [kW_{th}]$; base load: $\Phi'_{grid,min.} + \dot{Q}'_{DHW} = 106 [kW_{th}]$; grid length: $l_{grid} = 4000 [m]$; number of heat consumers: $n_{user,i} = 64 [1]$.

On the other hand the heat losses of the storage of Eibiswald exceed the losses in Moosburg. Reason for this could be a thicker insulation layer attached to the steel tank in Moosburg and a better volume-to-surface ratio of the large-scale steel tank with 200 m³ of volume. The minimum temperature of water fed into the district heating grid is lower in case of Eibiswald and is equal to the expected minimum during winter operation. For the simulated configuration in Moosburg the minimal

temperature of 55.9°C is higher because of an expected threshold of 75°C granted at the heating sub-stations.

In the next sub-chapter the solar-supported district heating system in Eibiswald in year 1997 and in Moosburg in year 2013 are evaluated and compared from an energetic point of view.

6.2.2 Evaluation of heat demand and energy balances for two solar-assisted biomass district heating systems: Moosburg 2013 and Eibiswald 1997

The energy balances listed in Table 6-6 are the results of simulation by SHWin based on the frame conditions given by the heat demand curve for Moosburg 2013 (see Figure 5-1) and the heat demand curve for Eibiswald 1997 (see Figure 5-4). In order to get an impression about the differences the delta values are listed in a separate column (see Table 6-6).

*Table 6-6: Comparison of key indicators of 2 solar-assisted biomass district heating systems. Moosburg 2013** and Eibiswald 1997*** (data source: simulation results of SHWin and own calculations).*

Indicator	Symbol	Value for Moosburg 2013	Value for Eibiswald 1997	Delta value (*)	Unit
Total heat produced by heat resources per year	$Q_{th,produced,an.}$	5330960	4520507	810453	[kWh _{th} /a]
Heat fed into the district heating grid per year	$Q_{th,demand,DH}$	5326745	4501483	825262	[kWh _{th} /a]
Useful head supplied and sold to the users per year	$Q_{th,useful,an.}$	4205945	3650000	555945	[kWh _{th} /a]
Heat produced by biomass boiler per year	$Q_{bio,prod.,an.}$	4525581	4040098	485483	[kWh _{th} /a]
Heat produced by oil boiler per year	$Q_{oil,prod.,an.}$	119804	12503	107301	[kWh _{th} /a]
Heat produced by solar thermal system per year	$Q_{sol.,prod.,an.}$	685575	467906	217669	[kWh _{th} /a]
Heat lost in the heating plant (e.g. buffer tank losses) per year	$\Phi_{HP,av.}$	4215	19024	-14809	[kWh _{th} /a]
Solar heat fed into the storage tank per year	$Q_{sol.,in,stor.}$	676823	460762	216061	[kWh _{th} /a]
Annual amount of heat fed into the	$Q_{aux.,in,stor.}$	4645389	4052605	592784	[kWh _{th} /a]

<i>Indicator</i>	<i>Symbol</i>	<i>Value for Moosburg 2013</i>	<i>Value for Eibiswald 1997</i>	<i>Delta value (*)</i>	<i>Unit</i>
storage tank by boiler(s)					
Heat lost in the solar circuit per year	$\Phi_{sol,av.}$	8752	7144	1608	[kWh _{th} /a]
Heat lost in the hot water storage tank per year	$\Phi_{stor,av.}$	10664	11891	-1227	[kWh _{th} /a]
Total annual electricity demand of heating plant	$W_{el,HP,aux.}$	90839	73809	17030	[kWh _{el} /a]
Annual thermal energy losses in DHG	$\Phi_{grid,an.}$	1120800	851483	269317	[kWh _{th} /a]

Explanations: * ... Delta of solar-ass. DHS Moosburg 2013 minus solar-ass. DHS Eibiswald 1997;
 ** ... Connected load: $Q'_{cl,DHN} = 3554$ [kW_{th}]; maximal effective connected load: $Q'_{cl,max,eff.} = 2130$ [kW_{th}]; base load: $\Phi'_{grid,min.} + Q'_{DHW} = 107$ [kW_{th}]; grid length: $l_{grid} = 5755$ [m]; number of heat consumers: $n_{user,i} = 104$ [1];
 *** ... Connected load: $Q'_{cl,DHN} = 3000$ [kW_{th}]; maximal effective connected load: $Q'_{cl,max,eff.} = 2114$ [kW_{th}]; base load: $\Phi'_{grid,min.} + Q'_{DHW} = 106$ [kW_{th}]; grid length: $l_{grid} = 4000$ [m]; number of heat consumers: $n_{user,i} = 64$ [1];
 DHG ... District Heating Grid.

Figure 6-6 represents the calculated energy balances in form of a bar diagram. Obviously, the energy balances of the solar district heating system in Moosburg 2013 succeed the balances of Eibiswald in each displayed energetic parameter except for annual losses in the heating plant and except for the heat lost in the hot water storage tank. Due to the fact that different storage volumes are available in Eibiswald and Moosburg the reason could be a better protection against heat losses and a better volume-to-surface ratio of the large-scale steel tank in Moosburg.

With respect to the auxiliary electricity demand the extended district heating grid and the large-scale solar thermal plant in Moosburg require 17.0 MWh_{el}/a more than the heating plant in Eibiswald. As shown later on (see Table 6-8) the highest shares can be assigned to the biomass boilers and the hot water circulation pumps.

Due to a longer heat distribution network the thermal energy losses by pipelines of Moosburg are higher. However, with average specific heat losses of 194.8 kWh_{th}/(m a) the grid in Moosburg shows a better result than the grid in Eibiswald (212.9 kWh_{th}/(m a)).

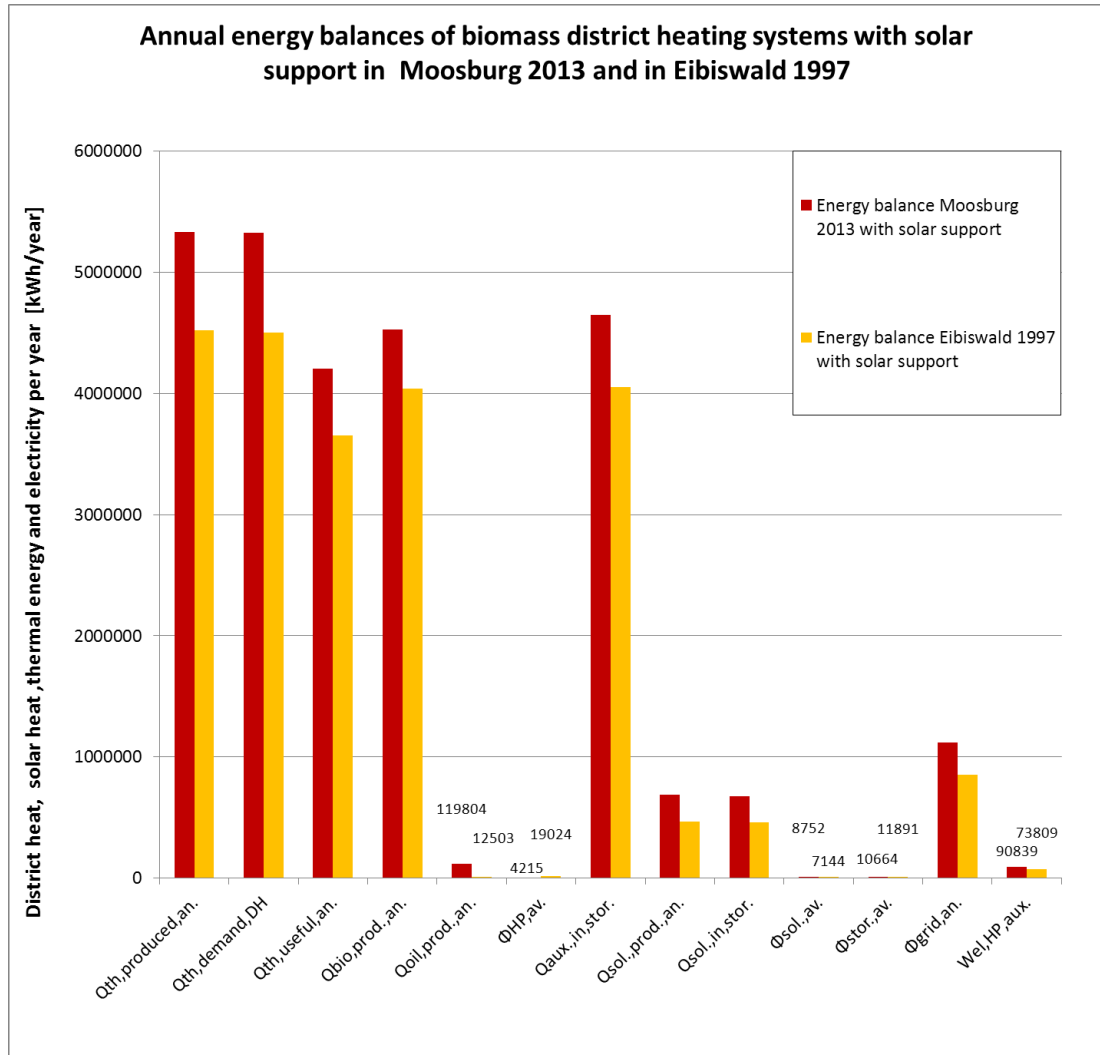


Figure 6-6: Annual energy balances of solar thermal supported biomass district heating systems in Moosburg 2013 and in Eibiswald 1997 (data source: simulation results of SHWin and own calculations).

Explanations: $Q_{th,produced,an.}$... Total heat produced by heat resources per year [kWh_{th}];
 $Q_{th,demand,DH}$... Heat fed into the district heating grid per year [kWh_{th}];
 $Q_{th,useful,an.}$... Useful head supplied and sold to the users per year [kWh_{th}];
 $Q_{bio,prod.,an.}$... Heat produced by biomass boiler per year [kWh_{th}];
 $Q_{oil,prod.,an.}$... Heat produced by oil boiler per year [kWh_{th}];
 $\Phi_{HP,av.}$... Heat lost in the heating plant (per year [kWh_{th}];
 $Q_{aux.,in,stor.}$... Annual amount of heat fed into storage tank by boiler(s) [kWh_{th}];
 $Q_{sol.,prod.,an.}$... Heat produced by solar thermal system per year [kWh_{th}];
 $Q_{sol.,in,stor.}$... Solar heat fed into the storage tank per year [kWh_{th}];
 $\Phi_{sol.,av.}$... Heat lost in the solar circuit per year [kWh_{th}];
 $\Phi_{stor.,av.}$... Heat lost in the hot water storage tank per year [kWh_{th}];
 $\Phi_{grid,an.}$... Annual thermal energy losses in DHG [kWh_{th}];
 $W_{el,HP,aux.}$... Total annual electricity demand of heating plant [kWh_{el}].

In the next sub-chapter a detailed evaluation of fuel demand, boiler operation mode and the respective primary energy content of the converted fuels are presented.

6.2.3 Evaluation of fuel demand, boiler operation mode and the respective primary energy content in case of two solar-assisted biomass district heating systems located in Moosburg (2013) and Eibiswald (1997)

In order to get comparable results the annual utilization ratio of biomass boiler ($\zeta_{bio,an} = 0.7178$) and the utilization ratio of oil boiler ($\zeta_{oil,an} = 0.8984$) is assumed to be equal in both plant configurations. The same applies to nominal efficiency of biomass boiler and oil boiler. The results for the annual fuel demand in both central heating stations, the related energy content of the combusted energy carriers and the calculated nominal power hours are listed in Table 6-7.

Table 6-7: Comparison of indicators for primary energy content of fuel used in 2 solar-assisted biomass district heating systems. Moosburg 2013* and Eibiswald 1997** (data source: simulation results of SHWwin and own calculations).

Indicator	Symbol	Value for Moosburg 2013	Value for Eibiswald 1997	Delta value (***)	Unit
Nominal capacity of biomass boiler	$Q'_{th,bio,nom.}$	1750	2000	-250	[kW _{th}]
Nominal capacity of oil boiler	$Q'_{th,oil,nom.}$	1500	500	1000	[kW _{th}]
Nominal power hours of bio. boiler	NPH_{bio}	2586	2020	566	[h/a]
Nominal power hours of oil boiler	NPH_{oil}	80	25	55	[h/a]
Biomass fuel demand per year	$FD_{bio,vol.}$	7930	7079	851	[SRM/a]
Heating oil (fuel) demand per year	$FD_{oil,vol.}$	13373	1396	11978	[l/a]
Primary energy content of biomass fuel input per year	$Q_{NCV,bio.,an.}$	6304952	5628587	676366	[kWh _{NCV/a}]
Primary energy content of heating oil input per year	$Q_{NCV,oil,an.}$	133347	13916	119430	[kWh _{NCV/a}]
Primary energy content of biomass converted above 30% capacity	$Q_{NCV,bio.,>30\%}$	5119396	4208951	910445	[kWh _{NCV/a}]
Primary energy content of biomass converted below 30% capacity	$Q_{NCV,bio.,<30\%}$	1185556	1419636	-234079	[kWh _{NCV/a}]
Primary energy content of oil converted above 30% boiler capacity	$Q_{NCV,oil,>30\%}$	100865	0	100865	[kWh _{NCV/a}]
Primary energy content of oil converted below 30% boiler capacity	$Q_{NCV,oil,<30\%}$	32482	13916	18566	[kWh _{NCV/a}]
Sum of primary energy content	$Q_{NCV,tot.,an.}$	6438299	5642503	795796	[kWh_{NCV/a}]

Explanations: * ... Wood chips (30%w.b.): $NCV_{wc30\%,vol.} = 795.1 \text{ [kWh}_{NCV}/\text{SRM}]$;
 ** ... Heating oil (0.845 kg/l): $NCV_{oil,mas.} = 11.8 \text{ [kWh}_{NCV}/\text{kg}]$;
 *** ... Delta of solar-ass. DHS Moosburg 2013 minus solar-ass. DHS Eibiswald 1997;
 + ... Connected load: $Q'_{cl,DHN} = 3554 \text{ [kW}_{th}]$; maximal effective connected load: $Q'_{cl,max,eff.} = 2130 \text{ [kW}_{th}]$; base load: $\Phi'_{grid,min.} + Q'_{DHW} = 107 \text{ [kW}_{th}]$; grid length: $l_{grid} = 5755 \text{ [m]}$; number of heat consumers: $n_{user,i} = 104 \text{ [1]}$;
 ++ ... Connected load: $Q'_{cl,DHN} = 3000 \text{ [kW}_{th}]$; maximal effective connected load: $Q'_{cl,max,eff.} = 2114 \text{ [kW}_{th}]$; base load: $\Phi'_{grid,min.} + Q'_{DHW} = 106 \text{ [kW}_{th}]$; grid length: $l_{grid} = 4000 \text{ [m]}$; number of heat consumers: $n_{user,i} = 64 \text{ [1]}$.

The figures of primary energy content of heating oil and wood chips converted at different boiler load levels are the basis for emission calculations based on emission factors later on.

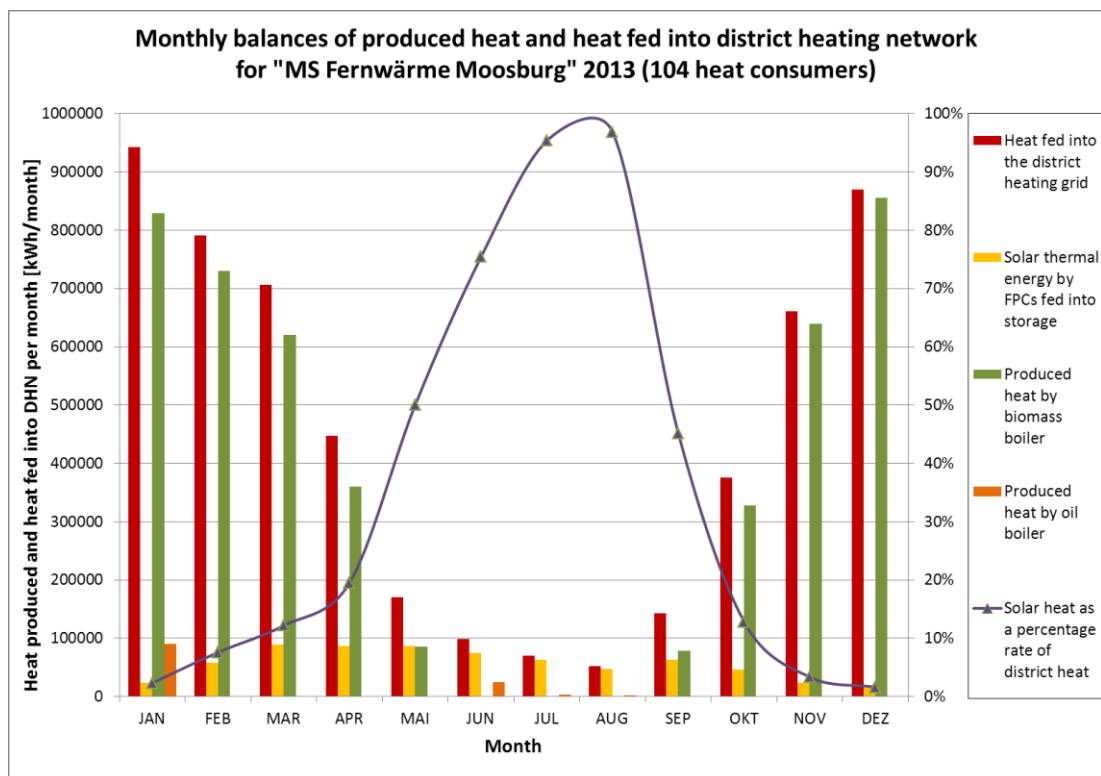


Figure 6-7: Monthly balances of heat produced by boilers, heat fed into the district heating grid, solar thermal energy fed into thermal energy storage and solar heat as a percentage rate of district heat determined for a solar-assisted biomass district heating system "MS Fernwärme Moosburg" in year 2013 (data source: simulation results of SHWin and own calculations).

With respect to boiler operation mode Figure 6-7 and Figure 6-8 display the assumed split of heat production on a monthly basis. In the assumed operation mode of the heating plant in Moosburg the biomass boiler is switched off in June, July and August, when the monthly solar saving fraction is high and the heat demand of the district heating system reaches its yearly minimum. The oil boiler

operates in stand-by mode and is used only in case the solar feed in is not sufficient. During the heating period the oil boiler is rarely started but is used for peak load coverage, if necessary.

If Figure 6-8 is analyzed in more detail a different usage of boilers will be found. As more biomass capacity is available, no peak load coverage of the oil boiler is necessary. The biomass boiler is able to provide the required thermal power during heating season. In July, August and September the biomass boiler is put out of operation and the oil boiler has to operate on low capacity level, if the required flow pipe temperature can not be granted by solar feed-in.

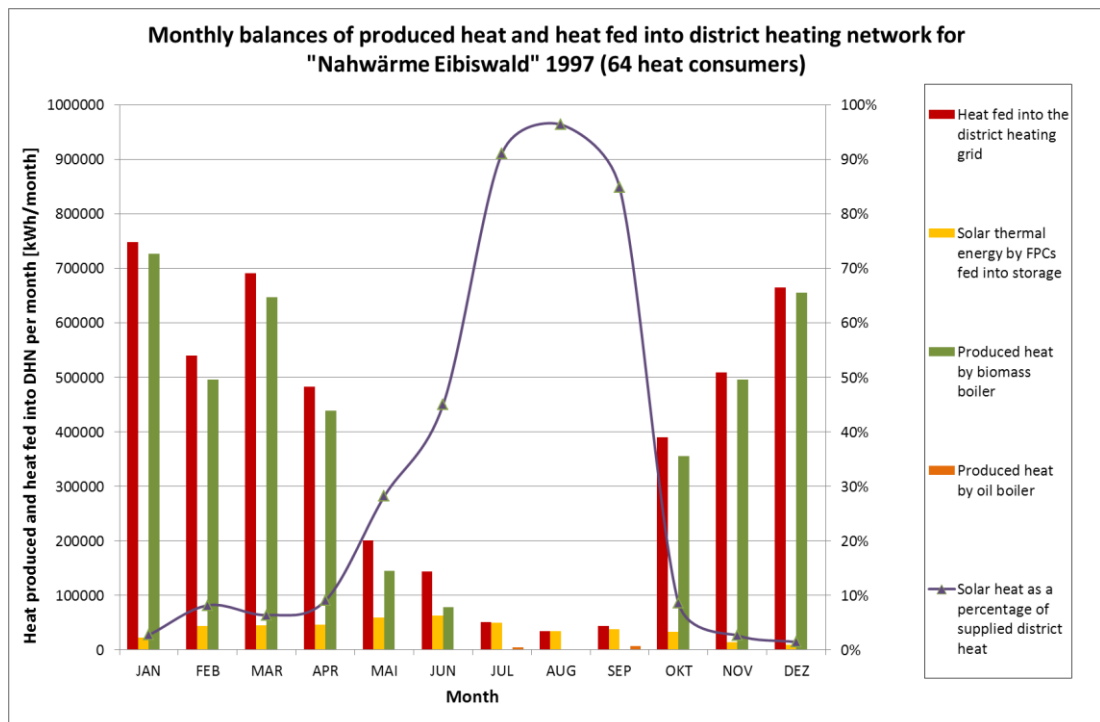


Figure 6-8: Monthly balances of heat produced by boilers, heat fed into the district heating grid, solar thermal energy fed into thermal energy storage and solar heat as a percentage rate of district heat determined for a solar-assisted biomass district heating system "Nahwärme Eibiswald" in year 1997 (data source: simulation results of SHWin and own calculation).

In the next sub-chapter the demand for consumables and further operation indicators for the two investigated applications are evaluated.

6.2.4 Evaluation of demand for consumables and further operation indicators in case of two solar-assisted biomass district heating systems: Moosburg 2013 and Eibiswald 1997

For a detailed overview on the determined operation indicators and the amount of consumables required by the two solar-assisted biomass district heating systems

during regular operation, please refer to Figure 6-8. In order to get an impression about the differences the delta values are listed in a separate column.

*Table 6-8: Comparison of consumables and operation indicators for solar-assisted biomass district heating systems. Moosburg 2013** and Eibiswald 1997*** (data source: simulation results of SHWwin and own calculations).*

<i>Indicator</i>	<i>Symbol</i>	<i>Value for Moosburg 2013</i>	<i>Value for Eibiswald 1997</i>	<i>Delta value (*)</i>	<i>Unit</i>
Total annual electricity demand of heating plant	$W_{el,HP,aux.}$	90839	73809	17030	[kWh _{el} /a]
Annual electricity demand for biomass boiler	$W_{el,bio,aux.}$	53132	47432	5700	[kWh _{el} /a]
Annual electricity demand for oil boiler	$W_{el,oil,aux.}$	5851	611	5240	[kWh _{el} /a]
Annual electricity demand for solar circulation pumps	$W_{el,sol.,aux.}$	7445	5068	2377	[kWh _{el} /a]
Annual electricity demand for hot water circulation pumps	$W_{el,Circ.,aux.}$	21294	18000	3294	[kWh _{el} /a]
Annual electricity demand for further devices (lighting, IT, etc.)	$W_{el,etc.,aux.}$	3118	2698	419	[kWh _{el} /a]
Biomass fuel demand per year	$FD_{bio,vol.}$	7930	7079	851	[SRM/a]
Heating oil (fuel) demand per year	$FD_{oil,vol.}$	13373	1396	11978	[l/a]
Operation hours of telescope loader per year	OpH_{loader}	99	88	11	[OpH/a]
Total diesel demand of telescope loader per year	FD_{diesel}	1318	1176	141	[l/a]
Annual working hours of personnel (e.g. boiler man)	$OpH_{pers.}$	255	281	-26	[OpH/a]

Explanations: * ... Delta of solar-ass. DHS Moosburg 2013 minus solar-ass. DHS Eibiswald 1997;

** ... Connected load: $Q'_{cl,DHN} = 3554$ [kW_{th}]; maximal effective connected load: $Q'_{cl,max,eff.} = 2130$ [kW_{th}]; base load: $\Phi'_{grid,min.} + Q'_{DHW} = 107$ [kW_{th}]; grid length: $l_{grid} = 5755$ [m]; number of heat consumers: $n_{user,i} = 104$ [1];

*** ... Connected load: $Q'_{cl,DHN} = 3000$ [kW_{th}]; maximal effective connected load: $Q'_{cl,max,eff.} = 2114$ [kW_{th}]; base load: $\Phi'_{grid,min.} + Q'_{DHW} = 106$ [kW_{th}]; grid length: $l_{grid} = 4000$ [m]; number of heat consumers: $n_{user,i} = 64$ [1].

Except for the working hours of personnel the results for Moosburg succeed the figures for Eibiswald. However, due to different biomass boiler capacities and different oil boiler operation modes the demand for heating oil in Moosburg is nearly ten times higher than in Eibiswald. Consequently, the related CO₂ emission balance

for the heating station in Moosburg should show a significant deflection. The following chapter will describe the results of calculating the emissions of CO₂, CO, C_xH_x, NO_x and particles based on the primary energy content of fuel determined in chapter 6.2.3.

6.3 Evaluation of emissions in case of biomass district heating systems without and with solar support

Based on the method in chapter 3.1.3 in the following the ecological effects of biomass district heating systems without and with solar thermal support in terms of gaseous emissions and particle emissions have been assessed. Detailed results for evaluating the emissions of CO₂, CO, C_xH_x, NO_x and particles based on the primary energy content of wood chips and heating oil can be found in Table 12-6, Table 12-7, and Table 12-8 in the annex. In each table the calculated emissions are listed in absolute figures for two different kinds of operation modes of biomass boiler and oil boiler. A graphical display in form of bar diagrams is shown in Figure 12-3 in the annex.

For later comparison the total emissions of CO₂, CO, C_xH_x, NO_x and particles are expressed as annual specific emissions related to the annual amount of heat fed into the district heating grid. The values are determined thanks to the emission factors defined in chapter 3.1.3, the different boiler operation modes assumed in chapters 6.1.2 and 6.2.3 and the calculated net calorific value of the converted biomass fuel and heating oil (see Table 6-2 and Table 6-7).

Table 6-9: Total, annual emissions based on primary energy content of fuel of a biomass district heating system without and with solar support in Moosburg 2013 (data source: simulation results of SHWin and own calculations).*

Type of heating plant	Unit	CO ₂	CO	C _x H _x	NO _x	Particles
Emissions of biomass DHS w/o solar support	[t/a]	32.136	7.048	0.471	2.754	3.743
Emissions of solar-assisted biomass DHS	[t/a]	36.004	5.440	0.362	2.392	2.930
ΔEMI /emission savings	[t/a]	3.868	-1.608	-0.109	-0.362	-0.814

Explanations: $\Delta EMI \dots EMI_{SADHS} - EMI_{DHS}$;
 $\Delta emi \dots emi_{SADHS} - emi_{DHS}$;
SADHS ... Solar-assisted district heating system;
DHS ... District heating system w/o solar support;
** ... Connected load: $Q'_{cl,DHN} = 3554 [kW_{th}]$; maximal effective connected load: $Q'_{cl,max,eff.} = 2130 [kW_{th}]$; base load: $\Phi'_{grid,min.} + Q'_{DHW} = 107 [kW_{th}]$; grid length: $l_{grid} = 5755 [m]$; number of heat consumers: $n_{user,i} = 104 [1]$.*

As distinct from operation mode of the pure biomass district heating system, for operation of a solar-assisted biomass district heating plant the biomass boiler is stopped during holiday season. With the results for total emissions given in Table 12-6 and Table 12-7 an emission balance can be established by comparing the emissions of a solar-assisted heating system with the emissions of a simple heating plant. The difference will show, if emission savings will be achieved by the solar supported heating station (see Table 6-9).

Obviously, the operation of an assisting solar plant can reduce the emissions of CO, C_xH_x, NO_x and particles, while the CO₂ emissions will grow. The same results are carried out, if the annual specific emissions are compared (see Table 6-10).

Table 6-10: Specific emissions per unit heat fed into district heating system of a biomass district heating system without and with solar support in Moosburg 2013 (data source: simulation results of SHWin and own calculations).*

Type of heating plant	Unit	CO ₂	CO	C _x H _x	NO _x	Particles
Annual specific emissions of biomass DHS w/o solar support per unit heat fed into DHN	[g/kWh _{th}]	6.031	1.323	0.088	0.517	0.703
Annual specific emissions of solar-assisted DHS per unit heat fed into DHN	[g/kWh _{th}]	6.759	1.021	0.068	0.449	0.550
Δemi /specific emission savings	[g/kWh _{th}]	0.728	-0.302	-0.020	-0.068	-0.153

Explanations: $\Delta EMI \dots EMI_{SADHS} - EMI_{DHS}$;
 $\Delta emi \dots emi_{SADHS} - emi_{DHS}$;
SADHS ... Solar-assisted district heating system;
DHS ... District heating system w/o solar support;
** ... Connected load: $Q'_{cl,DHN} = 3554 [kW_{th}]$; maximal effective connected load: $Q'_{cl,max,eff.} = 2130 [kW_{th}]$; base load: $\Phi'_{grid,min.} + Q'_{DHW} = 107 [kW_{th}]$; grid length: $l_{grid} = 5755 [m]$; number of heat consumers: $n_{user,i} = 104 [1]$.*

However, the balance of CO₂ emissions shows a significant increase of the main greenhouse gas, even though a solar thermal system is applied. The next section gives the results for annual greenhouse gas savings and air pollutant savings in case the district heating system's useful energy balance is compared with a reference system.

6.4 Evaluation of greenhouse gas and air pollutant savings compared to conventional district heating

In order to evaluate a set of figures for later comparison the following two sub-chapters assess the emission balance and the expected greenhouse gas and air

pollutant savings of solar-assisted biomass district heating plants in Moosburg in year 2013 and Eibiswald in year 1997.

6.4.1 Greenhouse gas and air pollutant savings compared to conventional district heating in case of a solar-assisted biomass district heating system in Moosburg 2013

To evaluate the annual greenhouse gas and air pollutant emission savings a solar-assisted biomass heating system in Moosburg, the amount of useful heat supplied and sold to heat consumers and the related greenhouse gas and air pollutant emissions are determined. The result is compared to the energy balance of a reference system and its related greenhouse gas and air pollutant emissions. The differences are either annual air pollutant savings measured in kg of SO₂-equivalents per year or annual greenhouse gas savings expressed in kg of CO₂-equivalents per year (see Table 6-11).

Table 6-11: Annual GHG emission savings and air pollutants savings by a solar-assisted biomass district heating system in Moosburg 2013 compared to conventional district heat supply by a district heating mix (data source: GEMIS (2010), Kaltschmitt & Streicher (2009), own calculations).*

Scenario	Annual air pollutants savings [kg SO ₂ -eq. / a]	Rel. air pollutants savings [% / a]	Annual GHG emission savings [kg CO ₂ -eq. / a]	Rel. GHG emission savings [% / a]
Solar-assisted biomass district heating system "MS Fernwärme Moosburg 2013" compared with a district heat supply mix	807.7	47.8%	993885.1	93.2%

Explanations: * ... Connected load: $Q'_{cl,DHN} = 3554 [kW_{th}]$; maximal effective connected load: $Q'_{cl,max,eff.} = 2130 [kW_{th}]$; base load: $\Phi'_{grid,min.} + Q'_{DHW} = 107 [kW_{th}]$; grid length: $l_{grid} = 5755 [m]$; number of heat consumers: $n_{user,i} = 104 [1]$.

For relative air pollutants and greenhouse gas savings the results for annual savings are related to air pollutants and greenhouse gas emissions of the reference system. The next chapter deals with an ecological appraisal of the reference system in Eibiswald, which is carried out for the year 1997.

6.4.2 Greenhouse gas and air pollutant savings compared to conventional district heating in case of a solar-assisted biomass district heating system in Eibiswald 1997

The annual air pollutant savings in kg of SO₂-equivalents and the annual greenhouse gas savings in kg of CO₂-equivalents of a solar-assisted biomass district heating system operated in Eibiswald in year 1997 are listed in Table 6-12.

Table 6-12: Annual GHG emission savings and air pollutants savings by a solar-assisted biomass district heating system in Eibiswald 1997 compared to conventional district heat supply by a district heating mix (data source: GEMIS (2010), Kaltschmitt & Streicher (2009), own calculations).*

Scenario	Annual air pollutants savings [kg SO ₂ -eq. / a]	Rel. air pollutants savings [% / a]	Annual GHG emission savings [kg CO ₂ -eq. / a]	Rel. GHG emission savings [% / a]
Solar-assisted biomass district heating system "Nahwärme Eibiswald 1997" compared with a district heat supply mix	700.9	47.8%	862512.7	93.2%

Explanations: * ... Connected load: $Q'_{cl,DHN} = 3000 [kW_{th}]$; maximal effective connected load: $Q'_{cl,max,eff.} = 2114 [kW_{th}]$; base load: $\Phi'_{grid,min.} + Q'_{DHW} = 106 [kW_{th}]$; grid length: $l_{grid} = 4000 [m]$; number of heat consumers: $n_{user,i} = 64 [1]$.

As a reference the annual emissions of conventional district heat supply according to GEMIS 4.6 (2010) is used. The figures in kg of CO₂-equivalents or kg of SO₂-equivalents respectively, as well as the percentage rates for relative air pollutant emission savings or relative greenhouse gas emission savings will be used for comparison and discussion in chapter 7.2 later on.

6.5 Economic assessment of an extended biomass district heating system with 104 heat consumers in Moosburg 2013

In the following sub-sections two detailed economic assessment based on the annuity method according to guideline VDI 2067 Blatt1 (2012) are conducted. In chapter 6.5.1 the economic feasibility of a pure grid extension in Moosburg is checked. Chapter 6.5.2 assesses the economic feasibility of an investment project, which includes an extended grid and a newly built solar thermal plant in Moosburg of year 2013.

6.5.1 Economic assessment based on annuity method in case of grid extension for a biomass district heating system without solar support in Moosburg 2013

Basis for the entire economic assessment is the extension of the existing district heating network in Moosburg. As already described in chapter 5.2.1 it is planned to have 1905 trench meters more and to connect additional 45 heating sub-stations. In the central heating station the existing 1500 kW_{th} biomass boiler shall be upgraded with an additional capacity of 250 kW_{th}.

In Table 6-13 initial investment costs for different district heating plant components and the related average lifetime (*TN*) are listed. Beside the investments foreseen for the grid extension in 2013 also the basic investment cost for the biomass district heating plant and the initial investment costs for the heat distribution network concerning the year 2009 up to year 2011 are included.

The economic assessment shall be done based on the approach, which is suggested by guideline VDI 2067 Blatt 1 (2012). It is the goal to show the economic feasibility of a simple grid extension project assuming a 40 % investment funding for environmentally relevant investments of the entire project scope. The investment horizon is set to twenty years counted from year 2009, when the project started.

*Table 6-13: Initial investment costs and specific investment costs for plant components of a biomass district heating system in Moosburg 2013** (data source: Biermayr, et al. (2012), SDH (2012), Kaltschmitt&Streicher (2009), QM-report (2012)).*

<i>Plant unit</i>	<i>Investment cost (A0₀₉) Year 2009</i>	<i>% of inv. 2009</i>	<i>Investment cost (A0₁₁) Year 2011</i>	<i>% of inv. 2011</i>	<i>Investment cost (A0₁₂) Year 2012</i>	<i>% of inv. 2012</i>	<i>TN*</i>
<i>Unit</i>	<i>[€]</i>	<i>[%]</i>	<i>[€]</i>	<i>[%]</i>	<i>[€]</i>	<i>[%]</i>	<i>[a]</i>
Biomass district heating plant							
Land	0.00	0.0%	0.00	0.0%	0.00	0.0%	50
Infrastructure and outside facilities	33427.00	1.5%	0.00	0.0%	0.00	0.0%	30
Buildings and building infrastructure	503343.00	22.7%	595.00	0.6%	0.00	0.0%	30
Biomass boiler incl. fire box (1.75 MW)	262800.00	11.9%	0.00	0.0%	12500.00	2.2%	25
Hydraulic installations	110723.00	5.0%	0.00	0.0%	0.00	0.0%	25
Permissions, contracting,	81703.00	3.7%	3000.00	3.1%	18420.82	3.3%	25

<i>Plant unit</i>	<i>Investment cost (A0₀₉) Year 2009</i>	<i>% of inv. 2009</i>	<i>Investment cost (A0₁₁) Year 2011</i>	<i>% of inv. 2011</i>	<i>Investment cost (A0₁₂) Year 2012</i>	<i>% of inv. 2012</i>	<i>TN*</i>
<i>Unit</i>	<i>[€]</i>	<i>[%]</i>	<i>[€]</i>	<i>[%]</i>	<i>[€]</i>	<i>[%]</i>	<i>[a]</i>
expert assessments							
Engineering, planning, project steering	35535.00	1.6%	0.00	0.0%	7894.64	1.4%	25
Grid connection to electric mains	2984.00	0.1%	2284.00	2.4%	0.00	0.0%	25
Oil boiler (peak load boiler)	12810.00	0.6%	0.00	0.0%	0.00	0.0%	20
Oil burner	6771.00	0.3%	0.00	0.0%	0.00	0.0%	12
Monitoring and controlling SW for boiler/heating station	65700.00	3.0%	0.00	0.0%	0.00	0.0%	10
Electric installations	27465.00	1.2%	0.00	0.0%	0.00	0.0%	15
Electronic installations (system control)	5986.00	0.3%	0.00	0.0%	0.00	0.0%	10
Vehicles (Telescope loader)	27600.00	1.2%	0.00	0.0%	0.00	0.0%	8
Monitoring and controlling SW for DHNW / consumer heat stations	10563.00	0.5%	7549.00	7.8%	13814.24	2.4%	10
Construction of district heating grid	952016.00	42.9%	83735.00	86.2%	512494.98	90.7%	40
Installation of consumer sub-stations	78291.00	3.5%	0.00	0.0%	0.00	0.0%	20
Sum investment costs biomass district heating plant:	2217717.00	100%	97163.00	100%	565124.67	100%	

Explanations: * ... Average lifetime of component in years according VDI 2067 Blatt 1;
 ** ... Connected load: $Q'_{cl,DHN} = 3554 [kW_{th}]$; maximal effective connected load: $Q'_{cl,max,eff.} = 2130 [kW_{th}]$; base load: $\Phi'_{grid,min.} + Q'_{DHW} = 107 [kW_{th}]$; grid length: $l_{grid} = 5755 [m]$; number of heat consumers: $n_{user,i} = 104 [1]$.

In a first step the initial investment costs of the overall project are evaluated. The considered components including the relevant average lifetime can be found in Table 6-13. Summing up the investment items of the relevant year, in year 2009 an amount of $A0_{09} = 2217717 \text{ €}$, in 2011 an amount of $A0_{11} = 97163 \text{ €}$ and in 2012 an

amount of $A_{0,12} = 565124.67 \text{ €}$ have been spent to get the plant configuration ready for operation. Obviously, the costs for grid extension have a 90 % share of the total investment volume in 2012, while about 43 % of the total investment in the year 2009 can be assigned to grid installations done for the initial district heating network.

Table 6-14 shows capital costs items in form of present values with respect to year 0 (i.e. year 2009) of the investment project. The other cost and income items are related to year 5 (i.e. year 2014). In year 2014 the balances of the first operating period with the new plant configuration are evaluated and will be taken as a basis for further comparison. Consumption costs, operation costs and other costs are computed based on the results, which are summarized in QM-report (2012) (please refer to chapter 4.1.3). For maintenance costs a percentage rate of the initial investments is used considering a discounting of investment items of year 2011 and 2012 to present values in year 0.

The income in year 2014 is determined by multiplying a net heat price of $79.31 \text{ € / MWh}_{th}$ with an amount of $Q_{th,useful,an.} = 4205.94 \text{ MWh}_{th}$ supplied and sold to heat consumers in year 2013. Other income items like a one-time connection fee or the income from a 40 % investment funding are not relevant in year 2014, but these proceeds are considered in the sum of present values or the present values of investments as well as in the specific annuities calculated for income from one-time connection fee and by income from funding (see Table 6-14).

Table 6-14: Cost items split according to VDI2067, Blatt1 (2012) and income items for a biomass district heating installation in Moosburg 2013 (data source: own calculations). Annuity items calculated according to VDI2067, Blatt1 (2012) (data source: own calculations)*

Cost / Income Item	Value	Unit	Annuity Item	Annuity	Unit
Capital costs (2009):					
Sum of PV of investment costs (A_0) calculated in year 0 (2009)	2801431.58	[€]	Annuity of investment costs ($A_{N,Inv.}$)	215923.47	[€]
Sum of present values ($A_0+A_1+A_2+ \dots -RW$) calculated in year 0 (2009)	2473591.00	[€]	Annuity of capital costs ($A_{N,K}$)	190654.79	[€]
Consumption costs (2014):					
Fuel costs (primary energy costs: wood chips)	152361.20	[€/year]	Annuity of fuel costs: wood chips ($A_{N,V,WC}$)	155781.07	[€]
Fuel costs (primary energy costs: heating oil)	7863.66	[€/year]	Annuity of fuel costs: oil ($A_{N,V,oil}$)	8087.91	[€]
Electricity costs (auxiliary demand)	12539.02	[€/year]	Annuity of electricity costs ($A_{N,V,El}$)	12748.45	[€]

Cost / Income Item	Value	Unit	Annuity Item	Annuity	Unit
Telecommunication costs (monitoring)	533.30	[€/year]	Annuity of Telco costs ($A_{N,V,Tel}$)	584.48	[€]
Costs for other consumables (water, chemicals, diesel, etc.)	1240.39	[€/year]	Annuity of costs for other consumables ($A_{N,V,OC}$)	1247.21	[€]
Costs for ash disposal, sewage disposal, chimney sweeper)	313.70	[€/year]	Annuity of costs for disposal ($A_{N,V,Disp}$)	335.44	[€]
Total consumption costs in year 5 (A_{V5})	174851.27	[€/year]	Annuity of consumption costs ($A_{N,V}$)	178784.54	[€]
Operation & Maintenance costs (2014):					
Annual working hours 2014	270	[h/year]			
Annual personal costs 2014	10029.89	[€/year]			
Total operation costs in year 5 (A_{B5})	10029.89	[€/year]	Annuity of operation costs ($A_{N,B}$)	10768.18	[€]
Annual maintenance costs in year 5 (A_{IN5})	40923.93	[€/year]	Annuity of maintenance costs (A_{IN})	42672.92	[€]
Total O&M costs per year	50953.82	[€/year]			
Other costs 2014:					
Other cost (miscellaneous: advertisement, service social rooms, etc.) 2014	772.73	[€/year]			
Insurance costs 2014	3116.66	[€/year]			
Administration costs (tax cons., admin.) 2014	6078.78	[€/year]			
Costs for taxes and fees (community tax, land tax, land fee, tourism fee, etc.)	2555.15	[€/year]			
Costs for land lease in 2014	5563.63	[€/year]			
Total other costs in year 5 (A_{S5})	18086.93	[€/year]	Annuity of other costs ($A_{N,S}$)	19376.76	[€]
Total costs (w/o capital costs) per year:	243892.03	[€/year]			
			Annuity of costs ($A_{N,K} + A_{N,V} + A_{N,B} + A_{N,S}$)	442257.19	[€]
Income 2014					
Net heat price	79.31	[€/MWh]			
Amount of heat supplied and sold to consumers	4205.94	[MWh/a]			
Income from useful heat supplied and sold to consumers	333584.09	[€/year]	Annuity of income from heat sold ($A_{N,FIT}$)	351870.95	[€]
Income from one-time connection fee in 2014	0.00	[€/year]	Annuity of income from one-time connection fee ($A_{N,Econ}$)	54529.84	[€]

Cost / Income Item	Value	Unit	Annuity Item	Annuity	Unit
Income from investment funding in 2014	0.00	[€/year]	Annuity of income from funding ($A_{N,Es\sub{ub}}$)	59572.41	[€]
Total annual income in year 5 (E5)	333584.09	[€/year]	Annuity of income ($A_{N,E}$)	465973.21	[€]
			Total Annuity		
			Total Annuity ($A_N = A_{N,E} - (A_{N,K} + A_{N,V} + A_{N,B} + A_{N,S})$)	23716.02	[€]
			Capital Recovery Factor (CRF) = Annuity factor (a)	0.07707612	[1]
			Net Present Value (NPV = $A_N \cdot 1/CRF$)	307696.08	[€]

Explanations: * ... Nominal capacity of biomass boiler: $Q'_{bio,nom.} = 1750 [kW_{th}]$;
 Nominal capacity of oil boiler: $Q'_{oil,nom.} = 1500 [kW_{th}]$;
 Storage volume of buffer tank: $V_{buf.} = 35 [m^3]$;
 Connected load: $Q'_{cl,DHN} = 3554 [kW_{th}]$;
 Maximal effective connected load: $Q'_{cl,max,eff.} = 2130 [kW_{th}]$;
 Base load: $\Phi'_{grid,min.} + Q'_{DHW} = 107 [kW_{th}]$;
 Grid length: $l_{grid} = 5755 [m]$;
 Number of heat consumers: $n_{user,i} = 104 [1]$.

Following VDI 2067, Blatt 1 (2012) costs and income items are grouped together with an interest rate of $i = 4.53 \%$ and an investment horizon of 20 years. The related annuity factor a , which equals the capital recovery factor (CRF), is calculated to $a = 0.07707612$. By taking into account a price change rate of 2.5% for capital costs, of 1.5% for consumption costs, of 1.5% for operation related costs, of 1.0% for maintenance costs and 1.0% for other costs the annuity of capital cost, consumption costs, operation costs, maintenance costs and other costs can be determined (see Table 6-14). The annuity of income, which is for the main part earned by supplying and selling heat to 104 heat consumers is shown as well. Because a net heat price in the amount of 79.31 €/MWh_{th} is assumed to grow with 2.15% within the period of observation, the proceeds by selling heat will change. Other income items will change with a change rate of 1.5%.

With the heat demand curve modeled for the extended district heating system in 2013 (see chapter 5.2.1) the useful energy sold and supplied to heat consumers is in the amount of $Q_{th,useful,an.} = 4205.94$ MWh/a. The annual proceeds achieved in the year 2014 are 333584.09 €/a. The annuity of income is calculated to 465973.21 €. Subtracting the annuity of costs from the annuity of income gives a total annuity of $A_N = 23716.02$ €. Under the specific side conditions the economic feasibility has been checked, the investment project could be accepted. The NPV will be positive

as well and the same result will be the outcome, if the *NPV*-method is used alternatively ($NPV = 307696.08 \text{ €}$).

When calculating the long run generation costs (*LRGC*) for the extended biomass district heating system of “MS Fernwärme Moosburg” the outcome will be $LRGC = 104.27 \text{ €/MWh}_{th}$. Compared to the average heat price of 79.31 €/MWh_{th} in year 2014 the result for long run generation costs seemed to be relatively high. However, a 40 % investment funding and the income from one-time connection fees still allow a successful economic operation within an investigation period of twenty years.

If the present value of investments is taken as a basis to determine the investment costs per unit of distributed useful heat, the result will be $inv_{grid,an.} = 666.07 \text{ €/(MWh}_{th}/a)$. Compared to the given range in Table 2-7 the specific cost of heat distribution will exceed the maximum for new biomass district heating systems erected in Austria since 2007.

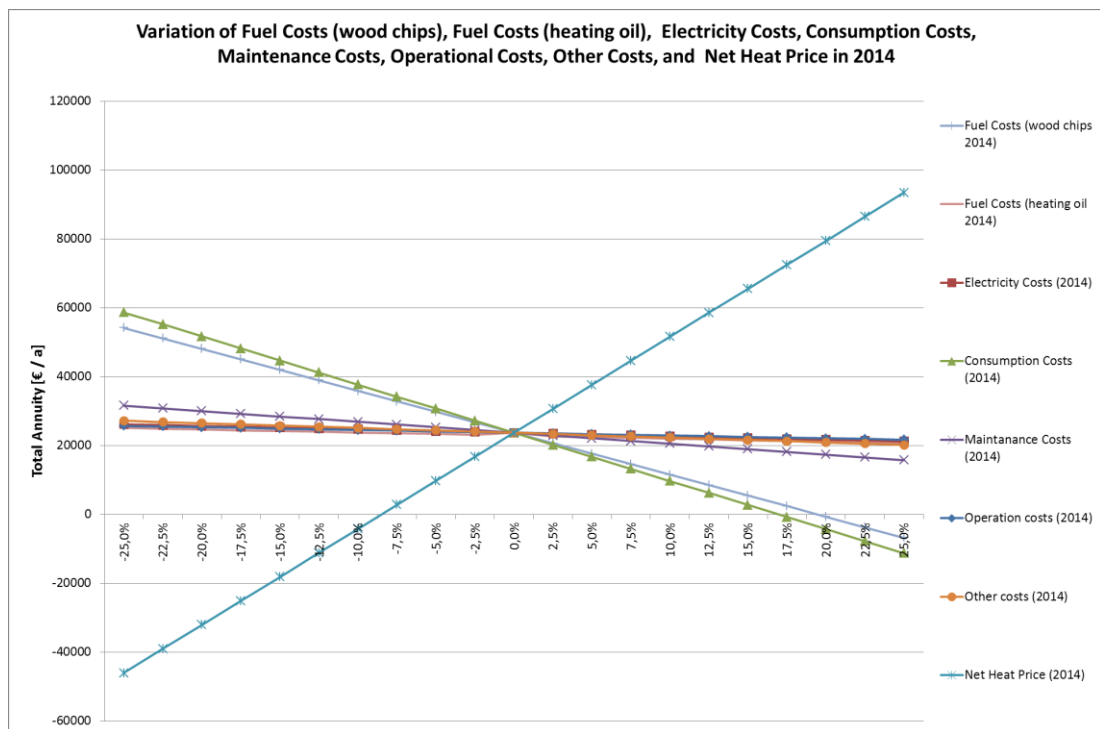


Figure 6-9: Sensitivity analysis of annuities for a biomass district heating system in Moosburg 2013. Total annuity of a district heating plant investment as a function of electricity costs, consumption costs, maintenance costs, other costs as well as net heat price valid for the year 2014 (Year 5 of operation). Variation done in the range of $\pm 25 \%$ (data source: own calculations).

In Figure 6-9 the results of a sensitivity analysis of the project's total annuity is displayed in one graph. For sensitivity analysis of the total annuity of electricity

costs, consumptions costs, maintenance costs, operational costs, other costs as well as the average net heat price of year 2014 are varied in a range of $\pm 25\%$.

As shown in Figure 6-9 the total annuity will still be positive, if the heat price in 2014 is reduced by a percentage rate of 8%. On the other hand the economic feasibility of the plant will be negative, if consumption costs and fuel costs would grow for another 17.5% up to 20%, respectively. Lower costs for maintenance or reduced other costs would slightly affect the positive economic performance of the biomass district heating system with the configuration described in chapter 5.2.1.

The next chapter will deal with an assessment of the biomass district heating system analyzed above, which have been extended by a solar thermal plant for support.

6.5.2 Economic assessment based on annuity method in case of a solar-assisted biomass district heating system in Moosburg 2013

In addition to the grid extension described before in the following sub-section an additional solar plant feeding into a prolonged district heating network will be assessed with respect to its economic feasibility. Based on the biomass district heating system's configuration outlined in chapter 6.5.1 the initial investment items listed in Table 6-16 are taken into account for applying the annuity method. The differences from overall investment's point of view are the cost items, which are necessary to install the plant components of a solar thermal application (see Table 6-15).

As already described in chapter 5.2 a ground mounted collector field with a net collector area of 1827.6 m^2 and a thermal energy storage with a volume of 200 m^3 are the main components of the extra investment project. For flat plate collectors about 55% of the overall investment costs for the solar thermal plant have to be considered (costs for FPCs = 535769.21 €), for the storage about 15% of investment costs has to be taken into account (costs storage = 142100 €). For detailed cost split in terms of initial investment costs related to specific components and the components average lifetime, please refer to Table 6-15.

Taking into account a 40 % investment funding for large-sized solar district heating applications the solar thermal plant's specific system costs are calculated to 285.56 €/m^2 (related to gross collector area). Without subsidies the specific system costs are evaluated to 475.93 €/m^2 , which is an acceptable result for large-scale applications (see Eicker (2012), page 94).

In order to determine the relevant maintenance costs the present value of the solar thermal plant's costs items have to be used. The relevant maintenance costs are computed based on a percentage rate as suggested by VDI 2067 Blatt 1 (2012).

*Table 6-15: Initial investment costs and specific investment costs for solar plant components of a solar-assisted biomass district heating system in Moosburg 2013** (data source: Biermayr et al. (2012), SDH (2012), Kaltschmitt & Streicher (2009), QM-report (2012)).*

Plant unit	Investment cost (A0₁₂) Year 2012	% of inv. 2012	TN*
Unit	[€]	[%]	[a]
Solar district heating plant			
Land for ground mounted installations	27500.00	2.8%	50
Flat plate collectors	535769.21	55.3%	20
Collector field installation including piping in the field	96804.79	10.0%	30
Anti-freeze fluid	6102.00	0.6%	25
Transmission piping (collector field to heat exchanger unit)	21106.75	2.2%	40
Heat exchanger (HX) unit (including pumps, expansion vessels, control, etc.)	29500.00	3.0%	20
Connection to existing district heating system	0.00	0.0%	40
Storage	142100.00	14.7%	25
Monitoring and controlling system (MSR software & hardware)	48402.39	5.0%	10
Engineering, planning, project steering	30089.04	3.1%	25
Infrastructure (access roads), outside facilities (building, ground shaping, fence, plants)	18673.68	1.9%	30
Expert assessments, permissions, contracting	12000.00	1.2%	25
Sum investment costs solar district heating plant:	968047.86	100%	

Explanations: * ... Average lifetime of component in years according VDI 2067 Blatt 1;
** ... Connected load: $Q'_{cl,DHN} = 3554 [kW_{th}]$; maximal effective connected load: $Q'_{cl,max,eff.} = 2130 [kW_{th}]$; base load: $\Phi'_{grid,min.} + Q'_{DHW} = 107 [kW_{th}]$; grid length: $l_{grid} = 5755 [m]$; number of heat consumers: $n_{user,i} = 104 [1]$.

Table 6-16 is more or less a copy of Table 6-13 from chapter 6.5.1. The only difference is the total sum of initial investments to be considered in year 2012. The solar thermal plant and the district heating grid extension will show up with a total investment of $A0_{12} = 1533172.53 \text{ €}$ (see Table 6-16).

*Table 6-16: Initial investment costs and specific investment costs for plant components (heating station, heat distribution grid) of a solar-assisted biomass district heating system in Moosburg 2013** (data source: Biermayr et al. (2012), SDH (2012), Kaltschmitt & Streicher (2009), QM-report (2012)).*

<i>Plant unit</i>	<i>Investment cost (A0₀₉) Year 2009</i>	<i>% of inv. 2009</i>	<i>Investment cost (A0₁₁) Year 2011</i>	<i>% of inv. 2011</i>	<i>Investment cost (A0₁₂) Year 2012</i>	<i>% of inv. 2012</i>	<i>TN*</i>
<i>Unit</i>	<i>[€]</i>	<i>[%]</i>	<i>[€]</i>	<i>[%]</i>	<i>[€]</i>	<i>[%]</i>	<i>[a]</i>
Biomass district heating plant							
Land	0.00	0.0%	0.00	0.0%	0.00	0.0%	50
Infrastructure and outside facilities	33427.00	1.5%	0.00	0.0%	0.00	0.0%	30
Buildings and building infrastructure	503343.00	22.7%	595.00	0.6%	0.00	0.0%	30
Biomass boiler incl. fire box (1.75 MW)	262800.00	11.9%	0.00	0.0%	12500.00	2.2%	25
Hydraulic installations	110723.00	5.0%	0.00	0.0%	0.00	0.0%	25
Permissions, contracting, expert assessments	81703.00	3.7%	3000.00	3.1%	18420.82	3.3%	25
Engineering, planning, project steering	35535.00	1.6%	0.00	0.0%	7894.64	1.4%	25
Grid connection to electric mains	2984.00	0.1%	2284.00	2.4%	0.00	0.0%	25
Oil boiler (peak load boiler)	12810.00	0.6%	0.00	0.0%	0.00	0.0%	20
Oil burner	6771.00	0.3%	0.00	0.0%	0.00	0.0%	12
Monitoring and controlling SW for boiler/ heating station	65700.00	3.0%	0.00	0.0%	0.00	0.0%	10
Electric installations	27465.00	1.2%	0.00	0.0%	0.00	0.0%	15
Electronic installations (system control)	5986.00	0.3%	0.00	0.0%	0.00	0.0%	10
Vehicles (Telescope loader)	27600.00	1.2%	0.00	0.0%	0.00	0.0%	8
Monitoring and controlling SW for DHNW / consumer heat stations	10563.00	0.5%	7549.00	7.8%	13814.24	2.4%	10
Construction of district heating grid	952016.00	42.9%	83735.00	86.2%	512494.98	90.7%	40
Installation of consumer sub-stations	78291.00	3.5%	0.00	0.0%	0.00	0.0%	20

<i>Plant unit</i>	<i>Investment cost (A₀₀₉) Year 2009</i>	<i>% of inv. 2009</i>	<i>Investment cost (A₀₁₁) Year 2011</i>	<i>% of inv. 2011</i>	<i>Investment cost (A₀₁₂) Year 2012</i>	<i>% of inv. 2012</i>	<i>TN*</i>
<i>Unit</i>	<i>[€]</i>	<i>[%]</i>	<i>[€]</i>	<i>[%]</i>	<i>[€]</i>	<i>[%]</i>	<i>[a]</i>
Sum investment costs biomass district heating plant:	2217717.00	100%	97163.00	100%	565124.67	100%	
Sum investment costs solar-assisted biomass DH plant:	2217717.00		97163.00		1533172.53		

Explanations: * ... Average lifetime of component in years according VDI 2067 Blatt 1
** ... Connected load: $Q'_{cl,DHN} = 3554 [kW_{th}]$; maximal effective connected load: $Q'_{cl,max,eff.} = 2130 [kW_{th}]$; base load: $\Phi'_{grid,min.} + Q'_{DHW} = 107 [kW_{th}]$; grid length: $l_{grid} = 5755 [m]$; number of heat consumers: $n_{user,i} = 104 [1]$.

Similar to chapter 6.5.1 this sum of present values and the sum of present values of investments are calculated as a starting point. The present values are determined for project start in year 0, which is 2009 as before. As a reference year the 5th year of operation is selected in order to consider one year of solar supported operation beforehand.

Table 6-17 shows the costs and income items of year 5 (i.e. 2014) as well as the specific annuity items. While the consumption costs in year 2014 are lower ($A_{V5} = 155582.05$ €) as in a configuration without solar assistance, the maintenance costs are significantly higher ($A_{IN5} = 55938.72$). The reason for this difference is the additional maintenance efforts for the solar components. Further saving can be identified in terms of annual working hours of plant personnel (see Table 6-17, left column).

On the right hand side of Table 6-17 the annuity of capital costs, of consumption costs, of maintenance and other costs are listed. Due to increased maintenance costs for a solar-assisted district heating system the related annuity of maintenance costs exceeds the value in Table 6-14, while the annuity of consumption costs results in a lower value as given in Table 6-14. However, the annuity of costs ($A_{N,C} = 499523.65$ €) is definitely higher than annuity of costs determined for a biomass district heating system without solar support (see $A_{N,C}$ in Table 6-14). This fact will result in higher long run generation costs for a solar-assisted biomass district heating system later on.

The annuity of income includes the annuity of income from sold heat and from one-time connection fees. In the annuity of income from funding a 40 % subsidy for grid

extension and a 40 % investment funding for large-scale solar district heating systems is included.

Table 6-17: Cost items split according to VDI2067, Blatt1 (2012) and income items for a solar-assisted biomass district heating installation in Moosburg 2013 (data source: own calculations). Annuity items calculated according to VDI2067, Blatt1 (2012) (data source: own calculations)*

Cost / Income Item	Value	Unit	Annuity Item	Annuity	Unit
Capital costs (2009):					
Sum of PV of investment costs (A_0) calculated in year 0 (2009)	3648998.46	[€]	Annuity of investment costs ($A_{N,Inv.}$)	281250.63	[€]
Sum of present values ($A_0+A_1+A_2+ \dots -RW$) calculated in year 0 (2009)	3246339.68	[€]	Annuity of capital costs ($A_{N,K}$)	250215.25	[€]
Consumption costs (2014):					
Fuel costs (primary energy costs: wood chips)	131925.38	[€/year]	Annuity of fuel costs: wood chips ($A_{N,V,WC}$)	138135.66	[€]
Fuel costs (primary energy costs: heating oil)	8810.12	[€/year]	Annuity of fuel costs: oil ($A_{N,V,oil}$)	8905.14	[€]
Electricity costs (auxiliary demand)	12897.88	[€/year]	Annuity of electricity costs ($A_{N,V,El}$)	13058.31	[€]
Telecommunication costs (monitoring)	533.30	[€/year]	Annuity of Telco costs ($A_{N,V,Tel}$)	584.48	[€]
Costs for other consumables (water, chemicals, diesel, etc.)	1101.66	[€/year]	Annuity of costs for other consumables ($A_{N,V,OC}$)	1127.42	[€]
Costs for ash disposal, sewage disposal, chimney sweeper)	313.70	[€/year]	Annuity of costs for disposal ($A_{N,V,Disp}$)	335.44	[€]
Total consumption costs in year 5 (A_{V5})	155582.05	[€/year]	Annuity of consumption costs ($A_{N,V}$)	162146.44	[€]
Operation & Maintenance costs (2014):					
Annual working hours 2014	255	[h/year]			
Annual personal costs 2014	9459.50	[€/year]			
Total operation costs in year 5 (A_{B5})	9459.50	[€/year]	Annuity of operation costs ($A_{N,B}$)	10275.68	[€]
Annual maintenance costs in year 5 (A_{IN5})	55938.72	[€/year]	Annuity of maintenance costs (A_{IN})	55244.20	[€]
Total O&M costs per year	65398.23	[€/year]			
Other costs (2014):					
Other cost (miscellaneous: advertisement, service social rooms, etc.)	772.73	[€/year]			

Cost / Income Item	Value	Unit	Annuity Item	Annuity	Unit
Insurance costs	5822.30	[€/year]			
Administration costs (tax cons., admin.):	6078.78	[€/year]			
Costs for taxes and fees (community tax, land tax, land fee, tourism fee, etc.)	2555.15	[€/year]			
Costs for land lease	5563.63	[€/year]			
Total other costs in year 5 (A_{S5})	20792.57	[€/year]	Annuity of other costs ($A_{N,S}$)	21642.08	[€]
Total costs (w/o capital costs) per year 2014:	241772.85	[€/year]			
			Annuity of costs ($A_{N,K} + A_{N,V} + A_{N,B} + A_{N,S}$)	499523.65	[€]
Income 2014					
Net heat price in 2014	79.31	[€/MWh]			
Amount of heat supplied and sold to consumers	4205.94	[MWh/a]			
Income from useful heat supplied and sold to consumers	333584.09	[€/year]	Annuity of income from heat sold ($A_{N,FIT}$)	351870.95	[€]
Income from one-time connection fee in 2014	0.00	[€/year]	Annuity of income from one-time connection fee ($A_{N,Econ}$)	54529.84	[€]
Income from investment funding in 2014	0.00	[€/year]	Annuity of income from funding ($A_{N,Esub}$)	84570.85	[€]
Total annual income in year 5 ($E5$)	333584.09	[€/year]	Annuity of income ($A_{N,E}$)	490971.64	[€]
			Total Annuity		
			Total Annuity ($A_N = A_{N,E} - (A_{N,K} + A_{N,V} + A_{N,B} + A_{N,S})$)	-8552.01	[€]
			Capital Recovery Factor (CRF) = Annuity factor (a)	0.07707612	[1]
			Net Present Value (NPV = $A_N * 1/CRF$)	-110955.32	[€]

Explanations: * ... Nominal capacity of biomass boiler: $Q'_{bio,nom.} = 1750 [kW_{th}]$;
 Nominal capacity of oil boiler: $Q'_{oil,nom.} = 1500 [kW_{th}]$;
 Storage volume of buffer tank: $V_{buf.} = 35 [m^3]$;
 Net collector area of installed FPCs: $A_{col,net} = 1828 [m^2]$;
 Storage volume of thermal energy storage: $V_{stor.} = 200 [m^3]$;
 Connected load: $Q'_{cl,DHN} = 3554 [kW_{th}]$;
 Maximal effective connected load: $Q'_{cl,max,eff.} = 2130 [kW_{th}]$;
 Base load: $\Phi'_{grid,min.} + Q'_{DHW} = 107 [kW_{th}]$;
 Grid length: $l_{grid} = 5755 [m]$;
 Number of heat consumers: $n_{user,i} = 104 [1]$.

By subtracting the annuity of costs from the annuity of income the total annuity A_N is computed. The result for a solar-assisted biomass district heating system is a negative total annuity of $A_N = -8552.01$ € considering annuity of income $A_{N,E} = 490971.64$ € and annuity of costs $A_{N,C} = 499523.65$ €. Under the specific side conditions the economic feasibility has been checked, the investment project cannot be accepted. The NPV will be negative as well ($NPV = -110955.32$ €) and the same result will be the outcome, if the NPV -method is used alternatively.

When calculating long run generation costs result is $LRGC = 117.77$ €/MWh_{th}. Compared with a net heat price of 79.31 €/MWh_{th} in year 2014 this value is relatively high. Even a 40 % investment funding would not be sufficient to facilitate a positive result, although the savings of consumption costs are considerable. The negative outcome of the appraisal shows that the investment costs for the solar plant's components will over-compensate this effect.

If the present value of investments is taken as a basis to calculate the investment costs per unit of distributed useful heat, the result will be $inv_{grid,an.} = 867.58$ €/(MWh_{th}/a). Compared to the values listed in Table 2-7 the specific cost of heat distribution will exceed the Austrian maximum for biomass district heating plants erected since 2007.

For sensitivity analysis of the project's total annuity electricity costs, consumptions costs, maintenance costs, operational costs, other costs as well as the net heat price in year 2014 are varied in a range of $\pm 25\%$. As shown in Figure 6-10 the total annuity will change to a positive value, if the net heat price for district heat supplied and sold to the heat consumers will be increased for about 2.5%. Further measures to get a positive total annuity A_N would be a reduction of consumption costs in general or fuel costs in this particular case. A change of at least -7.5% would change the investment project's total annuity to positive values. Further positive effects on the economic performance will be achieved, if maintenance costs could be reduced for more than 20%.

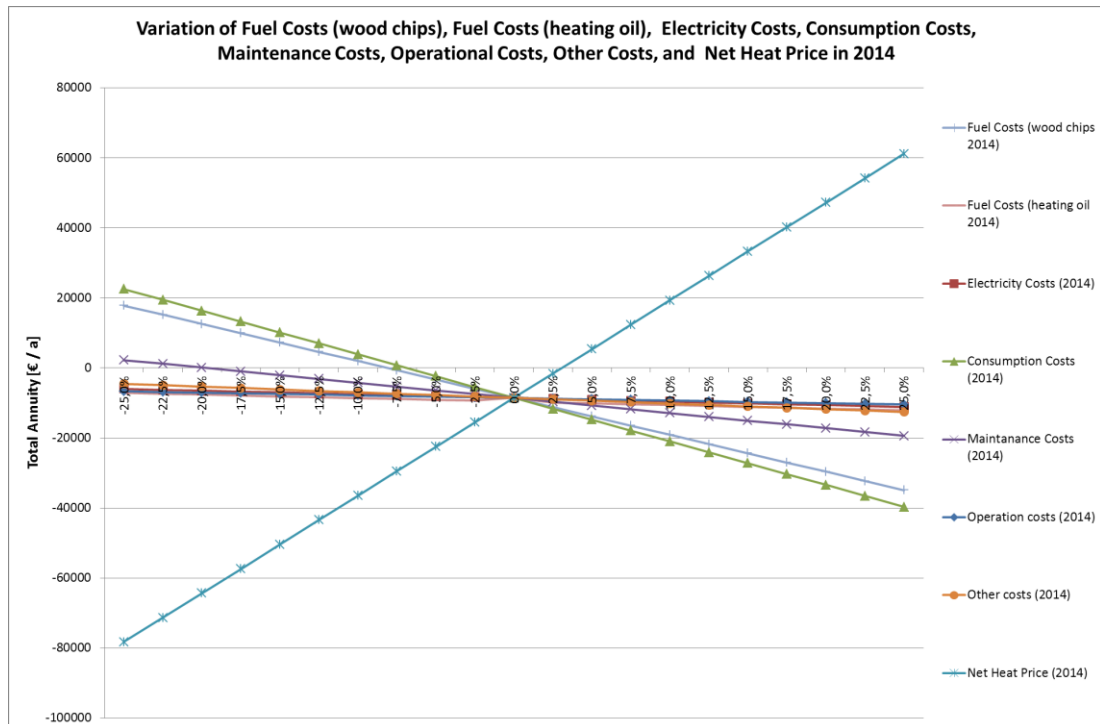


Figure 6-10: Sensitivity analysis of annuities for a solar-assisted biomass district heating system in Moosburg 2013. Total annuity of a district heating plant investment as a function of electricity costs, consumption costs, maintenance costs, other costs as well as net heat price valid for the year 2014 (Year 5 of operation). Variation done in the range of $\pm 25\%$ (data source: own calculations).

Similar to the approach selected to check an investment project's feasibility with 20 years of project life-time, a given interest rate and a given set of price change rates in the next chapter the economic feasibility of a solar-assisted biomass district heating system started in Eibiswald in year 1997 is assessed.

6.6 Economic assessment based on annuity method in case of reference system "Nahwärme Eibiswald"

In order to compare a modern solar-assisted biomass district heating system with a historical configuration from an economic point of view, the following assessment uses the same approach as applied in the two chapters before. Based on data given by Faninger & Weiss (2002), Streicher, et al. (1999) as well as Streicher & Oberleitner (1998) the annuity method according to guideline VDI 2067 Blatt 1 (2012) is used.

As already described in chapter 5.3 the main components of the solar plant in Eibiswald are roof-integrated collectors with a total net collector area of 1150 m^2 and an insulated steel tank with a storage volume of 105 m^3 integrated into the heating

house. For an overview on solar plant units, the assumed initial investment costs per component and the component's average life time, please refer to Table 6-18.

*Table 6-18: Initial investment costs for solar plant components of a solar-assisted biomass district heating system in Eibiswald 1997** (data source: Heimrath, et al. (2002), Faninger&Weiss (2002)).*

Plant unit	Investment cost (A0₉₆) Year 1996	% of inv. 1996	TN*
Unit	[€]	[%]	[a]
Solar district heating plant			
Land for ground mounted installations	0.00	0.0%	50
Flat plate collectors	188076.10	54.5%	20
Collector field installation including piping in the field	34488.90	10.0%	30
Anti-freeze fluid	3750.00	1.1%	25
Transmission piping (collector field to heat exchanger unit)	13788.58	4.0%	40
Heat exchanger (HX) unit (including pumps, expansion vessels, control, etc.)	7220.00	2.1%	20
Connection to existing district heating system	0.00	0.0%	40
Storage	54703.31	15.9%	25
Monitoring and controlling system (MSR software & hardware)	17244.45	5.0%	10
Engineering, planning, project steering	9238.84	2.7%	25
Infrastructure (access roads), outside facilities (building, ground shaping, fence, plants)	10878.78	3.2%	30
Expert assessments, permissions, contracting	5500.00	1.6%	25
Sum investment costs solar district heating plant:	344888.97	100%	

Explanations: * ... Average lifetime of component in years according VDI 2067 Blatt 1;
** ... Connected load: $\dot{Q}'_{cl,DHN} = 3000 [kW_{th}]$; maximal effective connected load: $\dot{Q}'_{cl,max,eff.} = 2114 [kW_{th}]$; base load: $\Phi'_{grid,min.} + \dot{Q}'_{DHW} = 106 [kW_{th}]$; grid length: $l_{grid} = 4000 [m]$; number of heat consumers: $n_{user,i} = 64 [1]$.

The calculated system costs including a 40 % investment funding are equal to 165.55 €/m² (per unit collector gross area). Using the initial total investment of 344888.97 € as a basis, the system costs are calculated to 275.91 €/m², which perfectly fits to the information given by Faninger & Weiss (2002) (see page 9). It is assumed that the solar thermal part of the plant had been erected in year 1996.

In Table 6-19 the initial investment costs for heating station and heat distribution grid are summarized. Start point of the twenty years investigation period is year 1993 (i.e. year 0), while year 1994 is taken as the first year the biomass district heating system run. It has to be pointed out, that the used figures in Table 6-18 and in Table 6-19 are estimated according to the used historical data. Deviations from real

investment costs are highly probable. However, the structure of cost split follows the scheme for the two configurations in Moosburg assessed before.

*Table 6-19: Initial investment costs for plant components (heating station, heat distribution grid) of a solar-assisted biomass district heating system in Eibiswald 1997** (data source: Streicher & Oberleitner (1998), Heimrath, et al. (2002), Faninger&Weiss (2002)).*

<i>Plant unit</i>	<i>Investment cost (A0₉₃) Year 1993</i>	<i>% of inv. 1993</i>	<i>TN*</i>
<i>Unit</i>	<i>[€]</i>	<i>[%]</i>	<i>[a]</i>
Biomass district heating plant			
Land	0.00	0.0%	50
Infrastructure and outside facilities	25607.18	1.1%	30
Buildings and building infrastructure	502998.21	21.7%	30
Biomass boiler incl. fire box (2 MW)	157040.61	6.8%	25
Hydraulic installations	178335.73	7.7%	25
Permissions, contracting, expert assessments	32008.98	1.4%	25
Engineering, planning, project steering	114317.77	4.9%	25
Grid connection to electric mains	2286.36	0.1%	25
Oil boiler (peak load boiler)	12500.88	0.5%	20
Oil burner	4115.44	0.2%	12
Monitoring and controlling SW for boiler/ heating station	41154.40	1.8%	10
Electric installations	105172.35	4.5%	15
Electronic installations (system control)	7773.61	0.3%	10
Vehicles (Telescope loader)	22863.55	1.0%	8
Monitoring and controlling SW for DHNW / consumer heat stations	59445.24	2.6%	10
Construction of district heating grid	932833.04	40.3%	40
Installation of consumer sub-stations	117061.40	5.1%	20
Sum investment costs biomass district heating plant:	2315514.74	100%	

Explanations: * ... Average lifetime of component in years according VDI 2067 Blatt 1;
** ... Connected load: $\dot{Q}'_{cl,DHN} = 3000 [kW_{th}]$; maximal effective connected load: $\dot{Q}'_{cl,max,eff.} = 2114 [kW_{th}]$; base load: $\Phi'_{grid,min.} + \dot{Q}'_{DHW} = 106 [kW_{th}]$; grid length: $l_{grid} = 4000 [m]$; number of heat consumers: $n_{user,i} = 64 [1]$.

Again, the present values of investments related to year 1993 are the basis to calculate maintenance costs according to percentage rates given by VDI 2067 Blatt 1 (2012). Like in the two assessments done before year 5 (i.e. year 1998) of the twenty years project runtime will be used for comparison. Consumption costs are estimated costs determined according to the heat demand curve in chapter 5.3.2 as well as according to results from simulation by SHWin. Operation costs and other

costs for year 1998 are evaluated based on data of the QM-report (2012) considering an appropriate price development during 15 years.

Income from heat supplied and sold to heat consumers is the result of multiplying the net heat price of 1998 (64.50 €/MWh_{th}) with the amount of useful heat delivered to heating sub-stations ($Q_{th,useful,an.} = 3650.0 \text{ MWh}_{th}/a$). In year 1998 no income from one-time connection fees or investment subsidies are taken into account.

Nevertheless, these income items will be considered in the annuity of income from one-time connection fees as well as in the annuity of income from funding (see Table 6-20, column at right hand side). The total annual proceeds achieved in year 1998 are $E_5 = 235409.97 \text{ €}$.

Thanks to the evaluated cost items the annuity for capital costs, operation costs, maintenance costs, and other costs can be calculated. With an interest rate of $i = 4.53\%$, an investment horizon of $T = 20$ years and identical price change rates as assumed before the annuity of costs is determined to $A_{N,C} = 357052.11 \text{ €}$, and the annuity of income results in $A_{N,E} = 356849.64 \text{ €}$.

Table 6-20: Cost items split according to VDI2067, Blatt1 (2012) and income items for a solar-assisted biomass district heating installation in Eibiswald 1997 (data source: own calculations). Annuity items calculated according to VDI2067, Blatt1 (2012) (data source: own calculations)*

Cost / Income Item	Value	Unit	Annuity Item	Annuity	Unit
Capital costs (1993)					
Sum of PV of investment costs (A_0) calculated in year 0 (1993)	2617479.63	€	Annuity of investment costs ($A_{N,Inv.}$)	201745.16	€
Sum of present values ($A_0 + A_1 + A_2 + \dots - RW$) calculated in year 0 (1993)	2446537.12	€	Annuity of capital costs ($A_{N,K}$)	188569.58	€
Consumption costs (1998):					
Fuel costs (primary energy costs: wood chips)	77635.68	€/year	Annuity of fuel costs: wood chips ($A_{N,V,WC}$)	84514.73	€
Fuel costs (primary energy costs: heating oil)	550.02	€/year	Annuity of fuel costs: oil ($A_{N,V,oil}$)	586.26	€
Electricity costs (auxiliary demand)	10907.74	€/year	Annuity of electricity costs ($A_{N,V,El}$)	11630.04	€
Telecommunication costs (monitoring)	318.41	€/year	Annuity of Telco costs ($A_{N,V,Tel}$)	339.39	€
Costs for other consumables (water, chemicals, diesel, etc.)	710.37	€/year	Annuity of costs for other consumables ($A_{N,V,OC}$)	769.89	€
Costs for ash disposal, sewage disposal, chimney sweeper)	212.27	€/year	Annuity of costs for disposal ($A_{N,V,Disp}$)	226.26	€

<i>Cost / Income Item</i>	<i>Value</i>	<i>Unit</i>	<i>Annuity Item</i>	<i>Annuity</i>	<i>Unit</i>
Total consumption costs in year 5 (A_{V5})	90334.49	[€/year]	Annuity of consumption costs ($A_{N,V}$)	98066.58	[€]
Operation & Maintenance costs (1998):					
Annual working hours 1998	281	[h/year]			
Annual personal costs 1998	10036.44	[€/year]			
Total operation costs in year 5 (A_{B5})	10036.44	[€/year]	Annuity of operation costs ($A_{N,B}$)	10620.76	[€]
Annual maintenance costs in year 5 (A_{IN5})	44769.70	[€/year]	Annuity of maintenance costs (A_{IN})	45548.63	[€]
Total O&M costs per year	54806.14	[€/year]			
Other costs (1998):					
Other cost (miscellaneous: advertisement, service social rooms, etc.)	772.73	[€/year]			
Insurance costs	2434.93	[€/year]			
Administration costs (tax cons., admin.):	3642.11	[€/year]			
Costs for taxes and fees (community tax, land tax, land fee, tourism fee, etc.)	1873.09	[€/year]			
Costs for land lease	4994.90	[€/year]			
Total other costs in year 5 (A_{S5})	13717.76	[€/year]	Annuity of other costs ($A_{N,S}$)	14246.56	[€]
Total costs (w/o capital costs) per year:	158858.39	[€/year]			
			Annuity of costs ($A_{N,K} + A_{N,V} + A_{N,B} + A_{N,S}$)	357052.11	[€]
Income 1998					
Net heat price	64.50	[€/MWh]			
Amount of heat supplied and sold to consumers	3650.00	[MWh/a]			
Income from useful heat supplied and sold to consumers	235409.97	[€/year]	Annuity of income from heat sold ($A_{N,FIT}$)	258451.46	[€]
Income from one-time connection fee in 1998	0.00	[€/year]	Annuity of income from one-time connection fee ($A_{N,Econ}$)	21197.31	[€]
Income from investment funding in 1998	0.00	[€/year]	Annuity of income from funding ($A_{N,Esub}$)	77200.87	[€]
Total annual income in year 5 ($E5$)	235409.97	[€/year]	Annuity of income ($A_{N,E}$)	356849.64	[€]
			Total Annuity		
			Total Annuity ($A_N = A_{N,E} - (A_{N,K} + A_{N,V} + A_{N,B} + A_{N,S})$)		
					-202.48 [€]

Cost / Income Item	Value	Unit	Annuity Item	Annuity	Unit
			Capital Recovery Factor (CRF) =		
			Annuity factor (a)	0.07707612	[1]
			Net Present Value (NPV = $A_N \cdot 1/\text{CRF}$)	-2626.98	[€]

Explanations: * ... Nominal capacity of biomass boiler: $\dot{Q}'_{bio,nom.} = 2000 [kW_{th}]$;
 Nominal capacity of oil boiler: $\dot{Q}'_{oil,nom.} = 500 [kW_{th}]$;
 Net collector area of installed FPCs: $A_{col,net} = 1150 [m^2]$;
 Storage volume of thermal energy storage: $V_{stor.} = 105 [m^3]$;
 Connected load of DHN: $\dot{Q}'_{cl,DHN} = 3000 [kW_{th}]$;
 Maximal effective connected load: $\dot{Q}'_{cl,max,eff.} = 2114 [kW_{th}]$;
 Base load: $\Phi'_{grid,min.} + \dot{Q}'_{DHW} = 106 [kW_{th}]$;
 Grid length: $l_{grid} = 4000 [m]$;
 Number of heat consumers: $n_{user,i} = 64 [1]$.

Subtracting the annuity of costs from the annuity of income gives a total annuity of $A_N = -202.48 \text{ €}$. As the value is negative also the net present value is negative ($NPV = -2626.98 \text{ €}$) and the investment project should not have been accepted in year 1993. However, the deviation from 0 is small, so that with the help of some improvements a change to a positive total annuity could have been achieved.

For long run generation costs of heat production by the solar-assisted biomass district heating system in Eibiswald 1997 the result is $LRGC = 97.82 \text{ €/MWh}_{th}$. Compared to the net heat price of 64.50 €/MWh_{th} in year 1998 this value seems to be relatively high. But as the sensitivity analysis will show later on, a small increase of the net heat price as well as the assumed price change rate of 2.15% per year would compensate the deviation in the long run.

If the present value of investments is taken as a basis to calculate the investment costs per unit of useful heat distributed, the result will be $inv_{grid,an.} = 717.18 \text{ €/(MWh}_{th}/a)$. Compared to the given range in Table 2-7 the specific cost of heat distribution will exceed the Austrian maximum.

In Figure 6-11 a graphical representation of a sensitivity analysis of the investment project is shown. By variation of electricity costs, consumptions costs, maintenance costs, operational costs, other costs as well as the net heat price in the range of $\pm 25 \%$ a sensitivity analysis of the total annuity is done. The outcome are several graphs with a common point of intersection at $A_N = -202.48 \text{ €}$.

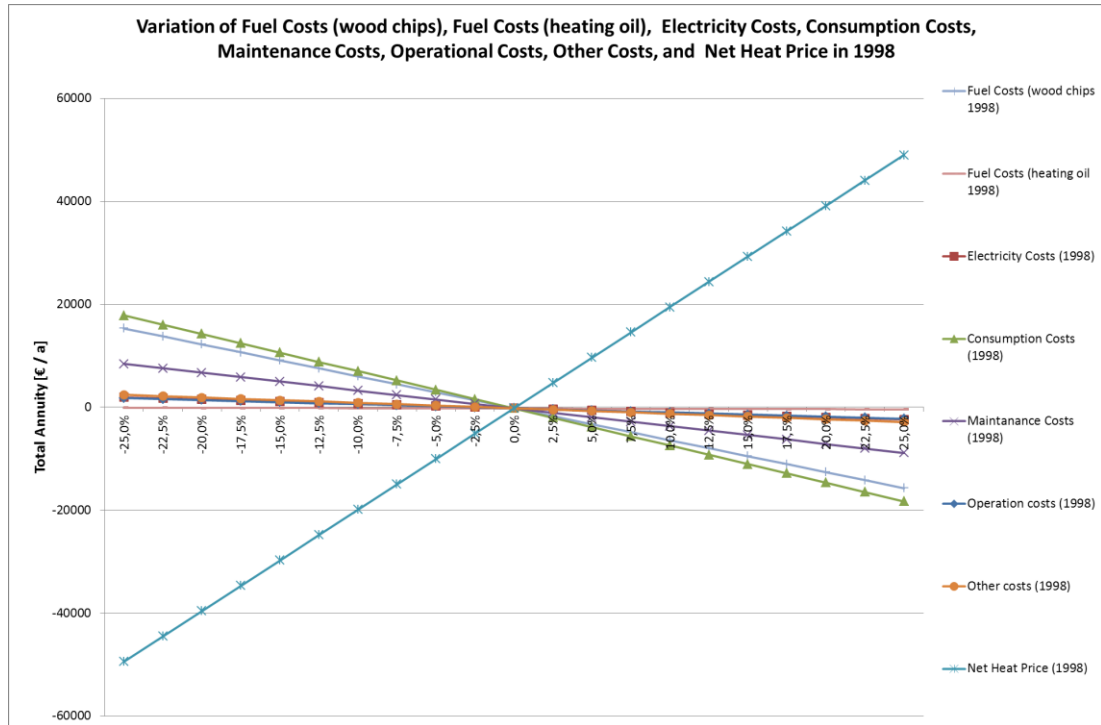


Figure 6-11: Sensitivity analysis of annuities for a solar-assisted biomass district heating system in Eibiswald 1997. Total annuity of a district heating plant investment as a function of electricity costs, consumption costs, maintenance costs, other costs as well as net heat price valid for the year 1998 (Year 5 of operation). Variation done in the range of $\pm 25\%$ (data source: own calculations).

As shown in Figure 6-11 the negative total annuity will grow, if consumption costs, fuel costs or maintenance costs are reduced for a small percentage rate below 5%. On the other hand a small increase of the net heat price in year 1998 would have the same effect, which would make the investment project's total annuity positive. However, the history of operating a solar-assisted biomass district heating system in Eibiswald has demonstrated that an operation with a positive economic performance has been possible in Eibiswald since 1993.

7 Discussion of Results

In the following chapters the results of assessments carried out in chapter 6 are finally summarized and discussed. Chapter 7.1 provides a technical and energetic comparison of the assessed applications based on key indicators evaluated for the central heating station, the heat distribution grid and the solar thermal plant of the investigated configuration. In chapter 7.2 the ecological effects due to gaseous emissions and particle emissions are summarized and discussed. Furthermore, a comparison of two solar-assisted biomass district heating systems in terms of greenhouse gas emission as well as air pollutants emission savings with conventional district heat supply is outlined. Finally, chapter 7.3 focusses on the results of the economic assessments, which have been executed for three different biomass district heating system configurations. Comparing cost and income related parameters for year 5 of operation as well as the resulting economic key indicators will provide a basis for decision, which kind of plant extension is suitable for investment.

7.1 Technical and energetic comparison of the proposed applications for district heat supply by biomass district heating systems

In the following chapters the three main parts of a solar-assisted district heating plant are compared and discussed from a technical and energetic point of view. Sub-chapter 7.1.1 focusses on the central heating station, its configuration and operating data as well as on its characterizing key indicators. In sub-chapter 7.1.2 the three distribution grid configurations and their related key indicators are compared to each other. Finally, sub-chapter 7.1.3 summarizes the main configuration data and operating data of the two investigated solar plants. The characterizing key indicators for the assisting solar thermal applications will be discussed with respect to their technological consequences.

7.1.1 Heating station related key indicators of a biomass district heating system without solar support and a solar-assisted biomass district heating system in Moosburg 2013 compared to heating station related indicators of a solar-assisted biomass district heating system in Eibiswald 1997

In Table 7-1 the characteristic indicators of the three central heating stations are listed. The heating station in Moosburg is equipped with two boilers (i.e. a 1750 kW_{th} biomass boiler and a 1500 kW_{th} oil boiler) in case of solar support and in case that no solar assistance is considered. In Eibiswald one 2000 kW_{th} biomass boiler is

operated in the central heating station, while the reserve of a 500 kW_{th} oil boiler is located in a connected school building. For boiler efficiencies the same values are assumed in each configuration. The energy balances in Table 7-1 have been discussed already and are mentioned for information only.

Table 7-1: Comparison of heating station related configuration and operating data of biomass district heating systems with and without solar support in Moosburg 2013 and a solar-assisted biomass district heating system in Eibiswald 1997** (data source: simulation results of SHWwin and own calculations).*

<i>Indicator</i>	<i>Symbol</i>	<i>Value for DHS Moosburg 2013 w/o solar support</i>	<i>Value for solar- assisted DHS Moosburg 2013</i>	<i>Value for solar- assisted DHS Eibiswald 1997</i>	<i>Unit</i>
Nominal capacity of biomass boiler	$Q'_{th,bio,nom.}$	1750	1750	2000	[kW _{th}]
Nominal efficiency factor of biomass boiler	$\eta_{bio,nom.}$	0.8570	0.8570	0.8570	[kW _{th} /kW _{NCV}]
Nominal capacity of oil boiler	$Q'_{th,oil,nom.}$	1500	1500	500	[kW _{th}]
Nominal efficiency factor of oil boiler	$\eta_{oil,nom.}$	0.8900	0.8900	0.8900	[kW _{th} /kW _{NCV}]
Total heat produced by heat resources per year	$Q_{th,produced,an.}$	5333547	5330960	4520507	[kWh _{th} /a]
Heat fed into the district heating grid per year	$Q_{th,demand,DH}$	5328213	5326745	4501483	[kWh _{th} /a]
Total annual electricity demand of heating plant	$W_{el,HP,aux.}$	88312	90839	73809	[kWh _{el} /a]

*Explanations: DHS ... District Heating System;
DHG ... District Heating Grid;
* ... Connected load: $Q'_{cl,DHN} = 3554$ [kW_{th}]; maximal effective connected load: $Q'_{cl,max,eff.} = 2130$ [kW_{th}]
** ... Connected load: $Q'_{cl,DHN} = 3000$ [kW_{th}]; maximal effective connected load: $Q'_{cl,max,eff.} = 2114$ [kW_{th}].*

From a technological point of view the different configurations of the central heating stations, the different modes of boiler operation and the influences of the assisting solar thermal plant determine the heating station's key indicators. Table 7-2 shows the results for characteristic parameters of the three involved heating stations.

Table 7-2: Comparison of heating station related key indicators of biomass district heating systems with and without solar support in Moosburg 2013* and a solar-assisted biomass district heating system in Eibiswald 1997** (data source: simulation results of SHWwin and own calculations).

Indicator	Symbol	Value for DHS Moosburg 2013 w/o solar support	Value for solar- assisted DHS Moosburg 2013	Value for solar- assisted DHS Eibiswald 1997	Unit
Annual efficiency of heat provision of heating plant	$\zeta_{tot,HP}$	0.7209	0.8283	0.8012	[kWh _{th} /kWh _{NCV}]
Annual biomass boiler utilization ratio	$\zeta_{bio,an.}$	0.7178	0.7178	0.7178	[kWh _{th} /kWh _{NCV}]
Annual oil boiler utilization ratio	$\zeta_{oil,an.}$	0.8984	0.8984	0.8984	[kWh _{th} /kWh _{NCV}]
Nominal power hours of biomass boiler	NPH_{bio}	2987	2586	2020	[h/a]
Nominal power hours of oil boiler	NPH_{oil}	71	80	25	[h/a]
Connected heat load per boiler output	$q'_{load,boiler}$	1.0935	1.0935	1.2000	[1]
Specific electricity demand of heating station	$W_{el,HP,aux.}$	16.56	17.04	16.33	[kWh _{el} /MWh _{th}]

Explanations: DHS ... District Heating System;

DHG ... District Heating Grid;

* ... Connected load: $Q'_{cl,DHN} = 3554$ [kW_{th}]; maximal effective connected load: $Q'_{cl,max,eff.} = 2130$ [kW_{th}];

** ... Connected load: $Q'_{cl,DHN} = 3000$ [kW_{th}]; maximal effective connected load: $Q'_{cl,max,eff.} = 2114$ [kW_{th}].

While in case of Moosburg the biomass boiler's and the oil boiler's capacity stay the same, in case of Eibiswald more biomass, but less oil boiler capacity is available.

Obviously, the solar thermal feed-in reduces the nominal power hours of the biomass boiler (NPH_{bio} : 2987 > 2586 h/a) and increases the nominal power hours of the oil boiler (NPH_{oil} : 71 < 80 h/a) in case of Moosburg.

In Eibiswald the biomass boiler's nominal power hours are less due to the fact, that a biomass boiler with greater capacity is applied and a higher level of heat load can be covered. The small amount of $NPH_{oil} = 25$ h/a for the oil boiler in Eibiswald is a clear indication, that heating oil is utilized mainly during summer load operation.

The different periods of operation for biomass boiler and oil boiler will have a direct impact on the amount of fuel that can be saved by feeding solar thermal heat into

the district heating network. Due to the fact that in all of the three scenarios the biomass boilers have the same efficiency the annual biomass utilization ratio is assumed to stay at the same level. For oil boilers the same assumption is made.

When comparing the annual efficiency of heat provision there is a significant increase in case of solar support. Due to less primary energy content of fuels utilized in case of solar-assisted biomass district heating systems the annual efficiency is higher in Moosburg's configuration with solar feeding as in Eibiswald.

Regarding the connected heat load per boiler output the value for Eibiswald is greater than the value for Moosburg. Because more boiler capacity is installed and less heat load is connected the result for Eibiswald is clear.

If the specific electricity demand of the different heating stations is compared to each other, the solar-assisted configuration in Moosburg will show the greatest demand per unit of produced heat. However, the outcome for all three applications is at the Austrian average as mentioned by Table 2-7.

The next sub-section will give a closer look to configuration data and operation data of heat distribution grids and their characteristic key indicators.

7.1.2 Distribution grid related key indicators of a biomass district heating system without solar support and a solar-assisted biomass district heating system in Moosburg 2013 compared to distribution grid related indicators of a solar-assisted biomass district heating system in Eibiswald 1997

In order to compare heat distribution grid related configuration and operating data of the three investigated scenarios, please refer to Table 7-3. As several times mentioned before the scenario in Moosburg of year 2013 with and without solar thermal assistance is based on the same district heating network configuration. Nevertheless, there are differences regarding the heat fed into the grid and the annual thermal energy losses in the heating network (see Table 7-3).

For district heating grid in Eibiswald in year 1997 the operating data differs because of a different nominal connected heat load, less heat consumers and a shorter grid length. The forward flow temperature levels and the return flow temperature levels are in the same order of magnitude as in Moosburg.

Table 7-3: Comparison of distribution grid related configuration and operating data of biomass district heating systems with and without solar support in Moosburg 2013 and a solar-assisted biomass district heating system in Eibiswald 1997 (data source: simulation results of SHWwin and own calculations).

Indicator	Symbol	Value for DHS Moosburg 2013 w/o solar support	Value for solar- assisted DHS Moosburg 2013	Value for solar- assisted DHS Eibiswald 1997	Unit
Sum of nominal connected heat load of users	$\sum Q'_{th,user,nom.,i}$	3554	3554	3000	[kW _{th}]
Number of connected heat users (consumer heating sub-stations)	$n_{user,i}$	104	104	64	[1]
Average connected nom. heat load per heat consumer	$Q'_{th,user,av.}$	34.2	34.2	46.9	[kW _{th} /us.]
Utilization factor in the district heating grid (calculated)	f_u	0.5812	0.5812	0.6836	[1]
Total connected heat load in the district heating grid	$Q'_{load,grid,tot.}$	2130	2130	2114	[kW _{th}]
Maximal effective heat load in DHG	$Q'_{load,max.,eff.}$	2066	2066	2051	[kW _{th}]
Average base load in DHG	$Q'_{load,base,av.}$	107	107	106	[kW _{th}]
Heat fed into the district heating grid per year	$Q_{th,demand,DH}$	5328213	5326745	4501483	[kWh _{th} /a]
Useful head supplied and sold to the users per year	$Q_{th,useful,an.}$	4205945	4205945	3650000	[kWh _{th} /a]
Annual thermal energy losses in DHG	$\Phi_{grid,an.}$	1122269	1120800	851483	[kWh _{th} /a]
Length of grid in trench meters (including connection lines)	l_{grid}	5755	5755	4000	[m]
Maximal forward flow temperature (winter)	$T_{FF,max}$	92	92	95	[°C]
Minimal forward flow temperature (summer)	$T_{FF,min}$	75	75	70	[°C]
Minimal return flow temperature (winter)	$T_{RF,min}$	50	50	50	[°C]
Maximal return flow temperature (summer)	$T_{RF,max}$	60	60	60	[°C]

Explanations: DHS ... District Heating System;
DHG ... District Heating Grid.

According to Zweiler (2011) the energy load level is recommended to reach a minimum of 1200 kWh_{th}/m, while the heat connection dense should exceed a level of 1 - 2 kW_{th}/m. As shown in Table 7-4 neither the energy load level in Moosburg's nor in Eibiswald's district heating grid shows the recommended result. For the heat connection dense, which have to be conducted for both heating grids, the results depend on the value taken as total heat load of the grid. If the total effective connected load is taken the results in Table 7-4 will be the outcome. If the sum of nominal connected heat load of users is the basis for calculation the outcome for Moosburg is an alternative heat connection dense of $NWA_{HL} = 0.6176$ kW_{th}/m and for Eibiswald an alternative value of $NWA_{HL} = 0.75$ kW_{th}/m (see Table 7-4).

Table 7-4: Comparison of distribution grid related key indicators of biomass district heating systems with and without solar support in Moosburg 2013 and in Eibiswald 1997 (data source: simulation results of SHWwin and own calculations).

Indicator	Symbol	Value for DHS Moosburg 2013 w/o solar support	Value for solar- assisted DHS Moosburg 2013	Value for solar- assisted DHS Eibiswald 1997	Unit
Energy load level in the district heating grid	ELL_{grid}	730.8	730.8	912.5	[kWh _{th} /m]
Heat connection dense	HCD_{grid}	0.3701	0.3701	0.5284	[kW _{th} /m]
Network allocation related to connected heat load of users	NWA_{HL}	0.6175	0.6175	0.7500	[kW _{th} /m]
Network allocation with respect to nom. thermal power of boiler	NWA_{TP}	0.5647	0.5647	0.6250	[kW _{th} /m]
Average power losses per trench meter in the DHG	$\varphi'_{grid,av.}$	0.0223	0.0222	0.0243	[kW _{th} /m]
Average heat losses per trench meter and year in the DHG	$\varphi_{grid,av.}$	195.0	194.8	212.9	[(kWh _{th} /a)/m]
Specific electricity demand of district heating grid	$w_{el,grid,aux.}$	0.0051	0.0051	0.0049	[kWh _{el} /kWh _{th}]
Annual grid utilization factor	$\zeta_{grid,an.}$	0.7886	0.7890	0.8074	[1]
Average nominal power hours per heat consumer	$NPH_{user,av.}$	1183.4	1183.4	1216.7	[(h/a)/user]

*Explanations: DHS ... District Heating System;
DHG ... District Heating Grid.*

If the network allocation with respect to the nominal thermal power of boilers is checked, the shorter grid length and the higher installed capacity in Eibiswald will cause a greater value of $NWA_{TP} = 0.6250 \text{ kW}_{th}/\text{m}$.

In order to check the specific grid loss indicators of the investigated grid configurations the average power losses ($\varphi'_{grid,av.}$) and the average heat losses per trench meters ($\varphi_{grid,av.}$) have to be compared. As shown in Table 7-4 the determined values for the grid in Moosburg are lower. That means that the applied measures for pipeline insulation are more efficient.

Regarding the specific electricity demand of district heating grid the three grid systems show nearly identical values of about $0.005 \text{ kWh}_{el}/\text{kWh}_{th}$ (see $w_{el,grid,aux.}$ in Table 7-4). This is below the determined average for Austrian heating systems erected since 2007 (see Table 2-7).

The annual grid utilization factor (see $\zeta_{grid,an.}$ in Table 7-4) is based on the annual heat production of the heating plant, which give a better ratio compared to the useful heat supplied and sold in Eibiswald.

With respect to the average nominal power hours per heat consumer the outcome of calculation gives a higher value for Eibiswald (see $NPH_{user,av.}$ in Table 7-4).

Obviously, a smaller number of heat consumers with a higher average nominal heat load per user utilize more useful heat supplied to the heating sub-stations in Eibiswald.

In the next sub-section a characterization of the applied solar thermal plants in Moosburg in year 2013 and in Eibiswald in year 1997 is carried out.

7.1.3 Solar plant related key indicators of a solar-assisted biomass district heating system in Moosburg 2013 compared to heating station related indicators of a solar-assisted biomass district heating system in Eibiswald 1997

For an overview on the two assisting solar thermal plants, which are compared to each other, please refer to Table 7-5. The installations comprise two large-scale collector fields made of flat plat collectors with similar collector characteristics. While the ground-mounted installment in Moosburg has a total gross area of 2034 m^2 , the roof-integrated system in Eibiswald requires 1250 m^2 of gross collector area. With respect to the thermal energy storage in both cases a cylindrical steel tank with insulation is applied. The storage volume of 200 m^3 of hot water in Moosburg exceeds the volume of 105 m^3 in Eibiswald (see Table 7-5).

Table 7-5: Comparison of solar plant related configuration and operating data of a solar-assisted biomass district heating system in Moosburg 2013 and a solar-assisted biomass district heating system in Eibiswald 1997 (data source: simulation results of SHWwin and own calculations).

Indicator	Symbol	Value for solar- assisted DHS Moosburg 2013	Value for solar- assisted DHS Eibiswald 1997	Unit
Name of collector		Solid Gluatmugl HT16.7	Gluatmugl Großfläche (1996)	
Type of collector		FPC	FPC	
Gross area of solar thermal collector field	$A_{col,gross}$	2034.0	1250.0	[m ²]
Aperture area of solar thermal collector field	$A_{col,net}$	1827.6	1150.0	[m ²]
Tilt of collector plane	$Ti_{col.}$	30	30	[°]
Azimuth (-90°:W, 0°:S, 90°:E)	$Az_{col.}$	-25	-20	[°]
Optical efficiency	η_0	0.811	0.754	[1]
1 st order heat loss coefficient	a_1	2.710	3.000	[W/(m ² K)]
2 nd order heat loss coefficient	a_2	0.010	0.002	[W/(m ² K ²)]
Storage volume of hot water tank	$V_{stor.}$	200	105	[m ³]
Number of charging cycles	CN	491	696	[a ⁻¹]
Maximal energy storage capacity of hot water tank (calculated)	$Q_{stor.,max.}$	39049041	23300218	[kJ]
Storage volume per unit collector area	$v_{col.}$	0.1094	0.0913	[m ³ /m ²]

Explanations: W ... West;
S ... South;
E ... East.

Based on the simulation results given by SHWwin (see chapter 6.2.1) a set of characteristic indicators for an assisting solar thermal plant feeding into a district heating network can be determined (see Table 7-6). As described in chapter 2.1.11, there are three definitions for the solar fraction (f_{sol}) in use, which have been applied on the outcome by SHWwin (see 6.2.1 and annex). In any case the results for the annual solar fraction are greater than the expected 10%. However, despite the fact, that Moosburg has got nearly double of storage volume than in Eibiswald only 3% more in terms of annual solar fraction can be achieved by the solar thermal application in Moosburg.

Looking at the results for solar fraction during summer load operation in July and August of year 2013 or 1997, respectively, the solar thermal installation in Moosburg in average gives the more promising results.

If the solar energy utilization ratio of Moosburg's solar plant is compared with the solar thermal application in Eibiswald, the roof-integrated collectors will reach a percentage rate of about 28% (see ζ_{sol} in Table 7-6). In order to assess the specific energy utilization performance of the installed solar thermal applications three key indicators are available. That is the specific energy yield of solar collectors, the degree of utilization of a solar thermal collector field and the specific energy savings per unit collector area and year (see y_{sol} , DU_{col} , $eS_{col,an}$ in Table 7-6).

For each of the mentioned key indicators the solar thermal system in Eibiswald shows up with greater indicator values. This fact leads to the conclusion that careful planning beforehand, and an excellent design adapted to the local conditions and an appropriate operation of the solar plant are the reasons for an optimized utilization of the available solar resources in Eibiswald. However, according to Streicher, et al. (1999) the specific energy yield of a solar thermal system can be seen as a quality criterion, which is an indication for the quality of design.

With regard to the system efficiency of a solar-assisted heating system again the application in Eibiswald gives a slightly better result. As for dimensioning of an assisting solar thermal application the nomogram algorithm presented by Streicher, et al. (1999) could be used, the specific collector area and the specific storage volume (see a_{sol} , v_{stor} in Table 7-6) are mentioned for information only.

During normal operation a solar thermal application is characterized by no emissions in terms of greenhouse gases, air pollutants, particles or noise. By combination with combustion technology for heat generation ecological effects will occur in that respect. The next chapter will summarize the results from ecological assessment carried out in chapter 6 before.

Table 7-6: Comparison of solar plant related key indicators of a solar-assisted biomass district heating system in Moosburg 2013 and a solar-assisted biomass district heating system in Eibiswald 1997 (data source: simulation results of SHWwin and own calculations).

<i>Indicator</i>	<i>Symbol</i>	<i>Value for solar- assisted DHS Moosburg 2013</i>	<i>Value for solar- assisted DHS Eibiswald 1997</i>	<i>Unit</i>
Solar savings fraction (def.1)	$f_{sol.}'$	12.8%	10.0%	[1]
Solar fraction (def.2)	$f_{sol.}''$	12.7%	10.2%	[1]
Solar fraction (def.3)	$f_{sol.}^{*}$	12.7%	10.2%	[1]
Solar savings fraction (def.1) for summer month (Jul., Aug.)	$f_{sol.}',_{sum.}$	96.0%	93.3%	[%]
Solar fraction (def.2) for summer month (Jul., Aug.)	$f_{sol.}''_{,sum.}$	90.1%	99.0%	[%]
Solar fraction (def.3) for summer month (Jul., Aug.)	$f_{sol.}^{*}_{,sum.}$	95.7%	93.6%	[%]
Solar energy utilization ratio	$\zeta_{sol.}$	26.1%	27.8%	[1]
Specific energy yield of solar collectors	$y_{sol.}$	370	401	[kWh/(a m ²)]
Degree of utilization of a solar thermal collector field	$DU_{col.}$	2915	3914	[kWh/(a m ²)]
Specific energy savings per unit collector area and year	$es_{col.,an.}$	335	390	[kWh/(a m ²)]
System efficiency of a solar-assisted heating system	$\zeta_{sys.,sol.}$	0.7903	0.8087	[1]
Specific collector area	$a_{col.}$	0.8580	0.5441	[m ² /kW _{th}]
Specific storage volume	$v_{stor.}$	0.0939	0.0497	[m ³ /kW _{th}]

Explanations: def. ... definition;
Aug. ... August;
Jul ... July.

7.2 Ecological comparison of the proposed applications for district heat supply by biomass district heating systems

In the following sub-chapters three different configurations of biomass district heating systems are compared with respect to their ecological effects by focusing on gaseous emissions and particle emissions. In chapter 7.2.1 the results of evaluations done in chapter 6.3 are summarized and discussed. Chapter 7.2.2 deals with the results of relative emission savings compared to conventional district heating supply as well as greenhouse gas savings and air pollutant savings of the

investigated solar-assisted biomass district heating systems in Moosburg 2013 and Eibiswald 1997 (see chapter 6.4).

7.2.1 Ecological comparison of the proposed applications for biomass district heat supply without and with solar support in Moosburg 2013 with the solar-assisted biomass district heating system in Eibiswald

For an overview on the total annual emissions of carbon dioxide (CO₂), carbon monoxide (CO), hydro carbons (C_xH_x), nitric oxide (NO_x) and particles, which have been evaluated based on emission factors given by Streicher, et al. (1999), please refer to Table 7-7.

Table 7-7: Total, annual emissions based on primary energy content of fuel utilized by district heating systems without and with solar support in Moosburg 2013 and by by a solar-assisted biomass district heating system in Eibiswald 1997 (data source: simulation results of SHWin and own calculations).

Type of heating plant	Unit	CO₂	CO	C_xH_x	NO_x	Particles
Emissions of biomass DHS w/o solar support in Moosburg 2013	[t/a]	32.136	7.048	0.471	2.754	3.743
Emissions of solar-assisted biomass DHS in Moosburg 2013	[t/a]	36.004	5.440	0.362	2.392	2.930
Emissions of solar-assisted biomass DHS in Eibiswald 1997	[t/a]	3.777	6.272	0.421	2.111	3.279

Explanations: DHS ... District Heating System.

As Table 7-7 represents absolute figures the emitted output for the biomass district heating system without solar support and the solar-assisted biomass district heating plant in Moosburg shows the factual change when introducing a solar thermal plant. While the CO₂ emission increases, the other types of emission are reduced. Main reason for this effect is an enhanced operation of the oil boiler on low capacity level.

The absolute figures for carbon dioxide (CO₂), carbon monoxide (CO), hydro carbons (C_xH_x), nitric oxide (NO_x) and particles emissions of the solar-assisted biomass district heating system are in the same magnitude of order, except the figures for CO₂ emissions. This is a clear indication that in Eibiswald the 500 kW_{th} oil boiler is used rarely.

Table 7-8 summarizes the results of specific emissions determined per unit heat fed into the district heating grid. As the figures are relative values, a direct comparison

of the three different district heating system configurations with respect to their gaseous and particle emissions can be performed.

Table 7-8: Specific emissions per unit heat fed into district heating system without and with solar support in Moosburg 2013 and per unit heat fed into solar-assisted biomass district heating system in Eibiswald 1997 (data source: simulation results of SHWin and own calculations).

Type of heating plant	Unit	CO ₂	CO	C _x H _x	NO _x	Particles
Annual specific emissions of biomass DHS w/o solar support per unit heat fed into DHN in Moosburg 2013	[g/kWh _{th}]	6.031	1.323	0.088	0.517	0.703
Annual specific emissions of solar-assisted biomass DHS per unit heat fed into DHN in Moosburg 2013	[g/kWh _{th}]	6.759	1.021	0.068	0.449	0.550
Annual specific emissions of solar-assisted biomass DHS per unit heat fed into DHN in Eibiswald 1997	[g/kWh _{th}]	0.839	1.393	0.094	0.469	0.728

*Explanations: DHN ... District Heating Network;
DHS ... District Heating System.*

While the solar-assisted biomass district heating system in Moosburg 2013 shows the lowest specific emission in terms of CO, C_xH_y, NO_x and particles, the specific emission of CO₂ are the highest compared to the two other evaluated applications. As the installed biomass boiler is stopped during holiday season and the oil boiler has to cover the additional heat load during summer operation, the share of specific CO₂ emissions is high.

In the scenario without solar assistance and in the biomass district heating plant of Eibiswald the specific emissions of CO, C_xH_y, NO_x and particles are quite similar. Except for specific CO₂ emissions the resulting figures are almost the same. A reason for this similarity could be a similar use of biomass boiler throughout the year. The difference in specific CO₂ emissions is again a consequence of a different use of the oil boiler. While in Moosburg the oil boiler has to cover peak load situations during heating season, to the main part the oil boiler in Eibiswald is started only during summer season.

In the next sub-chapter a comparison of greenhouse gas savings and air pollutant savings of two solar assisted biomass district heating plants with a reference system representing a mixture of conventional district heating systems is described.

7.2.2 Ecological comparison of the proposed applications for district heat supply by solar-assisted biomass district heating systems in Moosburg 2013 and Eibiswald 1997 with respect to relative emission savings

In order to compare the ecological parameters of a solar-assisted biomass district heating system in Moosburg in year 2013 with an application in Eibiswald in year 1997, please refer to Table 7-9. Table 7-9 summarizes the annual amount of greenhouse gas savings in tons of CO₂-equivalents and the annual amount of air pollutant savings in tons of SO₂-equivalents compared with a reference system. The basic figures for the reference district heating system (see GEMIS 4.6 (2010)) are the result of a mixture of measurements carried out for several conventional heating systems. Further on, the relative greenhouse gas savings and relative air pollutant savings of the two investigated applications are shown as a percentage rate (see Table 7-9).

Table 7-9: Ecological parameters of a solar-assisted biomass district heating system in Moosburg 2013 compared with a solar-assisted biomass district heating system in Eibiswald 1997 (data source: simulation results of SHWin and own calculations).

Ecological Parameter	Symbol	Unit	Solar-assisted biomass DHS in Moosburg 2013	Solar-assisted biomass DHS in Eibiswald 1997
Annual amount of CO ₂ -equivalents of GHG savings checked against conventional district heating mix	ΔEMI_{CO_2}	[t CO ₂ -equ./ a]	993.89	862.51
Annual amount of SO ₂ -equivalents of air pollutants' savings checked against conventional district heating mix	ΔEMI_{SO_2}	[t SO ₂ -equ./ a]	0.81	0.70
Relative GHG savings compared to conventional district heating mix	$\frac{\Delta EMI_{CO_2}}{EMI_{ref,CO_2}}$	[%]	93.2%	93.2%
Relative air pollutants savings compared to conventional district heating mix	$\frac{\Delta EMI_{SO_2}}{EMI_{ref,SO_2}}$	[%]	47.8%	47.8%

Explanations: $\Delta EMI \dots \Delta EMI = EMI_{ref} - EMI_{SADHS}$;
GHG ... Greenhouse Gas;
SADHS ... Solar-Assisted District Heating System.

For greenhouse gas emission and air pollutant emission balances the complete lifecycle of the two selected solar-assisted district heating applications and the reference system's lifecycle has to be considered. In each case the specific emissions per unit of supplied final energy at the consumer's heating sub-station is taken into account. Because of different amounts of heat supplied and sold to heat

consumers the annual amount of greenhouse gas savings and air pollutant savings by the application in Moosburg are higher than in Eibiswald. Approximately 1000 tons of CO₂-equivalents are saved in Moosburg and more than 860 tons of CO₂-equivalents are saved in Eibiswald compared to conventional district heating mixture.

If the relative greenhouse gas and air pollutant savings are checked, an identical percentage rate of 93.2% of GHG savings and 47.8% of air pollutant savings will be calculated. From an ecological point view the positive environmental effect of applying solar-assisted district heating plant for the supply of useful heat is evident.

Nevertheless, the image of environmentally friendly heat generation is not that strong motivation to introduce a solar thermal system for district heating. A lot more the economic performance of a solar-assisted biomass district heating system influences the decision to invest. In the following chapter the results of the economic assessment of three biomass district heating configurations are discussed.

7.3 Economic comparison of the proposed applications for district heat supply by biomass district heating systems

In order to compare the cost and income related economic parameters of the three investigated investment projects, please refer to Table 7-10. The parameters are valid for year 5 of operation of the three biomass district heating systems.

While in case of Moosburg the biomass and the oil boiler's capacity stay the same, in case of Eibiswald more biomass, but less oil boiler capacity is available. The different periods of operation for biomass boiler and oil boiler will have a direct impact on the amount of fuel that can be saved by feeding solar thermal heat into the district heating network. However, the effective savings of wood chips or heating oil depend on the operation mode and the seasonal use of boiler capacities.

Table 7-10: Cost and income related economic parameters of 2 district heating systems without and with solar support in Moosburg 2013 compared with the economic parameters of a solar-assisted biomass district heating system in Eibiswald 1997 (data source: simulation results of SHWwin and own calculations).

Cost & income related economic parameters	Symbol	Unit	DHS w/o solar support in Moosburg (year 5: 2014)	Solar-assisted DHS in Moosburg (year 5: 2014)	Solar-assisted DHS in Eibiswald (year 5: 1998)
Fuel costs for wood chips (30 wt.%; net price *)	$p_{bio,30\%wt}$	[€/SRM]	16.64	16.64	10.97
Fuel costs for heating oil (net price)	$p_{oil,light}$	[€/l]	0.66	0.66	0.39
Industrial electricity price (consumption < 1 GWh/a)	$p_{el,light}$	[€/kWh _{el}]	14.20	14.20	14.78
Nom. capacity biomass boiler	$Q'_{th,bio,nom}$	[kW _{th}]	1750	1750	2000
Nom. power hours of biomass boiler per year	NPH_{bio}	[h/a]	2987	2586	2020
Nom. capacity oil boiler	$Q'_{th,oil,nom}$	[kW _{th}]	1500	1500	500
Nom. power hours of oil boiler per year	NPH_{oil}	[h/a]	71	80	25
Average heat price for sold heat	$p_{heat,av.}$	[€/MWh _{th}]	79.31	79.31	64.50
Total effective, connected load in DHN	$Q'_{cl,grid,tot.}$	[kW _{th}]	2130	2130	2114
Useful head supplied and sold to the users per year	$Q_{th,useful,an.}$	[kWh _{th} /a]	4205945	4205945	3650000

Explanations: DHS ... District Heating System
DHN ... District Heating Network.

For a comparison of economic key indicators applied and evaluated by the annuity method according to VDI 2067 Blatt 1 (2012) please refer to Table 7-11. In any case of the investigated investment projects the same prerequisites for an economic feasibility study are given. Starting from year 0, when the original biomass district heating system has been started, a period of 20 years is used as investment horizon. Within the 20 years period the assisting solar thermal plant is operated for 16 years. In all three cases the same interest rate ($i = 4.53\%$) and the same annuity factor ($a = 0.07707612$) is applied in order to calculate the investment project's total annuity, its NPV and the expected long run generation costs.

Table 7-11: Economic key indicators of 2 district heating systems without and with solar support in Moosburg 2013 compared with the economic parameters of a solar-assisted biomass district heating system in Eibiswald 1997 (data source: simulation results of SHWin and own calculations).

Economic key indicators	Symbol	Unit	Biomass DHS w/o solar support in Moosburg	Solar-assisted biomass DHS in Moosburg	Solar-assisted biomass DHS in Eibiswald
Percentage rate for investment funding of solar plants		[%]	40%	40%	40%
Percentage rate for investment funding of biomass district heating systems		[%]	40%	40%	40%
Sum of PV of investment costs calculated in year 0	PV(A ₀)	[€]	2801431.58	3648998.46	2617479.63
Sum of present values (A ₀ +A ₁ +A ₂ +... -RW)	Σ PV	[€]	2473591.00	3246339.68	2446537.12
Investment horizon	n	[a]	20	20	20
Remaining project life time for solar plant	n _{sol}	[a]	16	16	16
Interest rate	i	[%]	4.53%	4.53%	4.53%
Annuity factor	a	[1]	0.07707612	0.07707612	0.07707612
Total Annuity	A _N	[€]	23716.02	-8552.01	-202.48
Net Present Value	NPV	[€]	307696.08	-110955.32	-2626.98
Annuity of Income	A _{N,E}	[€]	465973.21	490971.64	356849.64
Annuity of Costs	A _{N,C}	[€]	442257.19	499523.65	357052.11
Capital Recovery Factor	CRF	[1]	0.07707612.	0.07707612	0.07707612
Long Run Generation Costs	LRGC	[€/MWh _{th}]	104.27	117.77	97.82

Explanations: DHS ... District Heating System.

All three examples of investment projects are based on biomass district heating systems supplying useful heat via a district heating grid to a defined number of heat consumers. So the regular income from sold heat is the main driver for revenues in any of the three compared configurations. Consequently, the long run generation costs will decrease, if the number of connected heat consumers and the related amount of sold heat increases. So the economic efficiency of the biomass district heating system will be improved, if either the heat connection dense (HCD_{grid}) and

the energy load level (ELL_{grid}) of the grid is changed to a higher level or if the grid losses in the district heating grid are reduced to a minimum.

But the economic success in the long run is also influenced by the amount of subsidies granted at the very beginning of the investment project. As shown in Table 7-11 in each of the three case studies a 40% investment funding for both, the environmentally relevant investment costs of a biomass district heating system and the environmentally relevant investments of a solar district heating system are assumed. However, a percentage rate of 40% is the possible maximum, which is not granted in any case.

According to the analysis done in chapter 6.4, chapter 6.5 and chapter 6.6 the total annuity for a pure grid extension is positive, while the implementation of an additional solar thermal plant results in a negative total annuity. VDI 2067 Blatt 1 (2012) recommends to accept an investment project, which gives a positive value for total annuity or NPV . In case two projects are compared with each other, the project with the more positive result for total annuity A_N or NPV should be selected.

However, the outcome of the economic feasibility study is to accept and to invest in case of a pure grid extension project, but to reject in case of adding a solar thermal plant for solar assistance to an existing biomass district heating system.

From an economic point of view the solar-assisted biomass district heating system in Eibiswald shows the better economic performance than the solar-supported application in Moosburg. The main reasons are a higher specific energy yield of solar collectors or higher specific energy savings per unit collector area, respectively. As a consequence careful planning and exact technical design are prerequisites for an optimal utilization of the available solar potential. The economic success of the solar-assisted district heating plant should be more realistic in this case.

8 Conclusions

The entire chapter summarizes the conclusions, which can be derived from a technological, an economic, and from an ecological point of view. In addition, the conclusions a plant owner and/or district grid operator will come to are mentioned as well.

8.1 Conclusions from a technological point of view

Keeping in mind the results from the technical evaluation carried out in chapter 6 and the outcome of comparison performed in chapter 7 the following conclusions can be drawn from a technical point of view:

- The district heating grids flow pipe temperature and return pipe temperature level are the limiting factors with respect to the solar energy utilization ratio of an installed collector field. For an increase of the specific energy yield of the collectors the temperature levels applied in the district heating grid should be low. Especially the impact of a reduced return flow temperature on the collector field's performance is evident. If it is possible for the biomass district heating system's operator to lower the grid temperatures during holiday season to a minimum, the energy output of the assigned solar collectors will significantly increase.
- In order to enhance the collector's energy utilization factor, the average collector operating temperature has to be diminished. A proper reduction could be achieved if the heat exchange unit in the collector loop is able to cool down the collector's inlet temperature to the lowest temperature level of the secondary circuit coming from the central storage tank.
- In relation to the useful heat demand at the consumers heating sub-stations outside the heating season the heat losses in the district heating grid will be relatively high. Percentage rates of more than 65% could occur. As the grid losses depend on the forward flow temperature level the flow pipe temperature should be decreased as low as possible during summer load operation.
- Detailed and careful planning, an optimized design based on state-of-the-art technologies and an appropriate operation of the assisting solar plant will result in a high specific energy yield of solar collectors. In general, the

assisting solar thermal plant is dimensioned and designed according to the district heating system's demand during summer load operation.

- Large-scale thermal energy storages do not automatically increase the annual solar fraction of an assisting solar thermal application. The storage volume for a solar-assisted biomass district heating system should be dimensioned to cover 3- 5 times the daily demand of thermal energy for domestic hot water preparation.
- In order to optimize the storage capability of the solar thermal energy storage, the charging of the hot water storage tank should result in stratified layers. A mixture of solar heated water fed in by the collector field with colder water would result in heat losses due to circulation. Several inlets at different heights should be planned.

Further findings with regard to the economic analyzes can be found in the next chapter.

8.2 Conclusions from an economic point of view

With respect to the economic feasibility studies carried out in chapter 6.5 and chapter 6.6 as well as the outcome of comparisons made in chapter 7.3 the reader can come to the following conclusions from an economical point of view:

- The extension of an existing biomass district heating system with a solar thermal plant does not automatically change the plant's economic performance to a more positive result. As shown in the frame of this study it could be even a change to the other direction. The better the specific energy yield of solar collectors during long-term operation and the higher the specific energy savings per unit collector area and year, the better is the chance to get a positive result for the investigated project run time.
- With respect to the fuel input it has been shown, that the higher the costs for the substituted type of fuel, the better the profitability of an introduced assisting solar thermal application. The example of a solar-assisted biomass district heating system has pointed out that a shut-down of the biomass boiler during summer period could mean an increased fuel demand for heating oil. Consequently, a solar thermal support will not achieve the required effect, as the price development for fossil fuels has shown an over proportional growth in the last decade.

- From an economic point of view the use of supporting solar thermal systems in biomass district heating systems has to be planned carefully. Due to the frame conditions established by pure biomass district heating systems (e.g. supply flow temperature, return flow temperature, temperature difference in distribution grid) an optimal operation of the additional, cost intensive solar thermal plant is tricky. One possibility to achieve a better economic feasibility could be the prolongation of the projects overall run time and an intensified utilization of the solar thermal components within their total lifetime of twenty years.
- However, a sixteen years period for the solar thermal part of the investment project is short compared to an average life time of twenty years for flat plate collectors. An operation as long as possible, but at least twenty years would probably change the economic performance in a positive way.
- Generally, the economic performance of the district heating grid will increase, if the heat connection dense will be improved by a grid expansion. The more heat consumers will use the provided district heat especially during summer load operation, the better the economic efficiency during this period of inefficient boiler operation intensified by very high shares of grid losses along the heat distribution network. So it should be the solar district heating system operator's goal to have heat consumers with domestic hot water preparation as much as possible.
- A further learning from the examples assessed in the frame of this study is the fact, that solar plants will not show positive economic feasibility in any case. The combination of biomass combustion technology with solar thermal technology for district heat supply increases the investment costs and the related economic risk.

The next chapter provides a summary of conclusions, which can be reached from an ecological point of view.

8.3 Conclusions from an ecological point of view

Taking into account the outcome of analyses conducted in chapter 6.3 and chapter 6.4 regarding emission balances and emission savings and keeping in mind the comparisons performed in 7.2 the following conclusions can be reached from an ecological point of view:

- When applying a solar thermal system as an additional resource for district heat supply, the new setup of the district heating plant does not mean an automatic improvement of the overall system's environmental compatibility. If the ecological effects are focused on greenhouse gas emissions, air pollutants emissions, and the emissions of particles, the configuration of the plant's boilers will be the most influencing factor for a solar-assisted biomass district heating system's ecological balance.
- In cases of plants with fossil fueled peak-load boilers, which have to run during summer season as a reserve, the annual balance of CO₂ emissions could even be worse compared to plant operation with biomass boilers working in start / stop operation mode during this period. In case the oil boiler is not dimensioned as a reserve but as a summer load boiler, the output of greenhouse gas CO₂ cannot be prevented during the biomass boiler's standstill and the solar thermal plant's period of maximal thermal power output.
- In general, the substitution of heat generation by wood chips fueled boilers with solar thermal energy gained during summer time dramatically improve the heating plant's emission balance in terms of carbon monoxide (CO), hydro carbons (C_xH_y), nitrous gases (NO_x) and particles. For the CO₂ emission balance a correctly dimensioned oil boiler or gas boiler would help to lower the necessary CO₂ emissions to a minimum.

As mentioned before, the positive ecological effects of solar thermal supported district heating systems are not the main argument for system extension. The next chapter will give a summary of conclusions relevant for the plant owner and/or district grid operator.

8.4 Conclusions from a plant operator's / plant owner's point of view

Summing up the findings made and the conclusions drawn in the frame of this case study, the plant owner and /or district heating grid operator will come to the following conclusions:

- It has been shown, that a solar-assisted biomass district heating system will work on a high level of availability and security of supply. The example of "Nahwärme Eibilwald" is a best-practice-model to demonstrate the reliability of this technology over two decades of operation. The decision by the

owners in Eibiswald to reinvest in this kind of technology for district heat supply with a solar assistance for another twenty years of operation is exemplary.

- Further learnings from the Eibiswald example are the positive image effect, the good experience with the realization of big-scaled solar thermal plants and the increase of public acceptance for this kind of technology.
- If a municipality with an already up and running biomass district heating system would like to differentiate from other municipalities with similar district heating systems, the add-on of solar thermal system is still distinguishing feature. Even though, there has been installed more than 36 solar-assisted biomass district heating systems and more than 15 solar-assisted biomass micro-grids up to now in Austria the installation of big scaled solar district heating plants is still of public interest.

9 Further Outlooks

In the following chapters a short outlook on future perspectives and further measures for a sustainable development of solar-supported district heating is given.

9.1 Perspective for the current owner of the biomass district heating system and district heating grid operator of “MS Fernwärme Moosburg”

As the project history of “MS Fernwärme Moosburg” has shown, the success story of the biomass district heating system started quite early in the year 2004. Further five years went by before the system started regular operation. From today’s point of view this long lasting pre-phase of diligent planning, of careful economic assessments and professional construction work has been necessary to secure the biomass heating system’s survival.

Based on this knowledge further assessments and detailed project engineering is recommended to the plant owner before the decision for a plant extension with solar thermal components is taken. However, the final realization of a project for solar thermal support of the district heating plant will depend on the regular framework and the availability of a 40% investment funding in future.

In order to improve the district heating system’s economic performance in future, the following measures could help to gain more district heat users:

- Improve the citizens’ willingness to change to district heat supply as an alternative to environmentally unfriendly oil-fired heating stations.
- Initiate further promotion events like “Day of Sun” at plant site of “MS Fernwärme Moosburg” on a regular basis. This would help to bring this kind of renewable energy resource for space heating to public’s attention.
- Target on a further expansion of the heat distribution grid to various service areas. A moderate prolongation of pipeline length in parallel to more district heat sub-stations will increase the network’s heat connection dense.

With respect to Moosburg’s participation in the “e5-program” the next chapter summarizes an outlook and further measures for the municipality.

9.2 Outlook and further measures for the municipality of Moosburg

As the municipality of Moosburg has joint the “e⁵- Program” for sustainable and energy efficient municipalities in Austria, further energy projects based on the

utilization of renewable energy resources are of high interest. Since the introduction of biomass district heating plant in Moosburg mainly influenced the municipality's very positive rating for the first time the solar thermal extension of the current biomass district heating system would strengthen its position on the "eee" level.

As further measures to improve the municipality's sustainable development and to reach its 2020 targets the following proposals are made:

- Motivate Moosburg's citizens to replace their outdated oil-fueled heating systems by a connection to district heat supply.
- Invest in public promotion programs at community level. Small financial incentives could be effective as good publicity.
- Intensify advertising efforts. Via different media channels (e.g. via parish review or via the municipality's internet homepage) it should be emphasized how reasonable a connection to the available district heating system could be in terms of energy efficiency and energy savings.

10 Acknowledgements

First of all I will like to thank my supervisor, Dipl. Päd. Ing. Werner Weiss, for his continuous support, encouragement and patience. His continuous good mood and his motivating comments have always been welcome. In these months I have also benefited a lot from his willingness to accept this master thesis of about 200 pages, which contributed to finish my studies in time.

I also want to thank Mr. Max Sereinig, the plant owner of “MS Fernwärme Moosburg”. Based on his reflections the idea for this master thesis was born. I have been most fortunate to have him as a contact person for detailed information about his biomass district heating system, for technical questions and discussions.

Finally I want to thank my partner, Mag. Sonja Ertl, for her patience and her continuous support. Her ability to support me in writing in a foreign language in a very precise way has always been of great help.

11 References

11.1 Reports, papers, scripts, and books

AEA (2011), “Energiepreise für private Haushalte - Jahresrückblick 2011“, Österreichische Energieagentur, Wien, 2012;
http://www.energyagency.at/fileadmin/dam/pdf/energie_in_zahlen/jahresberichte_epi/epi-2011.pdf

AEA (2012) “Energiepreise für private Haushalte - Jahresrückblick 2012“, Österreichische Energieagentur, Wien, 2013;
http://www.energyagency.at/fileadmin/dam/pdf/energie_in_zahlen/jahresberichte_epi/epi-2012.pdf

Biermayr, P., et al. (2012), “Innovative Energietechnologien in Österreich Marktentwicklung 2011 - Biomasse, Photovoltaik, Solarthermie und Wärmepumpen“, Berichte aus Energie- und Umweltforschung 12/2012, Bundesministerium für Verkehr, Innovation und Technologie, Wien, Mai 2012;
<http://www.aee-intec.at/0uploads/dateien835.pdf>

CPC 14 XL (2012), “Evacuated Tube Collectors CPC XL Series“, Technical Specifications, Ritter XL Solar GmbH, Karlsbad, Germany, March 2012

Danfoss DAS 1 Mini (2012), “DSA 1 Mini- Advanced district heating substation from 16 to 90 kW“, product sheet no. VLGP302, Danfoss 04/2012;
http://heating.danfoss.com/PCMPDF/VLGP302_DSA_1_MINI_1204.pdf

Danfoss Termix BVX RO (2010), “Termix BVX RO – Indirect substation for single-family houses or apartments“, product sheet no. VLCWG202, Danfoss 10/2010;
http://heating.danfoss.com/PCMPDF/VLCWG202_Termix_BVX-RO-1010.pdf

Danfoss Termix Novi (2012), “Termix Novi- Instantaneous water heater for flats, single-family houses and small apartment buildings with up to 4 flats“, product sheet no. VLGEJ302, Danfoss 05/2012;
http://heating.danfoss.com/PCMPDF/VLGEJ302_Termix_Novi-1205.pdf

Duffie, J. A. & Beckman, W., “Solar engineering of thermal processes“, 3rd edition, John Wiley & Sons, New Jersey, 2006

Eicker, U., “Solare Technologien für Gebäude – Grundlagen und Praxisbeispiele“, 2. Auflage, Vieweg + Teubner Verlag, Wiesbaden, 2012

ESTIF (2007), “Objective methodology for simple calculation of the energy delivery of (small) Solar Thermal systems”, Solar Thermal Industry Federation, August 2007; http://www.estif.org/fileadmin/estif/content/policies/downloads/Simple_Calculation.pdf

Faninger, G. & Weiss, W. (2002), “Zentrale solare Wärmeversorgungsanlagen in Österreich - Betriebsdaten, Betriebserfahrungen und Zukunftsperspektiven“, Institut für Interdisziplinäre Forschung und Fortbildung, iff, Universität Klagenfurt & AEE INTEC, Gleisdorf, 2002

Fink, Ch., et al. (2007), “MoSol-Net - Entwicklung von modular erweiterbaren technischen Lösungen, die eine Wärmeversorgung von Neubaugebieten über solar unterstützte Nahwärmenetze ermöglichen“, Endbericht, Institut für Wärmetechnik der Technische Universität Graz und AEE INTEC, Gleisdorf. 2007

Fink, Ch. & Riva, R. (2004), “Solar-supported heating networks in multi-storey residential buildings – A planning handbook with a holistic approach”, Arbeitsgemeinschaft Erneuerbare Energie – Institut für nachhaltige Technologien (AEE INTEC), 1st edition, Gleisdorf, 2004; <http://www.aee-intec.at/0uploads/dateien540.pdf>

FNR (2010), “Marktübersicht Hackschnitzel-Heizungen“, 3., aktualisierte Auflage, Fachagentur Nachwachsende Rohstoffe e. V. (FNR), Gülzow, Mai 2010; http://www.fnr-server.de/ftp/pdf/literatur/pdf_293-mu_hackschnitzelheizungen_2010_web.pdf

GK3100 (2012), “GK 3000 Series Large-size Collectors”, Technical data, GREENoneTEC Solar Collectors, Sankt Veit a.d.Glan, Austria, May 2012

Heimrath, R., et al. (2002), “Solar unterstützte Wärmenetze – Technologie und Komponentenentwicklung“, Endbericht, Berichte aus Energie- und Umweltforschung 12/2002, BMVIT, Graz, April 2002; http://www.hausderzukunft.at/download/endbericht_streicher_1202.pdf

Hofbauer, H. (2010), “Plant engineering for thermal biomass utilization – Module 2: Biomass, Biogas and Biofuels”, script for module 2, MSc Program Renewable Energy in Central and Eastern Europe, October 2010

HT 4.2 m² (2009), “Datenblatt Gluatmugl HT“, ÖkoTech Produktionsgesellschaft für Umwelttechnik mbH, Graz, Juli 2009

Kalt, G. & Kranzl, L. (2009), "Bioenergieketten: Ein dynamischer Vergleich von Effizienzen, Kosten und Treibhausgaseinsparungen- Erneuerbare Energieträger; Biomasse"; 6. Internationale Energiewirtschaftstagung an der TU Wien, 11. - 13. Februar 2009

Kaltschmitt, M., et al. (2010), "Renewable Energy – Technology, Economics and Environment" Springer-Verlag Berlin Heidelberg 2010

Kaltschmitt, M., Hartmann, H. & Hofbauer, H. (2009), "Energie aus Biomasse – Grundlagen, Techniken und Verfahren", 2. Auflage, Springer-Verlag Berlin Heidelberg 2009

Kaltschmitt, M. & Streicher, W. (2009), "Regenerative Energien in Österreich – Grundlagen, Systemtechnik, Umweltaspekte, Kostenanalysen, Potenziale, Nutzung", Vieweg+Teubner GWV Fachverlage GmbH, Wiesbaden 2009

Konstantin, P. (2009), "Praxisbuch Energiewirtschaft", Springer-Verlag Berlin Heidelberg 2009

Kranzl, L. (2010), "Bioenergy and Biomass markets, heating calculation example – Introduction to Renewable Energy", script for module 1, MSc Program Renewable Energy in Central and Eastern Europe, October 2010

Leitfaden (2012), "Leitfaden Solarthermie – solare Großanlagen- 3. Ausschreibung", Klima- und Energiefonds, Vienna, June 2012;
<http://www.klimafonds.gv.at/assets/Uploads/Downloads-Forderungen/Solarthermie/Solarthermie.LF.2012.pdf>

LEV (2009), "Karte zu den Biomasse-Nahwärme-Netzen in Österreich, Stand 2008", LandesEnergieVerein Steiermark, Graz, March 2009;
http://www.lev.at/Download/Karte_Biom_Oesterreich_2008.pdf

LWK NÖ (2012), "Biomasse-Heizungserhebung 2011", Landwirtschaftskammer Niederösterreich, Abteilung Betriebswirtschaft und Technik, St. Pölten, June 2012;
<http://www.lk-noe.at/mmedia/download/2012.06.11/1339404035977882.pdf>

Meißner, R. & Abrecht, S. (2012), "Sinn und Unsinn von Solarspeichern – Das Beherrschen der Stagnation ist Voraussetzung für eine optimierte Speicherauslegung", FEE Heizungsjournal - Special, September 2012;
<http://heizungsjournal.de/Downloads/Themenarchiv/hzi/Forum-Erneuerbare-Energien-FEE/Solarthermie/HZJ-9-2012-Ritter-Solar-Solar-Speicher.pdf>

Meteonorm (2012), "Meteonorm Datensatz Moosburg/AT", Wetterprognosen - Erneuerbare Energien - Luft und Klima – Umweltinformatik - Genossenschaft METEOTEST, Bern, Oktober 2012

Obernberger, I. (1997), "Möglichkeiten der technologisch und wirtschaftlichen Optimierung von Biomasse-Nahwärme- und Mikronetzen", in: conference proceedings to international ALTENER conference in Salzburg "Mikronetze-Gebäudeübergreifende Wärmeversorgung auf Biomassebasis, Vienna, September 1997; <http://www.bios-bioenergy.at/uploads/media/Paper-Obernberger-OptimierungFWNetze-Altener-1997-09-30.pdf>

OeBV (2011), "Biomasse-Standorte - Biomasseheizwerke und KWK-Anlagen, Stand 2010", Österreichischer Biomasseverband (Austrian Biomass Association), 2011; http://www.biomasseverband.at/uploads/tx_osfopage/OeBV_BDB_TABs13_2.pdf

Ortner, M. (2010), "Planning, construction and implementation of plants for the use of biomass (electric, thermal)", script for module 2, MSc Program Renewable Energy in Central and Eastern Europe, October 2010

Promitzer, F. (2011), „Qualitätsmanagement für Biomasseheizwerke als Fördervoraussetzung“, LandesEnergieVerein (LEV) Steiermark, Graz 2011; http://www.biomasseverband.at/uploads/tx_osfopage/PSII_5_Promitzer.pdf

QM-report (2012), „Standardisierter Betriebsbericht für Biomasseheizwerke – Biowärme Moosburg – Betriebsjahr 2011“, qm-heizwerke, Moosburg 2012

Raab, S. (2006), "Simulation, Wirtschaftlichkeit und Auslegung solar unterstützter Nahwärmesysteme mit Heißwasser-Wärmespeicher", Dissertation Universität Stuttgart, 1. Auflage, Cuvillier Verlag, Göttingen 2006

Schallenberg, K. (1998), "Einfluß der Netztemperaturen in den Abnehmersystemen auf den Wärmegestehungspreis", Scientific Technical Report 98/09, GFZ Potsdam, September 1998; <http://bib.gfz-potsdam.de/pub/str9809/9809-6.pdf>

SDH (2012), "Solar district heating guidelines – collection of fact sheets WP3 –D3.1 & D3.2", Solar District Heating, April 2012; <http://www.solar-district-heating.eu/LinkClick.aspx?fileticket=lfFNaiyDxTk%3d&tabid=580>

SHWwin (1999), "Programmbeschreibung von SHWwin – Simulationsprogram für solare Brauchwasserbereitungs- und Heizungssysteme", Institute for Thermal Engineering - Graz University of Technology, Graz, April 1999

Sözen, A. , et al. (2008), “Determination of efficiency of flat-plate solar collectors using neural network approach”, Expert Systems with Applications, Volume 35, Issue 4, November 2008, Pages 1533-1539;

<http://www.sciencedirect.com/science/article/pii/S0957417407003685>

Stockinger, H. & Obernberger, I. (2005), “Systemanalyse der Nahversorgung mit Biomasse“, Schriftenreihe Thermische Biomassenutzung Band 2, 2. Auflage, Institut für Ressourcenschonende und Nachhaltige Systeme der Technischen Universität Graz, Graz, März 2005

Streicher, W., et al. (1999), “Kombination von Biomasse und Solarenergie in Nahwärmenetzen – Kriterienkatalog“, Institut für Wärmetechnik der Technischen Universität Graz, Graz 1999;

http://www.hausderzukunft.at/download/streicher_kriterienkatalog.pdf

Streicher, W. & Oberleitner, W. (1998), “Solar unterstütztes Biomasse-Nahwärmenetz Eibiswald – Ergebnisse einer einjährigen Meßperiode“, aus: „erneuerbare energie“, AEE - Arbeitsgemeinschaft ERNEUERBARE ENERGIE – Dachverband, Gleisdorf 1998

Urbas (2009), Screen shot of user interface for control & monitoring software by urbas energietechnik, Urbas Maschinenfabrik GmbH, Völkermarkt, Carinthia, 2009

VDI2067, Blatt 1 (2012), “Economic efficiency of building installations - Fundamentals and economic calculation”, VDI Richtlinien September 2012, VDI-Gesellschaft Bauen und Gebäudetechnik (GBG)

VDI2067, Blatt 40 (2012), ”Wirtschaftlichkeit gebäudetechnischer Anlagen – Energieaufwand der Erzeugung“, VDI Richtlinien Januar 2012, VDI-Gesellschaft Bauen und Gebäudetechnik (GBG)

Viessmann (2009), “Technical guide – Solar thermal systems”, Viessmann GmbH, 2009; http://www.viessmann.ee/etc/medialib/internet-ee/pdf/vitosol_200-f_200-t.Par.53007.File.File.tmp/PRHandbuchSolar9449829_05-2009_GB.pdf

VK 14 (2008), “Vakuumröhrenkollektoren VK 4000 – Serie“, Technical data, GREENoneTEC Solar Collectors, Sankt Veit a.d.Glan, Austria, June 2008

Wald&Holz (2012), “Wald und Holz in Kärnten“, Landesforstdirektion Kärnten, Abteilung 10 (Kompetenzzentrum Land- und Forstwirtschaft), 9020 Klagenfurt, Mai 2012; http://www.ktn.gv.at/218889_DE-FOLDER-Folder_WaldundHolz2013.pdf

Weiss, W. & Mahler, B. (2003), "Solare Nahwärme in Europa – Vergleich von unterschiedlichen Systemkonzepten und Leistungsdaten", Tagungsband, Solare Kombianlagen für Mehrfamilienhäuser im europäischen Vergleich, AEE INTEC, Gleisdorf 2003

Weiss, W. (2011), "Solar thermal systems and components – Module 3: Solar Energy – Solar Heating & Photovoltaics", script for module 3, MSc Program Renewable Energy in Central and Eastern Europe, January 2011

Winter, W., Haslauer, T. & Obernberger, I. (2001), "Untersuchungen der Gleichzeitigkeit in kleinen und mittleren Nahwärmenetzen", in: Euroheat & Power 09&10, September 2001; <http://www.bios-bioenergy.at/uploads/media/Paper-Winter-Gleichzeitigkeit-Euroheat-2001-09-02.pdf>

Winter, W. & Obernberger, I. (2002), "Netzberechnungsprogramm zur optimierten Dimensionierung und integrativen Berechnung von kleineren und mittleren unvermaschten Biomassenahwärmenetzen", TU Graz, September 2002; <http://www.bios-bioenergy.at/uploads/media/Paper-Winter-Rdesign-2002-09-20.pdf>

Weißensteiner, L. (2010), "Economics of electricity generation from renewable energy sources - Introduction on Renewable Energy", script for Module 1, MSc Program – Renewable Energy in Central and Eastern Europe, September 2010

Zweiler, R. (2011), "Operation, maintenance, economic evaluation, risk and cost aspects – Heat and electricity generation", script for module 2, MSc Program Renewable Energy in Central and Eastern Europe, June 2011

11.2 Internet resources

BMfWFJ (2013), Klimadatenrechner - Energie & Bergbau, Bundesministerium für Wirtschaft, Familie und Jugend, 1010, Wien, <https://www.bmwfj.gv.at/ENERGIEUNDBERGBAU/KLIMADATENRECHNER/Seiten/default.aspx>, last access: January, 15th 2013

Eibiswald (2013), Homepage of „Nahwärme Eibiswald eGen“, 8552, Eibiswald, <http://www.nahwaerme-eibiswald.at/>, last access: April, 15th 2013

KAGIS (2013), KAGIS - Das KÄRNTNER GEOGRAFISCHE INFORMATIONSSYSTEM, Amt der Kärntner Landesregierung, Abt.8 – Kompetenzzentrum Umwelt, Wasser und Naturschutz, Klagenfurt am Wörthersee, Austria, http://www.kagis.ktn.gv.at/19948_DE/, last access: Feb., 27th 2013

Klimafonds (2013), Klima- und Energiefonds, Wien, Austria,
<http://www.klimafonds.gv.at/>, last access: Feb., 20th 2013

LEV (2013), qm heizwerke - Qualitätsmanagement für Biomasseheizwerke und-nahwärmenetze, LandesEnergieVerein Steiermark, <http://www.lev.at/index.asp>, last access: Feb., 18th 2013

qm-heizwerke (2013), Quality and Efficiency Improvement of District Heating Systems and Biomass plants, <http://www.qm-heizwerke.at>, last access: Feb., 18th 2013

GEMIS (2010), Gemis 4.6: Globales Emissions-Modell Integrierter Systeme (GEMIS) Version 4.6, <http://www.gemis.de>, last access: Apr., 01th 2013

Google (2013), Google earth, Version 7.0.3.8542 - © 2013 Google Inc.,
<http://www.google.com/earth/index.html>, last access: April, 10th 2013

PVGIS (2013), Photovoltaic Geographical Information System (PVGIS), Geographical Assessment of Solar Resource and Performance of Photovoltaic Technology, European Commission, Joint Research Centre, Institute for Energy, Renewable Energy Unit, Ispra (VA), Italy,
<http://re.jrc.ec.europa.eu/pvgis/apps4/pvest.php#>, last access: April, 07th 2013

saisonalspeicher.de (2009), saisonalspeicher.de/Bestehende Projekte,
<http://www.saisonalspeicher.de/LinkClick.aspx?fileticket=UqtawVCB7es%3d&tabid=93&language=de-DE>, last access: November, 30th 2012

Schletter (2009), Schletter shade calculation tool, Verslon 4.1, © 2009 Schletter GmbH, <http://www.schletter.de/>, last access: April, 11th 2013

ZMAG (2000 – 2011), Jahrbuch - Monats- und Jahresübersichten aller Messstationen für die Jahre 2000 bis 2011, Zentralanstalt für Meteorologie und Geodynamik (ZAMG), 1190 Wien,
<http://www.zamg.ac.at/cms/de/klima/klimauebersichten/jahrbuch>, last access: December, 11th 2012

ZAMAG (1971 – 2000), Klimadaten von Österreich 1971 – 2000, Zentralanstalt für Meteorologie und Geodynamik (ZMAG), 1190 Wien,
http://www.zamg.ac.at/fix/klima/oe71-00/klima2000/klimadaten_oesterreich_1971_frame1.htm, last access: December, 11th 2012

12 Annex

Table 12-1: Solar-assisted biomass district heating systems in Austria 2012 (Part 1)

No.	Plant Site	Start of Operation (year)	Biomass Boiler(s) Type of Biomass Fuel (MW)	Annual Fuel Peak Load (Biomass) Type of Fuel (SRWt)	District Heating Net Length (km)	Type of Heating	Types of Heating	Connected Consumers (kW)	No. of Heat Consumers	Central Thermal Storage (m³)	Collector Area per unit collector (m²)	Storage volume per unit collector (m³)	Annual Heat Delivery (MWh/a)	Specific collector area per connected heat load (m²/MW)	Specific storage volume per connected heat load (m³/MW)	Remarks	Status	Source
1	Deutsch Teichmenseedorf / Burgenland	1984	600 Biomass	2800 non	n.a.	290 DHHW	290 DHHW	847	44	34	350	0.097	1500	0.413	0.60	1996: total heat demand for 2500 m DHHW: 1386 MWh/a (heat consumer + grid losses); 1997: total heat demand for 2500 m DHHW: 1386 MWh/a (heat consumer + grid losses); solar fraction: 10 %; grid losses 224 MWh/a = 19.3 % a.	2004	http://www.burgenland.at/news/146146 http://www.burgenland.at/news/146146 http://www.burgenland.at/news/146146
2	Bälden / Burgenland	1995	1000 Wood chips	1800 non	n.a.	4500 DHHW	4500 DHHW	1000	72	38	450	0.084	1250	0.460	0.038	1996: total heat demand for 2500 m DHHW: 1386 MWh/a (heat consumer + grid losses); 1997: total heat demand for 2500 m DHHW: 1386 MWh/a (heat consumer + grid losses); solar fraction: 10 %; grid losses 224 MWh/a = 28.1 % a.	2004	http://www.burgenland.at/news/146146 http://www.burgenland.at/news/146146 http://www.burgenland.at/news/146146
3	Chernikensdorf / Lower Austria	1995	840 + 340 Forest wood chips	3000 non	n.a.	3400 DHHW	3400 DHHW	n.a.	95	80	567	0.141	n.a.	n.a.	n.a.	n.a.	n.a.	http://www.burgenland.at/news/146146 http://www.burgenland.at/news/146146 http://www.burgenland.at/news/146146
4	Unterbach / Burgenland	1996	640 + 500 Forest wood chips	1800 non	n.a.	4500 DHHW	4500 DHHW	n.a.	84	58	477	0.122	1000	n.a.	n.a.	n.a.	n.a.	http://www.burgenland.at/news/146146 http://www.burgenland.at/news/146146 http://www.burgenland.at/news/146146
5	Langbaben / Burgenland	1997	450 Wood chips	1000 non	n.a.	2000 DHHW	2000 DHHW	n.a.	32	37	350	0.108	960	n.a.	n.a.	Full mix made of hardwood, softwood and shells of sunflower seeds	2004	http://www.burgenland.at/news/146146 http://www.burgenland.at/news/146146 http://www.burgenland.at/news/146146
6	Gnas / Styria	1996	1000 + 640 Wood chips	3000 non	n.a.	2800 DHHW	2800 DHHW	1700	29	60	441	0.136	2100	0.259	0.036	2 central heat storages, final number of heat storages is 115 m³ boiler tank, as yet into operation	n.a.	http://www.burgenland.at/news/146146 http://www.burgenland.at/news/146146 http://www.burgenland.at/news/146146
7	Ullersdorf / Burgenland	1996	650 Forest wood chips	1250	170 Fuel oil	2200 DHHW	2200 DHHW	594	30 / 60	30 + 30	340	0.178	850	0.572	0.101	2 central heat storages, final number of heat storages is 50 to 55	2006	http://www.burgenland.at/news/146146 http://www.burgenland.at/news/146146 http://www.burgenland.at/news/146146
8	Bad Mittersdorf / Styria	1997	4000 Wood chips	n.a.	n.a.	13000 DHHW	13000 DHHW	n.a.	130	130	1120	0.116	n.a.	n.a.	n.a.	Max. thermal power of collectors: 750 kW; supply / return temp.: 95 °C / 60 °C; solar fraction: 10 %; grid losses 224 MWh/a = 19.3 % a.	2004	http://www.burgenland.at/news/146146 http://www.burgenland.at/news/146146 http://www.burgenland.at/news/146146
9	Erlawatz / Styria	1997 / 2006 / 2012	2000 + 500 Wood chips	11500 non	n.a.	9500 DHHW	9500 DHHW	4000	> 70	(109) 175 + 1250 + 1000	2450	0.071	7000	0.613	0.044	Max. thermal power of collectors: 750 kW; supply / return temp.: 95 °C / 60 °C; solar fraction: 10 %; grid losses 224 MWh/a = 19.3 % a.	n.a.	http://www.burgenland.at/news/146146 http://www.burgenland.at/news/146146 http://www.burgenland.at/news/146146
10	Polysbrunn / Lower Austria	1997	1000 Forest wood chips	2500 non	n.a.	3400 DHHW	3400 DHHW	n.a.	102	80	870	0.092	2000	n.a.	n.a.	Max. thermal power of collectors: 750 kW; supply / return temp.: 95 °C / 60 °C; solar fraction: 10 %; grid losses 224 MWh/a = 19.3 % a.	n.a.	http://www.burgenland.at/news/146146 http://www.burgenland.at/news/146146 http://www.burgenland.at/news/146146
11	Malsch / Burgenland	1997	1600 + 600 Wood chips	5050 non	n.a.	10250 DHHW	10250 DHHW	n.a.	179	70	760	0.090	2000	n.a.	n.a.	Max. thermal power of collectors: 750 kW; supply / return temp.: 95 °C / 60 °C; solar fraction: 10 %; grid losses 224 MWh/a = 19.3 % a.	2004	http://www.burgenland.at/news/146146 http://www.burgenland.at/news/146146 http://www.burgenland.at/news/146146
12	Kneitsch Kneller / Burgenland	1997	700 + 150 Forest Wood chips	1800 non	n.a.	6000 DHHW	6000 DHHW	n.a.	95	65	626	0.096	1300	n.a.	n.a.	Biomass boiler 700 kW + Fired bed boiler: 550 kW	2004	http://www.bur

Table 12-2: Solar-assisted biomass district heating systems in Austria 2012 (Part 2)

Case No.	Plant Site	Start of Operation [year]	Biomass Briquet Type of Biomass Fuel [kW]	Annual Fuel Peak Load [kW]	Type of Fuel	Direct Heating Net Output [kW]	Type of Heating	Connected Thermal Load [kW]	Central Thermal Storage [m ³]	Collector Area and collector efficiency [m ²]	Storage Volume [m ³]	Annual Heat Delivery [MWh]	Specific collector gross area per connected heat load [m ² /kW]	Remarks	Status	Source
21	Neckarschlag / Emmstal / Styria	2006	500 Forest wood chips	1672	400 t/a	n.a.	1150 CHNW	680	1150	3	327 m ³ a.	n.a.	0.40 m ² a.		2006	

Table 12-3: Solar-assisted biomass micro grid systems in Austria – Status 2012

No.	Plant Site	Start of Operation (Year)	Biomass Substr.	Type of Biomass Fuel	Annual Fuel Demand (GWh _{th})	Peak Load (MW _{th})	Type of Fuel	Direct Heating Net Length (m)	Type of Heating Network (m)	Suspended Load (kW)	Connected Load (No. of Heat Consumers)	Central Thermal Storage (GJ)	Collector Area (m ²)	Storage volume per unit collector area (m ³ /m ²)	Annual Heat Delivery (MWh/a)	Specific collector gross area per connected heat load (m ² /kW)	Specific storage volume per connected heat load (m ³ /kW)	Remarks	Status	Source
1	Wieners / Upper Austria	1998	100 Wood chips	n.a.	non	n.a.	n.a.	7	MIN	n.a.	6	1	44	0.034	n.a.	n.a.	n.a.	1 buffer tank (100 l) + 1 domestic hot water tank 500 l	n.a.	http://www.solar.at/de/energie/technologie/technik/technik.htm http://www.solar.at/de/energie/technologie/technik/technik.htm http://www.solar.at/de/energie/technologie/technik/technik.htm http://www.solar.at/de/energie/technologie/technik/technik.htm http://www.solar.at/de/energie/technologie/technik/technik.htm
2	Gleisdorf / Styria	1998	40 Wood chips	n.a.	non	n.a.	n.a.	7	MIN	n.a.	3	14	235	0.069	n.a.	n.a.	n.a.	Solar-supported biomass micro-CHP system for 12 family houses and 2 residential buildings. Max. thermal power of solar collector: 150 kW	n.a.	http://www.solar.at/de/energie/technologie/technik/technik.htm http://www.solar.at/de/energie/technologie/technik/technik.htm http://www.solar.at/de/energie/technologie/technik/technik.htm http://www.solar.at/de/energie/technologie/technik/technik.htm http://www.solar.at/de/energie/technologie/technik/technik.htm
3	Liezen/Strassenehl / Styria	1999	125 Wood chips	n.a.	non	n.a.	n.a.	13	MIN	n.a.	28	5	106	0.047	280	0.934	0.045	domestic hot water and space heating for 13 family houses, 8 apartments and 1	2004	http://www.solar.at/de/energie/technologie/technik/technik.htm http://www.solar.at/de/energie/technologie/technik/technik.htm http://www.solar.at/de/energie/technologie/technik/technik.htm http://www.solar.at/de/energie/technologie/technik/technik.htm http://www.solar.at/de/energie/technologie/technik/technik.htm
4	St. Florian / Upper Austria	2000	700 Wood chips	1100 ton	n.a.	n.a.	n.a.	100	MIN	n.a.	7	7	7	n.a.	900	n.a.	n.a.	Space heating and domestic hot water for a vocational school and boarding home. DHW in summer by solar thermal system	2009	http://www.solar.at/de/energie/technologie/technik/technik.htm http://www.solar.at/de/energie/technologie/technik/technik.htm http://www.solar.at/de/energie/technologie/technik/technik.htm http://www.solar.at/de/energie/technologie/technik/technik.htm http://www.solar.at/de/energie/technologie/technik/technik.htm
5	Wernsmannsdorf / Styria	2001	125 Wood chips	350 n.a.	n.a.	n.a.	n.a.	95	MIN	n.a.	2	5	106	0.047	360	0.939	0.029		n.a.	http://www.solar.at/de/energie/technologie/technik/technik.htm http://www.solar.at/de/energie/technologie/technik/technik.htm http://www.solar.at/de/energie/technologie/technik/technik.htm http://www.solar.at/de/energie/technologie/technik/technik.htm http://www.solar.at/de/energie/technologie/technik/technik.htm
6	Saiburg / Salzburg	2002	160 Wood pellets	n.a.	500	n.a.	n.a.	7	MIN	n.a.	126	7	403	n.a.	n.a.	n.a.	n.a.	127 residential units + 1 Kindergarten	n.a.	http://www.solar.at/de/energie/technologie/technik/technik.htm http://www.solar.at/de/energie/technologie/technik/technik.htm http://www.solar.at/de/energie/technologie/technik/technik.htm http://www.solar.at/de/energie/technologie/technik/technik.htm http://www.solar.at/de/energie/technologie/technik/technik.htm
7	Saiburg / Salzburg	2003	150 Wood pellets	n.a.	n.a.	100	n.a.	7	MIN	n.a.	43	7	160	n.a.	n.a.	n.a.	n.a.	37 residential units + 6 row houses	n.a.	http://www.solar.at/de/energie/technologie/technik/technik.htm http://www.solar.at/de/energie/technologie/technik/technik.htm http://www.solar.at/de/energie/technologie/technik/technik.htm http://www.solar.at/de/energie/technologie/technik/technik.htm http://www.solar.at/de/energie/technologie/technik/technik.htm
8	Wernberg / Upper Austria	2004	110 Wood chips	n.a.	non	n.a.	n.a.	7	MIN	n.a.	4	7	46	0.169	n.a.	n.a.	n.a.	1 central boiler tank (7000 l) hot water tank (1000 l) + 1 hot water tank (1000 l) The original bio-oiled BHKW has been replaced by a 3. pellets boiler. The original BHKW is still in operation with a 300 tank for DHW. Solar collectors are mounted on the facade of the office building	n.a.	http://www.solar.at/de/energie/technologie/technik/technik.htm http://www.solar.at/de/energie/technologie/technik/technik.htm http://www.solar.at/de/energie/technologie/technik/technik.htm http://www.solar.at/de/energie/technologie/technik/technik.htm http://www.solar.at/de/energie/technologie/technik/technik.htm
9	Vilach / Carinthia	2005	32 + 32 + 32 (+ Biodiesel)	Wood pellets	n.a.	non	n.a.	120	MIN	n.a.	1 + 4	3.05	78	0.039	n.a.	n.a.	n.a.		n.a.	http://www.solar.at/de/energie/technologie/technik/technik.htm http://www.solar.at/de/energie/technologie/technik/technik.htm http://www.solar.at/de/energie/technologie/technik/technik.htm http://www.solar.at/de/energie/technologie/technik/technik.htm http://www.solar.at/de/energie/technologie/technik/technik.htm
10	Aischach / Upper Austria	2004 / 2006	500 Wood pellets	n.a.	non	n.a.	n.a.	7	MIN	n.a.	7	2 + 2 + 1	30	0.169	n.a.	n.a.	n.a.	Space heating and domestic hot water for a hotel complex	2009	http://www.solar.at/de/energie/technologie/technik/technik.htm http://www.solar.at/de/energie/technologie/technik/technik.htm http://www.solar.at/de/energie/technologie/technik/technik.htm http://www.solar.at/de/energie/technologie/technik/technik.htm http://www.solar.at

Table 12-4: Simulation report of for a solar-assisted biomass district heating system in Moosburg / Carinthia 2013

Simulationsprogramm "SHW"
zur Simulation von Systemen zur solaren
Raumheizung und Warmwasserbereitung mit Zusatzheizung

Erstellt von
W.Streicher, K.Schnedl, A.Thuer, A.Vilics
(c) Institut fuer Waermetechnik, TU Graz

Datum: 05.04.2013

Uhrzeit: 10:46

B E R E C H N U N G S E R G E B N I S :

GESAMTANLAGE: Nahwärmenetz_MS_FW_2013_min								
Monat	Global [kWh]	BeDauKol [h]	NutzKol [kWh]	ZirkVer [kWh]	SolSpei [kWh]	KolWiGr [%]	KolNuGr [%]	DeckGr [%]
JAN	115598	82.8	24265	489.5	23775	33.81	20.99	2.34
FEB	179127	149.7	59190	865.6	58324	40.09	33.04	7.59
MAR	242769	200.1	90707	1077.1	89630	44.36	37.36	12.20
APR	249167	190.4	87238	960.7	86278	45.83	35.01	19.52
MAI	296890	210.2	87846	990.6	86855	45.06	29.59	50.07
JUN	300304	187.9	75815	877.2	74938	44.64	25.25	75.43
JUL	318543	178.4	63412	822.5	62589	42.56	19.91	95.35
AUG	298055	130.9	47579	613.3	46966	42.60	15.96	96.86
SEP	243294	146.1	63315	728.6	62586	44.81	26.02	45.20
OKT	160616	129.4	46824	631.6	46193	41.94	29.15	12.85
NOV	97925	64.0	24319	350.0	23969	40.61	24.83	3.36
DEZ	86451	60.7	15059	345.4	14714	31.41	17.42	1.63
Jahr	2588745	1730.6	685575	8752.1	676823	42.83	26.48	12.79

(c) Institut fuer Waermetechnik, TU Graz

FERNWAERME:								
Monat	BeDauKol [h]	FwSpTmax [oC]	FwSpent [kWh]	FwSpVerl [kWh]	Kessel [kWh]	Elektr [kWh]	SolSpei [kWh]	DeckFw [%]
JAN	82.8	95.34	942306	868.8	920249	0	23775	2.34
FEB	149.7	98.63	790547	778.9	730532	0	58324	7.59
MAR	200.1	101.52	705906	850.8	619792	0	89630	12.20
APR	190.4	102.00	447822	845.9	360402	0	86278	19.52
MAI	210.2	101.42	170385	938.1	85081	0	86855	50.07
JUN	187.9	103.49	98921	929.8	24308	0	74938	75.43
JUL	178.4	99.97	69826	1012.6	3250	0	62589	95.35
AUG	130.9	97.91	51832	1008.7	1625	0	46966	96.86
SEP	146.1	103.54	142428	908.5	78055	0	62586	45.20
OKT	129.4	102.52	375717	860.5	327433	0	46193	12.85
NOV	64.0	100.18	661459	805.8	639241	0	23969	3.36
DEZ	60.7	97.28	869591	855.7	855417	0	14714	1.63
Jahr	1730.6	103.54	5326745	10664.3	4645389	0	676823	12.79

(c) Institut fuer Waermetechnik, TU Graz

WEITERE DATEN:						
Monat	BetrStr [kWh]	FwentTmi [oC]	FW-Deckg [%]	Fernw. [kWh]	Heizung [kWh]	Pass+Sp [kWh]
JAN	71775	55.98	88.62	1063269	940043	.0
FEB	147627	55.98	91.61	862978	739651	.0
MAR	204496	55.98	93.22	757260	621862	.0
APR	190356	55.98	95.91	466898	345205	.0
MAI	194949	55.97	99.12	171898	62584	.0
JUN	169855	55.98	99.75	99167	11299	.0
JUL	148983	55.97	100.00	69828	0	.0
AUG	111699	56.00	100.00	51832	0	.0
SEP	141301	55.96	98.54	144532	101678	.0
OKT	111660	55.94	96.01	391343	341911	.0
NOV	59880	55.98	91.99	719035	649054	.0
DEZ	47952	55.98	89.36	973148	871588	.0
Jahr	1600540	55.94	92.30	5771194	4684880	.0

ANLAGEDATEN:

Projekt:

Nahwärmenetz_MS_FW_2013_min
 Klimadatensatz: Moos_hor.dat

S I M U L A T I O N S T E C H N. D A T E N:

Simulationsbeginn mit Monatsnummer	[-]	=	7
Simulationsende mit Monatsnummer	[-]	=	19
Simulationsschritte je Stunde	[-]	=	10
Max. Anzahl von Schichten im Speicher	[-]	=	10
Min. Schichttemperaturdiff. fuer Splitten	[oC]	=	.600
Geographische Breite	[o]	=	46.664
Max. Temp.fehler bei Kollektorkreisiteration	[oC]	=	.300

KOLLEKTORDATEN: FPC Solid HT16,7

Kollektorflaeche	[m2]	=	1827.600
Kollektorneigungswinkel	[o]	=	30.000
Kollektorazimut -90:W, 0:S, 90:O	[o]	=	-25.000
c0 (= Kollektorkonversionsfaktor)	[-]	=	.811
c1 (= Kollektor k-Wert)	[W/m2,K]	=	2.710
c2 (= Quadrat. Glied f. Kol.Wirk.Grad)	[W/m2,K2]	=	.010
Spezifische Absorbermasse	[kg/m2]	=	3.040
Spez. Waermekap. Absorbermaterial	[J/kg,K]	=	651.900
Kol-Massenstr. bei Warmwassersp.-Ladung	[kg/s]	=	40.000
Kol-Massenstr. bei Heizenergiesp.-Ladung	[kg/s]	=	5.200
Winkelfaktor bei 50o Abweichung von Normaler	[-]	=	.960
Spezifischer Fluessigkeitsinhalt Kollektor	[m3/m2]	=	.001
Dichte Koll.-Fluessigkeit	[kg/m3]	=	1060.000
Spez. Waermekap. Koll.-Fluessigkeit	[J/kg,K]	=	3760.000
Rohrlaenge Waermetauscher-Kollektor	[m]	=	180.000
Rohrdurchmesser Waermetauscher-Kollekt	[m]	=	.100
Rohrwandstaerke Waermetauscher-Kollekt	[m]	=	.005
Daemmungsdicke Waermetauscher-Kollektor	[m]	=	.080
Daemmungsleitwert Waermet.-Kollektor	[W/m,K]	=	.040
Dichte Rohrleitungsmaterial	[kg/m3]	=	7850.000
Spez. Waermekap. Rohrleitungsmaterial	[J/kg,K]	=	500.000
Rohrlaenge Kollektor-Waermetauscher	[m]	=	180.000
Rohrdurchmesser Kollektor-Waermetausche	[m]	=	.100
Rohrwandstaerke Kollektor-Waermetausche	[m]	=	.005
Daemmungsdicke Kollektor-Waermetauscher	[m]	=	.080
Daemmungsleitwert Kollektor-Waermetauscr	[W/m,K]	=	.040
Dichte Rohrleitungsmaterial	[kg/m3]	=	7850.000
Spez. Waermekap. Rohrleitungsmaterial	[J/kg,K]	=	500.000

FERNWAERMSPEICHER: Fw-Speicher_MS_FW_2013

Allgemeines:

Warmwasserspeichervolumen	[m3]	=	200.000
Warmwasserspeicherhoehe	[m]	=	10.000
Daemmungsdicke	[m]	=	.400
Daemmungsleitwert	[W/m,K]	=	.040
Mittlerer vertikaler Waermeleitwert	[W/m,K]	=	.996
Zuflusshoehe Frischwasser	[m]	=	.000
Abflusshoehe Warmwasser	[m]	=	10.000
Alternat. Abflusshoehe Warmwasser	[m]	=	5.000

Zufuhr von Sonnenenergie ueber Waermetauscher 1:

Waermetauscherart	[-]	=	ext
int: Einbauh. WT; ext: Zuflusshoehe	[m]	=	4.500
Einbauhoehe Temperaturfuehler	[m]	=	.170
int: Bauhoehe WT; ext: Abflusshoehe	[m]	=	.010
alternative Zuflusshoehe	[m]	=	9.970
alternative Hoehe Temperaturfuehler	[m]	=	9.400
alternative Abflusshoehe	[m]	=	.010
Oberflaeche Waermetauscher	[m2]	=	1353.000
k-Wert Waermetauscher	[W/m2,K]	=	1000.000
ext: Sekundaermassenstrom	[kg/s]	=	35.981

Zufuhr von Kesselenergie ueber Waermetauscher 2:

Waermetauscherart	[-]	=	ext
int: Einbauh. WT; ext: Zuflusshoehe	[m]	=	9.970

Master Thesis
MSc Program
Renewable Energy in Central & Eastern Europe

Einbauhoehe Temperaturfuehler	[m]	=	9.970
int: Bauhoehe WT; ext: Abflusshoehe	[m]	=	5.640
Oberflaeche Waermetauscher	[m2]	=	257.000
k-Wert Waermetauscher	[W/m2,K]	=	39.360
ext: Sekundaermassenstrom	[kg/s]	=	51.510
Zufuhr von elektrischer Energie:			
Einbauhoehe E-Patrone	[m]	=	1.100
Einbauhoehe Temp.-Fuehler E-Patrone	[m]	=	.000
Leistung E-Patrone	[W]	=	.000

STEUERUNG: Steuerung_MS_FW_2013_FPC

Kollektor:

Vorrang f. Ladung v. (w=Warmw, h=Heiz, g=Gleichr)	=	w
Tempdiff. fuer Einschalten in Boiler	[oC]	= 5.000
Tempdiff. fuer Einschalten in Heizspeicher	[oC]	= 5.000
Hysterese fuer Ausschalten	[oC]	= 1.000
Laufzeit im Nachrang	[min]	= 12.000
Wartezeit im Nachrang	[min]	= 6.000

Warmwasserspeicher:

Max. Temp. bei solarer Energiezufuhr	[oC]	= 85.000
Hysterese fuer Einschalten solar	[oC]	= 5.000
Max. Temp. bei Kesselenergiezufuhr	[oC]	= 93.500
Hysterese fuer Einschalten Kessel	[oC]	= 10.000
Max. Temp. bei elektr. Energiezufuhr	[oC]	= .000
Hysterese fuer Einschalten E-Patrone	[oC]	= .000

FERNWAERME

FW: Tv,Tr aus HZ vorgeg., Massenfluss err.	
Spreizung der Fernwaerme fuer Warmw.	[oC] = 19.000
T-Aussen ab der Netz-Vorl.= BW.Temp.	[oC] = 12.000

WARMWASSERVERBRAUCH: :NWN_MS_FW_2013_min_2

Warmwasserverbrauch	[l/Tag]	= *****									
Warmwasserverbrauchstemperatur	[oC]	= 75.000									
Grundwassertemperatur	[oC]	= 55.000									
Verbrauchsart:											
h=stuendlich lmal / k=kontinuierlich	[-]	= k									
Schwank. Grundw.Temp (hinkt 3 Mon nach)	[oC]	= 10.000									
Stuendl. Tagesverteilung in Prozent											
0-1	1-2	2-3	3-4	4-5	5-6	6-7	7-8	8-9	9-10	10-11	11-12
2.7	3.6	4.7	4.2	3.5	4.1	8.8	7.4	4.9	4.3	3.5	3.6
12-13	13-14	14-15	15-16	16-17	17-18	18-19	19-20	20-21	21-22	22-23	23-24
5.4	4.5	4.1	3.3	3.4	2.8	3.0	4.0	4.2	3.4	3.2	3.4
Tagesverbr. in der Woche in Prozent des Warmwasserverbrauchs											
Mon	Die	Mit	Don	Fre	Sam	Son	Nr.1.d. Jahres				
100.0	100.0	100.0	100.0	100.0	100.0	100.0	0				
Tagesverbr. in den Monaten in Prozent des Warmwasserverbrauchs											
JAN	FEB	MAR	APR	MAI	JUN	JUL	AUG	SEP	OKT	NOV	DEZ
100.0	100.0	100.0	100.0	100.0	100.0	100.0	100.0	100.0	100.0	100.0	100.0

HEIZUNGSANLAGE und GEBAEUDE: 100

Normheizlast	[W]	= 2023540.0				
Auslegungstemperatur (Normaussentemperatur)	[oC]	= -16.300				
Vorlaufstemperatur im Auslegungspunkt	[oC]	= 92.500				
Ruecklaufstemperatur im Auslegungspunkt	[oC]	= 52.500				
Raumtemperatur	[oC]	= 20.000				
Heizbeginnntemperatur	[oC]	= 12.000				
Innere Waermeleistung	[W]	= .0				
Heizlast unbeheizter Gebaeudeteile	[W]	= .0				
Tagnr. START 1. unbeh. Zeit (1.5.=121)	[-]	= 183				
Tagnr. ENDE 1. unbeh. Zeit (1.10.=274)	[-]	= 212				
Tagnr. START 2. unbeh. Zeit (1.6.=152)	[-]	= 213				
Tagnr. ENDE 2. unbeh. Zeit (1.9.=244)	[-]	= 243				
Raumtemperatur bei Nachtabsenkung	[oC]	= 16.000				
Stunde Nachtabsenkung EIN	[h]	= 0				
Stunde Nachtabsenkung AUS	[h]	= 0				
Heizkoerperexp. (1.1 Fubo - 1.3 Rad.)	[-]	= 5.0				
**** Fensterflaechen ****						
1	2	3	4	5	6	
Flaeche	.0	.0	.0	.0	.0	[m2]
Neigung	90.0	90.0	90.0	90.0	90.0	[o]

Azimut	112.5	112.5	22.5	-22.5	.0	67.5	[°]
g-Wert	.460	.460	.460	.460	.460	.480	[-]

KESSEL: Urbas Bio + Viessmann Öl 3250 kW
Leistung der Zusatzheizung (Kessel) [W] = 3250000.0
Kesselart (f=fest, g=gleitend) [-] = g
Kesselminimaltemperatur [°C] = 75.000
Max. Kes-Massenstr. bei Warmw-Sp-Lad. [kg/s] = 51.510
Max. Kes-Massenstr. bei Heiz-Sp-Lad. [kg/s] = 51.510
Max. Kes-Massenstr. bei gleichz. Sp-Lad. [kg/s] = 51.510
Anteil Kes-Massenstr. Warmw. b. gleichz. Lad. [%] = 100.000

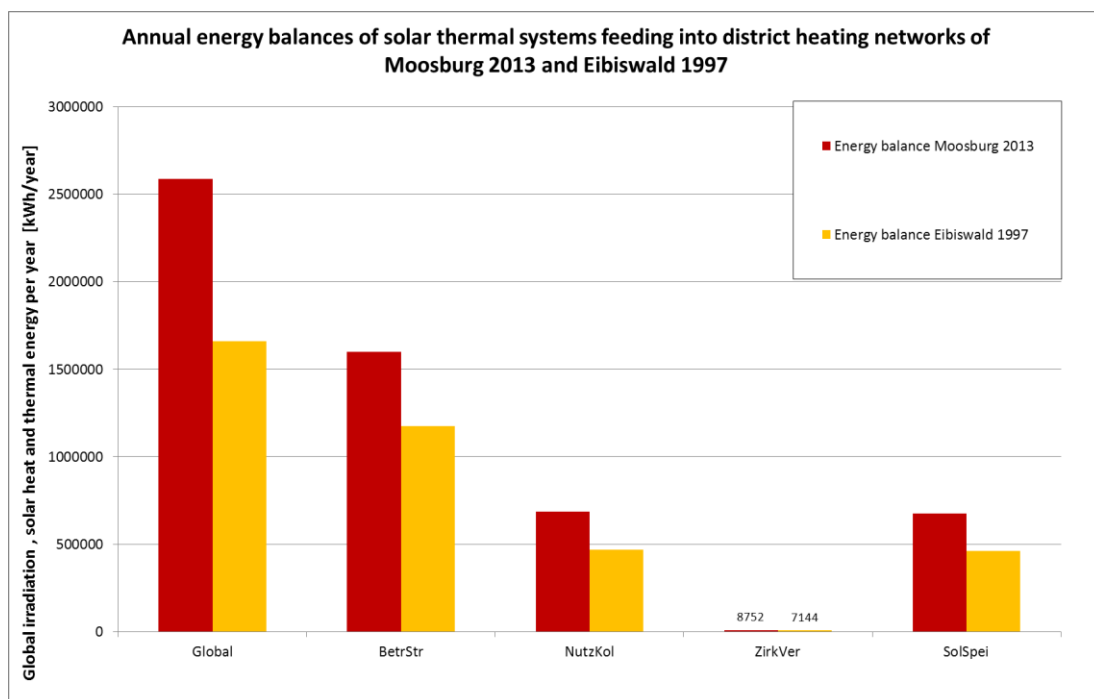


Figure 12-1: Annual balances of 2 solar thermal systems feeding into district heating networks of Moosburg 2013 and Eibiswald 1997 (data source: simulation results of SHWin).

Explanations: *Global ... Global irradiation on total collector area with inclined plane [kWh_{th}];*
BetrStr ... Global irradiation onto collector area, while collectors are operating [kWh_{th}];
NutzKol ... Useful energy gained by collectors [kWh_{th}];
ZirkVer ... Annual heat losses due to circulation in collector loop [kWh_{th}];
SolSpei ... Solar thermal energy fed into storage by collectors [kWh_{th}].

Table 12-5: Simulation report of for a solar-assisted biomass district heating system in Eibiswald / Styria 1997

Simulationsprogramm "SHW"
zur Simulation von Systemen zur solaren
Raumheizung und Warmwasserbereitung mit Zusatzheizung

Erstellt von
W.Streicher, K.Schnedl, A.Thuer, A.Vilics
(c) Institut fuer Waermetechnik, TU Graz

Datum: 11.03.2013

Uhrzeit: 10:57

B E R E C H N U N G S E R G E B N I S :

GESAMTANLAGE: Nahwärmenetz_Eibiswald_97								
Monat	Global	BeDauKol	NutzKol	ZirkVer	SolSpei	KolWiGr	KolNuGr	DeckGr
	[kWh]	[h]	[kWh]	[kWh]	[kWh]	[%]	[%]	[%]
JAN	82517	104.5	22914	477.4	22437	34.86	27.77	2.75
FEB	128883	191.0	44850	775.5	44074	38.15	34.80	8.19
MAR	142278	184.8	45519	764.7	44754	38.45	31.99	6.42
APR	150812	197.5	46797	754.1	46043	37.58	31.03	9.07
MAI	178720	201.9	60449	734.4	59715	43.67	33.82	28.20
JUN	189550	236.7	64254	805.6	63448	42.79	33.90	45.00
JUL	198156	208.1	50645	714.5	49931	40.96	25.56	91.12
AUG	179522	151.8	35164	530.4	34633	40.01	19.59	96.41
SEP	200086	134.9	38694	521.1	38173	42.67	19.34	84.82
OKT	108376	139.0	33717	536.7	33181	39.63	31.11	8.66
NOV	58313	70.7	14927	293.8	14633	36.43	25.60	2.67
DEZ	42610	56.0	9971	235.8	9735	32.82	23.40	1.46

Jahr	1659827	1876.9	467906	7144.0	460762	39.87	28.19	9.97

(c) Institut fuer Waermetechnik, TU Graz

FERNWAERME:								
Monat	BeDauKol	FwSpTmax	FwSpent	FwSpVerl	Kessel	Elektr	SolSpei	DeckFw
	[h]	[oC]	[kWh]	[kWh]	[kWh]	[kWh]	[kWh]	[%]
JAN	104.5	97.26	747825	963.3	727291	0	22437	2.75
FEB	191.0	100.59	539912	864.3	495702	0	44074	8.19
MAR	184.8	99.25	691187	952.2	646842	0	44754	6.42
APR	197.5	100.67	482920	898.2	439133	0	46043	9.07
MAI	201.9	102.23	201481	985.2	144665	0	59715	28.20
JUN	236.7	103.93	143555	983.0	78950	0	63448	45.00
JUL	208.1	102.84	50656	1090.2	4500	0	49931	91.12
AUG	151.8	97.83	34802	1135.8	1250	0	34633	96.41
SEP	134.9	98.48	44504	1184.0	6753	0	38173	84.82
OKT	139.0	101.25	390007	993.5	356241	0	33181	8.66
NOV	70.7	100.03	509582	904.5	495952	0	14633	2.67
DEZ	56.0	98.17	665047	937.0	655322	0	9735	1.46

Jahr	1876.9	103.93	4501483	11891.1	4052605	0	460762	9.97

(c) Institut fuer Waermetechnik, TU Graz

WEITERE DATEN:						
Monat	BetrStr	FwentTmi	FW-Deckg	Fernw.	Heizung	Pass+Sp
	[kWh]	[oC]	[%]	[kWh]	[kWh]	[kWh]
JAN	65728	50.17	88.41	845873	716056	.0
FEB	117572	49.96	84.07	642222	511539	.0
MAR	118385	49.99	91.79	752993	597954	.0
APR	124532	49.95	93.24	517958	380751	.0
MAI	138434	49.96	97.83	205945	90712	.0
JUN	150168	49.94	98.43	145846	55824	.0
JUL	123657	49.92	100.00	50656	0	.0
AUG	87899	49.87	100.00	34802	0	.0
SEP	90683	49.93	99.65	44662	9042	.0
OKT	85073	49.83	93.38	417671	364967	.0
NOV	40970	49.92	91.91	554466	482806	.0
DEZ	30380	49.99	90.35	736069	634627	.0

Jahr	1173486	49.83	90.95	4949169	3844281	.0

ANLAGEDATEN:

Projekt:

Nahwärmenetz_Eibiswald_97
 Klimadatensatz: Eibiho97.dat

S I M U L A T I O N S T E C H N. D A T E N:

Simulationsbeginn mit Monatsnummer	[-]	=	7
Simulationsende mit Monatsnummer	[-]	=	19
Simulationsschritte je Stunde	[-]	=	10
Max. Anzahl von Schichten im Speicher	[-]	=	10
Min. Schichttemperaturdiff. fuer Splitten	[oC]	=	.600
Geographische Breite	[o]	=	46.000
Max. Temp.fehler bei Kollektorkreisiteration	[oC]	=	.300

KOLLEKTORDATEN: Gluatmugl Großfläche (1996)_OK

Kollektorflaeche	[m2]	=	1150.000
Kollektorneigungswinkel	[o]	=	30.000
Kollektorazimut -90:W, 0:S, 90:O	[o]	=	-20.000
c0 (= Kollektorkonversionsfaktor)	[-]	=	.754
c1 (= Kollektor k-Wert)	[W/m2,K]	=	3.000
c2 (= quadrat. Glied f. Kol.Wirk.Grad)	[W/m2,K2]	=	.002
Spezifische Absorbermasse	[kg/m2]	=	2.500
Spez. Waermekap. Absorbermaterial	[J/kg,K]	=	394.000
Kol-Massenstr. bei Warmwassersp.-Ladung	[kg/s]	=	1.740
Kol-Massenstr. bei Heizenergiesp.-Ladung	[kg/s]	=	1.740
Winkelfaktor bei 50o Abweichung von Normaler	[-]	=	.900
Spezifischer Fluessigkeitsinhalt Kollektor	[m3/m2]	=	.001
Dichte Koll.-Fluessigkeit	[kg/m3]	=	1060.000
Spez. Waermekap. Koll.-Fluessigkeit	[J/kg,K]	=	3760.000
Rohrlaenge Waermetauscher-Kollektor	[m]	=	160.000
Rohrdurchmesser Waermetauscher-Kollekt	[m]	=	.090
Rohrwandstaerke Waermetauscher-Kollekt	[m]	=	.005
Daemmungsdicke Waermetauscher-Kollektor	[m]	=	.080
Daemmungsleitwert Waermet.-Kollektor	[W/m,K]	=	.040
Dichte Rohrleitungsmaterial	[kg/m3]	=	8900.000
Spez. Waermekap. Rohrleitungsmaterial	[J/kg,K]	=	394.000
Rohrlaenge Kollektor-Waermetauscher	[m]	=	160.000
Rohrdurchmesser Kollektor-Waermetausche	[m]	=	.090
Rohrwandstaerke Kollektor-Waermetausche	[m]	=	.005
Daemmungsdicke Kollektor-Waermetauscher	[m]	=	.080
Daemmungsleitwert Kollektor-Waermetauscr	[W/m,K]	=	.040
Dichte Rohrleitungsmaterial	[kg/m3]	=	8900.000
Spez. Waermekap. Rohrleitungsmaterial	[J/kg,K]	=	394.000

FERNWAERMSPEICHER: Fw-Speicher_Eibi_OK

Allgemeines:

Warmwasserspeichervolumen	[m3]	=	105.000
Warmwasserspeicherhoehe	[m]	=	12.000
Daemmungsdicke	[m]	=	.250
Daemmungsleitwert	[W/m,K]	=	.040
Mittlerer vertikaler Waermeleitwert	[W/m,K]	=	.900
Zuflusshoehe Frischwasser	[m]	=	.000
Abflusshoehe Warmwasser	[m]	=	12.000
Alternat. Abflusshoehe Warmwasser	[m]	=	6.000

Zufuhr von Sonnenenergie ueber Waermetauscher 1:

Waermetauscherart	[-]	=	ext
int: Einbauh. WT; ext: Zuflusshoehe	[m]	=	5.500
Einbauhoehe Temperaturfuehler	[m]	=	.200
int: Bauhoehe WT; ext: Abflusshoehe	[m]	=	.010
alternative Zuflusshoehe	[m]	=	11.900
alternative Hoehe Temperaturfuehler	[m]	=	11.900
alternative Abflusshoehe	[m]	=	.010
Oberflaeche Waermetauscher	[m2]	=	1566.000
k-Wert Waermetauscher	[W/m2,K]	=	500.000
ext: Sekundaermassenstrom	[kg/s]	=	1.565

Zufuhr von Kesselenergie ueber Waermetauscher 2:

Waermetauscherart	[-]	=	ext
int: Einbauh. WT; ext: Zuflusshoehe	[m]	=	11.950

Master Thesis
MSc Program
Renewable Energy in Central & Eastern Europe

Einbauhoehe Temperaturfuehler	[m]	=	11.950
int: Bauhoehe WT; ext: Abflusshoehe	[m]	=	5.450
Oberflaeche Waermetauscher	[m2]	=	197.000
k-Wert Waermetauscher	[W/m2, K]	=	39.500
ext: Sekundaermassenstrom	[kg/s]	=	39.600
Zufuhr von elektrischer Energie:			
Einbauhoehe E-Patrone	[m]	=	1.100
Einbauhoehe Temp.-Fuehler E-Patrone	[m]	=	.000
Leistung E-Patrone	[W]	=	.000

STEUERUNG: Steuerung_FW_Eibi97

Kollektor:

Vorrang f. Ladung v. (w=Warmw, h=Heiz, g=Gleichr)	=	w
Tempdiff. fuer Einschalten in Boiler	[oC]	= 5.000
Tempdiff. fuer Einschalten in Heizspeicher	[oC]	= 5.000
Hysterese fuer Ausschalten	[oC]	= 1.000
Laufzeit im Nachrang	[min]	= 12.000
Wartezeit im Nachrang	[min]	= 6.000

Warmwasserspeicher:

Max. Temp. bei solarer Energiezufuhr	[oC]	= 82.000
Hysterese fuer Einschalten solar	[oC]	= 5.000
Max. Temp. bei Kesselenergiezufuhr	[oC]	= 93.500
Hysterese fuer Einschalten Kessel	[oC]	= 10.000
Max. Temp. bei elektr. Energiezufuhr	[oC]	= .000
Hysterese fuer Einschalten E-Patrone	[oC]	= .000

FERNWAERME

FW: Tv, Tr aus HZ vorgeg., Massenfluss err.	
Spreizung der Fernwaerme fuer Warmw.	[oC] = 20.000
T-Aussen ab der Netz-Vorl.= BW.Temp.	[oC] = 13.500

WARMWASSERVERBRAUCH: :Nahwärmenetz_Eibi_97

Warmwasserverbrauch	[l/Tag]	= *****									
Warmwasserverbrauchstemperatur	[oC]	= 70.000									
Grundwassertemperatur	[oC]	= 53.000									
Verbrauchsart:											
h=stueendlich lmal / k=kontinuierlich	[-]	= k									
Schwank. Grundw.Temp (hinkt 3 Mon nach)	[oC]	= 10.000									
Stuendl. Tagesverteilung in Prozent											
0-1	1-2	2-3	3-4	4-5	5-6	6-7	7-8	8-9	9-10	10-11	11-12
2.7	3.6	4.7	4.2	3.5	4.1	8.8	7.4	4.9	4.3	3.5	3.6
12-13	13-14	14-15	15-16	16-17	17-18	18-19	19-20	20-21	21-22	22-23	23-24
5.4	4.5	4.1	3.3	3.4	2.8	3.0	4.0	4.2	3.4	3.2	3.4
Tagesverbr. in der Woche in Prozent des Warmwasserverbrauchs											
Mon	Die	Mit	Don	Fre	Sam	Son	Nr.1.d. Jahres				
100.0	100.0	100.0	100.0	100.0	100.0	100.0	0				
Tagesverbr. in den Monaten in Prozent des Warmwasserverbrauchs											
JAN	FEB	MAR	APR	MAI	JUN	JUL	AUG	SEP	OKT	NOV	DEZ
100.0	100.0	100.0	100.0	100.0	100.0	75.0	75.0	100.0	100.0	100.0	100.0

HEIZUNGSANLAGE und GEBAEUDE: 100

Normheizlast	[W]	= 2008060.0				
Auslegungstemperatur (Normaussentemperatur)	[oC]	= -15.000				
Vorlauftemperatur im Auslegungspunkt	[oC]	= 95.000				
Ruecklauftemperatur im Auslegungspunkt	[oC]	= 60.000				
Raumtemperatur	[oC]	= 20.000				
Heizbeginnntemperatur	[oC]	= 13.500				
Innere Waermeleistung	[W]	= .0				
Heizlast unbeheizter Gebaeudeteile	[W]	= .0				
Tagnr. START 1. unbeh. Zeit (1.5.=121)	[-]	= 196				
Tagnr. ENDE 1. unbeh. Zeit (1.10.=274)	[-]	= 196				
Tagnr. START 2. unbeh. Zeit (1.6.=152)	[-]	= 227				
Tagnr. ENDE 2. unbeh. Zeit (1.9.=244)	[-]	= 227				
Raumtemperatur bei Nachtabsenkung	[oC]	= 16.000				
Stunde Nachtabsenkung EIN	[h]	= 20				
Stunde Nachtabsenkung AUS	[h]	= 20				
Heizkoerperexp. (1.1 Fubo - 1.3 Rad.)	[-]	= 5.0				
**** Fensterflächen ****						
1	2	3	4	5	6	
Flaeche	.0	.0	.0	.0	.0	[m2]
Neigung	90.0	90.0	90.0	90.0	90.0	[o]

Azimut	112.5	112.5	22.5	-22.5	.0	67.5	[°]
g-Wert	.460	.460	.460	.460	.460	.480	[-]

KESSEL: Eibi_Biomasse_2500 kW

Leistung der Zusatzheizanlage (Kessel)	[W]	=	2500000.0
Kesselart (f=fest, g=gleitend)	[-]	=	g
Kesselminimaltemperatur	[°C]	=	75.000
Max. Kes-Massenstr. bei Warmw-Sp-Lad.	[kg/s]	=	39.600
Max. Kes-Massenstr. bei Heiz-Sp-Lad.	[kg/s]	=	39.600
Max. Kes-Massenstr. bei gleichz. Sp-Lad.	[kg/s]	=	39.600
Anteil Kes-Massenstr. Warmw. b. gleichz. Lad.	[%]	=	100.000

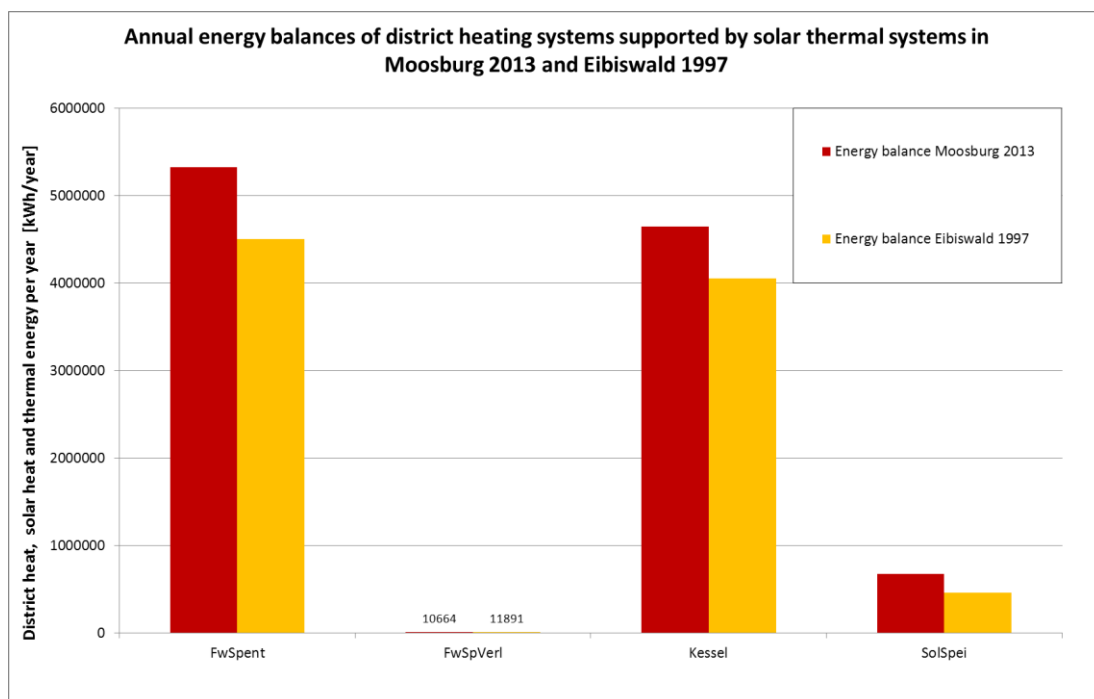


Figure 12-2: Annual energy balances of 2 district heating systems supported by solar thermal systems in Moosburg 2013 and Eibiswald 1997 (data source: simulation results of SHWwin).

Explanations: *FwSpent* ... Annual amount of thermal energy fed into district heating grid [kWh_{th}];
FwSpVerl ... Annual amount of heat losses by thermal energy storage [kWh_{th}];
Kessel ... Produced heat by boilers fed into thermal energy storage [kWh_{th}];
SolSpei ... Solar energy utilized by collectors, which is fed into thermal storage [kWh_{th}].

Table 12-6: Total, annual emissions based on primary energy content of fuel and specific emissions per unit heat fed into a biomass district heating system without solar support in Moosburg 2013*** (data source: simulation results of SHWwin and own calculations).

Fuel type	Mode of operation	CO₂ [g/a]	CO [g/a]	C_xH_x [g/a]	NO_x [g/a]	Particles [g/a]
Biomass*	Continuous operation	0	666770	28811	2140249	683233
Biomass*	Start/stop-operation	0	6368115	440055	585988	3060098
Oil**	Continuous operation	27233481	6064	1053	23602	0
Oil**	Start/stop-operation	4902269	7105	843	4249	0
Sum	[t/a]	32.136	7.048	0.471	2.754	3.743
Annual specific emissions per unit heat fed into DHN						
	[g/kWh_{th}]	6.031	1.323	0.088	0.517	0.703

Explanations: * ... Wood chips (30%w.b.): $NCV_{wc,30\%,vol.} = 795.1 [kWh_{NCV}/SRM]$;
 ** ... Heating oil (0.845 kg/l): $NCV_{oil,mas.} = 11.8 [kWh_{NCV}/kg]$;
 *** ... Connected load: $\dot{Q}'_{cl,DHN} = 3554 [kW_{th}]$; maximal effective connected load: $\dot{Q}'_{cl,max,eff.} = 2130 [kW_{th}]$; base load: $\Phi'_{grid,min.} + \dot{Q}'_{DHW} = 107 [kW_{th}]$; grid length: $l_{grid} = 5755 [m]$; number of heat consumers: $n_{user,i} = 104 [1]$.

Table 12-7: Total, annual emissions based on primary energy content of fuel and specific emissions per unit heat fed into a solar- assisted biomass district heating system in Moosburg 2013*** (data source: simulation results of SHWwin and own calculations).

Fuel type	Mode of operation	CO₂ [g/a]	CO [g/a]	C_xH_x [g/a]	NO_x [g/a]	Particles [g/a]
Biomass*	Continuous operation	0	597126	25802	1916702	611870
Biomass*	Start/stop-operation	0	4823697	333331	443872	2317952
Oil**	Continuous operation	27233481	6064	1053	23602	0
Oil**	Start/stop-operation	8770113	12711	1508	7601	0
Sum	[t/a]	36.004	5.440	0.362	2.392	2.930
Annual specific emissions per unit heat fed into DHN						
	[g/kWh_{th}]	6.759	1.021	0.068	0.449	0.550

Explanations: * ... Wood chips (30%w.b.): $NCV_{wc30\%,vol.} = 795.1 \text{ [kWh}_{NCV}/\text{SRM}]$;
 ** ... Heating oil (0.845 kg/l): $NCV_{oil,mas.} = 11.8 \text{ [kWh}_{NCV}/\text{kg}]$
 *** ... Connected load: $\dot{Q}'_{cl,DHN} = 3554 \text{ [kW}_{th}]$; maximal effective connected load: $\dot{Q}'_{cl,max.,eff.} = 2130 \text{ [kW}_{th}]$; base load: $\Phi'_{grid,min.} + \dot{Q}'_{DHW} = 107 \text{ [kW}_{th}]$; grid length: $l_{grid} = 5755 \text{ [m]}$; number of heat consumers: $n_{user,i} = 104 \text{ [1]}$.

Table 12-8: Total, annual emissions based on primary energy content of fuel and specific emissions per unit heat fed into a solar-assisted biomass district heating system in Eibiswald 1997*** (data source: simulation results of SHWwin and own calculations).

Fuel type	Mode of operation	CO₂ [g/a]	CO [g/a]	C_xH_x [g/a]	NO_x [g/a]	Particles [g/a]
Biomass*	Continuous operation	0	490932	21213	1575831	503054
Biomass*	Start/stop-operation	0	5776101	399145	531512	2775615
Oil**	Continuous operation	0	0	0	0	0
Oil**	Start/stop-operation	3757418	5446	646	3256	0
Sum	[t/a]	3.777	6.272	0.421	2.111	3.279
Annual specific emissions per unit heat fed into DHN		[g/kWh_{th}]	0.839	1.393	0.094	0.469
			0.728			

Explanations: * ... Wood chips (30%w.b.): $NCV_{wc30\%,vol.} = 795.1 \text{ [kWh}_{NCV}/\text{SRM}]$;
 ** ... Heating oil (0.845 kg/l): $NCV_{oil,mas.} = 11.8 \text{ [kWh}_{NCV}/\text{kg}]$
 *** ... Connected load: $\dot{Q}'_{cl,DHN} = 3000 \text{ [kW}_{th}]$; maximal effective connected load: $\dot{Q}'_{cl,max.,eff.} = 2114 \text{ [kW}_{th}]$; base load: $\Phi'_{grid,min.} + \dot{Q}'_{DHW} = 106 \text{ [kW}_{th}]$; grid length: $l_{grid} = 4000 \text{ [m]}$; number of heat consumers: $n_{user,i} = 64 \text{ [1]}$.

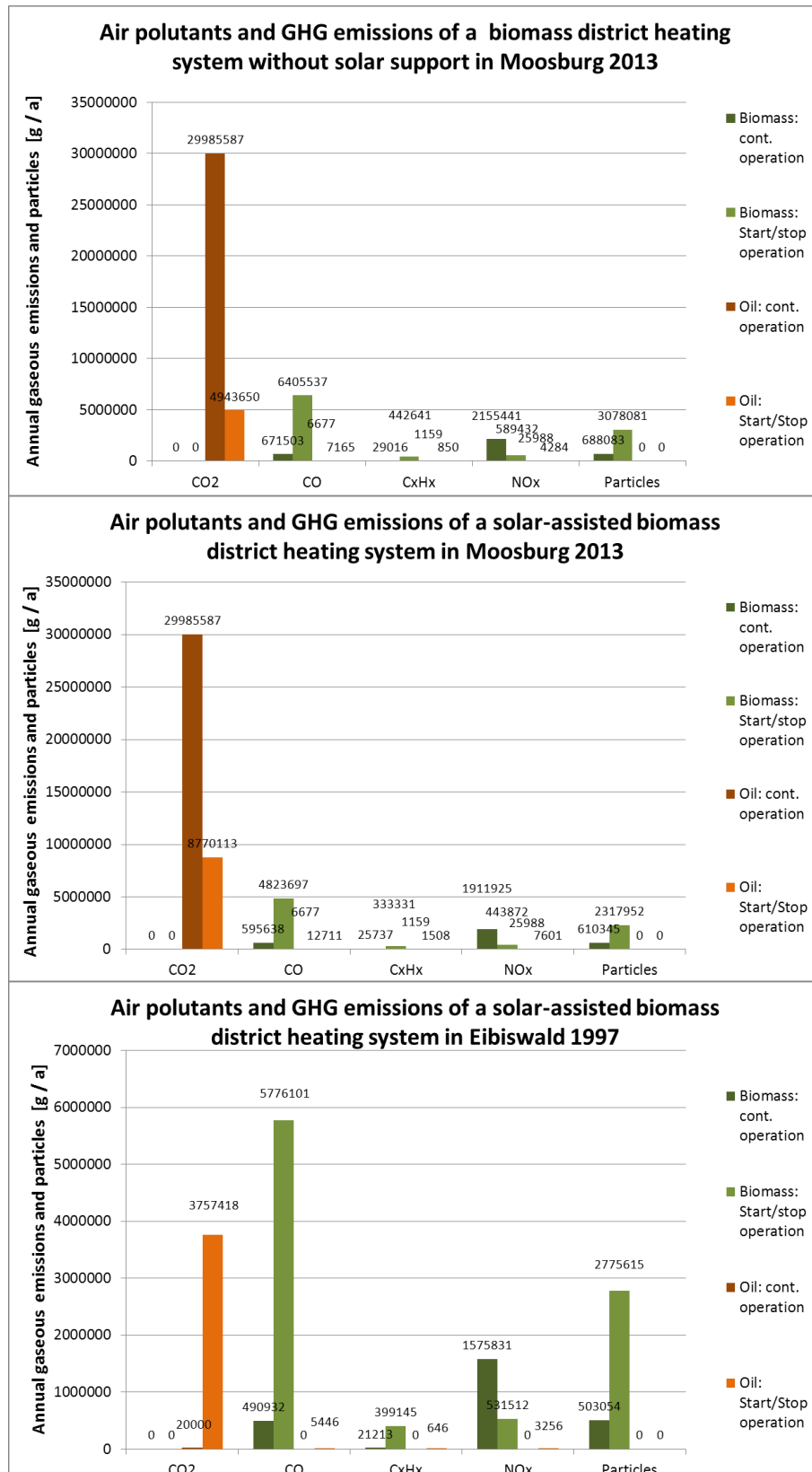


Figure 12-3: Total, annual emissions of CO₂, CO, C_xH_x, NO_x and fine particles based on primary energy content of fuel used in biomass district heating systems with and without solar support (data source: own calculations).